A role for the nuclear transport machinery in supporting positive-strand RNA virus infection and in regulating innate immune responses

by

Christopher John Neufeldt

A thesis submitted in partial fulfillment of the requirements for the degree of

Doctor of Philosophy

Cell Biology

University of Alberta

ABSTRACT

In eukaryotic cells, the genetic material is encapsulated in a double lipid membrane layer to form the nuclear compartment. This double membrane layer, termed the nuclear envelope, is fenestrated by pores, which are occupied by proteinaceous gateway structures termed nuclear pore complexes (NPCs). NPCs facilitate all traffic between the nucleus and cytoplasm effectively creating a selective barrier between these two compartments. Its key location at the interface between the nucleus and cytoplasm allows the NPC or it constituent proteins, termed nucleoporins or Nups, to regulate a large number of cellular pathways. This also makes the NPC an important target for many viral infections. Similar to the formation of organelles in eukaryotic cells, positive-strand RNA viruses, including hepatitis C virus, induce the formation of membrane bound replication and assembly compartments in the cytoplasm of infected cells. These membrane compartments function to both increase the efficiency of viral processes and to protect viral components from degradation or immune surveillance. The work presented here demonstrates a novel function for the NPC in cytoplasmic viral replication centers. Specifically, we show that Hepatitis C virus infection induces the relocalization of Nups to cytoplasmic regions enriched for viral proteins, which represent the viral replication complex (termed the membranous web). Our data also shows that components of the nuclear transport machinery support HCV replication and that nucleocytoplasmic transport is active at the membranous web. Moreover, our results indicate that NPCs residing in the membranous web are involved in a viral immune evasion strategy by facilitating the formation of a replication compartments that are protected from cellular immune receptors in the surrounding cytoplasm. Lastly, we present data the indicates one specific Nup, Nup358, is involved in generally regulating immune responses and is an important host factor that supports HCV infection. From these data we propose that

HCV utilizes the immune regulatory function of Nup358 to inhibit host cell immune activation and facilitate viral infection. These results demonstrate that the nuclear transport machinery pays a critical role in the life cycle of positive strand RNA virus infections and indicate that the NPC has an important function in regulating host cell immune responses.

DEDICATION

For my family
Their unfailing support made this possible

And for a few remarkable friends
Who never failed to impart a broader perspective

ACKNOWLEDGMENTS

Throughout my tenure as a graduate student, there have been a number of individuals that have provided guidance and support without which the completion of this thesis would not have been possible. First, I am grateful to Richard Wozniak for giving me the opportunity to join his research group and study under his supervision. Rick's enthusiasm for scientific exploration and his push for excellence have been truly inspiring. I am grateful for the knowledge and experience I have gained from Rick throughout my PhD.

I would also like to thank all of the members of the Wozniak Lab who have each significantly contributed to my education and experience as a graduate student. My success in the lab was only possible with the continual critical evaluation and insights provided by lab members.

The vast majority of the work presented here would not have been possible without Lorne Tyrrell and several members of his research group. It has been a great pleasure to work with Lorne whose generosity, love of biology and tireless efforts toward creating a better environment for both research and education are to be greatly admired. Additionally, I would like to specifically thank Michael Joyce for his constant efforts in the realization of the work presented here. Both Lorne and Michael provided significant support with insights and materials that were instrumental throughout my degree.

Finally, the support of my family and an extraordinary group of friends were foundational to my success throughout this journey. To my family, whose tenacious encouragement as well as steadfast support has been crucial for the success in every avenue of my life. To my remarkable friends, who have challenged and contributed to pushing my boundaries and perspectives over the years. Specifically, Michael Granzow, David Janzen, Lucas Cairo, Justin Pahara and Robert Janzen have each had a significant impact on my life as a graduate student and their support and continual efforts were indispensable in broadening the scope of my academic endeavors.

TABLE OF CONTENTS

LIST OF TABLES

LIST OF FIGURES

LIST OF SYMBOLS, ABBREVIATIONS AND NOMENCLATURE

µ	micron
µg	microgram
µm	micrometer
°C	degrees Celsius
aa	amino acid
ALL	acute lymphoblastic leukemia
AML	acute myeloid leukemia
Apo	apolipoprotein
BAR	Bin-Amphiphysin-Rvs
bp	base pair
CARD	caspase-recruitment domain
cDNA	complementary DNA
CLD	cyclophilin-like domain
cNLS	canonical NLS
ct	cycle threshold
CVB3	coxsackievirus B3
CypA	cyclophilin A
DENV	Dengue virus
DMV	double membrane vesicle
DNA	deoxyribonucleic acid
dsDNA	double-stranded DNA
dsRNA	double-stranded RNA
EM	electron microscopy
ER	endoplasmic reticulum
EVA	equine arterivirus
FG	phenylalanine-glycine
FFU	focus forming unit
FHV	flock-house virus
GAG	glycosaminoglycan
GAS	IFN-γ-activated site
GDP	Guanosine diphosphate
GTP	Guanosine triphosphate
GTPase	GTP hydrolase
HAT	histone acetyl-transferases
HAV	Hepatitis A virus
HBV	Hepatitis B virus
HCV	Hepatitis C virus
HDAC	histone deacetylase complex
IFN	interferon

IgG ..... Immunoglobulin G
IRF ..... interferon regulatory factor
IL ..... interleukin
Imp ..... importin
INM ..... inner nuclear membrane
InV/S ..... inverted vesicle or spherule
IRES ..... internal ribosome entry site
IRF ..... interferon regulatory factor
ISG ..... interferon-stimulated gene
ISGF3 ..... interferon-stimulated gene factor 3
ISRE ..... IFN-stimulated response elements
JAK ..... Janus activated kinase
Kap ..... karyopherin
KASH Klarsicht–ANC-1–SYNE
LD ..... Lipid droplet
LDL ..... low-density lipoprotein
LDLR ..... low-density lipoprotein receptor
LVP ..... lipoviroparticle
MOI ..... multiplicity of infection
miRNA ..... micro RNA
mL ..... milliliter
MMV ..... multimembrane vesicle
mRNA ..... messenger RNA
mRNP ..... messenger RNA protein
NE ..... nuclear envelope
NES ..... nuclear export signal
NET ..... nuclear envelope transmembrane
ng ..... nanogram
NPC ..... nuclear pore complex
NS ..... non-structural
NTF ..... nuclear transport factor
Nup ..... nucleoporin
ONM ..... outer nuclear membrane
PAMP ..... pathogen-associated molecular patterns
PBS ..... phosphate buffered saline
PCR ..... polymerase chain reaction
peg ..... polyethylene glycol
PIAS ..... protein inhibitor of activated STAT
PIC ..... pre-integration complex
PML ..... Promyelocytic Leukemia
POM ..... pore membrane

Pom ..... pore membrane protein
PRR ..... patter recognition receptors
PV ..... poliovirus
qPCR ..... quantitative PCR
RanGAP ..... Ran GTPase-activating protein
RanGEF ..... Ran Guanine nucleotide Exchange Factor
RLR ..... RIG-I-like receptor
RNA ..... ribonucleic acid
RNase ..... ribonuclease
RUBV ..... rubella virus
SARS-coV ..... sever acute respiratory syndrome coronavirus
SENP ..... sentrin-specific protease
SFV ..... Semliki Forrest virus
shRNA ..... small hairpin RNA
SIM ..... SUMO binding motif
SMV ..... single membrane vesicle
SOCS ..... suppressor of cytokine signaling
SR-B1 ..... scavenger receptor class B type 1
SREBP ..... sterol regulatory element-binding protein
ssRNA ..... single-stranded RNA
STAT ..... signal transducer and activator of transcription
SUMO ..... small-ubiquitin like modifier
SUN SAD1, UNC84
SVR ..... sustained virological response
TEM ..... transmission electron microscopy
TIR ..... toll-interleukin-1 receptor
TLR ..... toll-like receptors
UTR ..... untranslated region
VLDL ..... very-low-density lipoprotein
VSV ..... vesicular stomatitis virus
WNV ..... West Nile virus
Xpo ..... exportin
ZFD ..... zinc fingers domain

CHAPTER I: Introduction

1.1 Preface

Compartmentalization of cellular processes is a defining feature of eukaryotic cells. Partitioning of the cell into different compartments allows for increased efficiency of individual cellular process by both concentrating factors required for a process in a specific location and decreasing interference between cellular processes. This also enhances the complexity of cellular organization, which facilitates the formation of more sophisticated multicellular organisms. A common organelle in all eukaryotes, the nucleus, separates the cellular genetic material from the cytoplasm by surrounding it with a membrane layer termed the nuclear envelope (NE). Throughout the NE are large proteinaceous complexes (termed nuclear pore complexes or NPCs) that are selectively permeable thereby creating a link between nucleus and cytoplasm. NPCs regulate all traffic between nuclear and cytoplasmic compartments and are required to maintain nuclear segregation while still allowing selective transport between compartments. Situated at the interface between the nucleus and the cytoplasm, NPCs are involved in a vast number of cellular processes. Similar to the formation cellular organelles, many viruses also produce compartments that improve the efficiency of viral replication within the hostile environment of the host cell. Virus-induced compartments are often comparable to cellular compartments in that they encapsulate the viral genome while still maintaining links to the surrounding cellular environment. The small genome size of viruses suggests they have evolved highly effective ways of manipulating host cells to form viral replication complexes. The efficiency with which these viruses disrupt or alter host cells also makes them ideal to uncover or discern the nature of specific host cell processes. The work presented here focuses on the mechanisms by which a specific class of viruses rearranges host cell architecture to produce an environment conducive to viral propagation. Specifically, these studies examine the role of the

NPC or specific NPC components in viral replication and in regulating innate immune responses.

1.2 Positive-strand RNA viruses

Viruses, first discovered in tobacco plants, are defined as small infectious agents that replicate only inside a host. Since their discovery, thousands of viral species have been described, infecting all forms of life and often causing devastating diseases. In general, viruses can be classified into three groups based on their genomic material: DNA viruses, RNA viruses, and reverse transcribing viruses. RNA viruses can be further subdivided into three groups: those that contain an RNA molecule that codes directly for viral proteins (positive-strand RNA viruses), those that contain RNA that must be replicated before translation of the viral proteins (negative-strand RNA viruses), and those that contain double-stranded RNA (dsRNA viruses). Positive-stranded RNA viruses represent the largest viral class and infect nearly all eukaryotes. Two of the best characterized of the thirty families within this group are the *Flaviviridae* and the *Picornaviridae* families. *Flaviviridae* consists of four genera (including *flavivirus*, *hepacivirus*, *pegivirus*, and *pestivirus*) while *Picornaviridae* contains at least 13 different genera. Despite the diverse number of hosts infected by positive-strand RNA viruses, there is a remarkable conservation in their mechanisms of replication. Intriguingly, viruses within this group unanimously induce the production of specialized replication complexes from host cell membranes (reviewed in (Belov and van Kuppeveld, 2012)). The data discussed here focus on the membrane rearrangements induced by two members of the *Flaviviride* family, Hepatitis C virus (HCV) and Dengue virus (DENV) as well as one member of the *Picornaviride* family (Hepatitis A virus or HAV) with an emphasis on the HCV-induced replication compartment.

1.3 Hepatitis C virus

HCV is estimated to infect approximately 150 million people and is a major cause of liver disease worldwide (Gower et al., 2014). In approximately 80% of infected patients the virus persists in a chronic infection causing progressive liver disease, which goes through several stages of cirrhosis and leads to end stage liver disease in approximately 30% of chronically infected individuals (Alter et al., 1992). HCV infection is also the leading indication for liver transplantation in North America (Roberts et al., 2004). Owing to its high genetic variability, there are seven identified genotypes of HCV encompassing approximately 100 subtypes, the most prevalent North American strains originating from genotype 1a (Gower et al., 2014; Simmonds et al., 2005). HCV is spread through the blood from infected individuals; primarily being transferred through drug use by contaminated needles and, prior to 1989, through blood transfusions and organ transplants in North America. Since the identification of the causative agent for Non-A Non-B viral hepatitis in 1989, the incidence of HCV infection has drastically diminished as a result of extensive blood screening and increased public awareness (Choo et al., 1989). Currently, there is still no vaccine for HCV however; unlike many viruses, treatment of HCV infected individuals with various drugs leads to sustained viral response (SVR or viral clearance) in a high percentage of patients (reviewed in (Hayes and Chayama, 2014)). Until recently, this treatment involved pegylated interferon alpha (pegIFNα) combined with ribavirin: a treatment that caused severe side effects and was only effective in ~50 percent of patients infected with HCV genotype 1 (See section 1.4.4)(Hadziyannis et al., 2004; Heim, 2013; Manns et al., 2001). Current treatment plans are now 'interferon-free', instead containing a cocktail of several viral protein inhibitors that effectively clear chronic infection in >95 percent of patients (Feeney and Chung, 2014). These drugs can be classified into three groups: those that inhibit the HCV non-structural (NS) protein complex NS3/4A (protease inhibitors), those that block viral

NS5A activity (NS5A inhibitors), and those that prevent viral polymerase activity (NS5B inhibitors) (reviewed in (Feeney and Chung, 2014; Hayes and Chayama, 2014; Kohli et al., 2014)). Though levels of viral clearance in patients are now extremely high, there are many questions about the mechanisms of HCV infection that remain unanswered. Further research into the cell biology of HCV infection will yield important information both about general mechanisms of viral infection and host cell processes.

1.3.1 HCV viral particle composition and host cell entry

The HCV virion is composed of an outer lipid envelope layer surrounding the viral capsid, which houses the genomic material (Figure 1-1A). Interestingly, HCV particles collected from patent serum vary in composition and structure. Two predominant viral particle forms can be isolated by density gradient centrifugation of patient serum: one found in higher density fractions (1.17-1.25 g/mL) and one found in lower density fractions (1.06-1.15 g/mL)(Figure 1-1A)(Andre et al., 2002; Lindenbach et al., 2005; Miyamoto et al., 1992). Interestingly, in virus isolated from tissue culture cells, virions obtained from the lower density fractions had a higher specific infectivity than those isolated from higher density fractions (Lindenbach et al., 2005). Recent studies suggest that the relative levels of low-density and high-density virions produced by infected cells are influenced by a number of both viral and host factors. Characterization of the lower density viral particles revealed the incorporation of cellular components normally found in low-density lipoprotein (LDL) and very low-density lipoprotein (VLDL) particles (Owen et al., 2009). These observations, along with the lower buoyant density of viral particles, suggest that HCV can form a hybrid lipoviroparticle (LVP), which facilitates entry into hepatocytes and protects the virus from humoral immune responses (Figure 1-1A right). Though the composition of these particles has been well characterized, their overall architecture,

including the organization of viral glycoproteins and whether their association with serum lipoprotein particles is transient or represents a hybrid molecule, remains unclear (see section 1.3.4). Further study is needed to determine the morphology of LVPs as well as to determine the exact role of high-density and low-density particles in HCV entry and spread.

The viral nucleocapsid is composed of the viral RNA encapsulated by a multimeric core protein shell. Formation of the viral capsid involves oligomerization of the HCV core proteins through homotypic interactions between defined protein domains (Matsumoto et al., 1996). The interactions between core molecules are supported through the formation of disulphide bonds, which stabilize the capsid structure (Kushima et al., 2010). Core oligomers interacts with both the 5' and 3' untranslated regions (UTRs) of the viral RNA, as well as the viral E1 glycoprotein, which coordinates the packaging of the viral genome with the formation of the assembled viral particles (Nakai et al., 2006; Santolini et al., 1994; Yu et al., 2009). The HCV genome consists of a 9.6 kb positive-strand RNA molecule containing a 5'UTR, an open reading frame that codes for a ~3000 amino acid poly protein and a 3' UTR (Figure 1-2A). Both the 5' and 3' UTRs contain structural motifs that are critical for the regulation viral RNA translation and replication.

HCV viral particle entry into host cells is a complex multistep process involving several cell surface receptors (Figure 1-1B). The first entry receptor described for HCV, a tetraspanin family protein CD81, was identified through its capacity to bind the E2 HCV envelope glycoprotein (Cormier et al., 2004; Pileri et al., 1998). Subsequently, several other cellular proteins have been associated with HCV entry including glycosaminoglycans (GAGs), the low-density lipoprotein receptor (LDLR), and the scavenger receptor class B type 1 (SRB1) (Bartosch et al., 2003; Germi et al., 2002; Meuleman et al., 2008; Molina et al., 2007; Owen et al., 2009; Scarselli et al., 2002). Both *in vitro* and *in vivo* data indicate that the entry process involves viral particles binding sequentially to these surface receptors, which is initiated by the low affinity

binding to LDLR or GAGs follow by a higher affinity SR-B1 interaction. Interactions between viral particles and SRB1 are thought to rearrange the virion such that E2 can bind to CD81, which was demonstrated to have a post attachment function (Catanese et al., 2010; Zeisel et al., 2007). E2-CD81 binding initiates cell-signalling events, mediated by epidermal growth factor receptor (EGFR) and ephrin receptor A2 (EphA2), which recruit the tight junction protein claudin-1 (CLDN1) forming the HCV receptor complex (Evans et al., 2007; Lupberger et al., 2011). This complex interacts with occludin (OCLN) at tight junctions resulting in viral uptake into an endosome by clathrin-dependent endocytosis (Blanchard et al., 2006; Brazzoli et al., 2008; Ploss et al., 2009). Endosome acidification triggers a glycoprotein protein-dependent fusion event between the viral envelope and the endosomal membrane, releasing the viral capsid into the cytoplasm (Blanchard et al., 2006; Lavillette et al., 2007). More recently, the tetraspanin protein CD63 and transferrin receptor 1 have also been described as entry factors, though their role in viral entry is still uncertain (Martin and Uprichard, 2013; Park et al., 2013). Additionally, the inhibition of cellular uptake of lipids/cholesterols from bile identified Niemann Pick C1 like 1 (NPC1L1) as an entry receptor for HCV, though its exact function in viral entry has also not been described (Sainz et al., 2012). Essential functions for lipid and cholesterol receptors in viral entry further suggest an important role for cellular lipid metabolism and cholesterol uptake pathways in the HCV life cycle (see section 1.3.4).

Figure 1-1. **Hepatitis C virus: virions and entry**. **A**. Shows a representation of the HCV viral particles produced from infected cells. The left panel shows the hypothesized high-density viral particle depicting the lipid envelope layer, the viral glycoproteins (E1 and E2), and the nucleocapsid containing viral core protein and the viral genome. The right panel shows a hypothesized hybrid viral lipoviroparticle (VLP), which is thought to represent the low-density virions produced from infected cells. Here the viral nucleocapsid and envelope proteins are integrated into a LDL- or VLDL-like particle containing neutral lipids and surface apolipoproteins (namely ApoB and ApoE). **B**. The diagram depicts a representative model for the entry of HCV particles into host cells. HCV viral particles attach to the cell surface through initial associations with heparan sulphate proteoglycans (HSPGs), low-density-lipoprotein receptor (LDLR) and scavenger receptor class B member 1 (SRB1). These interactions lead to the formation of a stable complex between viral particles and CD81, which then, through EGFR signalling, mediates the recruitment of claudin-1. These virion receptor complexes are then recruited to tight junctions where they interact with occludin followed by clathrin-mediated endocytosis. Virion envelope fusion with the endosomal membrane is initiated by a pH dependent rearrangement in the viral envelope proteins, which facilitates release of the nucleocapsid into the cytoplasm. This figure was adapted from (Lindenbach and Rice, 2013).

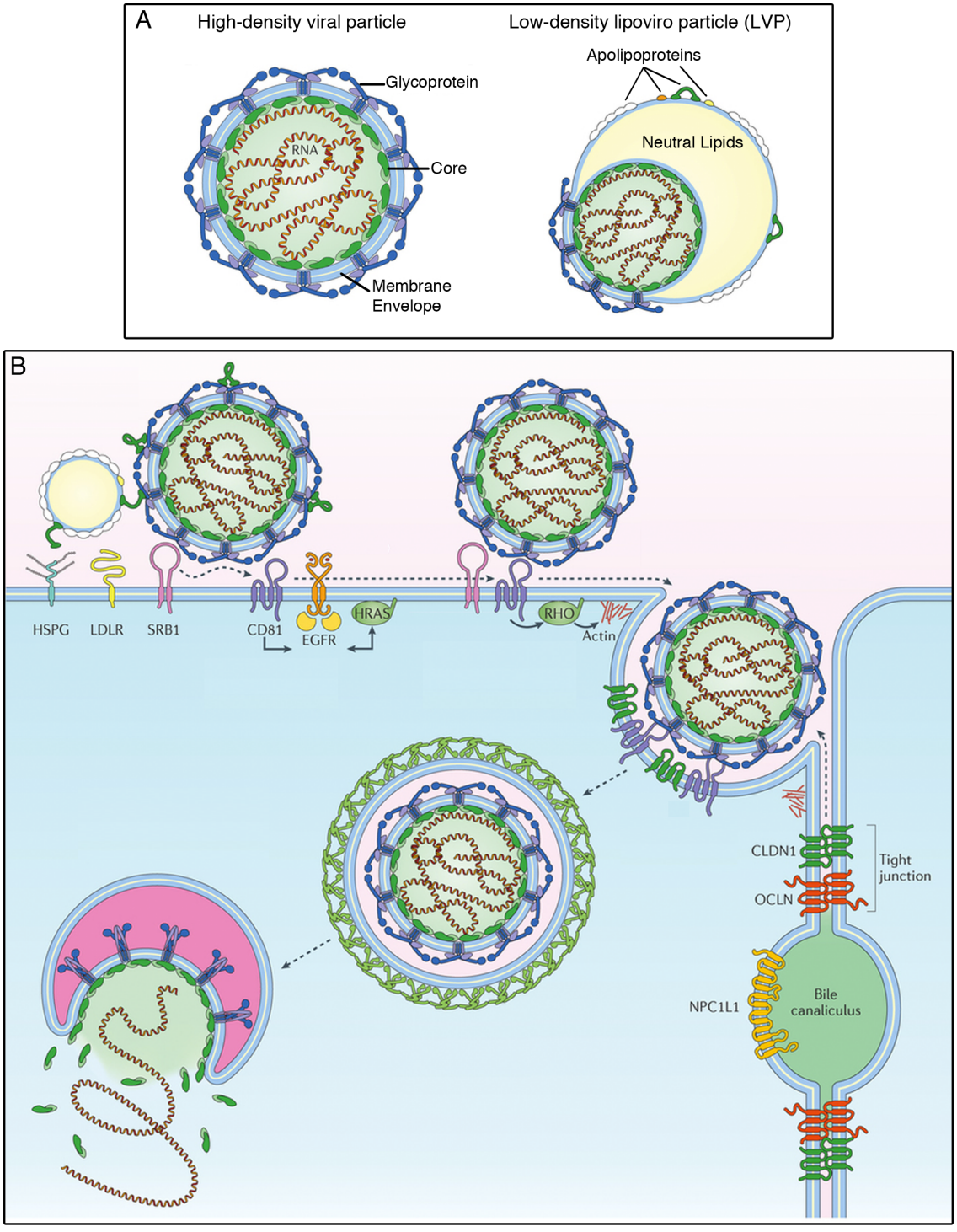

Figure 1-1. Hepatitis C virus: virions and entry

Figure 1-2. **Hepatitis C virus: replication and assembly**. **A**. The HCV genome is a positive-sense RNA molecule that contains an IRES element in its 5'UTR as well as stem loop structure in its 3' UTR, which are both required for the initiation of translation. The viral RNA is translated on the ER membrane to produce a poly-protein that is cleaved by both host proteases (white arrows) and viral proteases (black arrows) to form the mature forms of the ten viral proteins. **B**. Assembly and egress of viral particles is initiated by associations between viral proteins and cellular lipid droplets. This association is an intermediate step in the transfer of viral proteins and viral RNA from the replication complexes to viral assembly complexes. Assembly and egress involves both structural and non-structural viral proteins as well as cellular components of the VLDL export pathway. Panel D is adapted from (Lindenbach and Rice, 2013).

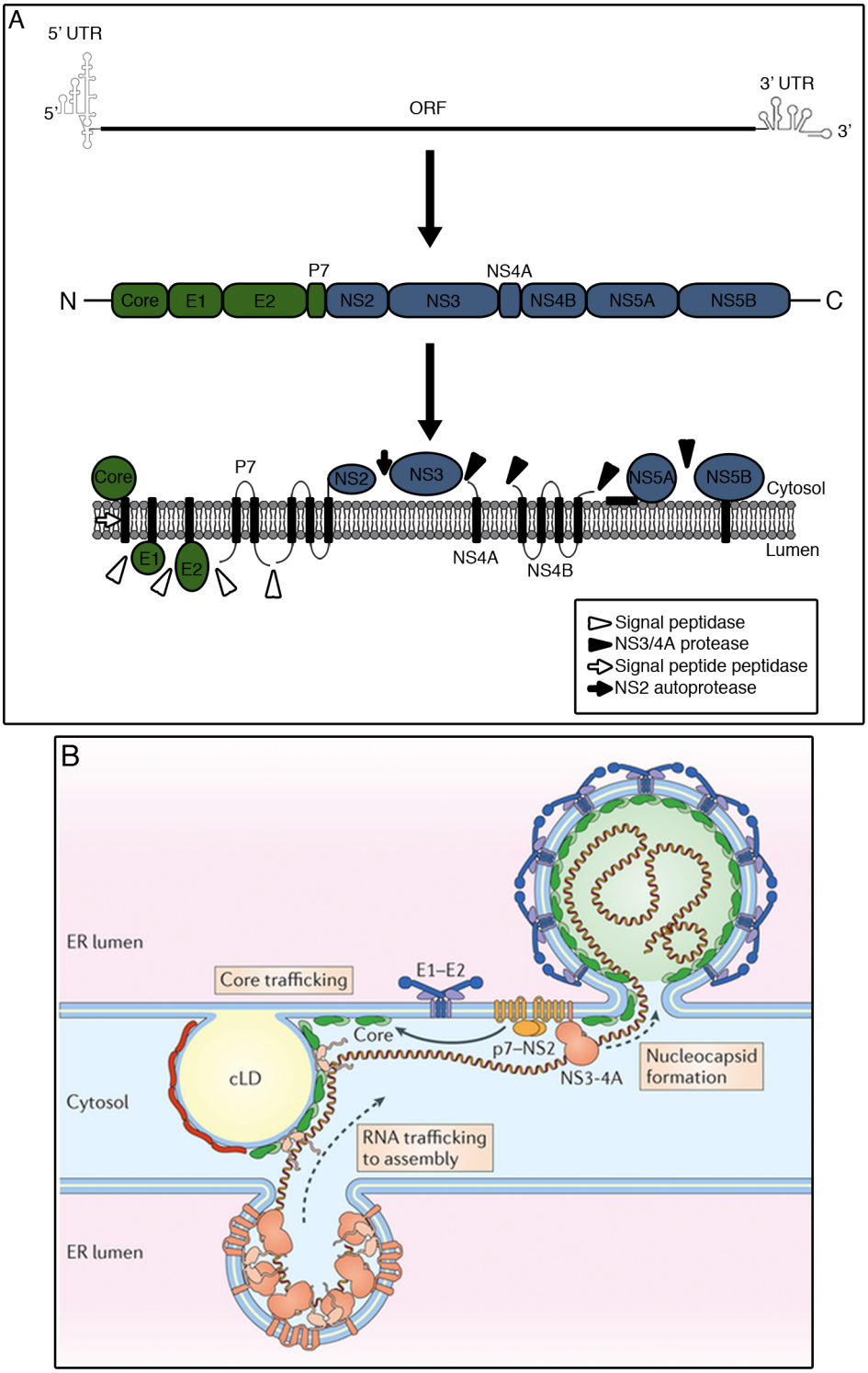

Figure 1-2. Hepatitis C virus: replication and assembly

1.3.2 Replication and assembly

Once released into the cytoplasm, the viral genome is directly translated into a long, 3006-3037 amino acid residue poly-protein. Instead of a 5' cap structure (namely the m7GpppN cap located at the 5' end of cellular mRNA transcripts), the 5'UTR of the viral genome contains an RNA regulatory element, termed the internal ribosome entry site (IRES), which is a structure common to many picornaviruses (reviewed in (Fraser and Doudna, 2007; Pineiro and Martinez-Salas, 2012). Translational initiation of most cellular mRNAs is facilitated by the recruitment of the (eIF)4F complex by the 5'cap, which then scans the mRNA molecule in a 5' to 3' direction until a start codon is found. In contrast, translation of many viral RNAs is initiated internally by IRES elements, which effectively allow for sustained viral protein production following the inhibition of normal translation initiation machinery induced by many viral infections (Figure 1-2A)(reviewed in (Niepmann, 2009)). In addition to the IRES element, the 5'UTR also contains two binding sites for microRNA-122 (miR-122), which is a cytoplasmic microRNA required for RNA translation and genome replication (Henke et al., 2008; Jopling et al., 2005). The 3'UTR of the viral genome includes a poly (U/C) tract followed by a X-loop region instead of a poly-A tail (Yanagi et al., 1999). This region has a translational enhancer function and has been demonstrated to associate with components of the IRES element (Romero-Lopez and Berzal-Herranz, 2009; Song et al., 2006). Association between the 5'UTR and 3'UTR leads to the formation of a 'kissing-loops' structure, which has a functional role in both RNA translation and replication (Friebe et al., 2005; Romero-Lopez and Berzal-Herranz, 2012; You and Rice, 2008).

The HCV poly-protein is co- and post-translationally cleaved by both host and viral factors to form the 10 individual viral proteins (Figure 1-2A). These proteins include three structural elements (core, E1, E2) and 7 non-structural proteins (p7, NS2, NS3, NS4A, NS4B, NS5A and NS5B). The C-terminal region of core contains the signal peptide, which targets the

nascent polyprotein to translocation sites at the ER membrane. Cellular signal peptidase is responsible for cleaving the poly-protein in the lumen of the ER to form the individual structural proteins (Figure 1-2A)(Hijikata et al., 1991). Additionally, the core protein is further processed by host cell signal peptide peptidase to produce the 'mature' form of the protein, which can associate with lipid droplets (LDs), an important initial step in viral assembly and egress (See section 1.3.4)(Miyanari et al., 2007). The two envelope glycoproteins, E1 and E2, are retained in the ER membrane where they are glycosylated and form heterodimers (Deleersnyder et al., 1997; Op De Beeck et al., 2004). The bulk of E1 or E2 is found in the ER lumen and their primary functions are in the assembly of viral particles and in facilitating viral particle entry. The p7 protein has ion-channel activity and is, therefore, included in a group of pore-forming viral proteins termed viroporins (reviewed in (Nieva et al., 2012)). Through associations with core and NS2, p7 is thought to coordinate links between viral replication and assembly (Boson et al., 2011; Jirasko et al., 2010a; Stapleford and Lindenbach, 2011). Additionally, p7 proteins can oligomerize to form an ion channel, which is thought to have a role in equilibrating pH gradients within specific secretory compartments thereby stabilizing viral particles during assembly and egress (OuYang et al., 2013; Wozniak et al., 2010). The region of the poly-protein containing the structural proteins, p7, and NS2 (core to NS2) is cleaved at the NS2-NS3 junction by the NS2/3 cysteine protease, spatially grouping p7 and NS2 with the structural proteins (Schregel et al., 2009). Though there is no evidence that NS2 is associated with assembled virions, it has an essential function late in viral assembly (Yi et al., 2009). The production of sustainable viral replicon cells that encode only the NS3 through NS5B region of the polyprotein also demonstrates that NS2 is not required for viral replication (Lohmann et al., 1999).

The remaining non-structural proteins, consisting of NS3 to NS5B, are liberated from the poly-protein by the NS3/4A protease complex (Steinkuhler et al., 1996). These proteins

constitute the minimal viral replicase, as demonstrated by the development of HCV replicon system, which has been used extensively to study HCV replication and develop viral inhibitors (Lohmann et al., 1999). Each of these non-structural proteins has a critical role in viral replication, functioning either in the formation of the viral replication complex or directly in viral replication. NS5B is the viral RNA-dependent RNA polymerase that forms a complex with NS3, NS4A, and NS5A to replicate the viral genome. In addition to its N-terminal protease domain, NS3 contains a C-terminal helicase domain that is required for both viral replication and assembly of virions. NS4A acts to target NS3 to the ER and also functions as a cofactor for both the helicase and protease activities of NS3 (Beran et al., 2009; Steinkuhler et al., 1996; Wolk et al., 2000). NS5A is a multi-domain phospho-protein required for both replication and assembly. Interactions between NS5A and the propyl-isomerase cyclophilin A (CypA) are required for the formation of NS5A dimers, which are essential for viral genome replication (Hanoulle et al., 2009). CypA associates with domain II and III of NS5A triggering cis/trans isomerization that stimulates NS5A RNA binding activity and dimerization (Foster et al., 2011; Verdegem et al., 2011; Yang et al., 2010). Indeed, several NS5A inhibitor drugs used to treat HCV patients act by disrupting either dimerization of NS5A or its RNA binding activity (Hayes and Chayama, 2014). NS4B is primarily involved in the reorganization of host cell membranes to form the viral replication and assembly compartments in the cytoplasm of infected cells. Similar to all positive-strand RNA viruses, HCV infection induces the formation of specialized membrane compartments for viral replication and assembly, a process that is achieved by the concerted actions of several non-structural proteins with a prominent role for NS4B.

Figure 1-3. Positive-strand RNA virus replication complexes. **A**. Uninfected or HCV infected Huh7.5 cells were grown for four days followed fixation in glutaraldehyde and embedding in epoxy resin. Thin sections of cells were cut and visualized by transmission electron microscopy. Boxes in the top panels represent the corresponding field of magnification in the bottom panel. In infected cell (right panels) the membranous web is seen as a collection of various membrane structures within cytoplasmic regions. **B-C**. EM tomography comparison between double membrane vesicle (DMV)(B) and inverted vesicle/spherule (InV/S)(C) type replication complexes as represented by HCV and DENV respectively. **B**. Three-dimensional reconstruction of the HCV membranous web from sequential thin sections visualized by EM. DMV represents double membrane vesicles and SMV represents single membrane vesicles. **C**. EM images (left) and 3-D reconstruction (right) of membrane alterations produced by DENV infection. These panels present a typical organization for InV type positive-strand RNA virus replication complexes. The arrow (left panel) and corresponding red vesicle (right panel) denote viral nucleocapsid in membrane structures near to the replication compartments. Panel B was adapted from (Romero-Brey et al., 2012) and panel was adapted from (Welsch et al., 2009).

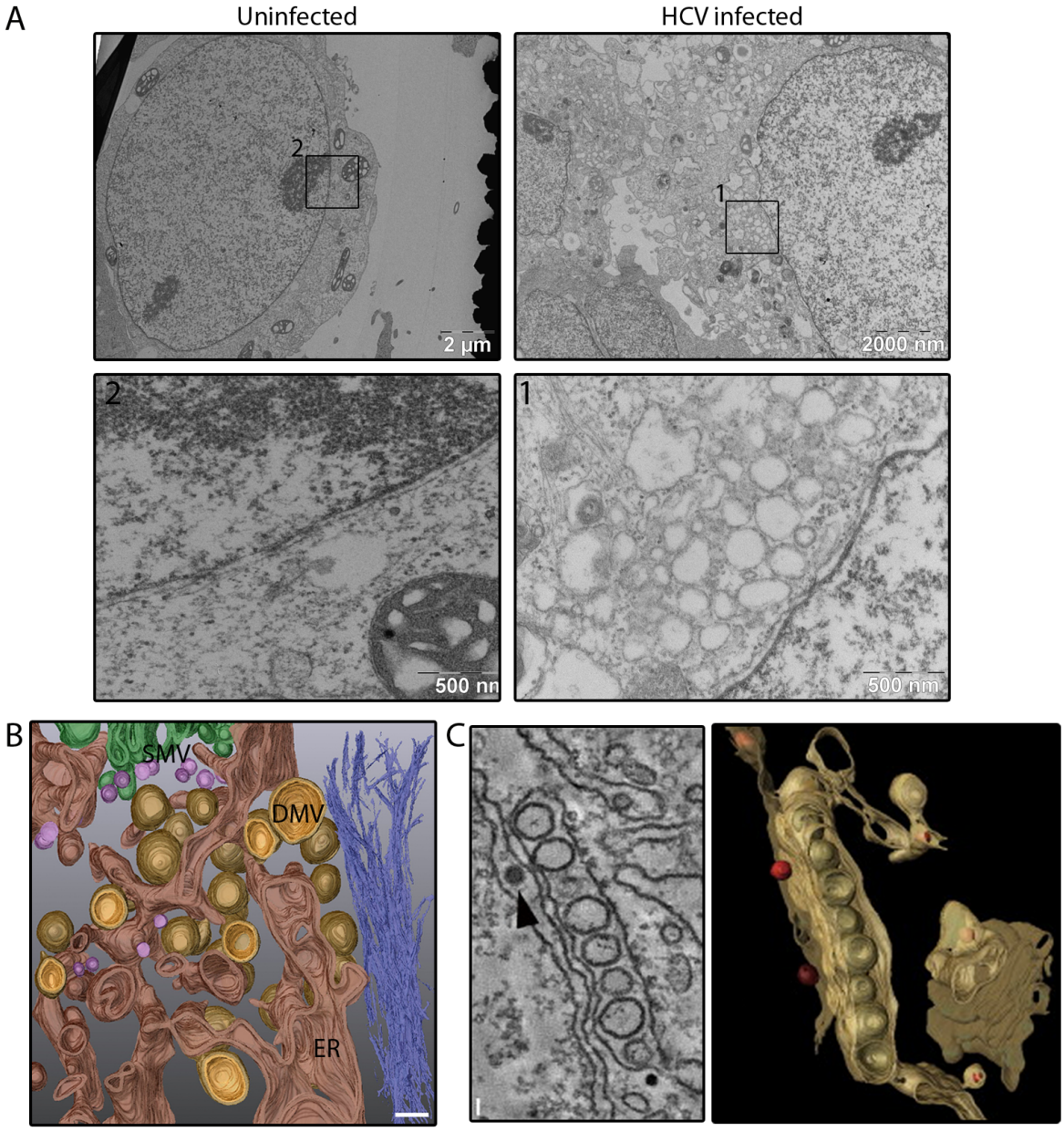

Figure 1-3. Positive-strand RNA virus replication complexes

1.3.3 The membranous web

Expression of HCV proteins induces the re-arrangement of cytoplasmic membranes to form cytoplasmic compartments that are conducive to viral replication and assembly. For many other viruses, these replication complexes appear as highly structured and well defined units. However, in the case of HCV infection, replication complexes appear as a disordered enrichment of various membrane structures within a region of the cytoplasm, giving rise to the term 'membranous web' (Egger et al., 2002; Gosert et al., 2003; Romero-Brey et al., 2012) (Figure 1-3A and 1-3B). Although the membranous web has been extensively studied, the precise structure, composition, and function of the membranous web are still not well defined. In general, these membrane rearrangements arise from the accumulation of ER membranes at sites of HCV infection. Single and double membrane vesicles (SMVs or DMVs) as well as multi-membrane vesicles (MMVs) have all been observed in HCV infected cells and cells containing a subgenomic replicon, but the specific roles of each of these structures are still largely unknown (Egger et al., 2002; Ferraris et al., 2010; Miyanari et al., 2007).

1.3.4.1 Functions of the membranous web

Though the precise structure and organization of the membranous web remains unclear, it is proposed to have a variety of functions in infected cells. The induction of cytoplasmic membrane compartments acts to concentrate factors needed for viral propagation into a specific region thereby significantly reducing the dependence on diffusion and increasing the efficiency of replication. The membranous web is also involved in the spatial coordination of viral processes, including RNA translation, genome replication, and viral particle assembly. In addition to increasing efficiency of specific viral processes, compartmentalization also promotes separation between different processes, thereby preventing interference. Indeed many viruses

produce replication factories that are assembled from ribosome-free membranes and form assembly complexes that are distinct from replication centers, suggesting an organized spatial separation between these processes (Fontana et al., 2010; Gillespie et al., 2010; Knoops et al., 2008; Welsch et al., 2009). Finally, the membranous web is also thought to provide a protective environment for viral replication and assembly forming a virus-induced organelle-like structure that is separate from the cytoplasm (Hsu et al., 2010; Miyanari et al., 2003). This membrane compartmentalization would effectively protect viral components from degradation by host proteases, and hide viral proteins and RNA molecules from cytoplasmic immune sensors (see Section 1.3.3.3 and Chapter 4)(den Boon et al., 2010; Overby and Weber, 2011).

1.3.3.2 Formation of the membranous web

Numerous viral proteins and host factors contribute to the formation of the membranous web. Studies examining the effects of individual HCV protein expression on host cell membrane topology found that each of the HCV replicase factors produce distinct membrane alterations. Ectopic expression of the NS3/4A complex caused the formation of large SMVs in the cytoplasm, whereas expression of NS4B induced the expression of smaller and more uniform SMVs (Egger et al., 2002; Romero-Brey et al., 2012). NS4B is a highly hydrophobic integral membrane protein that can form oligomers and has been shown to alter membrane integrity through the action of highly conserved C-terminal elements (Gouttenoire et al., 2010; Guillen et al., 2010; Palomares-Jerez et al., 2012; Paul et al., 2011). NS4B oligomers remodel intracellular membranes to aid in the formation of the membranous web, a process that is linked to active viral replication (Gouttenoire et al., 2010; Paul et al., 2011). Indeed, numerous mutations in NS4B alter the formation of DMVs and SMVs as well as inhibiting viral replication in infected cells (Paul et al., 2011). Additionally, active viral replication complexes can be isolated by pull-

down experiments using tagged versions of NS4B, further confirming its role in membranous web formation and viral replication (Paul et al., 2013). NS5A has also recently been found to facilitate the formation of DMVs, suggesting it has a role in the formation of the membranous web though the mechanisms of NS5A-mediated membrane rearrangements are still unclear (Romero-Brey et al., 2012). The current data suggest that the establishment of the complete membranous web is induced by a concerted effort from each of the viral proteins, which act directly on host cell membranes, or recruit host proteins to facilitate membrane rearrangement.

Numerous cellular factors are recruited to sites of HCV infection and have been associated with membrane alterations leading to membranous web formation. These host factors include components of the autophagy pathway, proteins involved in endocytosis or intracellular trafficking, and proteins involved in cellular lipid biogenesis. Similar to DMVs, autophagosomes are enclosed in a double lipid bilayer suggesting components of the autophagy pathway may function in membranous formation. Indeed, depletion of proteins critical for autophagosome formation inhibits HCV replication (Sir et al., 2012). However, while some studies suggest that components of the autophagy pathway are required for viral replication or viral egress, others indicate autophagy is required for translation of incoming viral RNA but dispensable for replication (Dreux et al., 2009; Sir et al., 2012; Tanida et al., 2009). Still others submit that autophagy is involved in immune responses and has an indirect effect on HCV infection (Ke and Chen, 2011). It may be that individual components of the autophagy pathway have divergent effects on HCV infection leading to the discrepancy in these reports.

Components of the intracellular membrane trafficking machinery, particularly proteins containing Bin-Amphiphysin-Rvs (BAR) domains, are also involved in HCV infection (Chao et al., 2012). For example, the BAR domain protein proline-serine-threonine phosphatase interacting protein 2 (PSTPIP2) has been observed to interact with NS4B and NS5A and has

been implicated in altering membranes required form membranous web formation (Chao et al., 2012). HCV-induced membrane compartments also rely on members of the phosphatidylinositol-4-kinase (PI4K) family, which produces phosphatidylinositol-4-phosphate (PI4P), for the production of functional replication complexes (Olmstead et al., 2012). HCV NS5A and NS5B both directly interact with PI4KIIIα leading to enrichment of PI4P in the membranous web (Bianco et al., 2012; Reiss et al., 2011). PI4KIIIα has also been identified as a HCV host dependency factor in numerous siRNA screens and specific depletion of PI4KIIIα causes a collapse of the membranous web into small, homogeneous vesicles that form tight clusters in the cytoplasm (Berger et al., 2009; Li et al., 2009; Reiss et al., 2011; Tai et al., 2009). Additionally, components of the sterol regulatory element-binding protein (SREBP) pathway are activated by HCV infection and are required for virion assembly (Waris et al., 2007). SREBP transcription factors, normally involved in activation of lipid biosynthesis, are thought to facilitate the production of specific lipids that promote the formation membranous web compartments (Olmstead et al., 2012). In general, the membranous web is derived from the combined function of several HCV proteins as well as host factors that contribute to the formation of the complex membrane network required for viral replication and assembly.

Several proteins required for endosomal trafficking or maturation have also been visualized in association with HCV replication complexes. The early endosome components, Rab-4 and Rab-5, are recruited to cytoplasmic compartments containing NS5A, a process facilitated by the C-terminal domain of NS4B (Aligo et al., 2009; Berger et al., 2009). Mutations in Rab-5 also leads to a dispersion of the membranous web thereby inhibiting viral replication (Stone et al., 2007). Additionally, NS5A interacts with TBC1D20, which normally functions in controlling endosomal trafficking and is required for HCV replication (Sklan et al., 2007). Moreover, siRNA screens have identified several ER-Golgi trafficking proteins (including

ARCN, COPA, COPB1, PI4KIIIα and VAP) as positive activators of infection, and inhibition of the coatomer COPI pathway decreases HCV replication efficiency (Berger et al., 2009; Li et al., 2014; Li et al., 2009). Viral reorganization of these protein and membrane networks leads to the aggregation of ER membranes and collapse of the Golgi and membrane trafficking pathways in infected cells. Together, these alterations in host cell membrane architecture and organization form an environment that is conducive to viral replication and maturation.

1.3.3.3 Architecture and topology of the membranous web

The membranous web has classically been characterized by the enrichment of various vesicle and membrane structures within a specific region of the cytoplasm (Figure 1-3). Recent electron tomography studies have suggested that DMVs are the predominant structure in HCV replication factories (Figure 1-3B)(Paul et al., 2013; Romero-Brey et al., 2012). These reports use various techniques to show that DMV formation occurs in association with ER membranes, and that the viral replication machinery is found in association with DMVs. Moreover, they show that isolated DMVs retain RNA replication activity suggesting these structures are the site of viral replication. However, current techniques lack sufficient resolution to determine whether viral replication occurs on the outer or inner surface of DMVs. Several groups have reported that viral proteins and RNA in isolated replication complexes are resistant to exogenously added protease or nucleases, indicating that RNA replication occurs in an environment that is segregated from the surrounding cytoplasm (Hsu et al., 2010; Miyanari et al., 2003; Paul et al., 2013; Quinkert et al., 2005). Interestingly, the majority of the DMVs (approximately 90%) appear closed from the surrounding cytoplasm. This morphology suggests that, if replication occurs on the interior surface of DMVs then there must be a transport mechanism to allow import of metabolites required for replication as well as export of viral RNA for translation or

virion assembly. Alternatively, in a model where replication occurs on the outer surface of DMV, a more complex architecture to the membranous web must exist to explain observation that viral RNA is protected from exogenously added nucleases. One group has suggested the RNA replication occurs on the interior surface of DMVs only while those structures are connected to the cytoplasm, and closed DMVs represent 'dead end' replication complexes (Paul and Bartenschlager, 2013). However, it is difficult to correlate such a model with efficient viral replication, as 90% of the observed replication complexes would be inactive (Romero-Brey et al., 2012). Additionally, the levels of negative-strand HCV RNA found in infected cells is relatively low, which would make the production of the observed amounts of viral protein and positive-strand RNA highly unlikely if the majority of replication complexes are inactive (Quinkert et al., 2005). Therefore, further research is required to determine the precise location of viral replication within membranous web (see chapters 3 and 4).

1.3.4 HCV associations with host cell lipids and their involvement in viral particle assembly

Association with host cell lipid metabolism pathways is integral to many viral infections. Early experiments in HCV infected cells demonstrated that the viral core protein associates with LDs, which are cytosolic lipid storage organelles composed of neutral lipids and cholesterol esters enclosed by a phospholipid monolayer (Figure 1-2B)(Barba et al., 1997). In depth analysis of this association revealed that cleavage of the signal peptide at the C-terminus of core by signal peptide peptidase leads to a relocalization of core from ER membranes to the surface of LDs, which are thought to be a storage site for core as well as providing a platform for the initial steps in viral assembly (Figure 1-2)(Boulant et al., 2005; Moradpour et al., 1996). Mutations in HCV core that prevent LD localization also inhibit viral assembly suggesting a prominent role for

cytosolic LDs in viral particle formation (Boulant et al., 2007; Miyanari et al., 2007; Shavinskaya et al., 2007). Interestingly, though usually localized predominantly to cytoplasmic compartments, several mutations in the C-terminal LD binding region of core lead to its nuclear accumulation (Cerutti et al., 2011). Additionally, mutations in the putative nuclear export signal (NES) sequence of core or general inhibition of nuclear export by leptomycin B also lead to an accumulation of core in the nucleus (Cerutti et al., 2011). Moreover, ectopic expression of HCV core leads to elevated levels of LDs in non-hepatic cells and causes steatosis in transgenic mice, suggesting that core has a significant role in regulating lipid metabolism (Barba et al., 1997; Moriya et al., 1997). Together these observations may suggest that, in addition to its direct role in viral assembly, core has a nuclear role in host cell gene regulation that facilitates viral replication and assembly and that this function of core may be regulated by the cellular levels of LDs.

Several host factors linked to viral assembly have been shown to mediate the trafficking of core to LDs. Depletion of diacylglycerol o-acyltransferase 1 (DGAT1), an enzyme involved in the synthesis of the triglycerides stored in LDs, leads to a decrease in LD trafficking of core and a subsequent decrease in virus production (Herker et al., 2010). Core trafficking is also regulated by cytosolic phospholipase A2 (cPLA2), an enzyme regulated by the mitogen-activated protein kinase (MAPK) pathway (Menzel et al., 2012). Inhibition of cPLA2 leads to a decrease in the association of core with LDs and inhibition of viral particle production, an effect that can be rescued by the exogenous addition of the enzymatic product of cPLA2, arachidonic acid (Menzel et al., 2012). The coordinated relocalization of core to LDs is thought serve as a preliminary step in the production of HCV particles, which is followed by the retrieval of core from LDs to form the viral capsids and assembled virions. Recently, studies using live cell imaging of fluorescently tagged core have provided insight into the dynamic nature of its LD association and retrieval for capsid assembly (Counihan et al., 2011). These studies show that

initial recruitment to LDs occurs rapidly in infected cells and is followed by a slow relocalization from LDs to motile puncta (Counihan et al., 2011). These puncta traffic on microtubules and are thought to represent viral particles undergoing secretion (Coller et al., 2012; Counihan et al., 2011).

The retrieval of core from LDs and the trafficking of viral RNA to assembly complexes in order to assemble viral particles are mediated by the combined function of all the HCV encoded non-structural proteins with the exception of NS4B. In addition to its essential function in viral replication, the C-terminal unstructured domain of NS5A (domain III) has been suggested to regulate the initiation of viral assembly by acting as a molecular switch between viral replication and assembly (Kim et al., 2011; Tellinghuisen et al., 2008). One of the first steps in the assembly of viral particles is the DGAT1-mediated association of NS5A with LD-bound core protein (Appel et al., 2008; Masaki et al., 2008; Miyanari et al., 2007). This relocalization of NS5A from replication complexes to LDs is mediated by the phosphorylation of specific serine residues in domain III of NS5A (Kim et al., 2011; Tellinghuisen et al., 2008). Indeed, mutations in these serine residues effectively blocks viral assembly, but not replication, indicating that phosphorylation of NS5A is an important step in assembly (Kim et al., 2011; Tellinghuisen et al., 2008). NS5A is also linked to later stages of viral assembly through interactions with ApoE (a component of the HCV LVP) and with annexin A2 (a trafficking protein required for viral assembly)(Backes et al., 2010; Benga et al., 2010; Evans et al., 2004). Association of NS2 with p7 is essential for the localization of NS2 to core bound LDs, which is thought to initiate the migration of core away from LDs to sites of viral nucleocapsid assembly (Figure 1-2B)(Gentzsch et al., 2013; Jirasko et al., 2010b; Popescu et al., 2011). The relocalization of core from LDs to assembly complexes also requires the NS2/p7 mediated recruitment of the NS3/4A enzyme complex to the surface of LDs prior to assembly (Figure 1-2B)(Counihan et al., 2011). These

observations suggest a prominent role for the NS2/p7 complexes in organizing and coordinating the steps of viral assembly. Interestingly, mutations that affect NS3 helicase activity also alter later stages of viral assembly suggesting that the NS3 helicase may facilitate RNA packaging during nucleocapsid formation (Beran et al., 2009; Phan et al., 2011; Pietschmann et al., 2009).

The formation of mature HCV particles is closely linked to lipoprotein secretion in hepatocytes. As stated above, multiple HCV particle variants can be isolated from the serum of both infected patients and tissue culture cells. A number of different observations indicate that the lower-density viral particles represent hybrid LVPs that mature and are secreted through a similar pathway as VLDL particles (Figure 1-1A right). First, inhibitors of the lipid transfer protein, microsomal triglyceride transfer protein (MTP) blocks HCV particle production (Gastaminza et al., 2008; Jiang and Luo, 2009; Nahmias et al., 2008). MTP is normally involved in neutral lipid transfer to the ER lumen, an important step in the production of VLDL particles (Huang et al., 2007). Additionally, HCV particles associate with apolipoproteins normally found in VLDL particles, but there remains some controversy over which components directly influence egress and assembly. Some groups report that the apolipoprotein, ApoB, which is critical for VLDL assembly, is not required for HCV particle production even though this protein has been found associated with virus in patient serum (Coller et al., 2012; Jiang and Luo, 2009). Instead, they report that the smaller apolipoprotein, ApoE, is required for trafficking of nascent viral particles and viral egress (Da Costa et al., 2012; Jiang and Luo, 2009; Long et al., 2011; Merz et al., 2011). Though not normally associated with VLDL export, ApoE has been suggested to act as an escape pathway for VLDL export in the absence of ApoB (Holwell et al., 1999). Interestingly, Huh7.5 cells (immortalized human hepatocytes used to propagate HCV) grown in bovine serum do not contain significant levels of ApoB and seem to be deficient in VLDL particle export (Blight et al., 2002; Steenbergen et al., 2013). Studies demonstrating that

HCV assembly and egress occurs in an ApoE-dependent and ApoB-independent manner were derived from experiments done in Huh7.5 cells grown in bovine serum suggesting that these observations may not accurately demonstrate *in vivo* conditions. These cells also produce significantly less low-density viral particles compared to virus found in patient serum (Andre et al., 2002; Lindenbach et al., 2005; Miyamoto et al., 1992). Alternatively, studies using cells propagated in human serum instead of bovine serum, which alters Huh7.5 cells to resemble primary liver cells, found that both ApoB and ApoE associate with VLPs in a step prior to cellular egress (Steenbergen et al., 2013). This study also reported increased ApoB levels in cells grown in human serum compared to bovine serum, and the authors suggest that propagation in human serum restores normal VLDL export in Huh7.5 cells. Together, these data strongly suggest that the VLDL export pathway is involved in HCV assembly and egress, and they also indicate that there might be multiple pathways for viral export that depend on lipid export pathway activity in host cells.

1.3.5 Replication factories induced by other positive-strand RNA viruses

Positive-strand RNA viruses manipulate the arrangement of cellular membranes in a variety of ways. Though there are many differences in the composition of viral particles and in genome organization, the three-dimensional architecture of replication complexes appears to have one of two general arrangements: those that produce DMVs and those that form invaginated vesicles or spherules (InV/S). Included in the first category are poliovirus (PV), coxsackievirus B3 (CVB3), severe acute respiratory syndrome coronavirus (SARS-CoV), equine arterivirus (EVA) and HCV (Belov et al., 2012; Knoops et al., 2012; Knoops et al., 2008; Limpens et al., 2011; Romero-Brey et al., 2012). The formation and architecture of this class of replication complex is described in detail above using HCV as an example. The formation of

InV/S type viral replication factories has been observed in cells infected with: alphaviruses (including Semliki Forrest virus (SFV) and Sindbis virus), flock-house virus (FHV), rubella virus (RUBV), DENV, and West Nile virus (WNV) (Fontana et al., 2010; Frolova et al., 2010; Gillespie et al., 2010; Kopek et al., 2007; Kujala et al., 2001; Welsch et al., 2009). In *flavivirus* infection, exemplified by DENV and WNV, membranes incorporated into replication complexes are most likely derived from the ER (Berger et al., 2009). In the case of DENV, studies using high-resolution electron tomography analysis have shown that viral infection induces the production of vesicular invaginations into the rough ER membrane (Figure 1-3C). These vesicles, measuring approximately 90 nm in diameter, are connected to the cytoplasm by a ~11 nm channel (Welsch et al., 2009). Viral RNA and replication proteins localize to the interior of these InVs indicating that viral genome replication occurs within these structures (Welsch et al., 2009). Interestingly, ribosomal proteins were excluded for InVs suggesting that viral RNA must exit the replication complex in order to be translated (Welsch et al., 2009). Assembled virus budding from the ER can be observed in close proximity to replication compartments demonstrating a spatial connection between viral replication and assembly complexes (Welsch et al., 2009). A similar morphology and organization of viral replication factories has also been reported for WNV (Gillespie et al., 2010). Comparisons between the membrane alterations induced by different positive-strand RNA viruses can be used to highlight morphological and functional differences as well as similarities of viral replication compartments. The significant number of parallels that can be drawn between different viral infections may point toward common pathways that could be targeted by antiviral therapeutics.

1.4 Interferon-Mediated Immune Responses

Host cell innate immune responses require the activation of a critical group of proteins bearing anti-pathogen activity. Included in this group of proteins are the interferons (IFNs), which were originally defined as molecules that 'interfere' with viral infection (Isaacs and Lindenmann, 1957). IFNs are cytokines, which interact with cell surface receptors to initiate innate immune responses. These cytokines are classified into type I, type II and type III IFNs based on the cell surface receptor binding. Type I IFNs, including one IFNβ and numerous -α molecules, bind a common cell-surface receptor, expressed by all cell types (reviewed in (Platanias, 2005). Association of either IFNα or IFNβ with the surface receptor leads to potent antiviral activity in cells (Isaacs and Lindenmann, 1957; Muller et al., 1994). In contrast to type I IFNs, IFNγ is the only type-II IFN in humans that is primarily involved in regulating inflammatory responses. IFNγ binds the type II IFN receptor, which is expressed on immune cells such as macrophages and dendritic cells, and has little homology in structure or function to type I IFNs (Bach et al., 1997; Pestka et al., 1997). Type III IFNs represent a recently classified group of cytokines having antiviral activity that includes IFNλ-1, IFNλ-2, and IFNλ-3/4 also called interleukin-29 (IL-29), IL-28A, and IL-28B (Kotenko et al., 2003). IFNλs are distinct from type I or type II IFNs and their specific role in antiviral responses is still unclear (Kotenko et al., 2003). Normal initiation of IFN responses is trigger through the recognition of common pathogenic markers by host cell immune receptors, leading to activation of immune effector molecules to fight infectious agents.

1.4.1 Pattern recognition receptors

One of the key pathways for activation of IFN-mediated immune responses is through recognition of recurring molecular patterns found in pathogens, termed pathogen-associated molecular patterns (PAMPs), by cellular pattern recognition receptors (PRRs). The discovery of PRRs transformed our perception of innate immune responses, revealing how multiple and diverse infectious agents can be identified by a limited number of innate immune receptors (Janeway, 1989). These PRRs predominantly fall into one of two different groups; signalling PRRs and endocytic PRRs. Endocytic PRRs, found on phagocytes, mediate attachment and phagocytosis of microorganisms without relaying intracellular signals. This process is important for the activation phagocytic cells and the stimulation of a type II IFN response. Signalling PRRs, which included toll-like receptors (TLRs), NOD-like receptors, and RIG-I-like receptors (RLRs), propagate immune activation upon ligand recognition through the initiation of intracellular signalling cascades. In virus-infected cells, recognition of PAMPs, including viral DNA, dsRNA, single ssRNA, and polyuridine signatures, is accomplished primarily by either TLRs or RLRs (Figure 1-4).

1.4.1.1 Toll-like receptors

TLRs are membrane bound receptors that recognize PAMPs by means of leucine-rich repeat domains found in the extracellular space or within intracellular vesicles. In humans, ten distinct TLRs have been identified, the majority of which are found on the cell surface and recognize extracellular PAMPs. Additionally, a subset of TLRs, including TLR3, TLR7, TLR8, and TLR9 recognize ligands in intracellular compartments such as endosomes. These intracellular TLRs are critical for the detection of viral PAMPs, having a shared ligand affinity for nucleic acids, including dsRNA (TLR3), ssRNA (TLR7 in mice and TLR8 in humans), and

CpG DNA motifs (TLR9) (Figure 1-4A)(Alexopoulou et al., 2001; Diebold et al., 2004; Heil et al., 2004; Hemmi et al., 2000; Lund et al., 2004). Ligand recognition by TLRs leads to activation of signalling through a common cytoplasmic toll-interleukin-1 receptor (TIR) domain (Akira and Takeda, 2004; Janeway and Medzhitov, 2002). TIR domains signal through recruitment of the adaptor proteins including MyD88, TRIF (TICAM-1), TRAM, and TIRAP (Mal), leading to a signalling cascade the results in the activation of inflammatory and antimicrobial genes (Figure 1-4A and reviewed in (Akira and Takeda, 2004; O'Neill et al., 2003).

Its recognition of dsRNA makes TLR3 a key receptor for detection of viral infections in cells. Unlike other TLRs, which universally signal through the MyD88 pathway, TLR3 signals primarily through activation of TRIF in a MyD88-independent pathway (Hoebe et al., 2003; Oshiumi et al., 2003; Yamamoto et al., 2003; Yamamoto et al., 2002). Ligand recognition by TLR3 activates TIRF, which recruits the cellular kinases TBK and IKK. Upon stimulation, these kinases activate transcription factors including IRF3, IRF7, and NFκB through specific phosphorylation events (Fitzgerald et al., 2003). Phosphorylation of IRF3 and IRF7 leads to homodimer or heterodimer formation, allowing the molecules to translocate into the nucleus and interact with the co-activators CBP (cyclic-AMP-responsive-element-binding protein (CREB)-binding protein) or p300 to form a holocomplex (Lin et al., 1998; Sato et al., 1998; Weaver et al., 1998; Yoneyama et al., 1998). This holocomplex acts as a transcriptional activator for the production of several immune effector molecules, the most prominent of which are the type I IFNs. Active IKK also phosphorylates the NFκB inhibitor I-κB, which triggers the release and activation the NFκB transcription factor complex stimulating production of proinflammatory and antiviral genes (Figure 1-4)(Karin and Ben-Neriah, 2000; Li and Verma, 2002). Signalling through the TRIF specifically activates IRF-3 leading to IFNβ production, a

key antiviral pathway, which is another reason TLR-3 plays a significant role in antiviral immune activation.

1.4.1.2 RIG-I-Like receptors

RLRs, including MDA5, RIG-I and LGP2 are cytosolic proteins that recognize specific non-self molecular structures within cells. Most notably, RLRs are essential for the recognition of viral RNA molecules within the cytoplasm of infected cells (Figure 1-4B). RLRs contain a C-terminal DExD/H-box helicase domain and, with the exception of LGP2, two N-terminal caspase-recruitment domains (CARDs)(Yoneyama et al., 2004). Both RIG-I and MDA5 bind viral dsRNA through the helicase domain; RIG-I preferentially binding to short (<300 bp) dsRNAs that have blunt ends and a 5' triphosphate (5'-ppp) moiety and MDA5 preferentially associating internally to long dsRNA (>1,000 bp) with no end specificity (Hornung et al., 2006; Kato et al., 2006; Pichlmair et al., 2006). In the absence of ligand, the RIG-I CARD domains remain in an autorepressed state, which sterically prevents interactions with other card domains, effectively inhibiting activation of downstream signalling molecules. Upon ligand recognition, RIG-I undergoes significant conformational rearrangement leading to filament formation and activation of mitochondrial antiviral signalling protein (MAVS)(Jiang et al., 2011; Kowalinski et al., 2011). Unlike RIG-I, the CARD domains of MDA5 are not repressed in the absence of ligand (Berke and Modis, 2012). Rather, the proximity of multiple MDA5 proteins binding to a single dsRNA molecule leads to oligomerization of CARD domains forming filaments that in turn lead to MAVS activation. Contrary to RIG-I andMDA5, LGP2 primarily functions to regulate rather than stimulate the activation of immune signalling cascades (Saito et al., 2007; Yoneyama et al., 2005).

The oligomerization of RIG-I or MDA5 into filaments along RNA molecules leads to a tetrameric structure that serves as a platform for MAVS recruitment on mitochondrial or peroxisomal membranes (Peisley et al., 2014). These structures have been proposed to facilitate the assembly of self-propagating MAVS polymers, which in turn lead to downstream RLR signalling (Hou et al., 2011). This self-propagation of activated polymers demonstrates a prion-like mechanism for MAVS activation and signalling (Peisley et al., 2014; Xu et al., 2014). MAVS activation leads to signalling through the cytosolic protein kinases IKK and TBK resulting in activation of NFkB, IRF7, and IRF3 transcription factors (Figure 1-4B)(Yoneyama et al., 2004). Active NFkB, IRF7 and IRF3 are translocated into the nucleus where they induce expression of type I IFNs and other inflammatory or antimicrobial genes.

Figure 1-4. **Innate immune response signalling pathways and their evasion by HCV**. Pattern recognition receptors, either toll-like receptors (TLRs)(**A**) or RIGI-like receptors (RLRs)(**B**), recognize viral PAMPs, which activate signalling cascades. These signalling cascades lead to the activation of transcription factors, including IRF-3, IFR-7 and NFκB, through specific phosphorylation events. Activated transcription factors are then translocated into the nucleus where they stimulate the production of IFNs and proinflammatory genes. Once produced, IFNs are secreted from cells where they can act on neighbouring cells to stimulate immune responses by interacting with IFN receptor subunits found on the cell surface. Once bound to IFN, the receptors activate JAK kinases, which initiates immune signalling cascade leading to the dimerization and nuclear localization of STAT transcription factors. Once in the nucleus STAT homo or hetero dimers interact with specific gene promoter elements to activate transcription and propagate immune response. HCV proteins inhibit immune signalling by blocking key steps in these signalling pathways (shown in red). The HCV NS3/4A protease inhibits immune signalling by cleaving and inactivating TRIF and MAVS. NS5A binds to and inhibits activation of MyD88 as well as stimulating the production of PP2A, which blocks STAT activation. HCV core protein also inhibits STAT signalling by stimulating production of the JAK inhibitors SOCS1 and SOCS3.

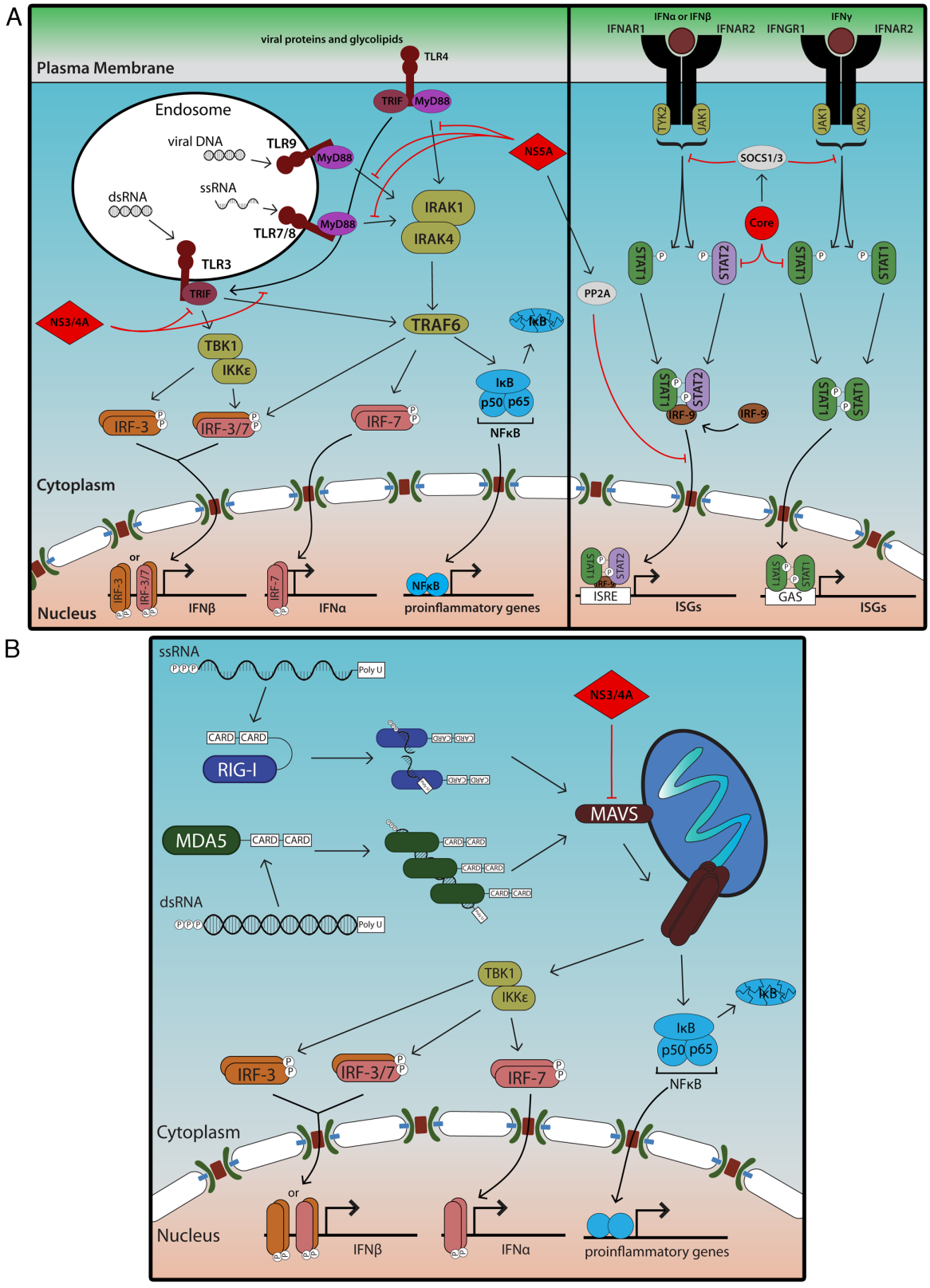

Figure 1-4. Innate immune response signalling pathways and their evasion by HCV

1.4.2 Interferon signalling and response

IFNs typically initiate immune activation through interaction with heterodimeric cell surface receptors (Figure 1-4A right). For type I IFNs, the receptor subunits are IFNAR1 and IFNAR2 where as IFNG1 and IFNG2 are receptors recognized by type II IFNs. Each of these receptor subunits interact with members of the Janus activated kinase (JAK) family, which are required for the initiation of downstream signalling (Muller et al., 1993; Velazquez et al., 1992; Watling et al., 1993). IFN receptor subunits bind selectively to a specific JAK protein leading to production of diverse downstream effects depending on which receptors are activated. Binding of IFN molecules to their respective receptor subunits stimulates the activation of JAK kinases and the subsequent phosphorylation of signal transducer and activator of transcription (STAT) proteins (Darnell et al., 1994; Platanias, 2005; Schindler et al., 1992; Silvennoinen et al., 1993). Classical STAT activation involves tyrosine phosphorylation, which drives the formation of homo or hetero dimers between STATs, mediating their translocation to the nucleus and the subsequent transcriptional activation of interferon-stimulated genes (ISG) (Figure 1-4A)(reviewed in (Platanias, 2005)).

Six different STAT proteins, STAT1-STAT6, have been identified as transcriptional activators in the IFN signalling pathway. A prominent transcriptional activation complex induced by type I IFN stimulation involves the association of STAT1-STAT2 heterodimers with IRF9 to form the ISG factor 3 (ISGF3) transcriptional activation complex (Darnell, 1997; Platanias, 2005). This complex interacts specifically with IFN-stimulated response elements (ISREs) that are present in the promoters of certain ISGs. Alternatively, STAT1 homodimers are the most prominent transcription factors induced by IFNγ, which recognize IFNγ-activated site (GAS) elements present in gene promoters (Darnell, 1997; Platanias, 2005). ISG promoters can contain only ISREs, only GAS elements or, in some cases, a grouping of both elements.

Combinations of different STAT-binding elements are likely required for optimal expression of specific genes leading to the documented complexity of ISG transcriptional activation. Other mechanisms leading to the diverse range in ISGs activation profiles include: cooperation with other transcription factors, post translational modification of STATs, and cell specific expression of various signalling molecules. For example, serine phosphorylation at position 727 (Ser727) of STAT1 and STAT3 leads to the recruitment of co-activators, including p300, CBP (cAMP-responsive-element-binding protein (CREB)-binding protein), and minichromosome maintenance deficient 5 (MCM5) (Bhattacharya et al., 1996; DaFonseca et al., 2001; Varinou et al., 2003; Zhang et al., 1996; Zhang et al., 1998). These proteins are involved in chromatin remodelling which is required for proper IFN-mediated transcriptional activation (DaFonseca et al., 2001; Hebbes et al., 1988; Zhang et al., 1998). Other chromatin remodelling enzymes, including histone acetyl-transferases (HATs) and histone deacetylases (HDACs) are also linked to the IFN response and play a role in either enhancing or regulating the transcriptional activation of specific gene loci (Chang et al., 2004; Nusinzon and Horvath, 2003; Sakamoto et al., 2004). Additionally, IRF proteins, which are up regulated by IFN stimulation, associate with regions that overlap with IRES and GAS elements enhancing the IFN response (Tamura et al., 2008). Importantly, IRFs, STATs, and ISGF3 bind simultaneously to many ISGs to form cooperative promoter complexes. Various combinations of these factors as well as numerous epigenetic factors generate the varied effects of IFN stimulation in different cell types and in different environments (Qiao et al., 2013).

1.4.3 Regulation of the interferon pathway

IFN responses are fine-tuned by both amplifying and regulating signals, which allow for effective anti-microbial or anti-tumour responses while limiting toxic side effects (reviewed in

(Ivashkiv and Donlin, 2014)). The signalling factors involved in type I IFN activation are constitutively expressed which allows for rapid immune activation in response to pathogens. However, the speed with which this pathway can be activated to combat infections also creates the potential for improper activation leading to toxic effects. Therefore, several mechanisms are in place to suppress or prevent basal activation of the IFN pathway. These include RNA polymerase pausing signals often found in genes association with IFN pathways and expression of microRNAs that inhibit translation of the corresponding transcripts (Gilchrist et al., 2012; Gracias et al., 2013; Lu et al., 2010; Papadopoulou et al., 2012). Additionally, several negative feedback loops exist to regulate the levels of immune activation and to eliminate signalling once it is no longer necessary. Included in the list of gene products elevated following IFN stimulation are the suppressor of cytokine signalling (SOCS) proteins and ubiquitin carboxy-terminal hydrolase 18 (USP18) (Sarasin-Filipowicz et al., 2009; Yoshimura et al., 2007). SOCS proteins reduce JAK activity and compete for STAT binding sites on IFNAR2 leading to an inhibition of IFN signalling. USP18 displaces JAK from IFNAR2, inhibiting receptor-mediated signalling (Sarasin-Filipowicz et al., 2009). Additionally, IFN signalling is regulated by the internalization or inhibition of IFNAR to limit IFN recognition on the cell surface. In some cases, IFNAR inhibition is initiated by phosphorylation of IFNAR causing internalization and degradation, while in others recruitment of phosphatases to IFNAR suppresses activation of the JAK-STAT signalling pathway (Du et al., 2005; Liu et al., 2009; Wang et al., 2010). IFNAR internalization can be stimulated by overexpression of the ISGs interleukin 1 (IL-1) and TLRs, which acts as another negative feedback loop for IFN signalling (Bhattacharya et al., 2013; de Weerd and Nguyen, 2012; Fuchs, 2013; Huangfu et al., 2012). Type 1 IFN activation is also controlled by specific miRNAs, such as miR-146a and miR-155, which have been shown to regulate JAK/STAT activation in different cell types (Gracias et al., 2013; Lu et al., 2010). Each

of the processes described above can act as negative feedback loops to fine tune and regulate immune responses to produce a precise immune response for a given pathogen. Moreover, dysfunction in one or more of these regulatory pathways often results in chronic inflammatory diseases. This is frequently exploited by tumour cells and intracellular pathogens, which inhibit regulatory pathways to suppress ISG stimulation and avoid the host immune response (Fuchs, 2013; Liu et al., 2009).

The activation of IFN-mediated transcription programs can also be regulated by controlling the levels or post-translational modification state of specific STATs proteins. Changes in the relative protein amounts of different STATs can significantly alter the downstream ISG activation profile (Murray, 2007). For instance, STAT1 is linked to the activation of pro-inflammatory genes while STAT3 activated genes suppress inflammatory responses (Ho and Ivashkiv, 2006). Regulation of the relative levels of STAT1 and STAT3 effectively controls the activation of specific genes upon IFN stimulation. Post-translational modification of STATs, including specific phosphorylation sites or modification with the small-ubiquitin like modifier (SUMO) can also suppress STAT activation or lead to STAT protein degradation (Rogers et al., 2003; Ungureanu et al., 2005). Interestingly, SUMO modification also suppresses the activation of several IRF signalling molecules and NFkB, suggesting a general regulatory role of the sumoylation pathway in immune responses (see section 1.7.1 and chapter 5)(Kim et al., 2008; Kubota et al., 2008; Mabb and Miyamoto, 2007; Nakagawa and Yokosawa, 2002; Scognamiglio et al., 2008). Protein inhibitor of activated STAT1 (PIAS1) is a SUMO modification enzyme that suppresses ISG activation by inhibiting interactions between STAT1 and DNA (Shuai and Liu, 2005; Tahk et al., 2007). However, this function of PIAS1 appears to be independent of its SUMO ligase activity (Liu et al., 2004). In general, activation of the proper

IFN-mediated immune response to combat specific pathogens relies on an intricate combination of both positive and negative effector proteins.

1.4.4 Treatment of diseases with IFN

Over the last 40 years, IFN has been used to treat a diverse range of human infections and diseases. The antiviral activity originally ascribed to IFNs stimulated research into the clinical application of these molecules. Original clinical studies demonstrated that type I IFN treatment had antiviral activity in patients with chronic hepatitis B virus infections (Greenberg et al., 1976). These findings eventually led to the adoption of IFNα therapy as a widely used treatment for patients with chronic hepatitis B virus infection. Even before the discovery of HCV in 1989, preliminary studies also showed that recombinant type I IFN therapy increased positive outcomes in patients with non-A, non-B hepatitis (Hoofnagle et al., 1986). However, increased surveillance of HCV infection revealed the efficacy IFN monotherapy to be relatively low, with only 15-20% of patients achieving a sustained virological response (SVR)(Poynard et al., 1995). Moreover, prolonged IFN treatment is associated with an abundance of debilitating side effects including: asthenia, neutropenia, myalgia, headache, an influenza-like syndrome, thrombocytopenia and depression (Poynard et al., 1995). These toxic side effects coupled with the low efficiency of type I IFN therapy stimulated extensive research into understating viral and host responses to IFN with the aim of uncovering new treatments for chronic HCV. In the early 1990s several studies demonstrated that the nucleoside ribavirin increased patient immune response to chronic HCV and in 1998 the combination of IFNα and ribavirin became the standard treatment for chronic HCV; increasing prevalence of SVR to ~38% (McHutchison et al., 1998). In 2001, the introduction of pegIFNα in combination with ribavirin increased SVR rates to ~50% (Fried et al., 2002; Manns et al., 2001). PegIFNα, produced by the covalent

attachment of a polyethylene glycol (peg) molecule to IFNα, has a significantly increased half-life of in the blood stream compared to recombinant IFNα, which is widely assumed to increase immune activation by providing constant IFNAR stimulation over a longer period of time. This combination therapy became the standard of care for chronic HCV until the recent discovery and clinical approval of direct-acting viral protein inhibitors in the last 5 years. Though these compounds were originally used in parallel with pegIFNα, recent studies demonstrate that a combination of viral protein inhibitors is effective in ~95% of chronic HCV patients without the requirement for IFN (Feeney and Chung, 2014). Interestingly, several recent studies have demonstrated that type III IFN, specifically pegIFNλ, has similar antiviral activity as pegIFNα with less severe side effects (Muir et al., 2010; Ramos, 2010; Witte et al., 2009). These results may initiate a permanent shift away from the use of highly toxic IFNα for the treatment of specific diseases.

In addition to treatment of viral infection, IFNα therapy has also been used to treat oncological diseases including myeloproliferative disorders, melanomas and renal cell carcinoma (reviewed in (Bracarda et al., 2010)). Numerous clinical studies have demonstrated that IFNα treatment improves the outcome of a significant number of patients suffering from these diseases. However, the complexity and broad spectrum of the systemic IFNα response in hosts make it difficult to determine the mechanisms of its anti-tumour activity. IFNα has been proposed to directly affect tumour cells by reducing proliferation, stimulating differentiation, altering the expression of surface receptors, and inducing apoptosis in tumour cells. Additionally, IFNα treatment has indirect affects against cancer cells through the production inflammatory responses leading to activation of immune cells that have anti-tumour activity. Despite the experimental effectiveness of type I IFN therapies against various cancers, concerns about the severity of its side effects compared to its clinical activity and the ability of cancers to evolve

IFN resistance undermines its widespread use as an oncological treatment. In general, type I IFN therapy has had a major role in the treatment of human diseases over the last 40 years. However, as drug discovery techniques improve and more targeted therapies are introduced, the standard IFN therapy for the treatment of human diseases will continue to diminish. Rather, the use of IFN treatments may have a more directed role in the treatment of diseases only in specific cases.

1.4.5 IFN response in viral infections

IFN stimulation leads to the transcriptional activation of hundreds of genes, which mediate various biological effects including having roles in antiviral, antitumor, and immunomodulatory responses (Der et al., 1998). Of these, the most characterized function of IFN induction is its role in combating viral infections within a host. However, the induction pattern of ISGs is highly variable between different cell types and different viral infections making elucidation of the exact mechanisms of action difficult. Moreover, for most ISG products, little is known about their specific modes of action or their antiviral potential. Though the complexity of IFN induced responses makes elucidation of specific ISG function difficult, recent advances in screening techniques have given novel insights into the role of specific ISGs in viral infection. Using large scale screening approaches, several ISGs have been identified as having common antiviral activity in a number of viral infections (Schoggins et al., 2011). These screens have also uncovered a number of ISGs whose antiviral potential is specific to certain viruses and, interestingly, a subset of ISGs that enhance the replication potential of certain viruses.

Microarray analysis of liver samples from both chronically infected patients and chimpanzees has shown that numerous ISGs are upregulated in response to HCV infection

(Bigger et al., 2001; Bigger et al., 2004; Helbig et al., 2005; Lanford et al., 2006; Smith et al., 2003; Su et al., 2002; Walters et al., 2006). Several of these ISGs have potent anti-HCV activity, including: protein kinase R (PKR), ISG56, ISG20, ADAR1, and Viperin. Additional analysis of these ISGs indicates that both PKR and ISG56 bind to translational initiation factors and inhibit the translation of viral RNA (Wang et al., 2003). Additionally, ADAR1 causes destabilization of viral RNA through deamination of adenosine residues (Taylor et al., 2005) and Viperin is an ER-associated protein that is linked to alterations in ER structure, which is thought to inhibit viral replication by interfering with membranous web formation (Hinson and Cresswell, 2009). Recently, siRNA screens have also identified IFIT3, TRIM14, PLSCR1, and NOS2 as ISGs that have anti-HCV activity, but the exact role of the proteins in constraining viral infection is still unknown (Metz et al., 2012). This screen also demonstrated that there is significant overlap between type I and type II IFN responses required for control of HCV infection. HCV has developed several mechanisms to disrupt the specific subset of ISGs that have anti-HCV activity leading to prolonged infection in a high percentage of patients (see section 1.4.6). Several studies examining patient responses to traditional IFN treatment have shown that the ability to stimulate specific ISGs is a key determinant for the efficacy of treatment (Sarasin-Filipowicz et al., 2008). Indeed, these studies and others done in chimpanzees have found that individuals that did not respond to treatment often had increased levels of ISGs suggesting that effective immune responses to HCV are determined by the subset of ISGs activated and not by the level of immune stimulation (Bigger et al., 2001; Bigger et al., 2004; Chen et al., 2005). Alternatively, studies showing that the IFN resistance or susceptibility of patient derived viruses is retained upon secondary infection in a mouse model system indicate that the HCV strain, and not the host immune response, is the major determinant for viral clearance and drug susceptibility.

Based on the current evidence, it is thought that control of HCV and response to treatments is likely determined by a combination of both host and viral factors.

1.4.6 Viral evasion of immune responses

Though there are similarities between the immune response profiles for different viral infections, the diverse range of effects induced by different patients or different viruses makes studying immune responses to specific infections difficult. One approach to this problem is to examine how viruses counter immune activation in order to determine how immune pathways are initiated during infection. Several common mechanisms of viral immune evasion involve blocking signalling cascades from immune receptors such as TLRs and RLRs. To achieve this, viral proteins often inhibit key signalling proteins that are involved in multiple pathways. For example, MyD88 is required for all TLR signalling cascades, with the exception of TLR3, and is, therefore a predominant target for many viral infections including HCV and DENV (Green et al., 2014; Horner et al., 2012). Additionally, viruses often target STAT proteins to eliminate or alter IFN signalling in infected cells. Inhibition of these two targets effectively blocks the major host pathways that facilitate antiviral activity. Another important immune evasion strategy employed by positive-strand RNA viruses is to conceal potential PAMPs, including dsRNA, from host cell receptors (Overby and Weber, 2011). Recognition of viral RNA by RLRs or TLRs is one of the most important mechanisms for activation antiviral immune responses. Compartmentalization of viral genome replication in organelle-like structures allows positive-strand RNA viruses to effectively evade detection by the immune responses and to create an environment conducive to viral propagation (see Chapters 3 & 4).

1.4.6.1 Hepatitis C virus immune evasion strategies

HCV has evolved a number of strategies to block immune activation through inhibition of RLR, TLR and IFN signalling cascades (Figure 1-4 red)(reviewed in (Horner and Gale, 2009; Liu and Gale, 2010)). First, in addition to its role in cleaving the viral poly-protein, the NS3/4A protease also cleaves TRIF and MAVS (Ferreon et al., 2005; Meylan et al., 2005). As described above, TRIF is an essential link in the TLR3 signalling pathway and MAVS is the major adaptor protein for the RLR signalling pathway. Inactivation of these proteins by the NS3/4A cleavage effectively blocks signalling through both of the key PAMP recognition pathways. Additionally, HCV core can inhibit IRF signalling through interactions with the DEAD box protein 3 (DDX3) (Mamiya and Worman, 1999; Owsianka and Patel, 1999; You et al., 1999). During infection, DDX3 has been shown to associate with IKK-ε to prevent IRF activation (Schroder et al., 2008). Core also blocks JAK/STAT signalling through several mechanisms. Interactions between core and the SH2 domain of STAT1 inhibit JAK/STAT signalling by preventing nuclear localization of STAT (de Lucas et al., 2005; Lin et al., 2006; Melen et al., 2004). Expression of HCV core also directly inhibits JAK phosphorylation and induces the expression of SOCS proteins, which in turn prevent JAK-mediated signalling (Bode et al., 2003). Additionally, chronic HCV infection is associated with increased cellular levels of protein phosphatase 2A (PP2A), which results in increased STAT1-PIAS1 binding and reduced STAT activity (Blindenbacher et al., 2003; Duong et al., 2004; Heim et al., 1999). The HCV glycoprotein E2 also blocks cellular antiviral activity by binding and inhibiting PKR (Taylor et al., 1999). Moreover, NS5A blocks PKR activity through direct binding, allowing for subversion of immune responses, and is also linked to the increased levels of IL-8 observed in patients who do not respond well to IFN treatment (Gale et al., 1998; Pflugheber et al., 2002; Polyak et al., 2001a; Polyak et al., 2001b). Finally, NS5A binds to the general TLR signalling adaptor protein

MyD88, effectively blocking cytokine induction in response to TLR activation (Abe et al., 2007). The combined effect of each of these immune evasion strategies is likely a major contributing factor to the prevalence of HCV worldwide.

1.5 The nuclear envelope

Cellular evolution leading to compartmentalization of specific organelles is the defining feature of eukaryotic cells. The development of intracellular membrane compartments in eukaryotic cells resulted in the encapsulation of chromatin by a continuous double-phospholipid bilayer, which created a selectively permeable barrier surrounding the DNA termed the nuclear envelope (NE)(reviewed in (Hetzer, 2010; Hetzer et al., 2005). Formation of this barrier separated cellular processes allowing for the development of more complex pathways that were not possible in prokaryotes. Located at the interface between the cytoplasm and the nucleoplasm, the NE is essential to the organization of many cellular processes. The outer membrane of the NE (outer nuclear membrane or ONM) is contiguous with the ER and is enriched for various ER components. The inner nuclear membrane (INM), separated from the ONM by a 40-50nm perinuclear space, harbours a unique subset of membrane proteins that have a variety of nuclear functions including forming structural links to the cellular cytoskeleton. Positioned throughout the NE are channels that form fusions between the INM and ONM (Figure 1-5)((Watson, 1954) reviewed in (Hetzer et al., 2005)). Within these channels reside large macromolecular structures termed nuclear pore complexes (NPCs), which facilitate selective traffic between the cytoplasm and nucleoplasm. Through the function of NPCs, eukaryotic cells form a spatial separation between specific cellular operations while still preserving a link between the nuclear and cytoplasmic compartments.

In vertebrate cells, the INM is lined by a layer of nuclear specific proteins, which create a stable protein meshwork termed the nuclear lamina (For review on lamins see (Burke and Stewart, 2013)). The lamina associates with structural proteins located in the INM, including SAD1 and UNC84 (SUN proteins), that are involved, through interactions with ONM KASH (Klarsicht–ANC-1–SYNE homology) domain proteins, in maintaining NE structure as well as coupling the nucleus to the cytoskeleton (Sosa et al., 2012). In addition to maintaining nuclear structure, the nuclear lamina has been associated with an array of cellular processes including gene expression, DNA damage repair, development, cell differentiation, cell proliferation, and cellular aging (reviewed in (Burke and Stewart, 2013)). Specific mutations in the genes encoding lamins have been linked to human diseases such as adult-onset autosomal dominant leukodystrophy, ataxia-telangiectasia, Emery-Dreifuss muscular dystrophy, and Hutchinson-Gilford progeria syndrome (reviewed in (Burke and Stewart, 2013)). These diseases arise from alterations in the nuclear lamina network, which disrupts the overall nuclear structure and organization.

Observations indicating a systematic genome organization within the nucleus were first made using salamander larvae in the late 1800s (Rabl, 1885). Since then, transmission electron microscopy (TEM) images of nuclei from various organisms have demonstrated a concentration of denser chromatin in association with the NE or surrounding nucleoli and centromeres. Higher levels of organization can also be observed at the chromosome level, as studies have shown that specific chromosomes have higher NE occupancy, while others tend to be localized to the interior of the nucleus (Croft et al., 1999). Though many aspects of chromatin organization remain obscure, current models suggest that interactions with NPCs, lamins, and INM proteins serve as reference points for maintaining 3-dimensional genome organization and controlling gene activation. The INM is populated by a distinct set of peripheral and integral

membrane proteins, generally referred to as nuclear envelope transmembrane (NET) proteins, not normally found in the ER (for review on INM proteins see (Zuleger et al., 2011)). A significant proportion of these membrane proteins are involved in forming stable links between chromatin and the INM which contributes to the overall organization of chromosomes and are thought to be involved in gene silencing. Building on observations that higher density heterochromatin is primarily located at the nuclear periphery, studies focused on the impact of chromatin spatial organization on gene regulation have demonstrated that the majority of chromatin found in contact with the NE is in a silent configuration (Pickersgill et al., 2006). Alternatively, chromatin found in association with NPCs is predominantly in an uncondensed active state, placing the NPC at transition points between active and inactive chromatin (Schmid et al., 2006; Taddei et al., 2006). Moreover, changes in overall chromatin organization or specific chromosome localization have been observed in diseases caused by NE protein mutations. For example, in patients with NE mutations leading to muscular dystrophy progeroid syndromes or mandibuloacral dysplasia, the chromatin in cells is not localized to the NE, but rather appears to have either broken away from the nuclear periphery or disappeared completely (Goldman et al., 2004; Maraldi et al., 2006; Sewry et al., 2001; Verga et al., 2003). In general, the NE contributions to the spatial arrangement of chromosomes are essential for proper nuclear organization and gene regulation.

1.6 The nuclear pore complex

NPCs are most often characterized for their role in shuttling molecules across the NE, effectively creating a selective barrier between nuclear and cytoplasmic cellular compartments. Located at the interface between the cytoplasm and nucleus, the NPC is ideally position to impact a large number of cellular processes. In addition to mediating transport, NPCs are also

involved in chromatin organization, gene expression, chromatin inheritance, DNA damage repair, and cell cycle regulation (Brickner et al., 2007; Krull et al., 2010; Strambio-De-Castillia et al., 2010; Therizols et al., 2006; Van de Vosse et al., 2013; Van de Vosse et al., 2011). Having influences over such a large number of cellular processes, it is not surprising that the NPC is targeted by a large number of diseases (discussed in section 1.6.3 and 1.9). The complexity of its structure as well as its control over numerous cellular processes makes the NPC an important topic for study.

Current theories suggest that NPCs evolved in a similar manner as vesicle coat proteins; namely through the divergent evolution of proteins originally involved coating and stabilizing the bent ends of membrane cisterna (Dacks and Field, 2007; Devos et al., 2004; Mans et al., 2004). The individual constituents that make up the NPC, and indeed the general structure of the NPC, are highly conserved, suggesting that many NPC components evolved from duplications of a smaller ancestral set of proteins (Alber et al., 2007b; DeGrasse et al., 2009; Devos et al., 2006). This high level of conservation is also reflected in a large number of different organisms that, even over large evolutionary distances, share homology in specific NPC protein motifs and domains, suggesting that NPCs evolved very early in eukaryotic lineages (Table 1-1)(DeGrasse et al., 2009; Devos et al., 2004; Field and Dacks, 2009). The highly conserved nature of NPCs across species has allowed extensive characterization of the NPC in more easily studied model organisms. Specifically, the use of yeast *Saccharomyces cerevisiae* as a model has allowed for advances in our understanding of NPC structure and function that would not have been possible in studying mammalian cells alone.

Table 1-1. List of nucleoporin orthologues from different species.

	Vertebrate	*S. cerevisiae*	*C. elegans*	*D. melanogaster*
Cytoplasmic Nups	Nup358	—	npp-9	Nup358
	Nup214	Nup159p	npp-14	Nup214
	Nup88	Nup82p	—	Nup88
	GLE1	Gle1p	—	GLE1
	hCG1	Nup42p	—	CG18789
Nup98 complex	Nup98	Nup145Np, Mup116p, Nup100p	npp-10	Nup98
	RAE1	Gle2p	npp-17	RAE1
Channel Nups	Nup58	—	—	—
	Nup45	Nup49p	npp-4	Nup58
	Nup54	Nup57p	npp-1	Nup54
	Nup62	Nsp1p	npp-11	Nup62
Core scaffold	Nup43	—	C09G9.2	Nup43
	Nup37	—	—	CG11875
	Nup85	Nup85p	npp-2	Nup75
	Nup133	Nup133p	npp-15	Nup133
	Nup107	Nup84p	npp-5	Nup107
	Nup96	Nup145Cp	npp-10C	Nup96
	Nup160	Nup120p	npp-6	Nup160
	Sec13	Sec13p	npp-20	Sec13
	Seh1	Seh1p	npp-18	Nup44A
Adaptor scaffold	Nup53	Nup53p, Nup59p	npp-19	CG6540
	Nup93	Nic96p	npp-13	CG7262
	Nup155	Nup170p, Nup157p	npp-8	Nup154
	Nup188	Nup188p	—	CG8771
	Nup205	Nup192p	npp-3	CG11943
Nuclear Nups	Nup153	Nup1p	npp-7	Nup153
	Nup50	Nup2p	npp-16	Nup50
	TPR	Mlp1/Mlp2	R07G3.3	—
	—	Nup60p	—	—
Transmembrane Nups	POM121	—	—	—
	NDC1	Ndc1p	npp-22	Ndc1
	GP210	—	npp-12	GP210
	TMEM33	Pom33p	Y37D8A.17	Kr-h2
	—	Pom152p	—	—
	—	Pom34p	—	—

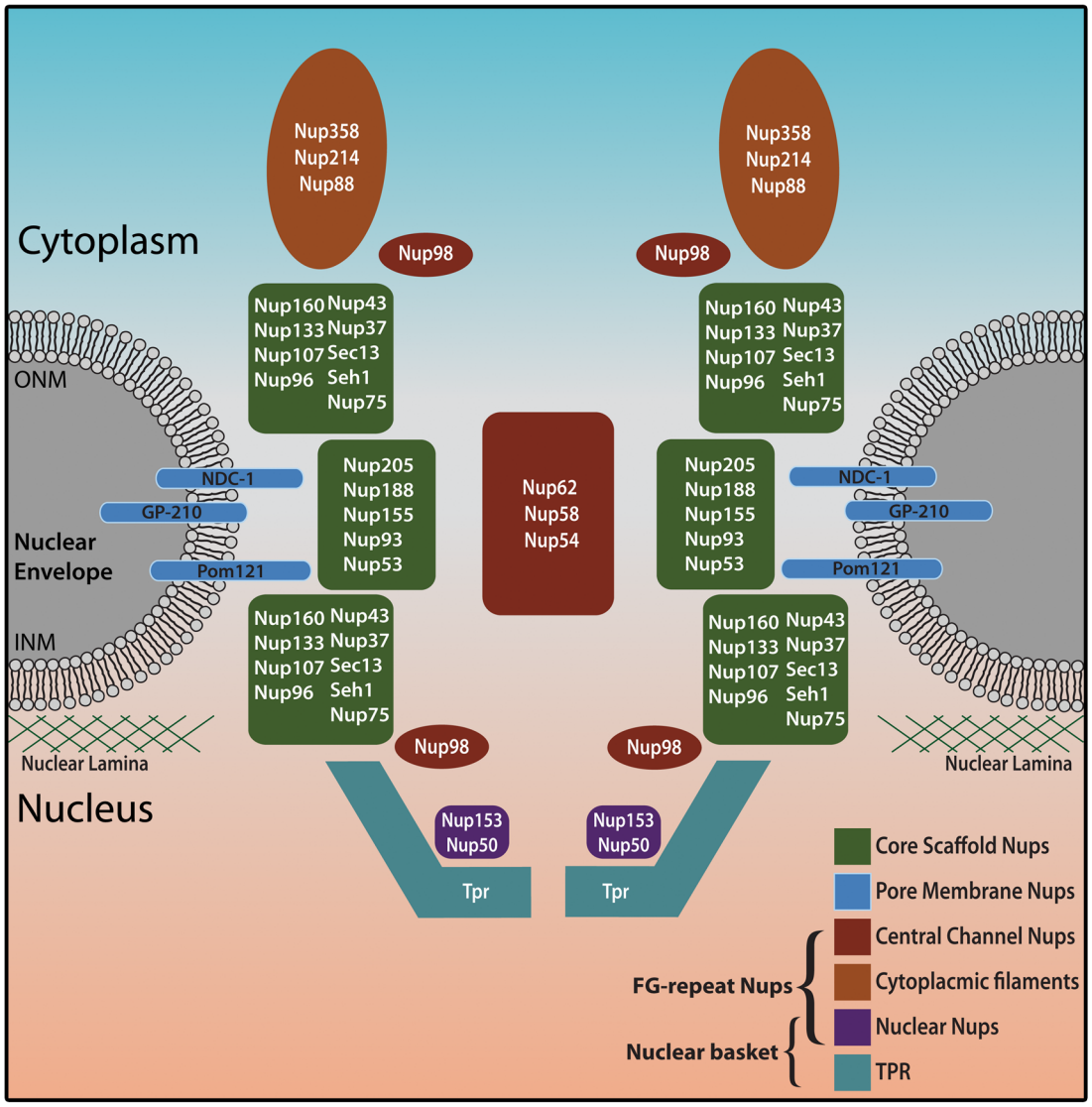

Figure 1-5. The nuclear pore complex. The NPC is a large macromolecular structure that extends across the nuclear envelope forming a channel between the cytoplasm and nucleoplasm. The NPC is composed of ~30 distinct proteins termed Nups, which are present in multiple copies giving the NPC a characteristic symmetrical structure. Two of the eight total NPC subunits are depicted. The pore membrane (Pom) Nups (blue) anchor the NPC in the NE. Core scaffold Nups (green) are involved in maintaining the NE membrane curvature and form a scaffold on which the central channel and asymmetric Nups are organized. Finally, the FG-repeat Nups function in forming associations with transport cargos and in maintaining the permeability barrier across the NE. FG-repeat Nups include symmetrical or central channel Nups (red) and asymmetrical Nups that make up the cytoplasmic filaments (orange) and the nuclear basket (purple).

1.6.1 Nucleoporins

Various imaging and biochemical techniques have shown that the NPC has a complex cylindrical structure that displays an octagonal symmetry around the central channel and two-fold symmetry along the plain of the NE (Akey, 1989; Akey and Radermacher, 1993; Stoffler et al., 1999; Unwin and Milligan, 1982). Extensive proteomic analysis of the structural components that compose the NPC has revealed that, though assembled mammalian NPCs are ~100MDa, the number of unique proteins within the complex is relatively low (reviewed in (Solmaz et al., 2013)). Each NPC is composed of ~30 distinct highly conserved proteins, termed nucleoporins or Nups (Cronshaw et al., 2002; Rout et al., 2000). A similar number of Nups has been observed in different species including, but not limited to, *Homo sapiens, Drosophila melanogaster, Caenorhabditis elegans, Xenopus laevis* and two yeast species, *Schizosaccharomyces pombe* and *S. cerevisiae* (Table 1-1). Structural analysis in *S. cerevisiae* and vertebrates has shown that Nups are organized into modular subunits, which assemble to form the larger macromolecular structure giving the NPC its characteristic symmetrical organization (Figure 1-5). Thus, the NPC, though only containing 30 unique proteins, is an assembly of ~500 distinct polypeptides.

Individual Nups can be organized into distinct subunits based on location and function within the NPC. Within eukaryotic cells, these subcomplexes of Nups can rapidly assemble into the complex array of proteins that allows for nuclear compartmentalization. The first group of Nups is composed of integral membrane proteins, which function to anchor the NPC in the NE (Figure 1-5, blue). In mammalian cells, this group of proteins, generally referred to as pore membrane domain or POM proteins, is involved in pore assembly as well as connecting the NE to the NPC core scaffold proteins. These core scaffold proteins comprise another group of Nups, which are involved in forming and maintaining the structural scaffold and characteristic membrane curvature of the NPC (Figure 1-5A green). Proteins components of this group often

contain domains involved in curving membranes that are homologous to those found in vesicle coat proteins (Brohawn et al., 2008; Field and Dacks, 2009). Finally, Nups containing unstructured phenylalanine-glycine (FG) repeats domains line the central channel of the NPC, and are critical for maintaining the permeability barrier between the cytosol and nucleoplasm (Frey and Gorlich, 2007; Patel et al., 2007). FG-repeat Nups mediate interactions between the NPC and transport proteins which facilitates active transport of large cargos across the NE. These Nups can be further subdivided into central channel Nups and peripheral Nups (Figure 1-5 red, orange and purple). In addition to direct roles in transport, the peripheral FG-repeat Nups also serve as platforms for numerous NPC-associated proteins.

1.6.1.1 Core scaffold nucleoporins

The scaffold of the NPC both maintains the membrane curvature of the NE at the NPC and forms the molecular framework on which FG-repeat Nups are organized. Within this framework are two predominant subcomplexes that make up the symmetric core (Nup107-160 complex containing Nup37, Nup43, Nup85, Nup96 Nup107, Nup133, Nup160, Sec13, and Seh1, termed Nup84p complex in yeast) and the adaptor scaffold (Nup53-93 and Nup155 complexes containing Nup53, Nup93, Nup155, Nup188, and Nup205) (Figure 1-5 green)((Belgareh et al., 2001; Grandi et al., 1997; Hawryluk-Gara et al., 2005; Loiodice et al., 2004) and reviewed in (Hetzer and Wente, 2009)). These subcomplexes are arranged in concentric rings, forming the outer and inner rings that make up the core structure of the NPC (Alber et al., 2007b). Early 2D EM studies on the *S. cerevisiae* homologue to the Nup107-160 complex (Nup84p complex) revealed that components of this complex can self assemble into a observable Y-shaped structure (Lutzmann et al., 2002). The assembly of multiple Y-shaped

Nup107-106 subcomplexes around the central channel, facilitated by the adaptor complexes, forms the structural framework of the NPC (Alber et al., 2007b).

Nup155 and several members of the Nup107-160 subcomplex contain two specific fold types, α-solenoid domains and β-propeller domains, which are found in one of three distinct arrangements: a single α-solenoid domain, a single β-propeller domain or an amino-terminal β-propeller domain followed by a carboxy-terminal α-solenoid (Berke et al., 2004; Devos et al., 2004; Devos et al., 2006; Schwartz, 2005). These domains have the capacity to bend cellular membranes or maintain high levels of membrane curvature, which is thought to function in the fusion of the ONM with the INM during formation of nuclear pores. Each of these domains shares a common architecture with protein domains found in vesicle coat complexes and the β-propeller followed α-solenoid configuration is a hallmark of clathrin-like proteins (Devos et al., 2004). Interestingly, components of the *S. cerevisiae* Nup84p complex, Sec13p and Seh1p are also shared components of COPII vesicle coat complexes (Devos et al., 2004). These observations formed the basis for the "protocoatomer" hypothesis, which predicts that components of the core scaffold Nups and the vesicle coat proteins originated from common ancestors during the evolution of the endomembrane system (Brohawn et al., 2008; DeGrasse et al., 2009; Devos et al., 2004; Field and Dacks, 2009; Field et al., 2011).

The similarities between specific Nups and vesicle coat proteins also inspired the hypothesis that the core scaffold Nups coat the nuclear membrane by forming interconnected lattice work that mimics the coat structures of COPI, COPII and clathrin-coated vesicles (termed the 'lattice model')(Brohawn et al., 2008). However, there are significant structural differences between these two complexes that make a direct comparison difficult. Most notably, unlike vesicle coats, which maintain only a positive membrane curvature, the donut-like shape of the NPC requires the maintenance of both a positive membrane curvature between the ONM

and INM and a concentric negative membrane curvature around the central channel. A second model for the organization of core scaffold Nups proposes a novel membrane coating arrangement of these Nups into a cylindrical structure formed from the higher-order assembly of Nup heptamers (termed the 'fence post' model)(Debler et al., 2008; Hsia et al., 2007). In-depth computational modeling of the NPC also suggests an arrangement of the NPC core-scaffold into heptamers that supports the 'fence post' model (Alber et al., 2007a; Alber et al., 2007b). However, current techniques cannot achieve the resolution required to definitively discern the arrangement of NPC membrane coat elements. Therefore, further development of new analysis methods for investigation into the structural elements of NPC is required to resolve the architectural framework of the NPC membrane coat.

1.6.1.2 Pore membrane nucleoporins

The NPC contains several Pom proteins that are predicted to anchor the pore in the NE as well as contribute to NPC assembly and nucleocytoplasmic transport. Poms identified in vertebrates include gp210, NDC1, and Pom121 (Figure 1-5 blue)(Gerace et al., 1982; Hallberg et al., 1993; Mansfeld et al., 2006c; Stavru et al., 2006). Both Pom121 and gp210 contain a single transmembrane domain that connects the luminal and cytoplasmic domains and links the NPC core scaffold to the pore membrane. However, Pom121 contains a much larger domain (~100 kDa) extending toward the NPC whereas gp210 contains a larger luminal segment. The third vertebrate Pom, NDC1, contains six predicted transmembrane domains with 3 luminal loops and a ~45 kDa C-terminal domain that associates with the NPC (Mansfeld et al., 2006a; Stavru et al., 2006). A fourth Pom recently identified in yeast (termed Pom33p) has a significant ER-associated pool in addition to its NE pool, and also has an important, though undefined, role in NPC assembly (Chadrin et al., 2010). Phylogenetic analysis revealed a human ortholog of

Pom33p, previously termed TMEM33; however, depletion experiments suggest that it is not required for NPC assembly in mammalian cells. Therefore, the role of TMEM33 in NPC biogenesis is still uncertain.

The specific role of Pom proteins has been difficult to discern, as they appear to have significant functional redundancy. For example, in yeast, single null mutations in either *POM152* or *POM34* did not have noticeable effects on nuclear import or NPC biogenesis. However, in the absence of both Pom34p and Pom152p cells exhibited defects in targeting of newly synthesized Nups to the NE (Onischenko et al., 2009). Additionally, both Nup53p and Nup59p have C-terminal amphipathic helices and have been demonstrated to be functionally redundant to Pom152p and Pom34p (Onischenko et al., 2009). Extrapolating functional information for mammalian Poms from yeast experiments was originally difficult as there was little obvious homology between Poms of different species. However, more recent experiments have shown that there are parallels between Poms from different species. For example, orthologues of NDC1 have been identified in numerous species from yeast to metazoan (DeGrasse et al., 2009). NDC1 has been shown to have important roles in both NPC assembly and maintenance of the NPC structure (Madrid et al., 2006; Mansfeld et al., 2006b; Onischenko et al., 2009; Stavru et al., 2006). In addition to NDC1, both Pom152p in yeast and Pom121 in vertebrates, have been linked to NPC biogenesis, further demonstrating an important role for integral membrane proteins in NPC assembly (Antonin et al., 2005; Madrid et al., 2006; Mitchell et al., 2010).

In vertebrates, NPC assembly can be broken into two categories: NPC assembly during NE reformation following mitosis and *de novo* NPC assembly during interphase. Following mitosis, ER membranes and disassembled NPC components are recruited to chromatin leading to simultaneous NE reformation and NPC assembly (Schooley et al., 2012). This pathway of assembly involves a stepwise association of Nups that is initiated by recruitment of the Nup107-

160 complex and subsequent formation of a 'pre-pore' structure to which other Nups are recruited (Dultz et al., 2008; Harel et al., 2003; Walther et al., 2003). Assembly of the 'pre-pore' is followed by the recruitment of Pom121 and NDC1 leading to binding of the adaptor complexes and the successive association of the remaining FG-repeat and peripheral Nups (Antonin et al., 2008; Antonin et al., 2005; Hawryluk-Gara et al., 2008; Mitchell et al., 2010). Whether this assembly occurs through a method of membrane enclosure around assembling NPCs or by insertion of NPCs into the NE membrane is still uncertain (Dultz and Ellenberg, 2010; Dultz et al., 2008; Schooley et al., 2012). Alternatively, *de novo* production of NPCs in interphase has been shown to occur through insertion into the NE. The process of NPC insertion during interphase differs from post mitotic assembly in that recruitment of Poms precedes the recruitment of the Nup107-160 complex (Doucet et al., 2010; Dultz and Ellenberg, 2010; Funakoshi et al., 2011; Talamas and Hetzer, 2011). Recruitment of Poms is followed by the rapid, synchronous association of the core scaffold Nup complexes leading to the recruitment of FG-repeat and peripheral Nups (Dultz and Ellenberg, 2010). In both pathways for NPC biogenesis, the Pom interaction network performs a vital function in NPC assembly through connecting the NE and the core scaffold of the NPC.

1.6.1.3 FG-repeat nucleoporins

Lining the central channel of the NPC is a subset of Nups that associate with the soluble transport machinery and facilitate movement of cargos across the NE (Figure 1-5)(reviewed in (Wente and Rout, 2010). This subset of Nups, representing approximately one-third of the total Nup population, is characterized by the presence of long, natively unfolded, domains that harbour FG, GLFG, and/or FXFG-repeats (Denning et al., 2003; Radu et al., 1995a; Radu et al., 1995b). The network of natively unfolded FG-repeat domains have a dual function in

maintaining the selective permeability of the NE: 1) to associate with transport complexes, allowing interchange between compartments, and 2) to passively form a permeability barrier, blocking access to macromolecules. Though the components that make of the FG-repeat Nups are well defined the exact organization of the FG-repeat domains and how these domains interact with import/export complexes and facilitate transport is still controversial (see section 1.6.2.2).

Categorized within this group of Nups are the symmetric FG-repeat Nups (Nup54, Nup58, Nup62, and Nup98) and two asymmetric subsets of Nups that extend into the cytoplasmic and nuclear compartments (Rout et al., 2000; Strawn et al., 2004). These asymmetrically positioned Nups, forming the cytoplasmic filaments and the nuclear basket of the NPC, provide docking sites for specific transport and regulatory proteins associated with the NPC. In vertebrates, the cytoplasmic filaments are composed of three proteins, Nup88, Nup214 (or CAN), and Nup358 (or RanBP2)(Figure 1-5 orange). Nup88 forms the NPC attachment point for both Nup214 and Nup358, and has been linked, along with Nup214, to the function of specific transport pathways (Bernad et al., 2006; Fornerod et al., 1997b). The largest of these proteins, Nup358, extends long filaments into the cytoplasm and is involved in facilitating nuclear transport as well as being linked numerous non-transport cellular pathways (see section 1.7). The nuclear face of the NPC contains two asymmetric Nups, Nup50 and Nup153, and the pore-associated protein TPR, which extends for the NPC to form a basket like structure. The nuclear basket structure is stabilized by the nuclear lamina and, similar to Nup358 in the cytoplasm, has been linked to regulating transport on the nuclear face of the NPC. Both the nuclear basket and the cytoplasmic filaments create platforms for the binding of NPC-associated proteins required to maintain nuclear traffic and facilitate links between the NPC and various other cellular pathways.

Like the Poms, the asymmetric FG-Nups have been shown to be functionally redundant as over half the total mass of these FG domains, can be removed without significant affects on cell viability (Strawn et al., 2004; Zeitler and Weis, 2004). These redundant FG-repeat Nups are predominantly located at the periphery of the NPC, as those residing within the central channel are essential for NPC transport function (Finlay et al., 1991; Guan et al., 1995; Strawn et al., 2004). Recent models for transport suggest that these essential channel FG-repeat Nups (including Nup54, Nup58 and Nup62), together with the core and adaptor scaffold Nups comprise a 'symmetric core' that can facilitate reversible dilation of the transport channel (Hoelz et al., 2011; Melcak et al., 2007; Solmaz et al., 2013; Solmaz et al., 2011). One of the evolutionary challenges faced by the emergence of transport channels across the NE was the ability of those channels to both accommodate transport of large macromolecules, while preventing concomitant bidirectional leakage of smaller proteins. The reversible alteration in NPC structure, moving from active to inactive conformations, could allow transport of a diverse set of transport cargos while still maintaining the barrier effect of the NPC (Solmaz et al., 2013).

1.6.2 NPC-mediated transport

Maintaining a selective boundary between cellular compartments requires both barrier and binding functions of the NPC. Early studies using fluorescently labeled dextran beads elegantly demonstrated that the NPC has a size exclusion barrier that blocks the passive diffusion of molecules ~40 kDa in mass or ~5 nm in diameter (Feldherr and Akin, 1997; Keminer and Peters, 1999). Larger molecules must overcome this barrier by interacting directly with the NPC or with soluble transport factors generally termed nuclear transport factors (NTFs)(Figure 1-6)(reviewed in: (Fried and Kutay, 2003; Guttler and Gorlich, 2011; Pemberton and Paschal, 2005)). Through various mechanisms the NPC is able to accommodate active transport of a

wide variety of cargos, including numerous RNA species and proteins, which can range in size up to a diameter of 39 nm (Feldherr et al., 1984; Pante and Kann, 2002; Wente and Rout, 2010). NPC have been estimated to accommodate a mass flow of nearly 100 MDa/second and can translocate ~1000 macromolecules per second; a feat that points towards a highly sophisticated nucleocytoplasmic transport system in eukaryotic cells (Ribbeck and Gorlich, 2001). In higher eukaryotes, the transport machinery consists of ~80 distinct proteins which can be clustered into the NPC components (Nups), soluble NTFs, and components that provide energy and directionality to the transport process (notably the RanGTP/RanGDP system)(Guttler and Gorlich, 2011). Though considerable progress has been made in the elucidation of the components required for NPC-mediated transport, there is still no unifying model explaining the process of transport.

1.6.2.1 Karyopherins and transport signal sequences

Targeting of proteins for transport through the NPC requires specific stretches of amino acid residues found within the cargo protein. These amino acid residue sequences, termed nuclear localization signal (NLS) sequences for nuclear import or nuclear export signal (NES) sequences for nuclear export, are sufficient for transport of proteins across the NE. This has been demonstrated by the increased nuclear localization of soluble cytoplasmic proteins observed after the addition of specific NLS sequences (Goldfarb et al., 1986). In general, NLS sequences contain stretches of basic residues, but the exact amino acid residue composition is variable between cargo proteins. For example, some cargo proteins contain a classical or canonical NLS (cNLS) sequence, comprised of a five-residue KKKRK sequence, which is sufficient for transport, while others require a "bipartite" sequence consisting of two regions of basic residues separated by ten amino acid residues (Dingwall et al., 1988; Goldfarb et al., 1986; Kalderon et al., 1984). In contrast to import cargos, nuclear export cargo NES sequences

generally contain short stretches of leucine rich amino acid residues (Wen et al., 1995). However, the constant fluctuations of nuclear transport pathways, which are regulated by cell cycle signals as well as numerous other cellular processes, and the dynamic nature of many cargos that cycle between the nucleus and cytoplasm makes defining specific NLS or NES sequences difficult for many cargo proteins (Wente and Rout, 2010).

Recognition of NLS or NES sequences and the subsequent transport of cargos across the NE are facilitated by soluble NTFs (Adam and Adam, 1994; Chi et al., 1995; Gorlich et al., 1994; Imamoto et al., 1995; Moore and Blobel, 1992). Most NTFs are members of a family of structurally conserved proteins known as karyopherins or Kaps (also called importins, exportins, or transportins). Kaps contain multiple binding sites for FG-repeat Nups, which allows them to interact with NPC in a way that overcomes the large molecule exclusion barrier of the NPC. Association with Kaps facilitates the transport of individual cargos as well as larger protein complexes or nucleic acid complexes, increasing the transport rate of a given cargo by factors of 100 to >1000 (Ribbeck and Gorlich, 2001). The majority of cellular NTFs have sequence homology to importin β (Impβ or Kapβ) and use a RanGTP-dependent transport pathway. The Impβ family of proteins consists of 14 members in *S. cerevisiae* and at least 20 members in metazoans (reviewed in: (Fried and Kutay, 2003; Pemberton and Paschal, 2005)). These Kaps use energy provided both through associations with GF-repeat Nups and by the RanGTPase system to overcome the selective barrier generated by the NPC and to provide directionality to nucleocytoplasmic transport (see section 1.6.2.1).

Kaps can be divided into those involved in nuclear export (recognizing NES signals), those involved in nuclear import (recognizing NLS signals), and at least one Kap that appears to be involved in both the import and export of cargos. For nuclear import, the most predominant importin in vertebrates, Impβ1 requires an adaptor protein to form stable complexes with

cargos. These adaptor proteins are members of the importin α (Impα or Kapα) family of proteins and can associate with NLS sequences but not with GF-repeat Nups. Alpha importins (Kap65p in yeast and Impα1-6 in metazoans) can act as a linker between Impβ1 (Kap95p in yeast) and cargo proteins forming a tetrameric complex that facilitates nuclear import (Goldfarb et al., 2004). Other importins, including Impβ3, do not require adaptor proteins, but rather they interact with both cargo proteins and Nups. Nuclear export of macromolecules is mediated by a separate group of Kaps referred to as exportins. Eight exportins have been identified in metazoans and four in *S. cerevisiae* but, so far, the vast majority of defined export cargos associate with CRM1 (Xpo1p in yeast) through a leucine rich NES domain (Fornerod et al., 1997a; Fukuda et al., 1997; Stade et al., 1997). The wide variety of structurally unrelated cargos recognized by either CRM1 or Impα/β complexes, each of which have each been associated with the transport of dozens of cargos, highlights the promiscuity of the nuclear transport pathway. In addition to individual Kaps shuttling a diverse range of proteins across the NE, specific cargo proteins can also be shuttled by multiple Kaps further demonstrating the significant level of redundancy in NPC-mediated transport pathways. Conversely, while multiple Kaps can mediate transport of some cargos, others required a specific Kap for transport suggesting a complex level of organization and regulation to the nucleocytoplasmic transport pathway.

1.6.2.2 Directionality of nuclear transport

The motion of NTF/cargo complexes within the central channel of the NPC is hypothesized to be a random process, occurring primarily through Brownian motion (see section 1.6.2.3)(reviewed in (Guttler and Gorlich, 2011; Stewart, 2007)). However, this system requires energy to overcome the energetically unfavourable process of entering the narrow NPC channel

and for retention of cargos within the proper compartment. The energy for maintaining directionality is provided to the nuclear transport pathway by the RanGTPase system (Figure1-6). Ran is predominantly found in the nucleoplasm where it is maintained primarily in its GTP bound state by the presence of the chromatin-associated Ran guanine nucleotide exchange factor (RanGEF) RCC1 (Ohtsubo et al., 1989; Seki et al., 1996). Importin/cargo import complexes entering the nucleus encounter RanGTP, which has a 1000 fold higher affinity for import Kaps than the GDP bound form of Ran (Bischoff and Gorlich, 1997; Gorlich et al., 1996; Rexach and Blobel, 1995). Interactions between importins and RanGTP disrupt the importin/cargo complex releasing the cargo into the nucleus (Figure 1-6). Alternatively, nuclear export complexes incorporate RanGTP, forming a trimeric structure that stabilizes the transport complex and allows transport through the NPC. On the cytoplasmic side of the NPC, RanGAP, associated with Nup358, hydrolyzes RanGTP into RanGDP triggering dissociation of the exportin/cargo/RanGTP complex and release of the cargo into the cytoplasm. RanGDP is recycled into the nucleus by the transport factor NTF2 to maintain the higher concentration of nuclear Ran (Ribbeck et al., 1998). Directionality in this system is a product of the differential concentration of RanGTP and RanGDP across the NE. This gradient is maintained by the predominant localization RCC1 in the nuclear compartment and RanGAP in the cytoplasmic compartment. As stated above, RanGAP, through association with Nup358, is localized to the cytoplasmic filaments facilitating efficient release of export cargos directly following NPC exit. Interactions with histones H2A and H2B tether RCC1 in the nuclear compartment preserve the high levels of nuclear RanGTP (Bischoff and Ponstingl, 1991; Nemergut et al., 2001; Ohtsubo et al., 1989).

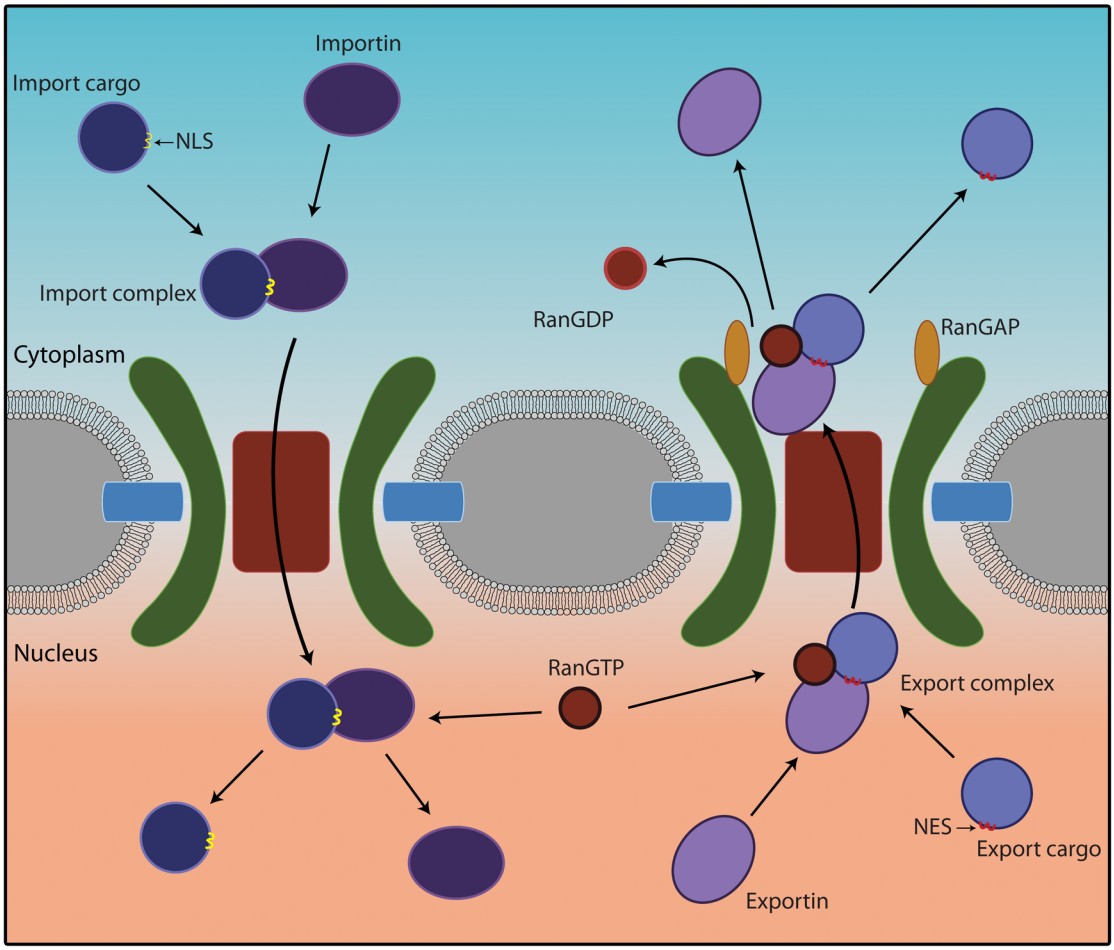

Figure 1-6. NPC-mediated transport. Cargo proteins that undergo nuclear import (dark blue) contain a nuclear localization signal (NLS) sequence that is recognized by an import karyopherin (importin, dark purple) on the cytoplasmic side of the NPC. The resulting cargo-importin complex can interact with Nups allowing translocation through the NPC. On the nucleoplasmic side of the NPC, the high concentration of RanGTP, maintained by the predominantly nuclear RanGEF, destabilizes the import complex releasing the cargo protein into the nucleus. Conversely, cargo proteins undergoing nuclear export (light blue) contain a nuclear export signal (NES) sequence, which facilitates the formation of a trimeric export complex with an export karyopherin (exportin, light purple) and RanGTP (red). The export complex can translocate through the NPC where RanGAP (orange), bound to Nup358 on the cytoplasmic side of the NPC, hydrolyzes RanGTP to form RanGDP. This process destabilizes the export complex and releases the export cargo into the cytoplasm.

Though the RanGTPase system provides directionality for the majority of defined cargos, other mechanisms also exist for maintaining substrates in the proper compartment. For instance, binding of a cargo protein to structures or proteins within a compartment could mediate Kap release and effectively trap cargos without independent of the Ran cycle. Additionally, large mRNA molecules do not utilize Ran-dependent export pathways, but rather employ an ATPase located on the cytoplasmic side of the NPC to prevent retrograde transport of transcripts (reviewed in (Stewart, 2010)). The major transport factors for mRNA transcripts are NXF1-NXT1 (Mex67-mtr2 in yeast), which coat mRNA transcripts in the nucleus and facilitates interactions with the NPC (Katahira et al., 1999). On the cytoplasmic face of the NPC, the export complex is remodelled by the Nup214-associated DEAD-box helicase DDX19 (dbp5 in yeast) in an ATP-dependent event, releasing NXF1-NXT1 into the cytoplasm and preventing retrograde transport of the mRNA molecule (Montpetit et al., 2011; Napetschnig et al., 2009). Consequently, movement through the NPC channel does not directly require energy, but energy sources are critical for the formation of transport complexes and to establish concentration gradients.

1.6.2.3 Models for nuclear transport

Since the discovery of the NPC, an immense amount of work has yielded a fairly comprehensive characterization of the machinery that governs nuclear transport. However, the mechanisms by which molecules are transported through the NPC are still poorly understood. Several different models have been proposed to describe how interactions between transport complexes at the NPC allow nucleocytoplasmic transport while still maintaining a selective barrier. Two of the predominant models are the selective phase/hydrogel model and the virtual gate/polymer brush model. The selective phase or hydrogel model proposes that FG-repeats are

cross-linked through their phenylalanine residues forming a dense gel like structure (Frey et al., 2006; Ribbeck and Gorlich, 2002). Multivalent interactions between NTFs and FG-repeats destabilize these associations between FG-repeats thereby forming a path for transport through the hydrogel-like structure (Frey and Gorlich, 2007). Molecules that do not interact with the FG-repeat domains would be excluded, as they would not disrupt the hydrogel structure. Alternatively, the virtual gate hypothesis argues that entry into the relatively small channel of the NPC is entropically unfavourable, blocking most molecules from entry (Rout et al., 2003; Rout et al., 2000). This model proposes that the energy of binding between FG-repeat Nups and transport complexes lowers the activation energy of translocation across the NE, there by allowing NTF-cargo complexes to enter the central channel of the NPC. Building on this model, several groups have suggested that the FG-repeats in the cytoplasmic and nuclear asymmetric Nups act as a 'polymer brush' to repel non-transport molecules and increase the efficiency of transport (Lim et al., 2007; Lim et al., 2006). Several hybrid models have also been proposed suggesting that the actual mechanism of transport may be more complicated than has yet been uncovered.

1.6.3 Non-transport functions of Nups

In addition to their classically defined role in nucleocytoplasmic transport, various components of the NPC and the nuclear transport pathway contribute to other cellular pathways. Several regulatory functions have been attributed to the NPC during the progression of the cell cycle. For example, the spindle assembly checkpoint is regulated by the dynamic association of Mad1 and Mad2 with the nuclear basket of the NPC in both mammalian and yeast cells (Campbell et al., 2001; Iouk et al., 2002; Scott et al., 2005). In yeast, this process is controlled by the Crm1 homologue Xpo1, which recognizes Mad1 in a RanGTP-dependent

manner and relocates it to kinetochores following activation of the spindle assembly checkpoint (Scott et al., 2009). Additionally, targeting of the Nup358/RanGAP1 to kinetochores in mammalian cells, a process essential for proper chromatin segregation, relies on dynamic associations with Kapβ and Crm1 (Joseph et al., 2004; Joseph et al., 2002). Overexpression of Kapβ1 causes relocalization of Nup358 away from kinetochores leading to several mitotic defects. This phenotype is rescued by the co-expression of Crm1 suggesting that the relative levels of Kapβ1 and Crm1 regulate Nup358 kinetochore association. These observations demonstrate important a links between the NPC and the cell cycle regulation.

The NPC also has a role in chromatin structure and gene regulation. Since the first EM descriptions of the NPC, they have been consistently associated with euchromatin channels through the heterochromatin normally located at the NE. This places the NPC at the interface between active and inactive chromatin states, generating theories that implicate the NPC in chromatin rearrangements leading to activation of specific gene loci. Indeed, several Nups interact with various components of the chromatin remodelling machinery and appear to have a significant role in gene regulation (Van de Vosse et al., 2013). Recent studies in *Drosophila* have also demonstrated that several Nups associate with distinct gene loci and mediate transcriptional activation of developmental genes (Capelson et al., 2010). Mutations in one of these nucleoplasmic Nups, Nup98, are associated with several human myeloid cancers including acute myeloid leukemia (AML), chronic myeloid leukemia in blast crisis, myelodysplastic syndrome, acute lymphoblastic leukemia (ALL), and bilineage/biphenotypic leukemia (reviewed in (Gough et al., 2011; Takeda and Yaseen, 2014)). In most cases, these mutations involve a fusion of the N-terminal FG-repeats domain of Nup98 to histone modifying genes leading to transcriptional activation of several cancer related genes. Several of these fusions can induce transformation and cell proliferation in cell culture and have been shown to inhibit cell differentiation of

hematopoietic precursor cells (Wang et al., 2007). Interestingly, both Nup98 and Nup153 have significant nuclear pools in mammalian cells and are dynamically associated with active transcription (Griffis et al., 2002; Griffis et al., 2004). It has been suggested that Nup98 is involved in both transcriptional activation and in shutting mRNA transcripts from active transcription site to the NPC for nuclear export. Several Nup214 gene fusions have also been shown to increase cell proliferation and have been associated with both AML and ALL patients (Takeda and Yaseen, 2014). However, the role of Nup214 in gene regulation is less clear as there is no observable nucleoplasmic pool of Nup214. These observations strongly suggest that NPC components have a critical function in gene regulation in addition to their role in nuclear transport.

1.7 Nup358 and cytoplasmic filament-associated proteins

Originally identified as a RanGTP binding protein, Nup358 (also called RanBP2) is a massive cytoplasmically positioned Nup that has a α-helical N-terminus and numerous functional domains in its C-terminus (Kassube et al., 2012; Wu et al., 1995; Yokoyama et al., 1995) (Figure 1-7A). Positioned on the cytoplasmic face of the NPC, Nup358 has the potential to interact with and affect cargos moving through the NPC. Indeed, Nup358 functional domains associate with a diverse range of factors involved in regulating cellular pathways. Nup358 has essential roles in CRM1 and mRNA nuclear export pathways, as well as functioning in importin α/β and transportin-mediated nuclear import (Bernad et al., 2004; Forler et al., 2004a; Hutten et al., 2009). Mutational analysis revealed that certain domains of Nup358 are required for the activity to specific transport pathways (Walde et al., 2012). Additionally, Nup358 is has several functions during mitosis both during and following NE breakdown. In general, Nup358 is a

multifaceted protein that acts as a platform for the regulation of numerous cellular pathways and is also a target of several diseases.

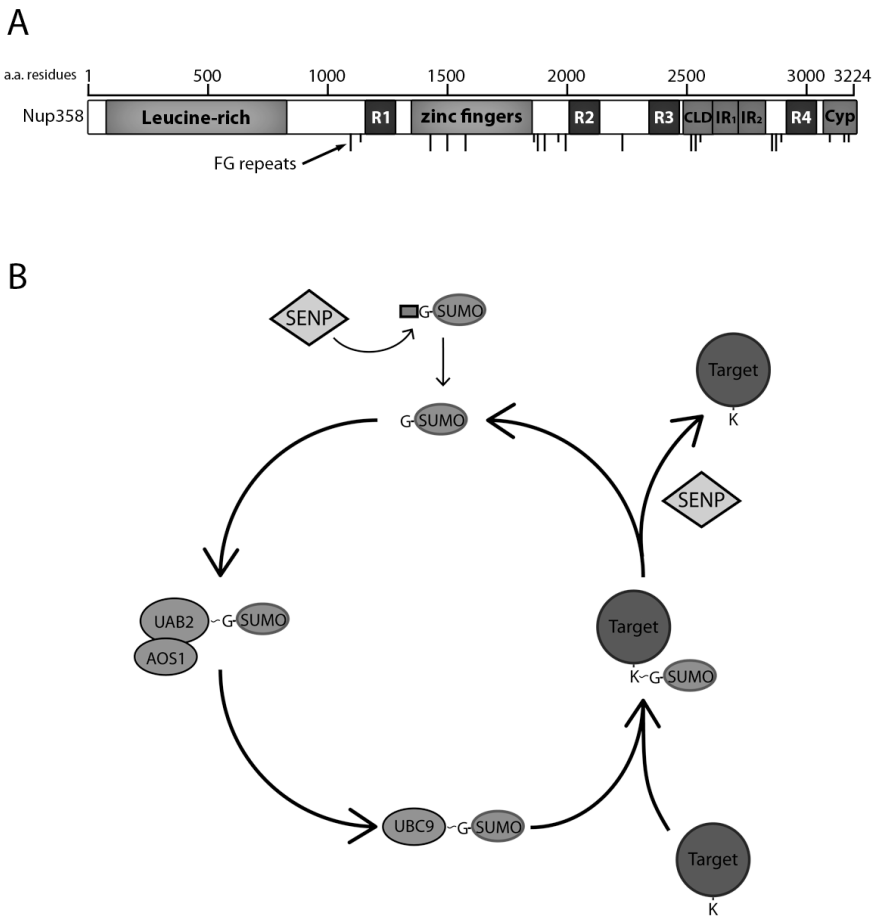

Figure 1-7. **Nup358 and the SUMO pathway**. **A**. Nup358 is a 358 KDa protein that forms a major part of the NPCs cytoplasmic filaments and contains numerous interaction domains. The N-terminal region of Nup358 targets it to the NPC and contains a leucine-rich domain that has RNA binding activity. The C-terminal region contains two internal repeats domains (IR1 and IR2) that act as a SUMO E3 ligase, and two domains that homology to the isomerase cyclophilin A (CLD and Cyp). The central zinc-fingers domain is involved in NE breakdown during mitosis and has been linked to efficient translation of select mRNA transcripts. Additionally, Nup358 contains four Ran binding domains and numerous FG-repeats. **B**. Schematic shows a representation of the SUMO pathway. Prior to entering the SUMO pathway, newly made SUMO is processed by SUMO-specific proteases, belonging to the SENP family, to expose a C-terminal glycine motif. This mature SUMO is then activated through association with the SUMO E1 activating enzymes Uba2 and Aos1. SUMO is then transferred from Uab2 to the E2 conjugation enzyme Ubc9. Ubc9 can then transfer the SUMO molecule to a target protein by catalyzing the formation of a bond between the C-terminal glycine of SUMO and a lysine residue found within specific amino acid sequences in target proteins. Transfer of SUMO from Ubc9 to target proteins is usually catalyzed by an E3 ligase. SUMO modification is reversible through cleavage of the bond between SUMO and target proteins by SENP isopeptidases.

1.7.1 Nup358 and SUMO

One well-characterized function of Nup358 is its activity as an E3 enzyme in the SUMO pathway (Pichler et al., 2002). Post-translational modification of substrates by SUMO has been shown to regulate a vast number of proteins in numerous cellular pathways (sumoylation reviewed in (Flotho and Melchior, 2013)). SUMO-modification or sumoylation of substrates is a reversible process that is achieved through an ATP-dependent enzymatic cascade that resembles the ubiquitin pathway. The process involves an E1 activating enzyme, consisting of 2 subunits (Aos2/Uba1), an E2 conjugating enzyme (Ubc9) and one of a number of SUMO specific E3 ligases (Figure 1-7B). Unlike ubiquitination, sumoylation does not generally lead to protein degradation; rather it is involved in mediating protein-protein interactions, altering protein subcellular location or affecting substrate stability. In many cases, multiple sumoylation events mediate protein interactions leading to the formation of larger protein complexes, which impact various cellular processes. The internal repeats domains (IR1 and IR2), located near the C-terminus of Nup358, binds stably to Ubc9 and acts as an E3-ligase, facilitating the transfer of SUMO to substrates (Figure 1-7B)(Zhang et al., 2002; Zhu et al., 2006). Interestingly, the Nup358 E3 ligase has a unique mode of action not shared by other E3's of either the SUMO or ubiquitin pathway. Instead of facilitating interactions between the conjugation enzyme and substrate proteins, binding to the IR domains of Nup358 alters the structure of Ubc9 resulting in an increase capacity for Ubc9 to transfer SUMO to target proteins (Pichler et al., 2004; Tatham et al., 2005). In this way, it was proposed that Nup358 acts as a general E3 enzyme instead of acting on specific substrates (Pichler et al., 2004). However, in vitro experiments have suggested that Nup358 has some specificity for certain targets (Pichler et al., 2002; Werner et al., 2009). It may be that the levels or morphology of Nup358 in cells determines that capacity of Nup358 to facilitate general or specific SUMO modification *in vivo*.

Various SUMO substrates have been identified for Nup358, the most prominent of which is the transport accessory protein RanGAP. SUMO-modification of RanGAP leads to the formation of a complex between Nup358, SUMO, RanGAP, and Ubc9, effectively sequestering RanGAP on the cytoplasmic face of the NPC (Figure 1-6)(Mahajan et al., 1997; Matunis et al., 1996; Matunis et al., 1998; Reverter and Lima, 2005; Saitoh et al., 1997; Zhu et al., 2006). Enrichment of RanGAP on the cytoplasmic face of the NPC is thought to increase the efficiency of nuclear transport by dissociating nuclear transport complexes as they exit the NPC (see Figure 1-6 and section 1.6.2). It was originally proposed that the formation of the Nup358/RanGAP*SUMO/UBC9 complex effectively blocked the further E3 ligase activity of Nup358, which raised questions about the functional relevance of the Nup358 E3 ligase in cells where the majority of Nup358 is bound by RanGAP (Reverter and Lima, 2005; Werner et al., 2012). However, it has recently been demonstrated that the second internal repeat domain (IR2), which is significantly less effective at *in vitro* SUMO-modification than the IR1 domain, becomes activated when the IR1 is bound to RanGAP (Pichler et al., 2004; Tatham et al., 2005; Werner et al., 2012). Thus, once the Nup358/RanGAP*SUMO/UBC9 complex is formed on the IR1 domain of Nup358, the sumoylation activity of the IR2 domain increases to maintain the E3 ligase activity of Nup358. These results also demonstrate a close proximity between the SUMO E3 ligase activity of Nup358 and nuclear export complex dissociation facilitated by RanGAP suggesting an intricate link between sumoylation and the RanGTPase cycle. Interestingly, the SUMO proteases (sentrin-specific proteases or SENPs), SENP1 and SENP2 associate with Nup153 and mediate SUMO deconjugation on the nuclear face of the NPC, giving further evidence for interconnection of nuclear transport and SUMO modification (Figure 1-7B)(Chow et al., 2012; Hang and Dasso, 2002). Additionally, SUMO modification is required for the proper subcellular localization of a number of transport substrates suggesting a role for Nup358 and the

SUMO pathway in regulating the traffic of specific cargo proteins ((Saitoh et al., 2006; Tatham et al., 2005) and reviewed in (Wang et al., 2012)).

Nup358 also plays an important role in the regulation of NE breakdown and cell division. The Nup358 zinc finger domain (ZFD), located near the middle of the protein, is thought to regulate NE breakdown through interactions with COPI (Prunuske et al., 2006). Sumoylated RanGAP has been shown to concentrate on the mitotic spindle and kinetochores, and the RanGAP-Nup358 complex is necessary for microtubule-kinetochore interactions (Joseph et al., 2004; Joseph et al., 2002). Additionally, through sumoylation of Topo IIα, Nup358 is required for the separation of sister chromatids and it was suggested to have a role in suppression of tumorigenesis (Dawlaty et al., 2008). The role of Nup358 in tumour suppression is supported by the observation that p53 is a potential SUMO substrate of Nup358 (Reverter and Lima, 2005). Depletion of Nup358 also disrupts the organization of nuclear PML bodies, a process which is thought to involve decreased SUMO modification of two prominent PML body proteins, SP100 and PML, suggesting that Nup358-mediated sumoylation may also be involved in the organization of nuclear sub-compartments (Saitoh et al., 2006; Tatham et al., 2005).

Nup358 is also linked to gene regulation through the SUMO-modification of specific HDAC proteins including HDAC4 (Kirsh et al., 2002). Sumoylation causes increased HDAC histone deacetylase activity, which is an important process in regulating transcription (Kirsh et al., 2002). Interestingly, HDAC4 specifically regulates genes involved in the innate immune response and depletion of either HDAC4 or Nup358 leads to increased transcriptional activation of IRF-1 and TNF-α (Scognamiglio et al., 2008). Furthermore, as stated above, several immune signalling proteins, including IRF-1, IRF-5, IRF-3, IRF-7, STAT1 and STAT2, are negatively regulated by SUMO modification (Kim et al., 2008; Kubota et al., 2008; Mabb and Miyamoto, 2007; Nakagawa and Yokosawa, 2002; Rogers et al., 2003; Ungureanu et al., 2005; Ungureanu et

al., 2003). Therefore, though Nup358 has not yet been linked with SUMO modification of immune signalling proteins, its position at the NPC as well as its connection to HDAC-mediated gene regulation suggest that Nup358 may be involved in regulating cellular immune responses (see chapter 5).

1.7.2 Additional functions of Nup358

Nup358 has also been linked to a number of other cellular pathways and processes. The C-terminal end of Nup358 contains a domain that is structurally and functionally similar to CypA (Figure 1-7A)(Lin et al., 2013). Cyclophilins are peptidyl-prolyl isomerases that are characterized by their ability to catalyze the interconversion of cis and trans proline isomers (Reviewed in (Davis et al., 2010)). Cyclophilins were originally described as receptors for certain immune suppressing molecules like cyclosporine, and they have been linked to several viral infections, including HCV and HIV. Structural and biochemical analysis of the C-terminal domain of Nup358 ($Nup358^{CTD}$) uncovered several structural differences from the CypA active site, but have also demonstrated that it retains a low level of isomerase activity (Lin et al., 2013). Both CypA and the Nup358 have been shown to support HIV infection, though the exact mechanism of action is still uncertain (Konig et al., 2008; Meehan et al., 2014; Schaller et al., 2011). One hypothesis for the role of Nup358 in HIV infection suggests that direct binding between the HIV capsid protein and $Nup358^{CTD}$ releases CypA from the viral pre-integration complex (PIC) promoting nuclear import of the RNA and integration into the host cell genome (Lin et al., 2013; Schaller et al., 2011). However, other studies have found that Nup358 impacts HIV infection independent of its C-terminal domain, suggesting that the N-terminal domain is sufficient for HIV infection (Meehan et al., 2014). Therefore, though HIV infection requires Nup358, the exact role of Nup358 is still unclear. Like HIV, there are several studies that show

CypA is required for HCV infection. However, a direct role for Nup358 in HCV infection has not yet been described (see chapter 5). In addition to the C-terminal cyclophilin domain, Nup358 also contains a cyclophilin-like domain (CLD), which has low but significant homology to Nup35^{CTD} (Figure 1-7A)(Ferreira et al., 1995). This domain binds to components of the 26S proteasome and is involved in regulating the steady-state levels of several proteins (Yi et al., 2007).

Nup358 is also a key component of the mRNA export pathway and is linked to efficient translation of specific mRNA transcripts. Nup358 forms a stable complex with components of the mRNA export machinery and depletion of Nup358 leads to decreased release of the mRNA transport complex into the cytoplasm, significantly decreasing mRNA export efficiency (Bachi et al., 2000; Forler et al., 2004b). Additionally, the evolutionarily conserved N-terminal domain of Nup358 has a positive electrostatic potential and can bind ssRNA (Kassube et al., 2012). From these observations, it has been suggested that Nup358 has a role in mRNA export and in mRNP remodelling on the cytoplasmic face of the NPC (Kassube et al., 2012). Moreover, the Nup358 zinc fingers domain (ZFD) is required for efficient translation of mRNA transcripts containing ER target sequences, linking mRNA export to the efficient production of membrane or ER lumen proteins (Figure 1-7A)(Mahadevan et al., 2013). Together, these observations indicate that Nup358 has a prominent role in the trafficking and translation of mRNA transcripts.

The multifaceted nature of Nup358 along with its cellular location makes it as a key regulator of several cellular processes. As such, Nup358 is a major target for many human diseases. Gene expression analysis in multiple myeloma patients showed that the levels of Nup358 were elevated in at least 50 percent of patients (Felix et al., 2009). Additionally, fusions between anaplastic lymphoma kinase and Nup358 have been characterized in patients with inflammatory myofibroblastic tumours (Ma et al., 2003). Mutations in Nup358 have also been

linked to post infection acute necrotizing encephalopathy (Neilson et al., 2009). Finally, as mentioned above, Nup358 is required for several viral infections (see chapter 3 and 4). In general, the different domains of Nup358 have the potential to affect a vast number of cellular pathways which, coupled with its location at the nuclear gateway, makes Nup358 a key protein for future study and perhaps a target for therapeutics.

1.8 The NPC in innate immune responses

The location of the NPC at the interface between the nucleus and cytoplasm indicates that all immune signalling cascades must interact with the NPC in order to facilitate the activation of immune effector genes in cells. Therefore, the NPC has the potential to function as a general regulator of immune responses by controlling the traffic of specific molecules. In addition to its role in transporting immune signalling factors, specific components of the NPC are also ISGs and can facilitate cellular immune responses. The promoter for the Nup98/Nup96 gene contains both GAS and ISRE sequences and the encoded polyprotein is upregulated in macrophage cells in response to IFNγ treatment (Enninga et al., 2002). Once translated, the Nup98/Nup96 protein is cleaved by autoproteolysis leading to the production of individual Nup98 and Nup96 proteins. The overexpression of Nup98 has been shown to rescue the mRNA export block caused by vesicular stomatitis virus (VSV) or influenza infection (Enninga et al., 2002; Satterly et al., 2007). As discussed above, Nup98 also has a significant role in transcription and mRNA export, which may be important for the increase in mRNA transcript production caused by immune stimulation (Capelson et al., 2010; Griffis et al., 2002; Griffis et al., 2004). Indeed, treatment of cells with IFNγ leads to increased levels of intranuclear Nup98 suggesting a transcriptional or gene activation role for Nup98 in immune responses (Enninga et al., 2002). Depletion of Nup96 inhibits export of specific mRNA transcripts including MHCI and MHCII,

which are required for proper immune surveillance (Faria et al., 2006). Additionally, both Nup88 and Nup214 are required for the nuclear import and signalling of the *Drosophila* homologue to NFκB, suggesting a regulatory role for cytoplasmic Nups in immune signalling pathways (Xylourgidis et al., 2006; Yi et al., 2012). Regulation of immune responses at the cytoplasmic face of the NPC is also supported by experiments showing that depletion of Nup358 leads to increased levels of the immune signalling proteins IRF1 and TNF-α (see chapter 5)(Scognamiglio et al., 2008). Together, these data suggest that some components of the NPC, in addition to their general role in transporting immune signalling molecules, may have specific functions in propagating immune responses that may or may not be directly related to nucleocytoplasmic transport. Future research into the functions of the NPC or specific Nups in the innate immunity may provide important insights into the activation and propagation of cellular immune responses.

1.9 The NPC in viral infection

Viruses impact or utilize the NPC and nuclear transport machinery in a variety of ways. First, all viruses that have a nuclear replication phase must interact with the NPC during their life cycle. For a number of nuclear viruses, NPCs or components of the nucleocytoplasmic transport machinery are involved in removing the capsid coat from the viral genome to allow import into the nucleus. For example, targeting of the adenovirus nucleocapsid to the nucleus requires active CRM1-mediated export and capsid uncoating is mediated by association with Nup214 on the cytoplasmic side of the NPC (Strunze et al., 2005; Trotman et al., 2001). One study suggests a model where the adenovirus nucleocapsid tracks along microtubules on kinesin motors to the NPC where it associates with Nup214 while maintaining binding to the kinesin

light chain (Strunze et al., 2011). Nup358 then activates the kinesin heavy chain, which is proposed to exert a pulling force on the capsid and NPC facilitating capsid disassembly. The pulling force is also suggested to disrupt NPC structure, increasing the NE permeability and promoting viral DNA entry into the nucleus. Additionally, Herpes virus capsid uncoating and genome import requires docking with the NPC, facilitated by interactions with Nup214, Nup358 and Impβ (Copeland et al., 2009; Ojala et al., 2000; Pasdeloup et al., 2009). In other viruses, such as Hepatitis B virus, the intact viral capsid appears to be transported to the nuclear face of the NPC were interactions with Nup153 facilitate capsid uncoating and genome release into the nucleus (Schmitz et al., 2010). These observations demonstrate the importance of the NPC and, more specifically, Nup153, Nup214, and Nup358, in nucleocapsid uncoating and genome localization for several viral infections.

Retroviruses, such as human immunodeficiency virus 1 (HIV-1), have an RNA genome that is reverse transcribed into DNA in the cytoplasm before it is imported into the nucleus and integrated into the host cell genome. During the reverse transcription process, several viral and cellular proteins associate with the DNA to form the pre-integration complex (PIC) (Jayappa et al., 2012). A number of viral proteins incorporated into PIC contain NLS sequences and are thought to contribute to nuclear import of the viral genome, but the exact mechanism is still uncertain. Interestingly, HIV infection induces a substantial change in NPC morphology leading to a significant decrease in the levels of 18 of the 30 Nups (Monette et al., 2011). Several siRNA screens have reported that nine different Nups (Nup85, Nup98, Nup107, Nup133, Nup153, Nup155, Nup160, Nup214, and Nup358) and two transport proteins (CRM1 and transportin 3) are host factors required for HIV infection (Brass et al., 2008; Konig et al., 2008; Zhou et al., 2008). However, specific functions in the viral life cycle have only been defined for a subset of these proteins. Nup358 interacts with the viral capsid protein, which promotes docking of the

PIC at the NPC and is thought to regulate transportin dependent import (Di Nunzio et al., 2012; Lin et al., 2013; Schaller et al., 2011). As discussed above, several groups have reported that this process requires the Nup358 CypA domain; however, the role of this domain in HIV infection is still controversial (see section 1.7.2)(Lin et al., 2013; Meehan et al., 2014; Schaller et al., 2011). Nup153 is involved in PIC exit from the NPC and release into the nucleoplasm, but the mechanisms behind this process are also not clear (Di Nunzio et al., 2013; Lee et al., 2010; Matreyek and Engelman, 2011). Additionally, HIV infected leads to increased nuclear localization of Nup62, Nup98, and Nup153, where they function in promoting viral genome integration (Ao et al., 2012; Di Nunzio et al., 2012). Finally, export of the viral RNA also requires association with the nuclear transport machinery, and it is mediated by interactions between the viral Rev protein and Crm1 (Bogerd et al., 1998).

In contrast to the above examples, a number of viruses have developed strategies to inhibit or augment nuclear transport in order to create an environment conducive to viral growth or to avoid immune activation. Several picornaviruses disrupt general transport through the NPC by targeting specific Nups for degradation. Virus derived 2A proteases produced by either poliovirus or human rhinovirus specifically cleave several Nups, including Nup62, Nup98, and Nup153, and a second rhinovirus protease (3C protease) also cleaves Nup214 and Nup358 (Belov et al., 2004; Castelló et al., 2009; Ghildyal et al., 2009; Gustin and Sarnow, 2001; Gustin and Sarnow, 2002; Park et al., 2008; Park et al., 2010; Watters and Palmenberg, 2011). Proteolysis of these Nups leads to a disruption of the NPC permeability barrier and an inhibition of nuclear transport. Encephalomyocarditis virus (EMCV) alters nuclear trafficking by targeting and modifying specific transport Nups. The ECMV leader (L) protein alters NPC-mediated transport through the hyperphosphorylation of Nup62, Nup153, and Nup214 as well as suppressing the activity of RanGTPase and altering the Ran gradient, thereby changing the

transport capacity of the nuclear transport system (Porter et al., 2006; Porter and Palmenberg, 2009). Other viruses disrupt NPC-mediated transport without physically altering the NPC structure. Both SARS-CoV and Ebola virus inhibit specific import pathways by competing for binding sites on certain Kaps or by causing the mislocalization of Kaps (Frieman et al., 2007; Mateo et al., 2010; Reid et al., 2006). Importantly, both these viruses specifically inhibit pathways required for the nuclear localization of STAT1 (Frieman et al., 2007; Kopecky-Bromberg et al., 2007; Mateo et al., 2010; Reid et al., 2006).

Several HCV non-structural proteins have also been shown to interact with Kaps leading to disruption of specific nuclear transport pathways. The HCV NS5A protein interacts with Impβ3 and disrupts its nuclear import pathway (Chung et al., 2000). Proteomics analysis of HCV infected cells revealed that viral NS3 interacts with two other importins and two exportins (Germain et al., 2014). Additionally, four of the ten HCV proteins, including core, NS2, NS3, and NS5A, contain putative NLS sequences, and can enter the nucleus when mutated or produced outside of the context of viral infection (de Chassey et al., 2008; Ide et al., 1996; Isoyama et al., 2002; Kim et al., 1999; Levin et al., 2014; Suzuki et al., 2005). However, only the core protein has been suggested to enter the nucleus of HCV-infected hepatocytes (Cerutti et al., 2011). The physiological relevance of these interactions in situations where the virus life cycle has no clear nuclear intermediate is unclear (see chapters 3 and 4).

Interference with host mRNA export is common strategy for several viruses, since inhibiting host cell protein production can limit immune responses to viral infection. Influenza viruses are negative-strand segmented RNA viruses that replicate in the nucleus of infections cells. In influenza A virus infection, the viral NS1 protein interacts with several components of the mRNA export machinery, including Nup98, Rae1, and NXF1, leading to degradation of Nup98 and a block in the mRNA export pathway (Satterly et al., 2007). Influenza NS1 protein

also disrupts mRNA processing by cleaving several polyadenylation factors (Satterly et al., 2007). To avoid deleterious effects on viral RNA production and export, influenza polymerase functions to polyadenylate viral RNA, which is exported through the CRM1 export pathway rather than the normal host mRNA export pathway (Elton et al., 2001; Watanabe et al., 2001). Therefore, the inhibition of host cell mRNA processing and export pathways by influenza virus acts to both prevent the expression of immune effectors and promote viral replication. Though VSV replicates in the cytoplasm of infected cells, it also inhibits mRNA export by a similar mechanism to that of influenza (Enninga et al., 2002). The VSV M protein is targeted to the nucleus by an internal NLS sequence where it forms a complex with Nup98 and Rae1 leading to the disruption of host mRNA export (Faria et al., 2005; Quan et al., 2014). The inhibition of mRNA export caused by either influenza or VSV can be reversed by the addition of IFNγ, which upregulates components of the mRNA export pathway including Nup98 and Rae1 (Enninga et al., 2002; Satterly et al., 2007). Exogenous overexpression of Nup98, Rae1, or NXF1 can also reverse the mRNA export block induced by influenza infection (Satterly et al., 2007). An mRNA export block has also been observed at later stages of adenovirus infection (Yatherajam et al., 2011). However, this is currently thought to be the result of competition between the highly abundant viral mRNA transcripts and host cell mRNAs for NXF1 and other transport factors (Yatherajam et al., 2011).

1.10 Thesis focus

The NPC is a large multifunctional protein structure that is located at a site of convergence for numerous cellular pathways, and comprises a major regulatory complex for the overall function and organization of eukaryotic cells. The capacity of the NPC to interact with and regulate a diverse range of cellular pathways makes it an ideal target for many diseases and

also makes it a potential focus for the discovery of therapeutic drugs. The work presented here outlines a novel function for the NPC in virus-infected cells as well as a general role for Nups in regulating innate immune activation. Specifically, results shown in chapters 3 and 4 indicate a cytoplasmic role for the nuclear transport machinery in positive-strand RNA virus infection, and they implicate the NPC is a key component in the passive immune evasion strategies of several different viruses. In addition to uncovering a novel role for the NPC in viral infection, these data provide important information about the interactions between viruses and their hosts. Furthermore, data presented in chapter 5 outline a role for the NPC in mediating innate immune responses. On the basis of this work, we propose a dual role for Nup358 in regulating immune activation and supporting viral infection. We hypothesize that Nup358 may function to suppress innate immune responses making it an important target for many diseases. The work presented in this thesis highlights the NPC as a key structure both for viral infection and for the host cell immune responses required to combat viral infection.

CHAPTER II: Experimental Procedures

2.1 Expression Constructs

Descriptions of the constructs used in these studies are provided in (Table 2-1). Expression constructs for production of HCV proteins were generated based on DNA sequences from the H77 strain of HCV by Michael Joyce from the lab of Lorne Tyrrell. The cNLS-2XGFP construct has been previously described (Cardarelli et al., 2007). The FLAG-tagged RIG-I constructs, including pEF-BOS-RIG-I and pEF-BOS-RIG-I-K270A were provided by Michael Gale (University of Washington). DNA fragments for the GFP-RIG-I constructs were amplified from the PEF-BOS-RIG-I plasmids using the Phusion© High-Fidelity PCR Kit (New England BioLabs, E0553L). For NLS (PKKKRKVRRR) or SLN (RRRVKRKKKP) tagged RIG-I, primers were designed containing the NLS or SLN sequences and used to amplify RIG-I. All PCR products were separated on agarose gels followed by purification using the QIAquick gel extraction kit (Qiagen, 28706). Plasmids were propagated in *Escherichia coli* at 37°C using media containing the appropriate antibiotics that pertain to the resistance gene present in each plasmid. Plasmids were isolated from *E. coli* using the QIAprep Spin Miniprep Kit (Qiagen, 27106). PCR products and plasmids were digested using 10 units of the restriction endonucleases described in Table 2-1 for 4 hours follow by separation on agarose gels and purification using the QIAquick gel extraction kit. DNA fragments were then ligated into vectors at a 3:1 molar ratio using T4 DNA ligase (New England Biolabs, M0202S) for 10 minutes and transformed into MAX efficiency© DH5α chemically competent cells (Life Technologies, 18258-012). Successful ligations were selected for by plating on antibiotic plates overnight and confirmed by test digestion followed by sequencing (TAGC applied genomics core).

MDA5 expression constructs were generated by first producing and amplifying cDNA pertaining to MDA5 using the SuperScript® One-Step RT-PCR System with Platinum® Taq

DNA Polymerase (Life Technologies, 10928-034). Primers for amplification were designed with attB recombination sites to allow for recombination into plasmids using the Gateway cloning system (Life Technologies). PCR products were separated on agarose gels followed by purification using the QIAquick gel extraction kit (Qiagen). DNA fragments were then recombined into the pcDONR201 donor plasmid using BP clonase (Life Technologies, 11789013) followed by transformation into One Shot© ccdB Survival™-T1R Chemically Competent Cells (Life Technologies). Positive clones were determined by test digestion followed by DNA sequencing. Positive clones were then recombined into pcDNA3.1/NV5-DEST plasmids from the pcDONR201 constructs using LR clonase (Life Technologies, 11791019) followed by transformation into MAX efficiency© DH5α chemically competent cells (Life Technologies). Transformed cells were grown on lysogeny broth (LB) agar plates containing ampicillin for 16 hours and positive clones were confirmed by test digest and sequencing.

2.2 Cell culture

2.2.1 Immortalized cell lines and HCV replicon cells

Human cell lines including HEK293T (ATCC), A549 (ATCC), HeLa (ATCC), Huh7.5 (Blight et al., 2002), and Huh7 (ATCC) cells, as well as mouse RAW 264.7 cells (ATCC) and African Green Monkey Vero cells (ATCC) were maintained in Dulbecco's modified Eagle's medium (DMEM)(Sigma, D5797) containing 10% fetal bovine serum (FBS) (Sigma, F6178) and penicillin-streptomycin (Sigma, P4333) at 37°C. U937 cells were propagated in RPMI1640 (Life Technologies, 11875-093) media containing 10% FBS (Sigma, F6178) and penicillin-streptomycin (Sigma, P4333) at 37°C. Four days before transfection, cells were switched to media without penicillin and streptomycin to increase transfection efficiencies. All work on tissue culture cells was done in laminar flow cabinets to prevent cell contamination. Huh7 cell

harbouring the JFH-1 HCV replicon (Lohmann et al., 1999) were maintained in DMEM containing 10% FBS and 400 μg/mL Gentamicin (Sigma, A1720). Cell lines were preserved by freezing in 10% dimethyl sulfoxide (DMSO) at -80°C overnight and then transferred to liquid nitrogen for long-term storage.

Table 2-1. Expression constructs

		Insert		Tag		Restriction enzyme		
Vector	Protein	aa Start	aa Stop	N-Term	C-Term	N-Term	C-Term	Template
pcDNA3.1/nV5-DEST	Core	1	118	V5	X	X	X	HCV H77
pcDNA3.1/nV5-DEST	NS3	1027	1649	V5	X	X	X	HCV H77
pcDNA3.1/nV5-DEST	NS4A	1638	1711	V5	X	X	X	HCV H77
pcDNA3.1/nV5-DEST	NS5A	1973	2416	V5	X	X	X	HCV H77
pEGFP-C1	RIG-I	1	926	GFP	X	XbaI	HindIII	pEF-BOS-RIG-I
pEGFP-C1	RIG-I-K270A	1	926	GFP	X	XbaI	HindIII	pEF-BOS-RIG-I-K270A
pEGFP-C1	NLS-RIG-I	1	926	GFP	X	XbaI	HindIII	pEF-BOS-RIG-I
pEGFP-C1	NLS-RIG-I-K270A	1	926	GFP	X	XbaI	HindIII	pEF-BOS-RIG-I-K270A
pEGFP-C1	SLN-RIG-I-K270A	1	926	GFP	X	XbaI	HindIII	pEF-BOS-RIG-I-K270A
pEGFP-C1	cNLS-GFP	N/A	N/A	X	2 X GFP	N/A	N/A	N/A
pcDNA3.1/nV5-DEST	MDA5	1	1025	V5	X	X	X	Huh7.5 rtPCR
pcDNA3.1/nV5-DEST	MDA5-I923V	1	1025	V5	X	X	X	Huh7.5 rtPCR
pcDNA3.1/nV5-DEST	NLS-MDA5	1	1025	V5	X	X	X	Huh7.5 rtPCR
pcDNA3.1/nV5-DEST	NLS-MDA5-I923V	1	1025	V5	X	X	X	Huh7.5 rtPCR
pEF-BOS	RIG-I	1	926	FLAG	X	N/A	N/A	N/A
pEF-BOS	RIG-I-K270A	1	926	FLAG	X	N/A	N/A	N/A
pEGFP-C1	$Nup358^{CTD}$	3062	3224	GFP	X	Xho1	BamH1	TOPO-Nup358
pEGFP-C1	$Nup358^{IR}$	2546	2838	GFP	X	Xho1	BamH1	TOPO-Nup358

2.2.2 Mouse primary macrophages

Five days before collection 3mL of thioglycolate was injected into the peritoneal cavity of 3-5 month old male C57BL/6 mice. For each experiment, 6 to 8 mice were injected in order to collect sufficient peritoneal macrophages for an *in vitro* stimulation experiment. On day 5 after injection, mice were euthanized and the skin was removed from the abdomen by cutting through

the epidermis from a fold of skin pulled away from the midline on the abdomen. Care was taken not to cut into the peritoneum. After the skin was nicked it was torn back from the abdomen to reveal the peritoneal cavity. A 10 mL syringe filled with room temperature phosphate buffered saline (PBS)(137 mM NaCl, 2.7 mM KCl, 4.3 mM Na_2HPO_4, 1.4 mM KH_2PO_4, pH 7.4) was injected into the peritoneal cavity with a 26-gauge needle. Care was taken not to hit the intestines, as this would release *E. coli*. The PBS was massaged throughout the cavity, and the mouse was left on a shaker for 6 minutes. Each mouse was processed, and then PBS was collected from the mice. PBS was removed using a 10 mL syringe and an 18-gauge needle. The needle was inserted into the cavity, the cavity was distended, and the media was aspirated by syringe. PBS was pooled from mice and kept on ice. Cells were collected by centrifugation at 500 x g for 8 minutes and rinsed in ice cold PBS. Cells were resuspended in growth media (DMEM containing 10% FBS) and seeded at a concentration of 2 x 10^6 cells per well in 6-well tissue culture plates. The dish was incubated for 2 hours at 37°C followed by aspiration and replacement of the media with 1 mL fresh growth media. This removed non-adherent cells, which are not macrophages.

Table 2-2. List of buffers

Buffer	Composition
Phosphate buffer saline (PBS)	137 mM NaCl, 2.7 mM KCl, 4.3 mM Na_2HPO_4, 1.4 mM KH_2PO_4, pH 7.4
SDS-sample buffer	0.5 M Tris-base, 100 mM DTT, 15% glycerol, 6.5% SDS, 0.25% bromophenol blue
Phosphate buffer saline with 0.1% tween (PBS-T)	137 mM NaCl, 2.7 mM KCl, 4.3 mM Na_2HPO_4, 1.4 mM KH_2PO_4, 0.1% tween pH 7.4
Isolation Buffer (IB)	225 mM Mannitol, 75 mM Sucrose, 30 mM Tris-HCl (pH 7.4), 0.1 mM EGTA
Mitochondrial Resuspension Buffer (MRB)	250mM Mannitol, 5mM HEPES (pH 7.4)
Percoll Isolation Medium (PIM)	225 mM Mannitol, 25 mM HEPES (pH7.5), 1 mM EGTA, 30% v/v Percoll
IP lysis buffer	10 mM Tris-HCl pH 7.5, 150 mM NaCl, 2 mM EDTA, 0.1% Triton-X100, 1 mM PMSF, 2 μg/ml aprotinin, 2 μg/ml leupeptin and 0.1 units/μl RNasin
IP wash buffer	50 mM Tris-HCl pH7.5, 150 mM NaCl, 0.05% Triton-X100

2.2.3 Virus production and infections

For HCV infection, Huh7.5 cells were seeded at a density of 2.5×10^5 cells/well in 6-well tissue culture plates, and 24 hours after plating, they were infected with 3 RNA genome equivalents of a serially passaged JFH-1 strain of HCV (provided by Takaji Wakita through Lorne Tyrrell)(Wakita et al., 2005). For HAV infection, Huh7.5 cells were grown to 70% confluency and infected with HAV/p16 virus (provided by Stanley M. Lemon, UNC North Carolina USA) at and MOI of 0.1. Cells infected with HAV were propagated for 3 weeks before harvesting. For dengue virus infection, A549 or Vero cells were grown to a density of 2.5×10^5 cells/well in 12-well tissue culture plates, and infected with DENV-2 strain of dengue virus (provided by Tom Hobman, UofA Alberta Canada) at an MOI of 1. Dengue virus-infected cells were harvested 48 hours after infection.

2.2.4 Transfection and reverse transfection

DNA constructs used for transfection protocols were isolated from bacteria using a PerfectPrep Endofree Plasmid Maxi Kit (5 PRIME) to obtain transfection quality DNA. Transfection reactions for each sample were assembled as per the manufacturers protocol using Lipofectamine 2000 (Life Technologies, 11668-019), Fugene 6 (Promega, E2691) or transit LT1 (MirusBio, MIR 2300) transfection reagents. For 6 well plates 4 μg of total RNA was used and 1 μg of total RNA was used. For normal transfection, transfection reagent was added to 6 or 12 well tissue culture plates containing cells at 80% confluency and left overnight. Culture media was then replaced with fresh growth media. For reverse transfection, cells were seeded into wells containing the transfection reagent at a concentration of 7×10^5 cells/well for 6 well plates and 3×10^5 cells/well for 12 well plates. 6 hours after transfection, culture media was replaced with fresh growth media. Cells were harvested 24 or 48 hours after transfection as indicated in each

experiment.

2.2.5 Production of stable cell lines

HeLa cells stably expressing GFP-Nup358^{CTD}, GFP-Nup358^{IR} or GFP were produced by first expressing the constructs into HeLa cells as by normal transfection. 24 hours after transfection, culture media was removed and growth media and 400 μg/mL G418 was added to cells. Cells were passaged in G418 for 2 weeks by plating at a low density (~2.5 × 10^4 per well) into 6 well tissue culture dishes. Individual colonies of cells were then removed from the tissue culture plates and moved to 24 well tissue culture plates containing growth media with 400 μg/mL G418. Once confluent, cells were sequentially seeded into larger plates. Expression of the proper protein was evaluated by western blot and qPCR analysis.

2.3 Lenti virus production and shRNA mediate gene depletion

The lentivirus packaging vectors (pHCMVG and HIV-gag-pol) were provided by Charles Rice (Rockefeller University New York NY)(Schoggins et al., 2011) and the pLKO.1 vectors containing the various shRNA sequences were purchased from Sigma (Sigma)(Table 2-3). To produce lentivirus particles, HEK293T cells, grown in T75 tissue culture flasks (Falcon) to ~80 percent confluency, were co-transfected with pHCMVG, HIV gag-pol and one of the pLKO.1 vectors at a 1:3.5:3.5 ratio (1.6 μg pHCMVG , 5.6 μg HIV gag-pol, and 5.6 μg pLKO.1) in 7 mL DMEM containing 3% FBS. After 6 hours, supernatant was removed and 10mL of fresh DMEM containing 3% FBS was added to each dish. The supernatant containing viral particles was harvested at 3 and 4 day following transfection and cellular debris was removed by filtration through 0.45 μm membrane filters (Millipore). Samples were aliquoted and stored at -80°C. Lentiviral titers were determined by infecting HEK293T cells with serially diluted lentiviral

stocks and selecting for transduced cells with Puromycin (Sigma). Six days after Puromycin selection, colonies in each well were counted to the number of infections units calculated. For lentiviral mediated transduction in Huh7.5 cells, 2.5×10^5 cells were plated in 6-well tissue culture plates and, after 24 hours, infected with lentivirus at a multiplicity of infection (MOI) of 2. For lentiviral transduction in U937 cells, 1×10^6 cells were centrifuged at 800 X g for 5 minutes followed by removal of the old culture media. Cells were then resuspended in growth media containing lentivirus at and MOI of 2. Western blotting and qPCR were used to monitor shRNA mediated gene depletions.

Table 2-3 lentiviral shRNA sequences

Gene	shRNA sequence
Scrambled Control	CCGGGCGCGATAGCGCTAATAATTTCTCGAGAAATTATTAGCGCTATCGCGCTTTTTG
Nup98	CCGGCCCTTGCAGATGGCTCTTAATCTCGAGATTAAGAGCCATCTGCAAGGGTTTTTG
Nup153	CCGGTCTGCTGGTGGTGGCATATTTCTCGAGAAATATGCCACCACCAGCAGATTTTTG
Nup155	CCGGCCCTATCCAAATCCATCCTTTCTCGAGAAAGGATGGATTTGGATAGGGTTTTTG
Kapβ3	CCGGCCATCACTGAAGCACATCGTTCTCGAGAACGATGTGCTTCAGTGATGGTTTTTTG
NDC1	CCGGCCTGTATAGTTCCTATGTAATCTCGAGATTACATAGGAACTATACAGGTTTTTG
Nup153-2	CCGGGCTACAAAGATACTTCAACAACTCGAGTTGTTGAAGTATCTTTGTAGCTTTTTG
Nup155-2	CCGGGCTCTTTAGTATTGCCCTTTACTCGAGTAAAGGGCAATACTAAAGAGCTTTTTG
Nup358	CCGGGCTTGTCAGAATCCAGGTAAACTCGAGTTTACCTGGATTCTGACAAGCTTTTT

2.4 Quantitative real-time PCR (qPCR)

2.4.1 qPCR

For analysis of intracellular RNA transcript levels, total RNA was extracted from confluent cells using TRIzol® reagent (Life Technologies, 15596-018) and cDNA was synthesized using random primers (Life Technologies, 48190-011) and superscript II (Life Technologies, 18064-014) according to the manufacturers specifications. Primers for qPCR were designed using Primer3 software and were used at a concentration of 0.625 μM per reaction (Table 2-4). PCR

efficiency for each primer was determined using the slope of a standard curve derived from qPCR analysis of cDNA serial dilutions. qPCR reaction solutions were made using a SYBR green super mix (Quanta Biosciences, CA101414-258) and samples were run on a Stratagene Mx3005p real time PCR machine. Samples were run in duplicate on each plate to minimize technical error. The PCR parameters were 1 cycle for 1 minute at 95°C followed by 40 cycles of 20 seconds at 95°C, 20 seconds at 58°C and 20 seconds at 72°C. To obtain the relative abundance of specific RNAs from each sample, cycle threshold (ct) values were corrected for the specific PCR efficiency of the primer used, and normalized to hypoxanthine phosphoribosyltransferase 1 (HPRT) ct values. These values were then used to represent the relative transcript level for a given mRNA. For analysis of extracellular HCV RNA levels, RNA was isolated from 200 μL of the media obtained from infected cells using a High Pure Viral Nucleic Acid Kit (Roche, 11858874001). The cDNA was synthesized using superscript III (Life Technologies, 18080044) and an HCV specific primer (see HCV reverse primer sequence Table 2-4). qPCR was done using TaqMan Master Mix with HCV primers and labeled probe (Table 2-4). Results for all qPCR experiments were analyzed in excel. Graphs representing the data obtained from qPCR were produced using excel or GraphPad Prism 5 software, and statistical analysis of values was done using students t-tests.

Table 2-4. Real time qPCR primers used in this study

Primer Name	Sequence
Nup53 Forward	5'-tcctggaacagggcaaagta-3'
Nup53 Reverse	5'-tccaactgggcaggagataa-3'
Nup62 Forward	5'-gtggctccagctaccacatc-3'
Nup62 Reverse	5'-ggctgaattccctgctgag-3'
Nup88 Forward	5'-ggaaagctgttgggtccatt-3'
Nup88 Reverse	5'-gggacacagggtaagcagagta-3'
Nup98 Forward	5'-accacccagaacactggctt-3'
Nup98 Reverse	5'-ggctgtgaggcttgggttac-3'
Nup107 Forward	5'-gagcgccacaaactgtacct-3'
Nup107 Reverse	5'-tgggtcaagtccctggtcta-3'
Nup153 Forward	5'-agcctgtgaaacaccgaaac-3'
Nup153 Reverse	5'-agctggaagatgaagcagtca-3'
Nup155 Forward	5'-ctccactgctgcctgtgata-3'
Nup155 Reverse	5'-cggaagagtggttggaaatc-3'
Nup214 Forward	5'-gctccgcctttacaaacaga-3'
Nup214 Reverse	5'-cacaggctttccaggtcact-3'
Nup358 Forward	5'-tgcaactactggcccttca-3'
Nup358 Reverse	5'-catagactgggccctttgtg-3'
Nup205 Forward	5'-caggcagaggatcgacaact-3'
Nup205 Reverse	5'-gcgaccacaggcattaactc-3'
NDC1 Forward	5'-catttgcagaagggtcagatg-3'
NDC1 Reverse	5'-tcaggtcctgcaaggctaaa-3'
Kap β3 Forward	5'-taatgccgtgggacagatg-3'
Kap β3 Reverse	5'-ccttggtcttccatggtctg-3'
IRF-1 Forward	5'-ggattccagccctgatacct-3'
IRF-1 Reverse	5'-cctgcatgtagcctggaact-3'
HPRT Forward	5'-cctggcgtcgtgattagtg-3'
HPRT Reverse	5'-acaccctttccaaatcctcag-3'
HCV Forward	5'-tctgcggaaccggtgagta-3'
HCV Reverse	5'-gtgtttcttttggtttttctttgaggtttagg-3'
HCV probe	5'-FAM-cacggtctacgagacctcccggggcac-TAMARA-3'
Kap α1 Forward	5'-tgttggctctccttgcagtt-3'
Kap α1 Reverse	5'-ttcttgttgcggcaaagatt-3'
Kap α7 Forward	5'-cttgctgggccctttcttat-3'
Kap α7 Reverse	5'-tgtgcatcagcagctctacc-3'
Kap β1 Forward	5'-atgcgaagggagcactacag-3'
Kap β1 reverse	5'-gggttccagtcatcgtcatc-3'

2.4.2 qPCR immune gene array

ISG transcript levels were evaluated using a TaqMan® OpenArray® RT PCR (Applied Biosystems)(See Table 5-1 for list of ISG specific primer sets). Cell lysis, RNA extraction and cDNA production were done as described (section 2.5.1). Following reverse transcription, 300 ng of cDNA was added to each of the eight sample wells at top of the plate and distributed to each well containing primer sets by centrifugation using the manufacturer's protocol. The plates were then run on an ABI qPCR machine and the resulting data were analyzed in Excel. Samples were normalized to both HPRT and actin transcript levels. Changes between samples and control relative transcript level of >1.5 fold were deemed significant using this assay.

2.5 Antibodies

Antibodies directed against Nup155, NDC1 and Nup98 (Mitchell et al., 2010), as well as Nup53 (Hawryluk-Gara et al., 2005), Lamin B (Chaudhary and Courvalin, 1993), Nup358/RanBP2 (Joseph et al., 2004), Nup153 (Bodoor et al., 1999), HCV NS4B (Paul et al., 2013), HCV NS5A (Lindenbach et al., 2005) and HCV NS5B (Wilson et al., 2003) have been previously described. Commercially available antibodies were used to detect Nup62, Nup153, Nup214, and Nup358 (mAb414)(Covance, MMS-120p), α-tubulin (Sigma-Aldrich, T6074), mouse anti-HCV core (Thermo Scientific, MA1-080), rabbit anti-HCV core (Abcam, ab58713), HCV NS3 (Millipore, MAB8691), karyopherin β3 (Santa Cruz Biotechnology, sc-84578), karyopherin α1/6 (Santa Cruz Biotechnology, sc-6918), FACL4 (Abcam, ab155282), VDAC1 (Abcam, ab15895), Ran (Abcam, ab4781), the FLAG epitope (Abcam, ab1257), S6 ribosomal subunit (Signalway Antibody Co. Ltd., 21225-100), dsRNA (Scicons, J2), HAV capsid (Feng et al., 2013)and the V5 epitope (Abcam, ab27671). For western blotting, the HRP-conjugated and fluor-conjugated secondary antibodies used to detect primary antibodies included: donkey anti–rabbit IgG-HRP

(GE Healthcare, NA934V), sheep anti–mouse IgG-HRP (GE Healthcare, NA931V), Alexa Fluor 750 goat anti-rabbit IgG (Life Technologies, A21039), and Alexa Fluor 680 goat anti-mouse IgG (Life Technologies, A21057). For indirect immunofluorescence microscopy, primary antibodies were detected using Alexa Fluor 488 donkey anti-rabbit IgG (Life Technologies, A21206), Alexa Fluor 488 donkey anti-mouse IgG (Life Technologies, A21202), Alexa Fluor 594 donkey anti-mouse IgG (Life Technologies, A21203), Alexa Fluor 594 donkey anti-rabbit IgG (Life Technologies, A11012), Alexa Fluor 594 donkey anti-goat IgG (Life Technologies, A11058) Alexa Fluor 647 donkey anti-mouse IgG (Life Technologies, A-31571), Alexa Fluor 647 donkey anti-rabbit IgG (Life Technologies, A-31573) and Alexa Fluor 647 Goat anti-mouse IgG (Life Technologies, A21236) secondary antibodies.

2.6 Western Blotting

Cells were washed with PBS and lysed using SDS-sample buffer (0.5 M Tris-base, 100 mM DTT, 15% glycerol, 6.5% SDS, 0.25% bromophenol blue) followed by brief sonication and denaturation at 95°C for 5 min. Total protein concentration in each sample was determined using the Bio-Rad DC™ (detergent compatible) Protein Assay kit (Bio-Rad, 500-0111). 10 μg of total protein from each sample was resolved by SDS-PAGE and transferred to nitrocellulose membranes using a wet transfer system (Bio-Rad) at 4°C. Membranes were blocked with PBS-T (PBS containing 0.1% Tween-20) containing 5% skim milk for 2 hours at room temperature, followed by incubation with anti-sera containing primary antibodies overnight at 4°C. Following incubation with primary antibodies, membranes were washed 3 times for 5 minutes each with PBS at room temperature followed by incubation for 2 hours at room temperature with either the HRP-conjugated or fluor-conjugated secondary antibodies. Primary and secondary antibodies used for western blotting are described in the previous section. For HRP-conjugated

secondary antibodies, membranes were washed in PBS-T followed by initiation of HRP chemiluminescence with ECL detection reagent (GE Healthcare, RPN2106) and the signal was detected using Fuji RX film (Fujifilm, 47410 08399). For fluorescent labeled blots, membranes were sequentially washed in PBS-T, PBS and H_2O and secondary antibodies were detected with an Odyssey infrared imaging system (Licor). Quantification of protein levels detected with the Licor system was done using Odyssey V3.0 software.

2.7 Immunofluorescence

2.7.1 Sample preparation

Tissue culture cells grown on glass cover slips to a confluency of 60-80% were washed with room temperature PBS followed by fixation with 3.2% formaldehyde (Sigma, F8775-500ML) at room temperature for 10 minutes. Samples were then washed 3 times with room temperature PBS followed by permeabilization in 0.2% Triton X-100 (VWR, CA97062-208) for 2 minutes at room temperature and three more washes with room temperature PBS. To visualize lipid droplets, samples were incubated with BODIPY 493/503 (Life Technologies, D3922) for 15 minutes after permeabilization. Cover slips were then blocked in PBS-T containing 2.5% skim milk for two hours at room temperature then incubated with the indicated primary antibodies at 4°C overnight. Samples were then washed with room temperature PBS-T 3 times for 10 minutes each and incubated with secondary antibodies for 45 minutes at room temperature. Coverslips were mounted onto microscope slides using Dapi-Fluoromount-G (Southern BioTech, 0100-20) and stored in the dark at 4°C for up to 5 days. For in situ hybridization of RNA probes using the QuantiGene® ViewRNA ISH Cell Assay (Affymetrix), following secondary antibody incubation, cells were re-fixed for 30 minutes in 3.2% formaldehyde. Samples were then re- permeabilized using detergent solution provided by the kit for 5 minutes. Probe sets pertaining to the positive-

strand (aa 4127-5044) or negative-strand (aa 4127-5044) of the JFH-1 HCV genome (produced by Affymetrix) were the hybridized to the samples by incubating at 40°C for 3 hours. The primary probe signal was amplified by sequential hybridization of pre-amplifier and amplifier DNA probes each at 40°C for 30 minutes. Samples were then incubated with label probes, containing the fluorescent molecules, for 30 minutes at 40°C. Coverslips were mounted onto microscope slides using Dapi-Fluoromount-G (Southern BioTech, 0100-20) and stored in the dark at 4°C for up to 5 days. For evaluation of specific infectivity, cells grown in 96 well optical plates were infected with serial dilutions of supernatants containing virus (described in section 2.12). Three days after infection, cells were fixed and permeabilized in the 96 well plates, followed by incubation with primary and secondary antibodies as described above. Samples were stored in PBS in the dark at 4°C for up to 5 days.

2.7.2 Image acquisition

Epifluorescence images were obtained with an Axio Observer Z1 microscope (Carl Zeiss, Inc.) using a 63x/1.40 NA Oil UPlanS-Apochromat objective lens (Carl Zeiss Inc.). Images taken on the epifluorescence microscope were deconvolved using the 'constrained iterative' algorithm in Axiovision software (Carl Zeiss, Inc.). Confocal images were obtained with a LSM 710 Axio Observer microscope (Carl Zeiss Inc.) using a 63x/1.40 NA Oil DIC Plan-Apochromat objective. Image acquisition from the LSM 710 microscope was done using ZEN software (Carl Zeiss Inc.). Images were acquired either as a single plane or as a z-stack series (with a distance of 0.24 μm between slices). Cells grown on 96 well optical plates were imaged using an Operetta high content imaging system and the images were evaluated using harmony software (PerkinElmer).

2.7.3 Image processing and quantification

Z-series are displayed as average intensity z-projections. Z-projection and merging of channels was done using ImageJ software (National Institutes of Health). Quantification of nuclear and cytoplasmic fluorescence levels was done using ImageJ by calculating to total fluorescence intensity of the nucleus or whole cell followed by subtraction of the nuclear value (cytoplasmic fluorescence). The percent cytoplasmic colocalization of Nups with HCV core or the NS5A protein was calculated in ImageJ using the Manders overlap coefficients as previously described (Manders et al., 1993). Line plots showing relative fluorescence levels were calculated using the line plot toll in ImageJ. Pearson's colocalization coefficients were calculated as previously described using the JACoP plugin for ImageJ (Manders et al., 1992). Photoshop 5.0 (Adobe) software was used for further processing of images and for assembling images into figures.

2.8 Subcellular fractionation

Subcellular fractionation was performed as previously described (Horner et al., 2011; Wieckowski et al., 2009). Huh7.5 cells were infected with HCV as described in section 2.2.3. On day 4 after infection 1 X 10^8 cells were removed from 8 T150 tissue culture plates by scraping in 4 mL isolation buffer (IB)(225 mM Mannitol, 75 mM Sucrose, 30 mM Tris-HCl (pH 7.4), 0.1 mM EGTA) per plate at 4°C. Cells were centrifuged at 100 x g at 4°C and washed two times in 25 mL ice cold IB buffer. Cells were then resuspended in 5 mL of ice cold IB and lysed using 30 strokes of Balch homogenizer (18 μm ball diameter), on ice. The nuclear fraction was isolated from the lysate by low speed centrifugation at 600 x g at 4°C. Crude mitochondria and associated membranes were pelleted from the supernatant obtained after the 600 x g spin by centrifugation at 7000 x g 2 times at 4°C for 10 minutes each. The supernatant was collected and

the microsomal fraction was isolated from the supernatant by centrifugation at 150000 x g at 4°C for 60 minutes followed by removal of the supernatant and resuspension of the microsomal pellet in ~500 μL mitochondrial resuspension buffer (MRB)(250mM Mannitol, 5mM HEPES (pH 7.4)). The mitochondria and associated membranes in the pellet were resuspended in 2mL MRB and layered onto 10mL of Percoll Isolation Medium (PIM) (225 mM Mannitol, 25 mM HEPES (pH7.5), 1 mM EGTA, 30% v/v Percoll). Samples were then centrifuged at 95000 x g for 40 minutes at 4°C to separate the MAM fraction from the mitochondrial fraction. The MAM fraction was removed from the top of gradient and centrifuged for 10 minutes at 6300 x g at 4°C and the resulting supernatant (containing the MAM) was diluted to 10mL with ice cold MRB. These samples were then centrifuged for 60 minutes at 100000 x g at 4°C to pellet the MAM fraction. The pellet containing the MAM fraction was resuspended in ice cold MRB. The mitochondria containing fraction (isolated from the bottom of the Percoll gradient) was further purified by centrifugation for 10 minutes at 6300 x g at 4°C. The pellet was resuspended in ice cold IB and centrifuged again at 6300 x g for 10 minutes at 4°C to pellet the purified mitochondrial fraction. Purified mitochondrial fraction was resuspended in ~500 μL ice cold MRB. All samples were immediately moved to -80°C for storage once isolated. The total amount of protein was calculated for each sample with a DC protein assay kit (Bio-Rad, 500-0116) using the manufacturers protocol. SDS sample buffer was added to each fraction and protein contents were evaluated by western blotting.

2.9 Immunoprecipitation

HEK293T cells were transfected with the constructs encoding for HCV proteins as described in section 2.1. 48 hours after transfection, cells were lysed with 500 μL ice-cold lysis buffer (10 mM Tris-HCl pH 7.5, 150 mM NaCl, 2 mM EDTA, 0.1% Triton-X100, 1 mM PMSF,

2 μg/ml aprotinin, 2 μg/ml leupeptin and 0.1 units/μl RNasin) and incubated on ice for 15 min. Lysates were clarified by centrifugation at 14000 rpm for 15 minutes at 4°C. The resulting supernatant was incubated with anti-V5 antibodies for 4 hours at 4°C and then overnight with protein G sepharose beads. Beads were washed 8 times with 1 mL of ice cold wash buffer (50 mM Tris-HCl pH7.5, 150 mM NaCl, 0.05% Triton-X100). After each wash, the beads were collected by centrifugation (5000 rpm for 5 minutes at 4°C) and the supernatant was removed. Following the last wash, the supernatant was removed and protein was stripped from the beads by adding SDS-sample buffer and incubation at 95°C for 10 minutes. For the immunoprecipitation experiments done in HCV infected cells, Huh7.5 cells were infected for 4 days as described in section 2.2.3. Using the same protocol as the subcellular fractionation experiments, 1 X 10^8 cells were scraped and lysed with a Balch homogenizer in 25 mL IB and the nuclear fraction was removed from the lysate by low speed centrifugation (600 x g for 5 minutes). The remaining cytoplasmic fraction was incubated with mAb414 antibodies for 4 hours at 4°C and then overnight with protein G Dynabeads (Novex, 10004D). Beads were washed 8 times with 1 mL ice cold wash buffer (50 mM Tris-HCl pH7.5, 150 mM NaCl, 0.05% Triton-X100). After each wash, the beads were collected by magnet and the supernatant was removed. Following the last wash, the supernatant was removed and protein was stripped from the beads by adding SDS-sample buffer and incubation at 95°C for 10 minutes. Samples were analyzed by western blotting.

2.10 Synthetic peptides and cell viability

Synthetic peptides including Kap α-NLS-penetratin, Kap β3/IPO5-NLS (Levin et al., 2010a; Levin et al., 2010b), and penetratin (Pietersz et al., 2001) have been previously described. Peptides were manufactured and purified to at least 85% purity by GL Biochem Ltd (Shanghai,

China). For immunoprecipitation experiments, 125 μM of the indicated peptide was added to the culture medium 12 hours post transfection. To assess the effects of peptide treatments on HCV replication, 125 μM of the indicated peptide was added to HCV infected Huh7.5 cells 4 hours after infection and again 2 days after infection. Intracellular and extracellular HCV titers were determined 4 days after infection by qPCR. A MTT (3-(4,5-dimethylthiazol-2-yl)-2,5-diphen yltetrazolium bromide) cell viability assay was used to determine cytotoxicity of shRNA expression or peptide treatment (Levin et al., 2009; Mosmann, 1983).

2.11 Specific infectivity assay

HCV particles were harvested from the culture media of cells infected with just HCV or coinfected with HCV and lentivirus. Total HCV RNA in each sample was calculated using qPCR with HCV specific primers (Table 2-4). Media was then diluted to make viral stocks containing 1 X 10^5 HCV RNA copies/mL. These viral stocks were serially diluted into 100 μL of DMEM containing 10% FBS, which was then added to Huh7.5 cells grown in optical 96 well plates. 2 days after infection, viral focus-forming units were determined by indirect immunofluorescence microscopy using antibodies specific to HCV core protein and counting virus-infected clusters of cells. Images were obtained using the Operetta high content imaging system. The values for specific infectivity were calculated by dividing the number of focus forming units by the total number of HCV RNA copies added to the cells (FFU/HCV RNA copy). The values for specific infectivity show an average over a count of 6 wells, and each experiment was repeated 3 times.

2.12 Immune stimulation and immune gene promoter activation assay

For immune stimulation experiments, cells were incubated over a time course of 24 hours with human recombinant interferon alpha (1000 units/mL)(Intron A, DIN02238675), human

recombinant interferon gamma (500 units/mL)(PBL interferon source, 11500-1), human recombinant TNF-α (100 ng/mL)(Sigma, T15) or γ-irradiated LPS (100 ng/mL)(Sigma, L7770). For the immune gene promoter activation assays, HEK293T cells were first transduced with constructs encoding for the specified shRNA sequences (described in Table 2-3). 24 hours after transduction, cells were trypsinized and ~1 X 10^5 cell were added to each well of a 24 well tissue culture dishes. These cells were then transfected, using the reverse transfection technique described 2.3.4, with constructs encoding for a luciferase reporter gene under the control of the ISRE, GAS, STAT3 or a control promoter sequence. These constructs are part of the cell-signalling pathway profiling system (Clonetech). 48 hours after transfection, cells were harvested by adding 500 μL of the Bright-Glo™ luciferase assay solution (Promega, E2620) to each well for 2 minutes. 200 μL was then taken for each well and added to a 96 well plate and measures for luminescence using an EnSpire® Multimode Plate Reader (Perkin Elmer, 2300-001M).

CHAPTER III: Hepatitis C virus-induced cytoplasmic organelles use the nuclear transport machinery to establish an environment conducive to virus replication

A version of this chapter has been previously published in: Neufeldt, C.J., M.A. Joyce, A. Levin, R.H. Steenbergen, D. Pang, J. Shields, D.L. Tyrrell, and R.W. Wozniak. 2013. Hepatitis C virus-induced cytoplasmic organelles use the nuclear transport machinery to establish an environment conducive to virus replication. *PLoS Pathogens*. 9:e1003744.

3.1 Overview

Hepatitis C virus (HCV) infection induces formation of a membranous web structure in the host cell cytoplasm where the viral genome replicates and virions assemble. The membranous web is thought to concentrate viral components and hide viral RNA from pattern recognition receptors. We have uncovered a role for nuclear pore complex proteins (Nups) and nuclear transport factors (NTFs) in the membranous web. We show that HCV infection leads to increased levels of cytoplasmic Nups that accumulate at sites enriched for HCV proteins. Moreover, we detected interactions between specific HCV proteins and both Nups and NTFs. We hypothesize that cytoplasmically positioned Nups facilitate formation of the membranous web and contribute to the compartmentalization of viral replication. Accordingly, we show that transport cargo proteins normally targeted to the nucleus are capable of entering regions of the membranous web, and that depletion of specific Nups or Kaps inhibits HCV replication and assembly.

3.2 Results

3.2.1 HCV recruits Nups to sites of viral assembly

Observations that several HCV proteins, such as core and NS5A, interact with nuclear transport factors are perplexing, given that these proteins are membrane associated and detected in the cytoplasm, where they participate in HCV replication or assembly. Core, for example, is detected in distinct regions of the cytoplasm and associated with membranes surrounding lipid droplets (Figure 3-1A) (Miyanari et al., 2007). These regions of core concentration lie primarily within areas of the cytoplasm that contain the membranous web (Miyanari et al., 2007). Consistent with this concept, regions of the cytoplasm containing the bulk of the core protein appear largely devoid of microtubules, presumably being excluded by the membranous web (Figure 3-1B). NS5A and NS3 are also detected in the membranous web (Miyanari et al., 2007) and in these regions of microtubule exclusion (Figure 3-1C). However, like several nonstructural proteins, NS5A and NS3 exhibit a broader cytoplasmic distribution outside the membranous web owning to their presence within the ER (Deleersnyder et al., 1997; Miyanari et al., 2007).

We postulated that interactions between HCV components and the nuclear transport machinery could contribute to cytoplasmic processes. Cytoplasmic functions for Kaps have been documented (Harel and Forbes, 2004), and in many cell types a population of NPCs (termed annulate lamellae) are present in the ER where they form transcisternal pores across parallel ER membranes similar to those in the NE. These cytoplasmic NPCs are transport competent, however, what roles they play are unknown (Kessel, 1983; Merisko, 1989). We hypothesized that, during HCV infection, cytoplasmic NPCs might function in the membranous web. To investigate this idea, we first examined subcellular localization of various Nups in Huh7.5 cells infected HCV genotype 2a strain JFH-1. In uninfected cells, immunofluorescence microscopy analysis using antibodies directed against various Nups, including Nup358, Nup155, Nup53,

Nup153, Nup98, and NDC1, an integral membrane component of NPCs, revealed a punctate NE pattern representative of NPCs and cytoplasmic foci characteristic of annulate lamellae (Figure 3-2A). In HCV-infected cells, a similar NE signal was observed, however cytoplasmic levels of each Nup were increased (Figure 3-2A, 3-2B, and Figure 3-3A). Strikingly, the cytoplasmic Nup signals often colocalized with core protein, notably around lipid droplets, and in regions of the cytoplasm with reduced microtubules and containing NS5A-positive membranes (Figure 3-2A, 3-3B, 3-5, and 3-8). A spatial relationship between core and the Nups was further demonstrated by line graphs of fluorescence intensity through regions containing lipid droplets (Figure 3-4). Interestingly, this redistribution of Nups to cytoplasmic compartments was also observed in cells infected other positive-strand RNA viruses, including Hepatitis A virus and Dengue virus, suggesting that there may be a conserved role for cytoplasmic Nups in positive-strand RNA virus infection (Figure 3-6).

We further evaluated the consequences of HCV infection on Nup localization and the physical proximity of Nups and HCV proteins using subcellular fractionation. Subcellular fractionation procedures have previously detected HCV proteins in membranes fractions with sedimentation characteristics similar to microsomes and mitochondrial-associated membranes (MAM) (Horner et al., 2011; Schwer et al., 2004; Wieckowski et al., 2009). We also detected an enrichment of HCV proteins in similar membrane fractions but not in more rapidly sedimenting nuclei and mitochondria containing fractions (Figure 3-2C). In uninfected cells, Nups are primarily detected in nuclear fractions, with the lower levels of these proteins detected in microsomes and the more rapidly sedimenting MAM fraction likely arising from annulate lamellae. Consistent with our immunofluorescence microscopy analysis showing a close association of Nups with core and the membranous web, we observed that HCV infected cells contained increased amounts of various Nups in the microsomal and MAM fractions together

with core and the non-structural proteins NS3 and NS5A (Figure 3-2C). By contrast, Nup amounts in nuclear fractions were unchanged in the HCV infected cells as compared to their uninfected counterparts. Barely detectable amounts of lamin B are seen in the MAM fractions of infected cells, perhaps reflecting a minor nuclear contamination of these fractions or the binding of lamin B to the Nups in these fractions. Nuclear contamination does not explain the increased levels of Nups in the MAM fraction as the Nup:lamin B signal ratio is strikingly higher in this fraction as compared to the nuclear fraction.

To investigate the molecular basis for the interactions of HCV core and other viral proteins with NPCs, we performed immunoprecipitation experiments. Two approaches were used to assess HCV protein-Nup interactions. To examine the interactions of core with NPCs, Nups present in a post-nuclear supernatant derived from HCV infected cell lysates were immunoprecipitated using a monoclonal antibody (mAb414) that binds a shared epitope present in several Nups, including Nup358, Nup214, Nup153, and Nup62. Consistent with our immunofluorescence results, western analysis of the immunopurified Nups detected associated core protein (Figure 3-7A). Similarly, we examined whether immune-purified HCV proteins were bound to Nups. As the purification of HCV proteins from infected cells was unsuccessful, we chose to introduce genes encoding individual HCV proteins tagged with a V5 epitope into HEK293T cells and immunoprecipitate the tagged proteins using anti-V5 antibodies. Western analysis of immunopurified core, NS5A, and NS4A detected Nups associated with a subset of these proteins (Figure 3-7B). Nup107 and Nup153, components of the NPC scaffold and attached filaments, were detected in association with HCV core and NS5A, while Nup358, Nup214, Nup98, and Nup62 were not detected in these immunoprecipitates. Another component of the NPC scaffold, Nup155, was detected in association with NS5A but not with the core protein. By contrast, we failed to detect any Nups bound to immunoprecipitated NS4A.

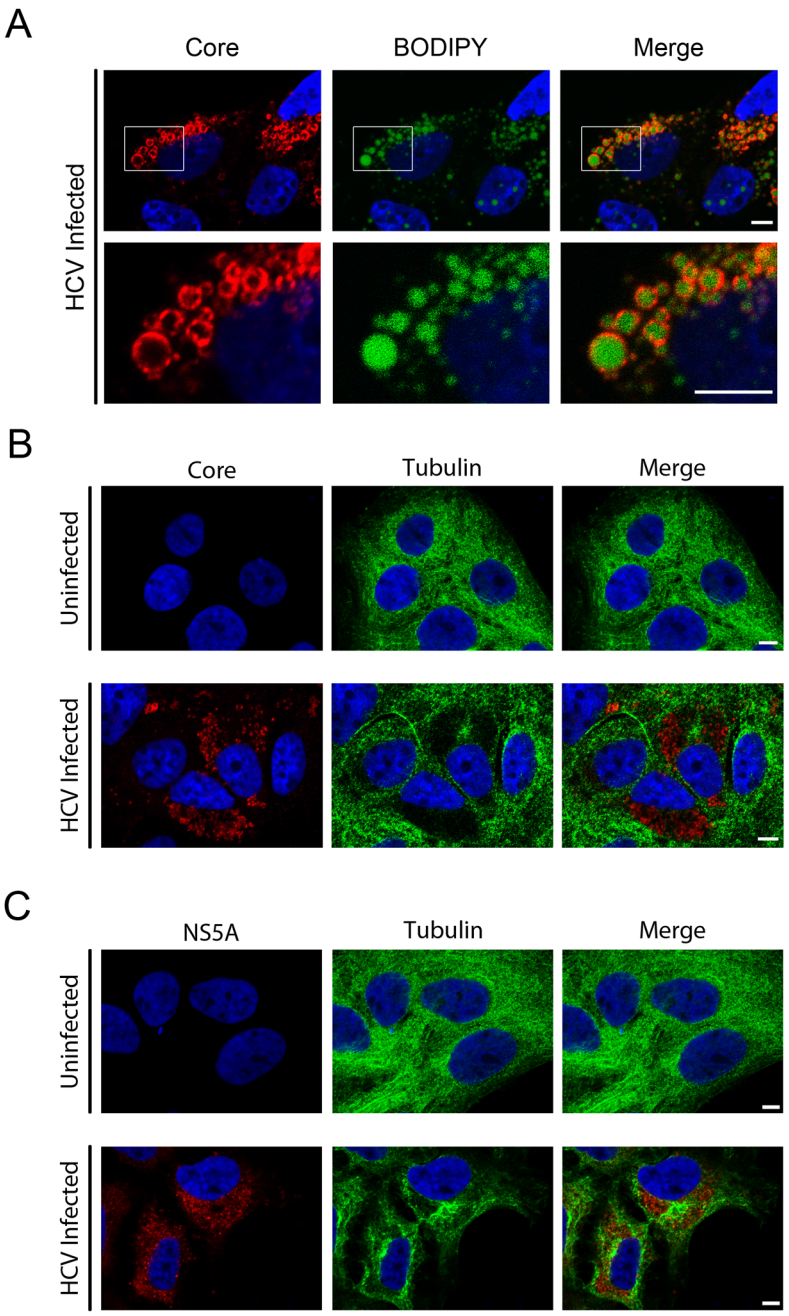

Figure 3-1. Localization of core and NS5A proteins in HCV infected Huh7.5 cells. Huh7.5 cells were infected with HCV for four days. A) The subcellular localization of lipid droplets and HCV core was determined by fluorescence confocal microscopy using BODIPY (green) and antibodies directed against HCV core (red). Boxed areas in the top rows of images are show at higher magnification in the bottom row. DNA was stained with DAPI (blue). B and C) The subcellular localization of tubulin (green) and HCV core (panel B, red) or NS5A (panel C, red) was examined by indirect immunofluorescence confocal microscopy using antibodies directed against the indicated proteins. DNA was stained with DAPI (blue). Scale bars, 5 μm.

Figure 3-2. **Cytoplasmic localization of Nups in HCV-infected tissue culture cells.** Huh7.5 cells were uninfected or infected with HCV for four days. A) Localization of Nups in cells either uninfected (Un) or HCV-infected (HCV) was evaluated by indirect immunofluorescence microscopy using antibodies specific for the indicated Nups or lamin B (green) and HCV core (red). DNA was stained with DAPI (blue). Scale bar, 2 μm (A). B) Changes in the cytoplasmic levels of Nups induced by HCV infection were quantified. The ratio of cytoplasmic to nuclear fluorescence levels were calculated for the indicated Nups and lamin B in uninfected and HCV-infected cells (n ≥10). The statistical significance of differences between uninfected and infected ratios was determined (p-values less than 0.05 (*), 0.01 (**) and 0.001 (***) are indicated). C) Total cell lysates were isolated from uninfected (UN) or infected (HCV) Huh7.5 cells and subjected to subcellular fractionation. Western blotting using antibodies specific for the indicated proteins was used to evaluate the protein levels in each of the indicated subcellular fractions. In addition to the Nups and HCV proteins indicated, markers for residue ER (calnexin), NE (lamin B), mitochondria (VDAC), and MAM (FacL4) proteins are shown. Equal amounts of total protein were loaded into each lane. All samples were run on the same gel and images shown are derived from scans of the same membrane. Data from C were produced with the help of R.H. Steenbergen.

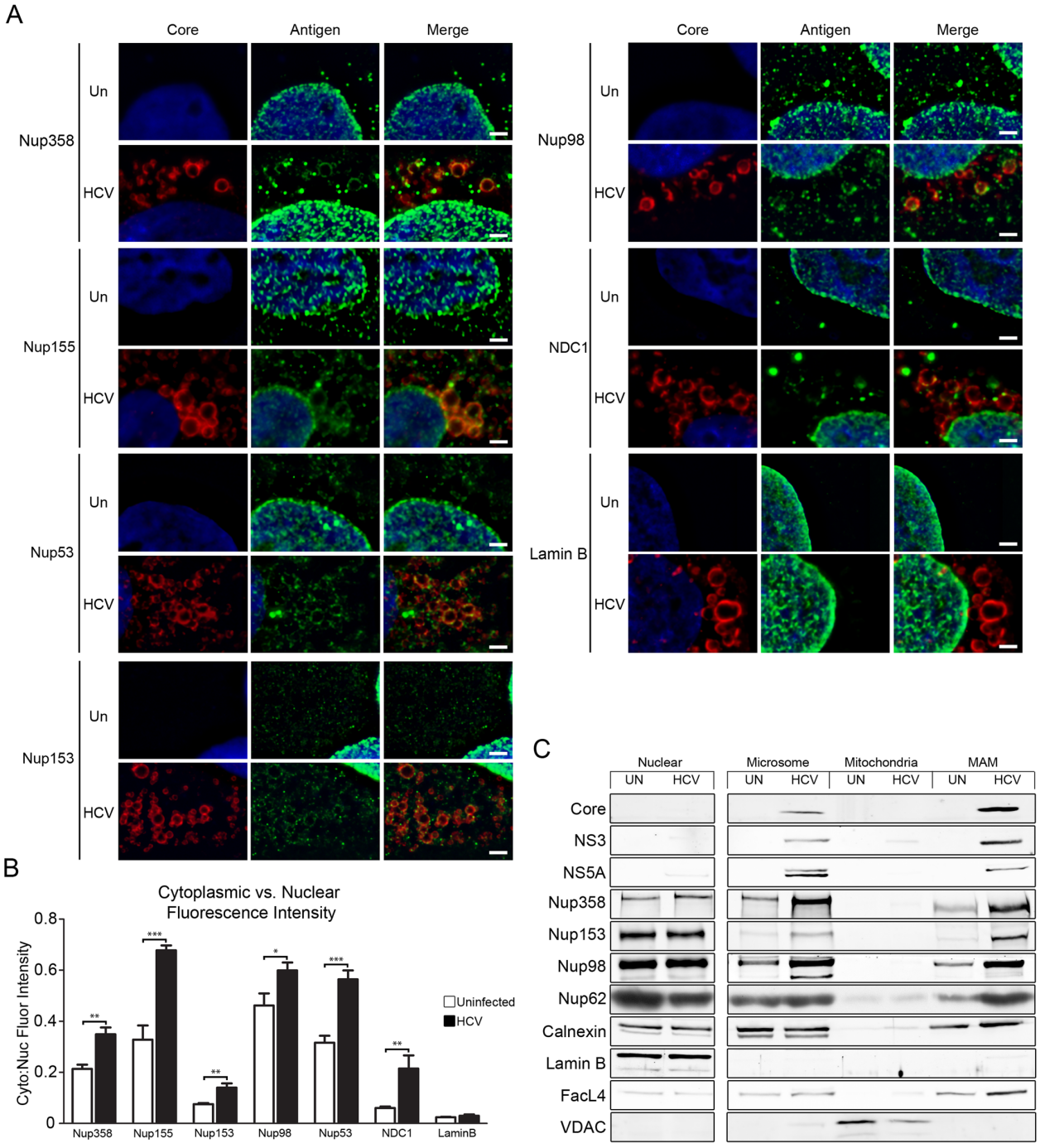

Figure 3-2. Cytoplasmic localization of Nups in HCV-infected tissue culture cells

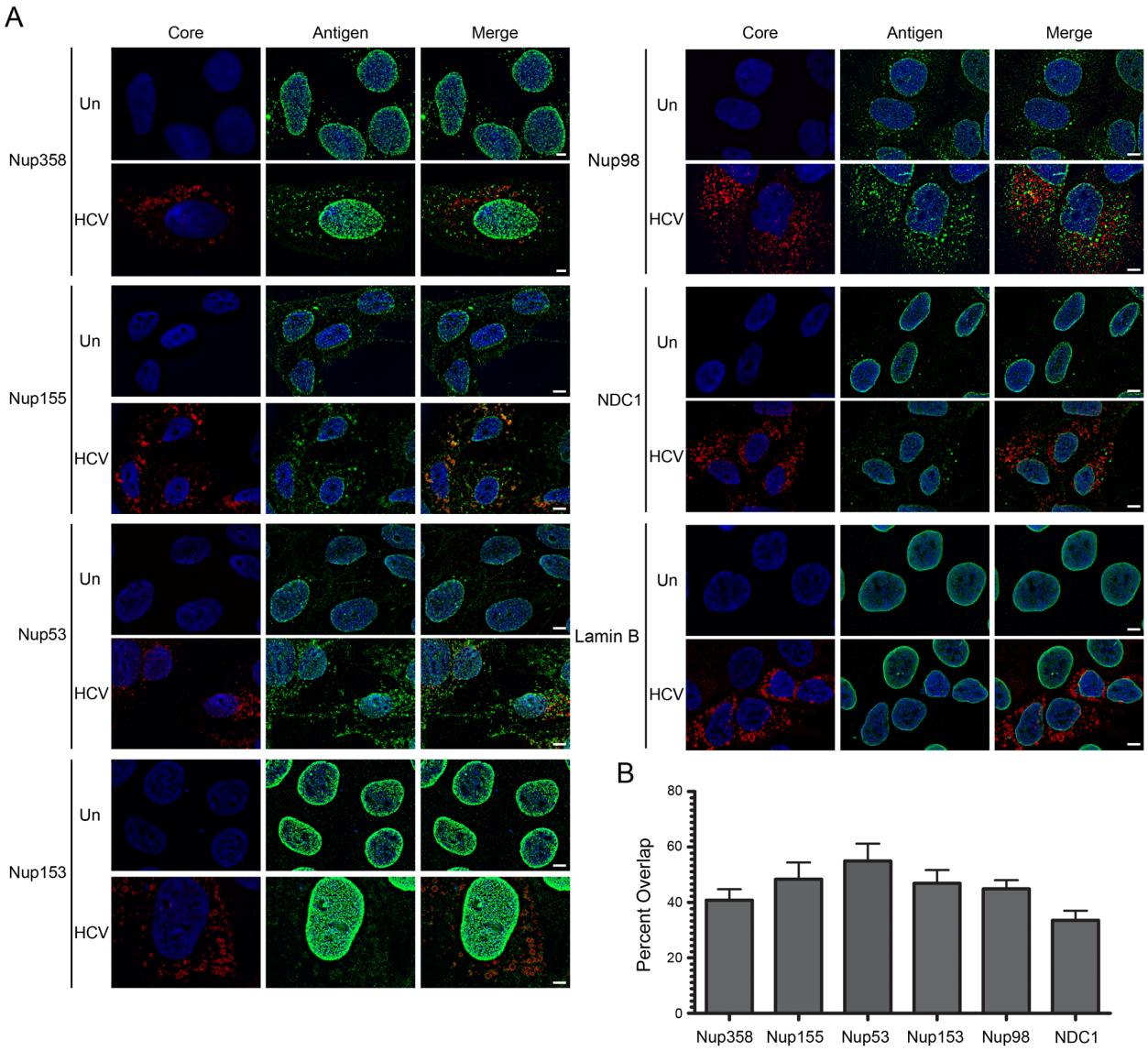

Figure 3-3. Localization of Nups and lamin B in HCV infected cells. A) Localization of Nups and the nuclear lamina was evaluated in uninfected Huh7.5 cells (Un) or 4 days following infection with HCV (HCV) by indirect immunofluorescence microscopy using antibodies specific for the indicated Nups or lamin B (green). HCV core protein localization was determined using anti-core antibodies (red). DNA is stained with DAPI (blue). These images provide lower magnification views of similar test samples examined in Figure 3-2. Scale bars, 5 μm. B) Percent colocalization between cytoplasmic Nups and HCV core protein in an average of ≥ 10 cells processed as in panel A was determined. Values represent the percent of the cytoplasmic Nup fluorescence signal overlapping with the HCV core fluorescence signal calculated using the Manders colocalization coefficient.

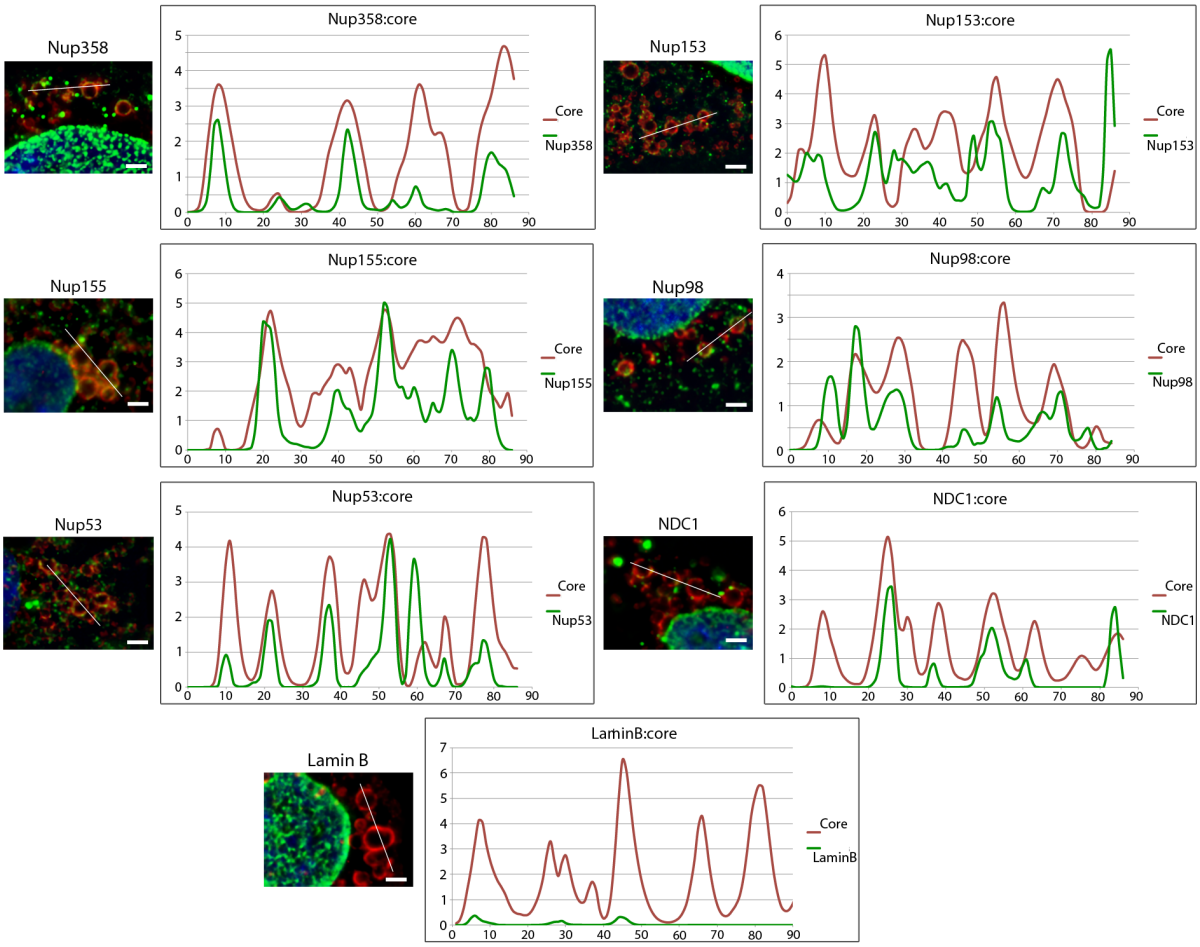

Figure 3-4. Colocalization between Nups and HCV core proteins. Huh7.5 cells were infected with HCV for 4 days. The localization of Nups and lamin B compared to HCV core was evaluated using indirect immunofluorescence by staining with antibodies specific for Nups and lamin B (green) or HCV core (red). Fluorescence intensity line graphs were plotted using pixel intensity data obtained from red and green fluorescence channels along lines (white) drawn through regions containing core protein and lipid droplets. Values on the Y-axis represent relative fluorescence intensity and values on the X-axis represent distance in pixels. DNA was stained with DAPI (blue). Scale bars, 2 μm.

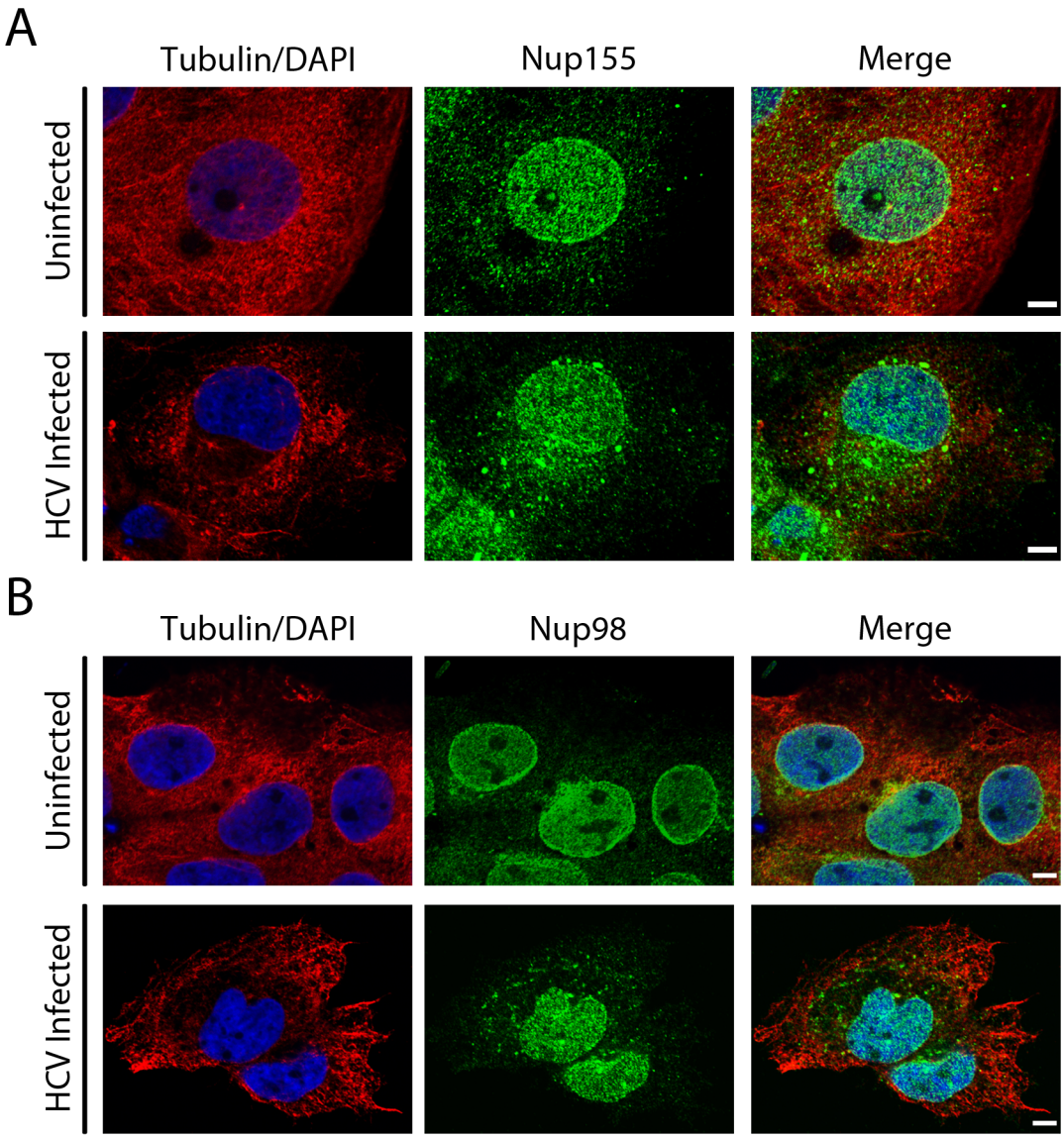

Figure 3-5. Localization of Nups and tubulin in HCV infected cells. A-B) The localization of Nup98 or Nup155 and tubulin was evaluated in uninfected or HCV infected Huh7.5 cells four days after infection. Cells were examined by indirect immunofluorescence confocal microscopy using antibodies directed against Nup155 (panel A, green) or Nup98 (panel B, green) and tubulin (red). DNA was stained with DAPI (blue). Scale bars, 5 μm.

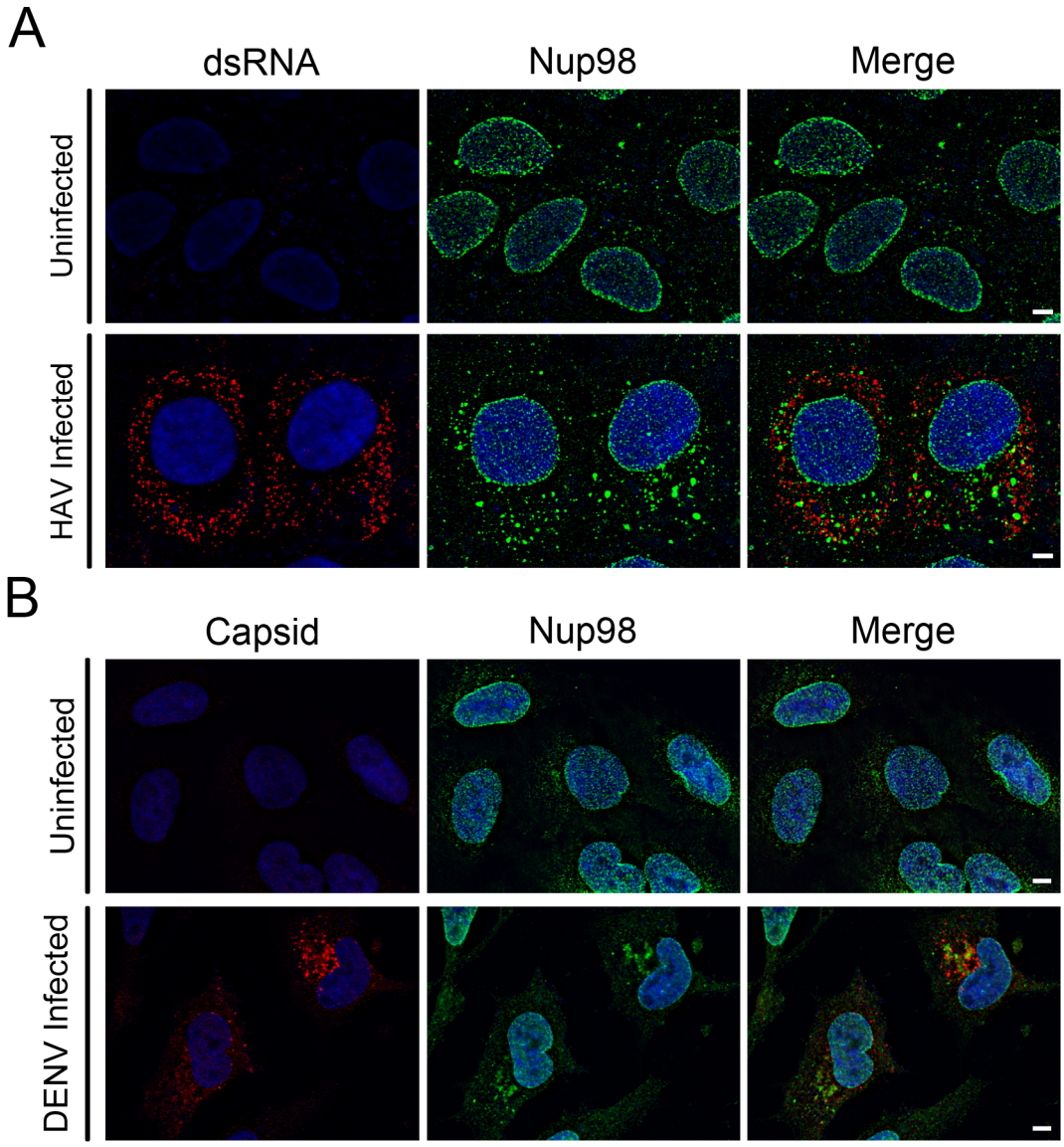

Figure 3-6. Cytoplasmic localization of Nups in dengue and hepatitis A virus infected cells. A) The localization of Nup98 was examined by indirect immunofluorescence microscopy in uninfected Huh7 cells and cells infected with hepatitis A virus (HAV infected) for three weeks using anti-Nup98 antibodies (green). Hepatitis A viral RNA was detected using anti-dsRNA antibodies (red). B) Localization of Nup98 was also examined in dengue virus (DENV) infected A549 cells (2 days post infection) as described in panel A (green) and compared to the localization of dengue virus capsid protein using capsid specific antibodies (red). In both panels, DNA was stained with DAPI (blue). Scale bars, 5 μm. Images in A were produced with the aid of D. Pang.

The interactions of core and NS5A with Nups were further evaluated by immunofluorescence analysis of cells expressing genes encoding these tagged HCV proteins or the JFH-1 subgenomic replicon. In cells producing core or NS5A, regions of the cytoplasm containing these proteins also showed colocalizing Nups, including Nup155 and Nup98 (Figure 3-7C and 3-8A); moreover, these Nups appeared reduced at the NE. A similar phenotype was not observed in cells expressing NS4A, leading us to conclude that core and NS5A are among those HCV proteins that interact with Nups. We also examined the localization of several Nups in cell expressing the JFH-1 subgenomic replicon, which lacks the coding region for core through the NS2 protein of the HCV polyprotein. Cells containing the replicon develop membrane alterations similar to the HCV-induced membranous-web (Gosert et al., 2003). In these cells we detected increased cytoplasmic levels of Nup358 and extensive colocalization of Nup155 with membrane-associated NS5A (Figure 3-9). Consistent with these observations, in HCV infected cells, cytoplasmic Nup155 exhibited an ~ 55% overlap with NS5A (Figure 3-8B and 3-8C), and, more generally, the increased cytoplasmic NPC foci seen during infection occupy similar regions of the cytoplasm as membranous web-associated NS5A (as revealed using anti-Nup98 antibodies; Figure 3-8). Interestingly, some Nups that were recruited to the cytoplasmic membranes in the HCV infected cells were not altered in their distribution in the replicon containing cells, including Nup98 and NDC1 (Figure 3-9). These results imply that those HCV proteins missing from the replicon containing cells, such as core, are required for the recruitment of additional Nups to cytoplasmic membranes.

Figure 3-7. Identification of Nups that physically interact with HCV proteins. A) Cell lysates were isolated from uninfected (Un) and HCV-infected (HCV) Huh7.5 cells four days after infection. The nuclear fraction was removed from the lysates by sedimentation and the remaining cytoplasmic fraction was incubated with the monoclonal antibody mAb414 specific for a subset of Nups. Proteins present in cell lysates and mAb414 immunoprecipitates (mAb414 IP) were analyzed by western blotting using antibodies specific for HCV. B) Constructs encoding for the indicated V5-tagged HCV proteins or an empty V5 vector (ctrl) were transfected into HEK293T cells and expressed for 48 hours. V5-tagged proteins were immunoprecipitated with anti-V5 antibodies and associated proteins were evaluated by western blotting using antibodies against the indicated Nups and the V5 epitope. C) Subcellular localization of Nup155 in Huh7.5 cells expressing the indicated V5-tagged HCV proteins was examined by indirect immunofluorescence microscopy using antibodies directed against Nup155 (green) and the V5 epitope (red). DNA is visualized with DAPI (blue) and arrows point to transfected cells. Pearson's colocalization coefficients were calculated to assess colocalization of Nup155 and the indicated V5 tagged protein and are shown at the top of the merged panel. Values > 0.5 are considered significant. Scale bar, 10 μm. Data shown in panel B were obtained by A. Levin.

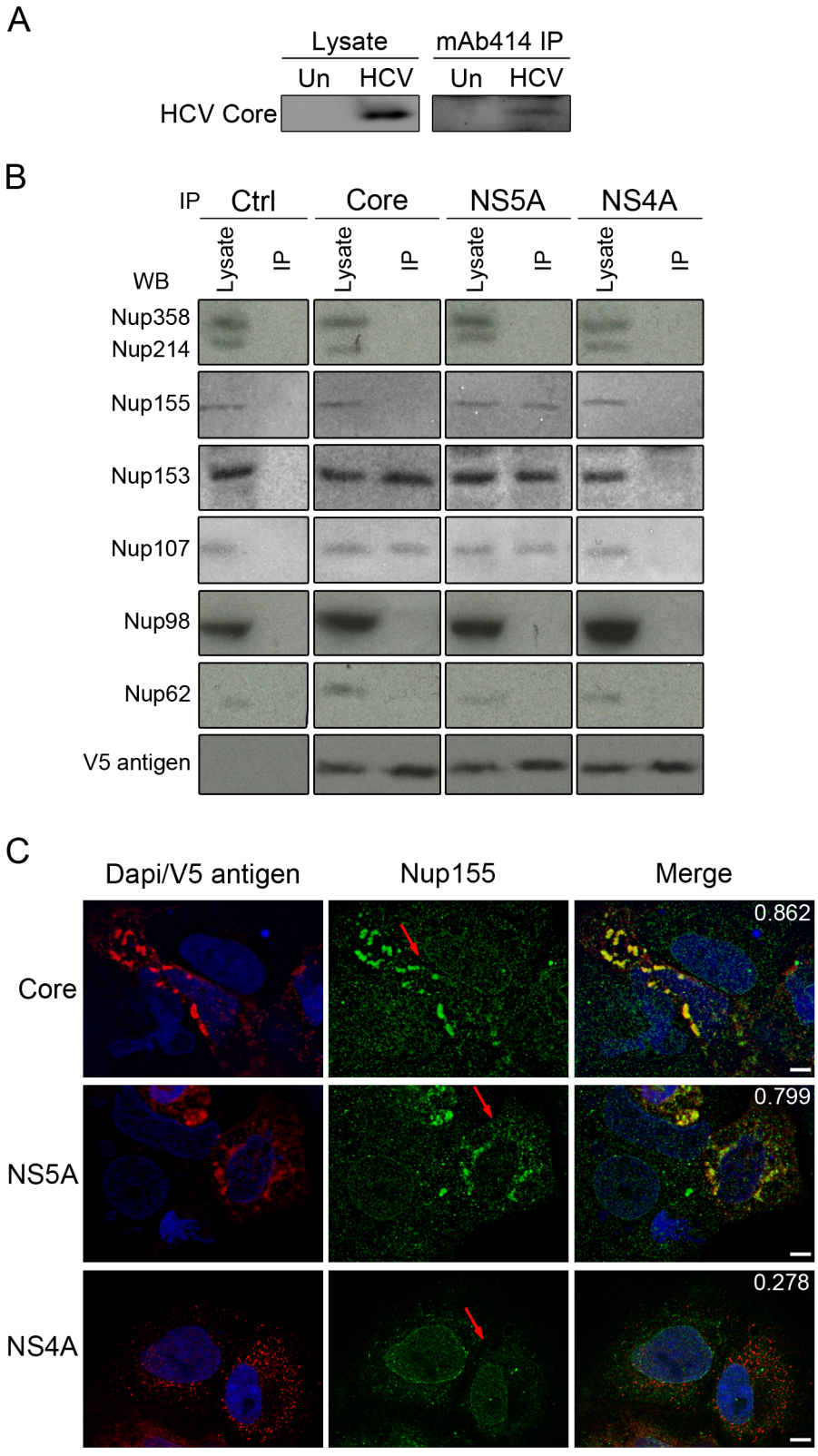

Figure 3-7. Identification of Nups that physically interact with HCV proteins

Figure 3-8. Localization of Nups and HCV proteins in transfected or HCV-infected cells. A) Huh7.5 cells were transfected with constructs encoding for V5-tagged HCV core, NS5A, or NS4A. The localization of the Nup98 and tagged HCV proteins was examined 48 hours later, by indirect immunofluorescence confocal microscopy using anti-Nup98 (green) and anti-V5 (red) antibodies. Arrows point to cells expressing the indicated HCV protein and Pearson's colocalization coefficients are specified in the merge panel. DNA is stained with DAPI (blue). Scale bars, 10 μm. B) The localization of Nup155 and Nup98 was evaluated in uninfected Huh7.5 cells (Un) or 4 days following infection with HCV (HCV) by indirect immunofluorescence confocal microscopy using antibodies specific for the indicated Nups (green) and HCV NS5A protein (red). Boxed areas in the middle rows of images are show at higher magnification in the bottom row. DNA is stained with DAPI (blue). Scale bars, 5 μm. C) Percent colocalization between cytoplasmic Nups and NS5A in an average of ≥ 10 cells processed as in panel B was determined. Values represent the percent of the cytoplasmic Nup fluorescence signal overlapping with the HCV core fluorescence signal calculated using the Manders colocalization coefficient.

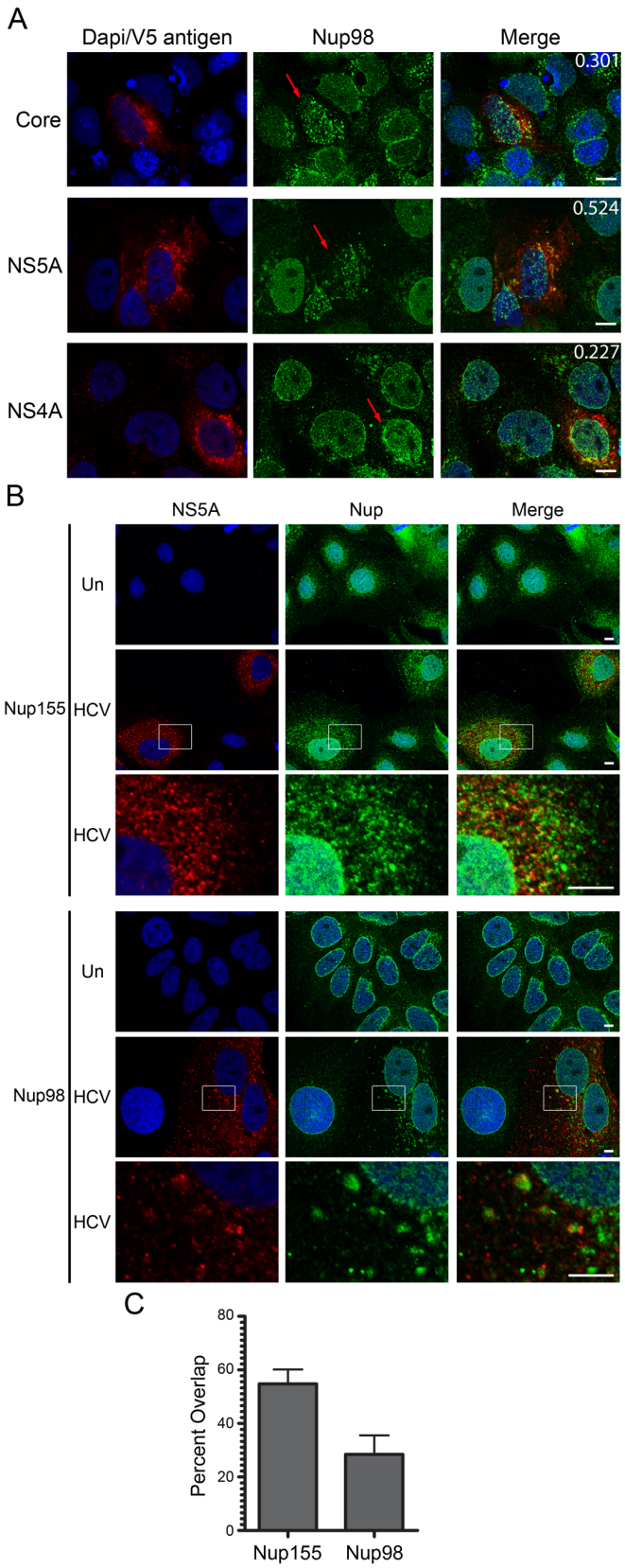

Figure 3-8. Localization of Nups and HCV proteins in transfected or HCV-infected cells.

Figure 3-9. Localization of a subset of Nups in Huh7 cells expressing the JFH-1 subgenomic replicon. Huh7 cells expressing or not expressing the JFH-1 subgenomic replicon (encoding NS3 through to the C-terminus of the HCV polyprotein) were analyzed by indirect immunofluorescence using antibodies directed against the HCV protein NS5A (red) and the indicated Nups (green). DNA is stained with DAPI (blue). Scale bars, 5 μm.

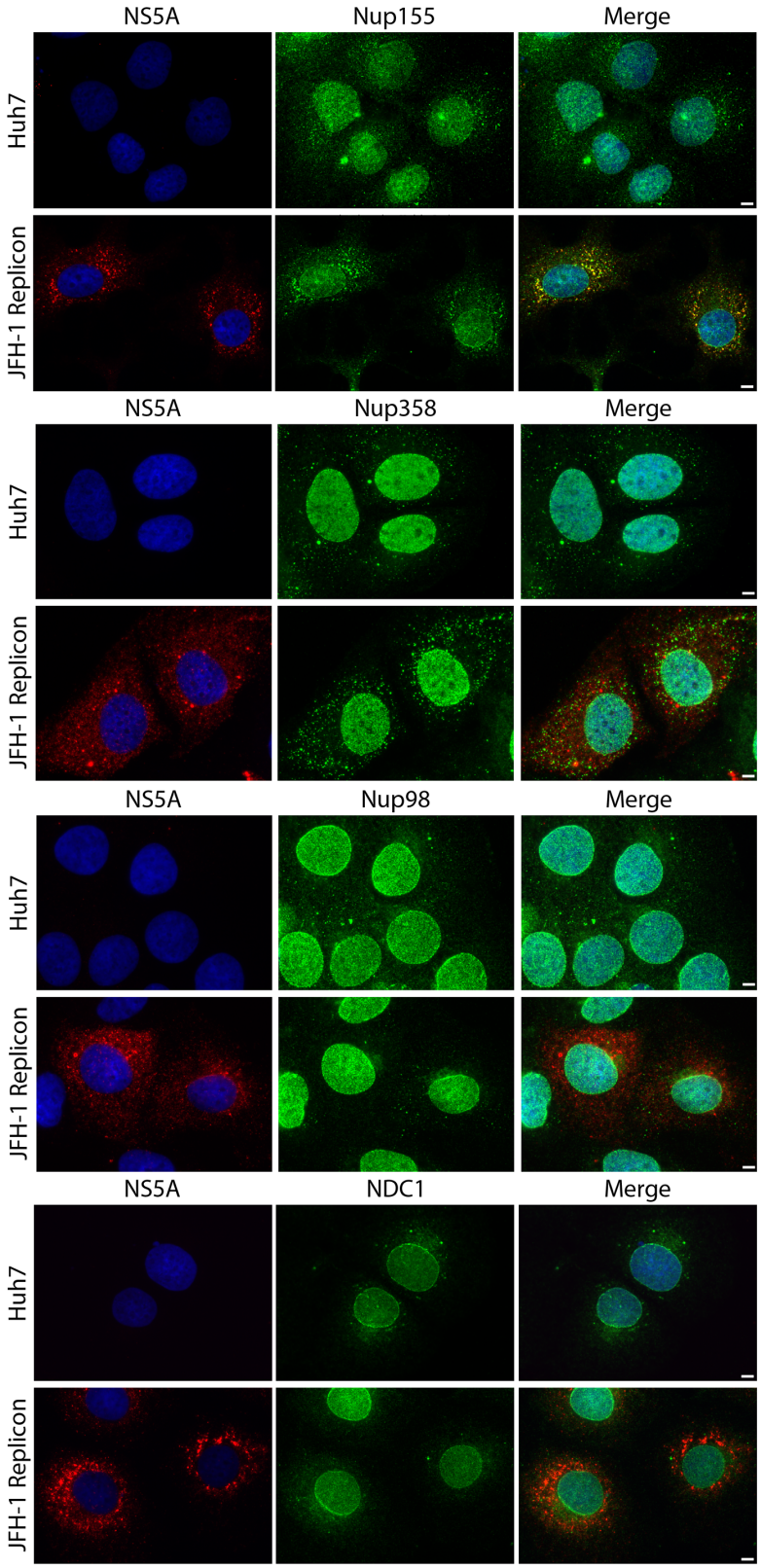

Figure 3-9. Localization of a subset of Nups in Huh7 cells expressing the JFH-1 subgenomic replicon.

3.2.2 HCV infection alters Nup mRNA and protein levels

The accumulation of Nups in the vicinity of HCV assembly sites could arise from redistribution of cellular pools, increased cellular levels of these proteins, or a combination of both events. To assess the potential contribution of increased Nup synthesis, we examined cellular levels of various Nup mRNA transcripts at time points after HCV infection of Huh7.5 cells (Figure 3-10A). We found that mRNA levels of Nups composing the cytoplasmic filaments of the NPC (Nup88, Nup214 and Nup358), and one that is part of the nuclear basket (Nup153) were reproducibly elevated 1.5- to 2-fold four days after HCV infection (Figure 3-10A) in a manner that qualitatively paralleled increasing HCV RNA levels. In addition, Nup358 showed a reproducible biphasic pattern with an additional peak visible at 2 days after infection. By contrast, levels of transcripts encoding for several Nups that make up the scaffold of the NPC (including Nup155, Nup107, Nup53, and Nup205) and two associated Nups, Nup62 and Nup98, showed little or no change during HCV infection. Consistent with the changes in transcript levels, quantitative analysis of a subset of these Nups by western blotting showed increased levels of Nup98, Nup153, and Nup358, but not Nup155 (Figure 3-10B). These results indicate that a subset of Nups are up-regulated during HCV infection while others show no statistically significant change. Thus, the Nups recruited to sites of viral assembly are likely to arise from both constitutive and HCV-induced Nup expression.

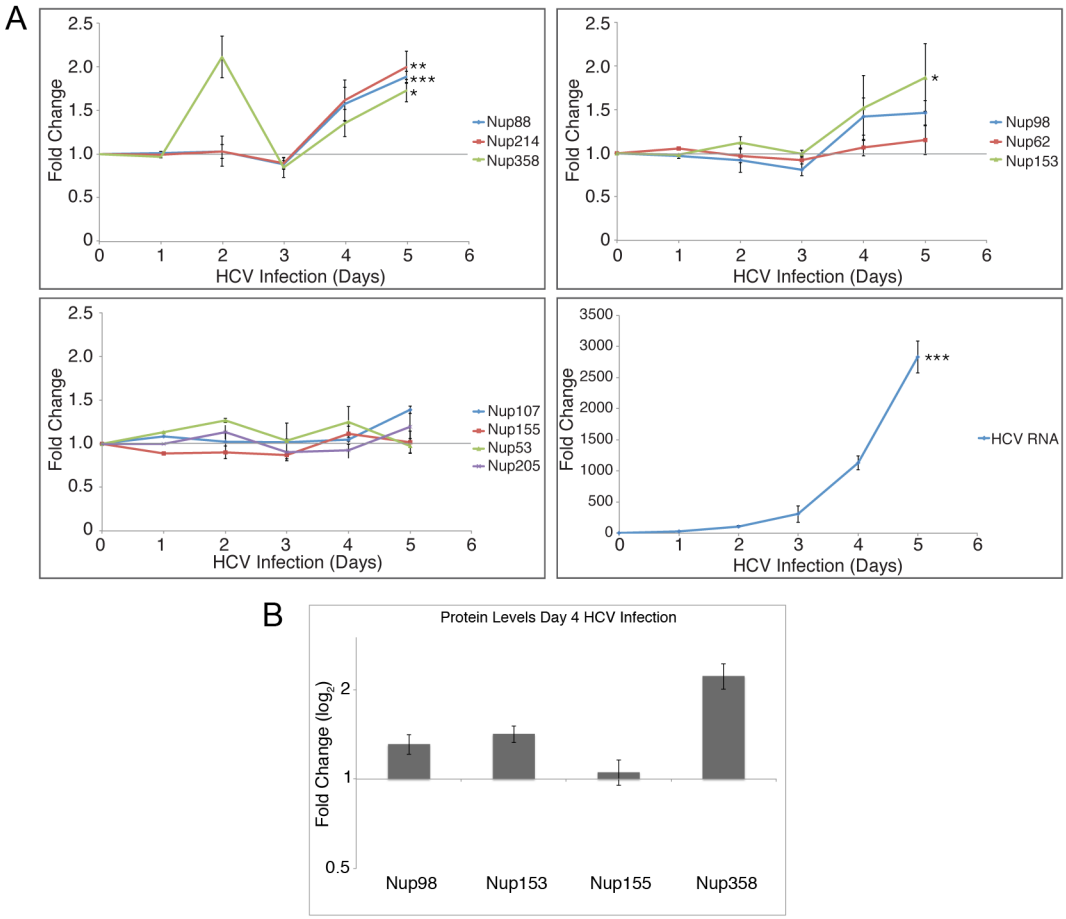

Figure 3-10. HCV infection increases RNA and protein levels of a subset of Nups. A) Total RNA was isolated from cell lysates at the indicated time points after infection of Huh7.5 cells with HCV, and levels of specific mRNA transcripts were assessed by qPCR. Values for each sample were normalized to HPRT and are expressed relative to uninfected cells (day 0 time point). HCV RNA levels are shown as fold change relative to HPRT. Error bars indicate standard error (based on ≥ 3 experiments) and statistical significance was evaluated using t-tests comparing each infected sample to an uninfected control sample. p-values less than 0.05 (*), 0.01 (**), and 0.001 (***) are indicated. B) Cell lysates were harvested from HCV infected Huh7.5 cells four days after infection and Nup proteins levels were determined by western blotting using antibodies specific for Nup98, Nup153, Nup155, and Nup358. Protein levels were quantified and normalized to tubulin levels and the fold-change is relative to uninfected cells. Error bars were determined using data from ≥ 3 experiments.

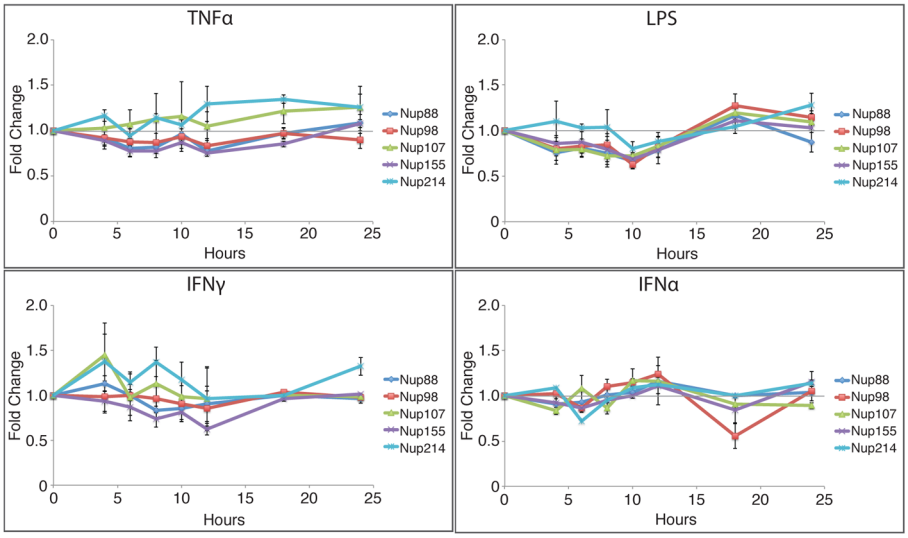

Figure 3-11. Activation of innate immune pathways does not significantly alter levels of various Nups in Huh7.5 cells. Huh7.5 cells were treated with IFNγ (500 units/mL), TNF-α (100 ng/mL), LPS (0.1 μg/mL), or IFNα (1000 units/mL). At various time points transcript levels of the indicated Nups were evaluated by qPCR. Samples were normalized to HPRT transcript levels and fold change is relative to samples derived from untreated cells.

3.2.3 HCV core and NS5A interact with Kap β3 and Kap α

To further understand the physical and functional basis for the interaction of HCV proteins with Nups, we considered the potential role of putative NLS sequences (i.e. potential nuclear transport factor binding domains) present in several HCV proteins, including core and NS5A. NLS sequences can bind Kaps, which, in turn, could mediate the interactions of the HCV proteins with Nups. Therefore, we tested whether these HCV proteins were capable of binding Kaps and whether this interaction was responsible for their binding to Nups. The NLS sequences in Core and NS5A are predicted to bind specific members of the Kap family: Kap β3/IPO5 and the Kap α/β1 complex (Chung et al., 2000; Isoyama et al., 2002; Levin et al., 2014). Thus, we immunoprecipitated V5-tagged core, NS5A, or NS4A from cell extracts and probed for associated Kap β3/IPO5 and the Kap α/β1 complex. Antibodies directed against Kap β3/IPO5 and Kap α detected these proteins in association with core and NS5A but not NS4A, which lacks a predicted NLS (Figure 3-12A). These interactions could be inhibited by competing NLS-containing peptides. Treatment of cells with cell-penetrating Kap β3/IPO5-specific NLS peptides or the overexpression of a Kap α-specific NLS (cNLS)-containing reporter protein blocked the interactions of core and NS5A with these Kaps. However, disruption of Kap interactions with core and NS5A did not alter their binding to Nup153, Nup107, or Nup155, showing that binding of these HCV proteins to Nups is not mediated by Kaps (Figure 3-12A and 3-13A).

Considering the redistribution of Nups observed in HCV infected cells, we examined whether the cellular distribution of Kap β3/IPO5 was also altered in these cells. In uninfected cells, immunofluorescence microscopy analysis detected Kap β3/IPO5 both within the nucleus and the cytoplasm. In HCV infected cells, a similar distribution was observed, however Kap β3/IPO5 appeared enriched in regions of the cytoplasm adjacent to, or occupied by, HCV core

protein (Figure 3-12B). This recruitment of Kap β3/IPO5 to centers of HCV assembly does not appear to arise from increased expression of the Kap β3/IPO5 encoding gene, as cellular levels Kap β3/IPO5 mRNA were not significantly increased in HCV infected cells (Figure 3-13B). Similarly, levels of Kap β1 and Kap α mRNAs were also not significantly changed.

Figure 3-12. Identification of Kaps that physically interact with HCV proteins through NLS sequences. A) Constructs encoding the indicated V5-tagged HCV protein or an empty V5 vector (Ctrl) were transfected into HEK293T cells. 12 hours after transfection, cells were subjected to no treatment, treatment with Kap β3/IPO5-NLS peptides, treatment with control penetratin peptides, or transfection with a construct encoding for a cNLS-GFP fusion protein and incubated for an additional 36 hours. Following treatment, cells were lysed and V5-tagged HCV proteins were immunoprecipitated with anti-V5 antibodies (IP). Associated proteins were detected by western blotting using antibodies against the indicated Nup or Kap (WB). B) The subcellular localization of Kap β3/IPO5 in Huh7.5 cells uninfected or infected with HCV was determined by indirect immunofluorescence microscopy using antibodies specific to Kap β3/IPO5 (green) and HCV core (red). DNA was stained with DAPI (blue). Scale bars, 5 μm. Data shown in panel A were obtained by A. Levin.

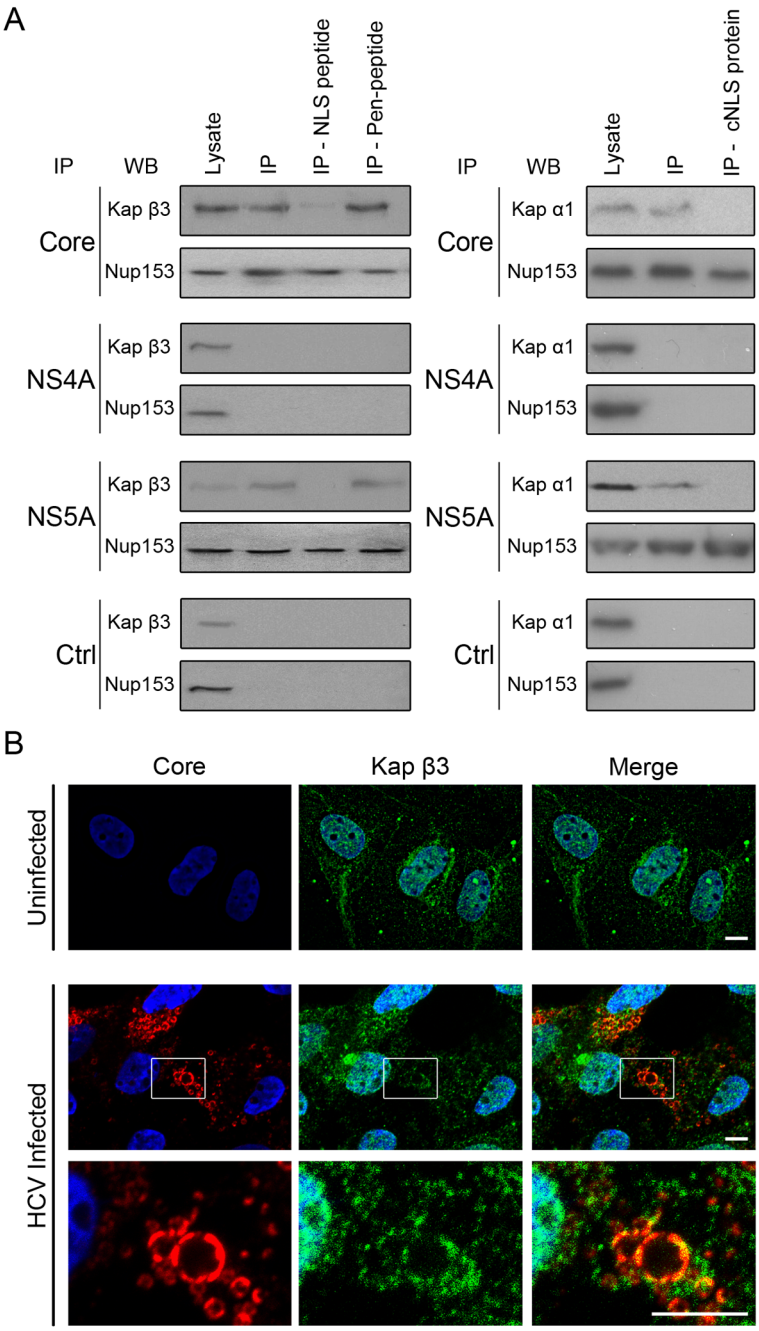

Figure 3-12. Identification of Kaps that physically interact with HCV proteins through NLS sequences.

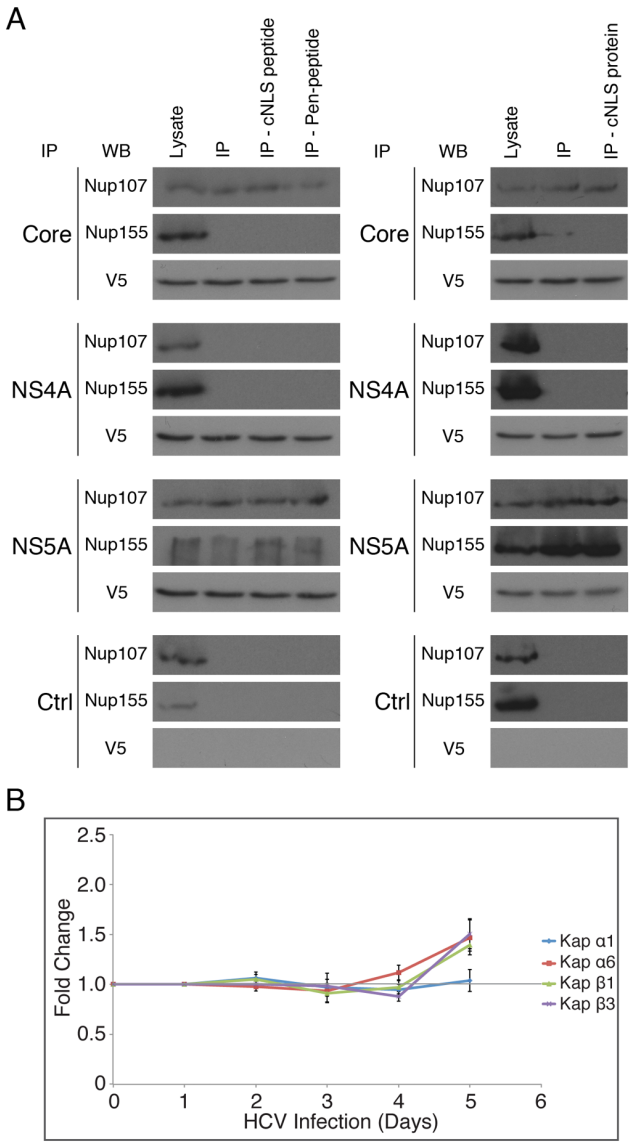

Figure 3-13. NLS peptides and NLS-containing proteins do not disrupt interactions between HCV proteins and Nups. A) Constructs encoding for the indicated V5-tagged HCV proteins were transfected into HEK293T cells and expressed for 48 hours. Twelve hours after transfection, cells were subjected to no treatment, treatment with Kap β3/IPO5-NLS peptides, or treatment with control penetratin peptides. Alternatively, cells were transfected with a construct encoding for a cNLS-GFP fusion protein 12 hours after transfection with HCV protein encoding constructs. Cells were then lysed and V5-tagged proteins were immunoprecipitated with anti-V5 antibodies (IP). Associated proteins were detected by western blotting using antibodies against the indicated proteins (WB). B) Huh7.5 cells were infected with HCV and total RNA was isolated from cell lysates at the indicated time points after infection. The mRNA transcript levels of the indicated Kaps were measured by qPCR analysis over a time course of infection. Values for each sample are normalized to HPRT mRNA and are expressed relative to mRNA levels of the indicated Kaps prior to infection (day 0 time point). Error bars indicate standard error (n=3 experiments). Data shown in panel A were obtained by A. Levin.

3.2.4 Nups and Kap β3/IPO5 support HCV infection

To examine the relevance of interactions between HCV proteins and Nups or Kaps, we investigated the consequences of reducing cellular levels of specific Nups and Kap β3/IPO5 on HCV replication. Lentivirus expressing shRNAs were used to reduce levels of targeted proteins. Using this approach, mRNA and protein levels for each of the targeted genes were decreased by > 60% in Huh7.5 cells by 4 days after lentivirus transduction (Figure 3-14A and 3-14B) with little effect on cell viability (Figure 3-14C). Cells were coinfected with lentivirus and HCV and, 4 days post infection, intracellular and extracellular HCV RNA levels were determined using quantitative real-time PCR (qPCR)(Figure 3-15A, 3-15B, and 3-14E). The results of these experiments revealed that intracellular levels of viral RNA were significantly decreased upon depletion of Nup98 or Nup153 (Figure 3-15A and 3-14E), while reduced levels of Nup155, NDC1, or Kap β3/IPO5, or treatment with lentivirus encoding a scrambled control sequence, had no effect. Consistent with these observations, quantitative western blotting revealed a decrease in HCV core protein levels in Nup98- or Nup153-depleted cells (Figure 3-15C). In accordance with decreased intracellular viral RNA levels, cells depleted of Nup98 or Nup153 also showed similar decreases in the levels of secreted virus (Figure 3-15B). Although Nup155- or Kap β3/IPO5-depleted cells showed no change in intracellular levels of HCV RNA, extracellular levels of secreted virus were decreased in these cells (Figure 3-15B), suggesting a requirement for Nup155 and Kap β3/IPO5 at a post-replication stage of virus assembly or in viral egress. These divergent effects of Nup depletions on intracellular versus extracellular RNA levels suggest functions for Nups at different stages of the HCV infectious cycle.

On the basis of our results, we concluded that at least a subset of Nups and Kap β3/IPO5 function in the production of secreted HCV. To further evaluate the relationship between the extracellular HCV RNA and the state of extracellular virus in the Nup and Kap

depleted cells, cells were co-infected with HCV and lentivirus, and the infectious titer of virus in the medium was determined (Figure 3-15D). Consistent with our results showing decreases in extracellular HCV RNA levels, we also observed decreases in HCV infectious titers following depletion of Nup98, Nup153, Nup155, and Kap β3/IPO5 (Figure 3-15D). When normalized to the amount of released HCV RNA, we observed that, with the exception of Nup155 depleted cells showing a slight decrease in the specific infectivity of viral particles, none of the knockdown cells produced viral particles with a significantly lower specific infectivity than virus from control cells (Figure 3-14D). Thus, we concluded that depletion of specific Nups decreases the efficiency of HCV replication and/or assembly but did not change viral particle infectivity.

Our observation that depletion of Kap β3/IPO5 reduces levels of secreted virus led us to further examine the role of Kaps in HCV infection by inhibiting interactions with NLS-containing targets *in vivo* using synthetic NLS-containing peptides (Levin et al., 2010a; Levin et al., 2010b). As discussed in the previous section, these peptides can disrupt interaction of HCV proteins with Kaps in cells, however, they do not significantly affect cell viability (Figure 3-14F). As shown in Figure 3-15E and 3-15F, treatment of HCV infected cells with the Kap α-NLS peptides significantly decreased both intracellular and extracellular HCV RNA levels. In comparison, Kap β3/IPO5-NLS peptides resulted in only a slight decrease in intracellular HCV RNA levels, but a significant decrease in the levels of secreted virus (Figure 3-15E and 3-15F). These data are similar to that obtained upon depletion of Kap β3/IPO5 (Figure 3-15A, 3-15B, and 3-15D). Combined with the decrease in HCV titers observed upon depletion of Kap β3/IPO5 (Figure 3-15B and 3-15D), the decrease in HCV titers following treatment of infected cells with NLS peptides provides further evidence that the nuclear transport pathways are important for viral infection and that, like Nups, different Kaps may contribute to distinct stages in the viral life cycle.

Figure 3-14. shRNA-mediated knockdown of Nups and Kaps and their effects on cell survival and the specific infectivity of HCV. A-D) Huh7.5 cells were coinfected with HCV and lentivirus encoding shRNAs directed against Nup98, Nup155, Nup153, NDC1, Kap β3, or a scrambled control sequence for four days. A) The level of mRNA transcript depletion following shRNA expression was evaluated by qPCR using primers specific for Nup98, Nup153, Nup155, Kap β3, or NDC1. Each sample is normalized to HPRT mRNA levels and expressed as a percent knockdown relative to cells infected with HCV and the lentivirus encoding the scrambled control shRNA sequence. B) Protein depletion following shRNA expression was evaluated by quantitative western blotting using antibodies specific for the indicated proteins. Protein levels were normalized to that of a-tubulin. Fold-change is relative to cells infected with HCV and the lentivirus encoding the scrambled control shRNA sequence. C) The cytotoxic effects of expressing the various shRNA constructs in Huh7.5 cells were evaluated using an MTT cell viability assay. Values for the survival of cells depleted of the indicated proteins represent fold change relative to cells not infected with lentivirus. D) The specific infectivity of HCV particles produced from cells coinfected with lentivirus was assessed by first determining total number of HCV RNA copies/mL in the culture supernatant for each sample. Huh7.5 cells were then infected with identical amounts of HCV RNA copies/mL harvested from each of the coinfected cells and focus-forming units were determined using indirect immunofluorescence microscopy. Values represent focus-forming units per copy of viral RNA. E) Huh7.5 cells were coinfected with HCV and lentivirus encoding a scrambled control sequence or an shRNA directed against a secondary site in either Nup155 or Nup153 distinct from that used in the analysis shown in A-D. Four days after infection, the levels of extracellular and intracellular HCV RNA were determined by qPCR. The values are presented as fold change relative to cell infected with HCV but not lentivirus. F) The cytotoxic effect of treating Huh7.5 cells with penetratin alone, Kap b3-NLS peptides, or penetratin peptides containing a N-terminal Kap α NLS sequence was determined using an MTT cell viability assay. Values for the survival of cells treated with peptides represent fold change relative to untreated cells. Data from E (right graph) were obtained with the help of J. Sheilds.

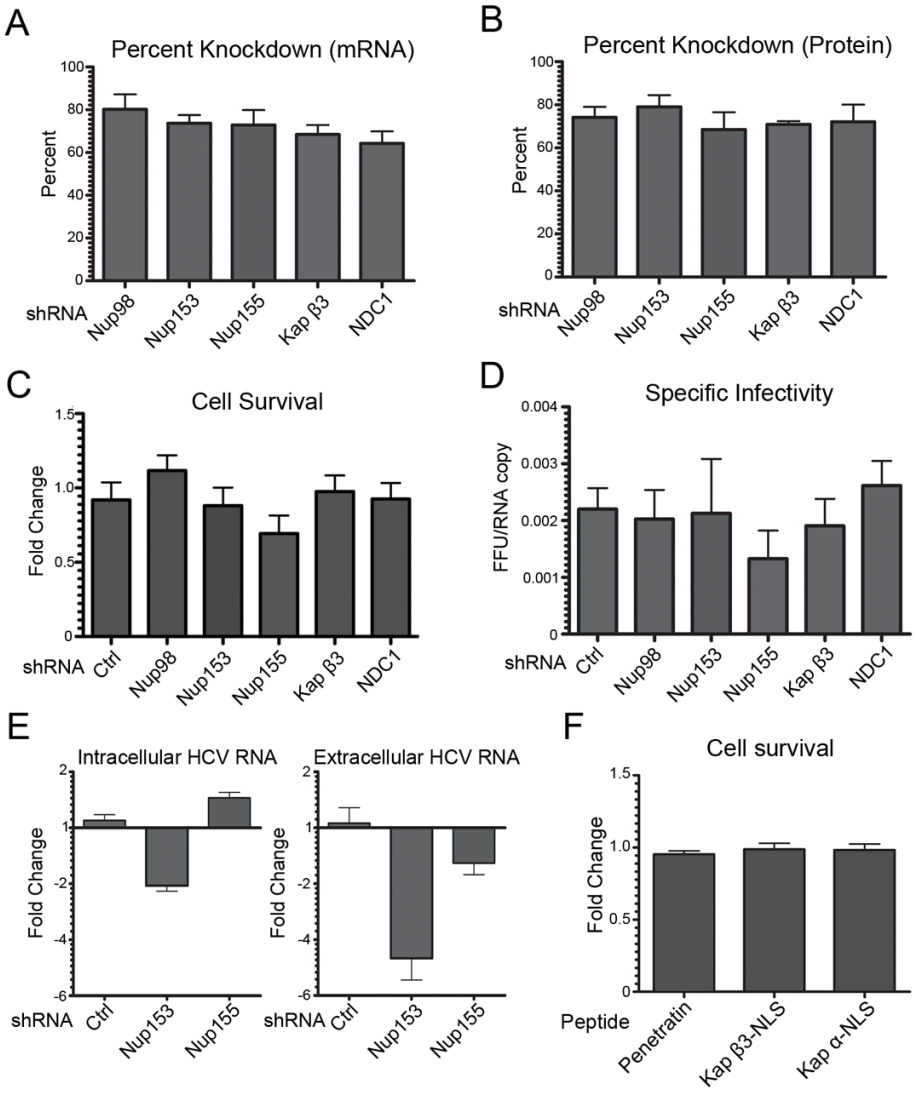

Figure 3-14. shRNA-mediated knockdown of Nups and Kaps and their effects on cell survival and the specific infectivity of HCV.

Figure 3-15. Depletion of Nups and Kaps inhibits HCV replication. A-D) Huh7.5 cells were coinfected with HCV and lentivirus encoding shRNAs directed against Nup98, Nup155, Nup153, Kap β3/IPO5, NDC1, or a scrambled control sequence for four days. The effects of Nup or Kap depletion on HCV titers were evaluated by qPCR analysis of HCV RNA levels in cell extracts (panel A) or in the culture supernatant (panel B) from HCV infected Huh7.5 cells co-infected with and without lentivirus. In addition, intracellular levels of the HCV core protein were examined by quantitative western blotting using antibodies specific for HCV core (panel C). Values for each sample are normalized to HPRT mRNA (Panel A and B) or a-tubulin (Panel C) and are expressed as fold-change relative to HCV infected cells not treated with lentivirus. Error bars indicate standard error (based on ≥ 3 experiments) and statistics are based on t-tests comparing each Nup or Kap specific shRNA treated sample to samples expressing the scrambled shRNA control. D) Huh7.5 cells were grown as described in panel A and the infectious titers of HCV particles present in the media of cells depleted of the indicated proteins were determined. Focus-forming units were determined using indirect immunofluorescence microscopy. Values shown represent focus-forming units per mL of medium (FFU/mL). E-F) Huh7.5 cells were infected with HCV and 4 hours post infection a penetratin peptide, a Kap b3-NLS peptide, or a penetratin peptide containing a N-terminal Kap α NLS (Kap α-NLS) was added to the media. Four days later the effects of these peptides on HCV RNA levels in intracellular (panel E) and extracellular (panel F) compartments were assessed by qPCR analysis. Values for each sample are normalized to HPRT mRNA levels and expressed as fold change relative to cells receiving no peptide. Error bars indicate standard error (based on ≥ 3 experiments) and statistics based on t-tests comparing cells treated with penetratin alone to those treated with the Kap b3-NLS peptide or the Kap α-NLS containing peptide. p-values less than 0.05 (*), 0.01 (**), and 0.001 (***) are indicated. Data from panels B and F was obtained with the help of J. Shields.

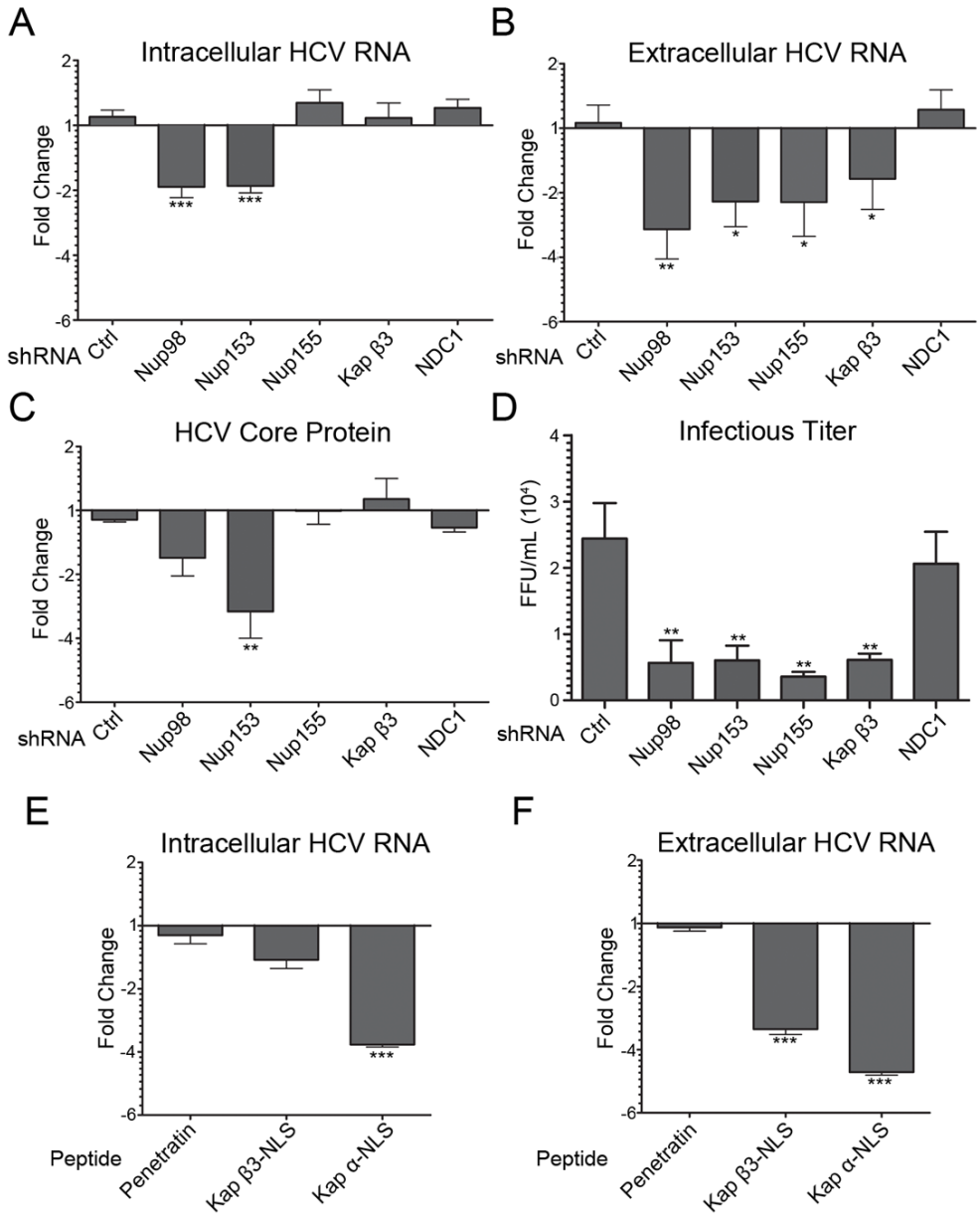

Figure 3-15. Depletion of Nups and Kaps inhibits HCV replication.

3.2.5 Nuclear transport substrates accumulate in regions of HCV assembly

The HCV-induced membranous web is thought to restrict access of cytoplasmic factors, such as pattern recognition receptors, from sites of HCV replication and assembly. The accumulation of Nups and Kap β3/IPO5 in the vicinity of HCV replication and assembly sites led us to investigate the potential role of the nuclear transport machinery in mediating access of molecules to compartments within the membranous web. We hypothesized that, like their role at the NE, the presence of nuclear transport factors within the membranous web could facilitate access of NLS-containing molecules, including NLS-containing HCV proteins such as core and NS5A, into regions within the membranous web through their interactions with Kaps. Therefore, we examined whether NLS-containing proteins could access regions of the membranous web in HCV-infected Huh7.5 cells using a chimeric gene encoding two tandemly repeated GFP proteins fused to a canonical SV40 NLS (cNLS). The cNLS-GFP fusion protein accumulated efficiently in the nuclei of uninfected cells, with little or no signal visible in the cytoplasm or associated with cytoplasmic membrane structures (Figure 3-16A). HCV infected cells also exhibited a robust nuclear accumulation of the cNLS-GFP fusion protein suggesting nuclear import was functional in these cells. However, in the HCV infected cells significantly higher levels of cytoplasmic signal were detected (Figure 3-16C). Importantly, the cNLS-GFP fusion protein was not diffusely distributed throughout the cytoplasm, but rather it appeared in distinct regions of the cytoplasm that were adjacent to or occupied by core and NS5A (Figure 3-16A and 3-17).

The concentration of the cNLS reporter in regions of the cytoplasm occupied by the membranous web are consistent with a role for Kaps and NPCs in regulating access to compartments within the membranous web. A key factor responsible for the accumulation of cargoes in the nucleoplasm is the small GTPase Ran, which, when bound to GTP, binds import

Kaps and induces release of attached cargoes. Therefore, we examined whether, in HCV infected cells, Ran was present in the cytoplasm in addition to it normal concentration in the nucleoplasm. In uninfected Huh7.5 cells, Ran was detected primarily to the nucleus, consistent with previous studies (Moore and Blobel, 1993). However, in HCV infected cells, we detected a clear change in the localization pattern of Ran. While still present in the nucleus, infected cells contained cytoplasmic pools of Ran largely concentrated in multiple foci (Figure 3-16B). Quantification of the fluorescent intensity in cytoplasmic and nuclear compartments of uninfected and HCV infected cells confirmed the increase in cytoplasmic Ran levels (Figure 3-16C). This cytoplasmic localization of Ran further supports the conclusion that the nuclear transport machinery functions in the cytoplasmic compartment to support HCV replication/assembly.

Figure 3-16. cNLS-GFP reporter protein and Ran accumulated in the vicinity of HCV replication/assembly. A) Uninfected or HCV-infected Huh7.5 cells were transfected with a construct encoding a chimeric protein consisting of an N-terminal cNLS sequence followed by two tandemly repeated GFP molecules 2 days after infection. On day 4 after HCV infection, the cNLS-GFP reporter was visualized by fluorescence microscopy (green) and its location compared to HCV NS5A (red) detected by immunofluorescence microscopy**.** DNA was detected with DAPI (blue). All cell producing the cNLS-GFP reporter exhibited a nuclear signal. Visible levels of the cNLS-GFP reporter were also detected in the cytoplasm of ~81% of infected cells (n=193) and ~23% of uninfected cells (n=198). Scale bars, 5 μm. B) Localization of Ran in Huh7.5 cells, either uninfected or infected with HCV for four days, was evaluated by indirect immunofluorescence microscopy using antibodies specific for Ran (green) and HCV NS5A (red). DNA was stained with DAPI (blue). Scale bar, 5 μm. C) Cytoplasmic and nuclear fluorescence signal levels produced by the cNLS-GFP reporter protein or the Ran specific antibodies were used to determine cytoplasmic to nuclear fluorescence ratios in uninfected and HCV infected cells. Fluorescence levels were calculated using ImageJ software and the statistical significance of differences in the ratios detected in uninfected versus HCV-infected cells was evaluated using t-tests. Asterisks (***) denotes a p-value of less than 0.001

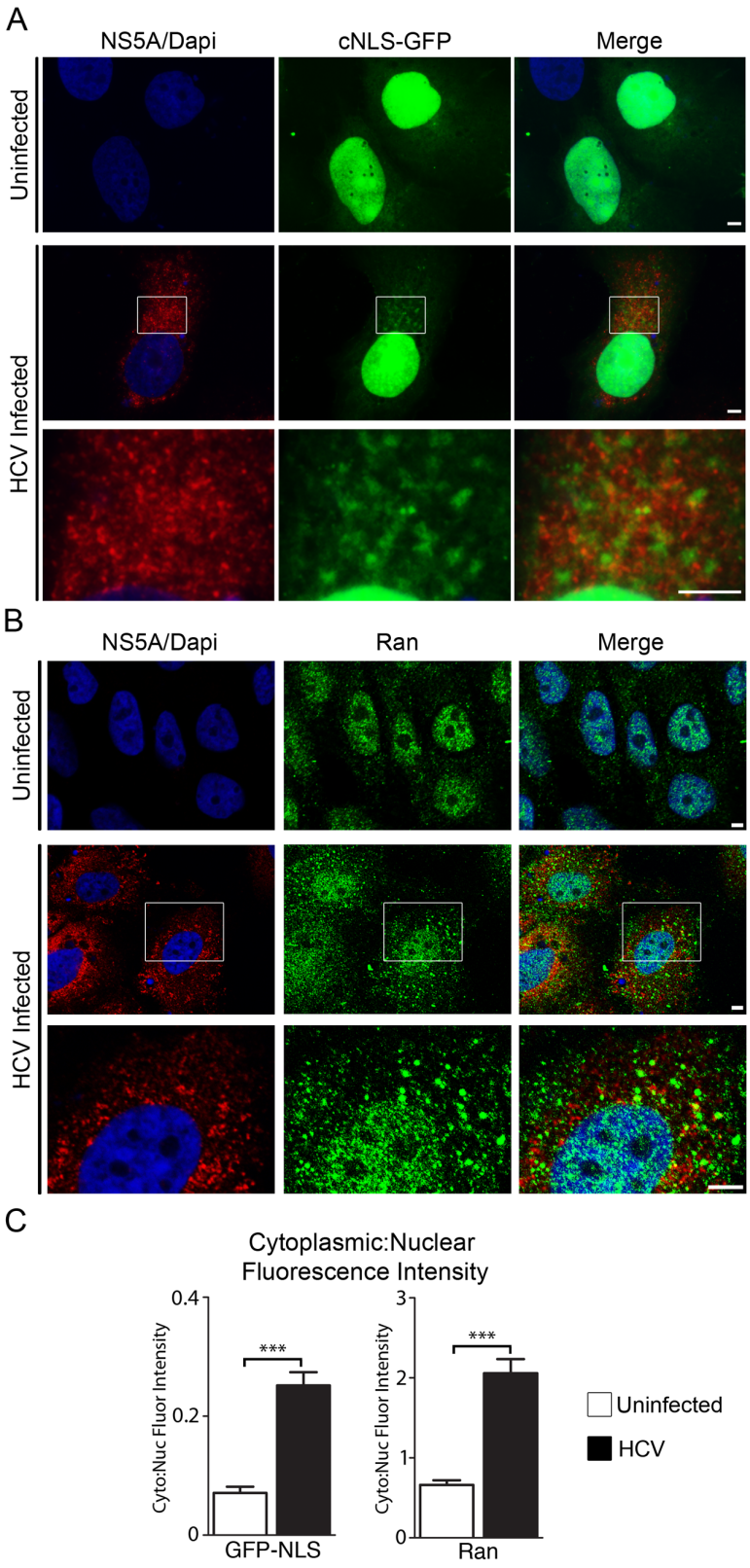

Figure 3-16. cNLS-GFP reporter protein and Ran accumulated in the vicinity of HCV replication/assembly.

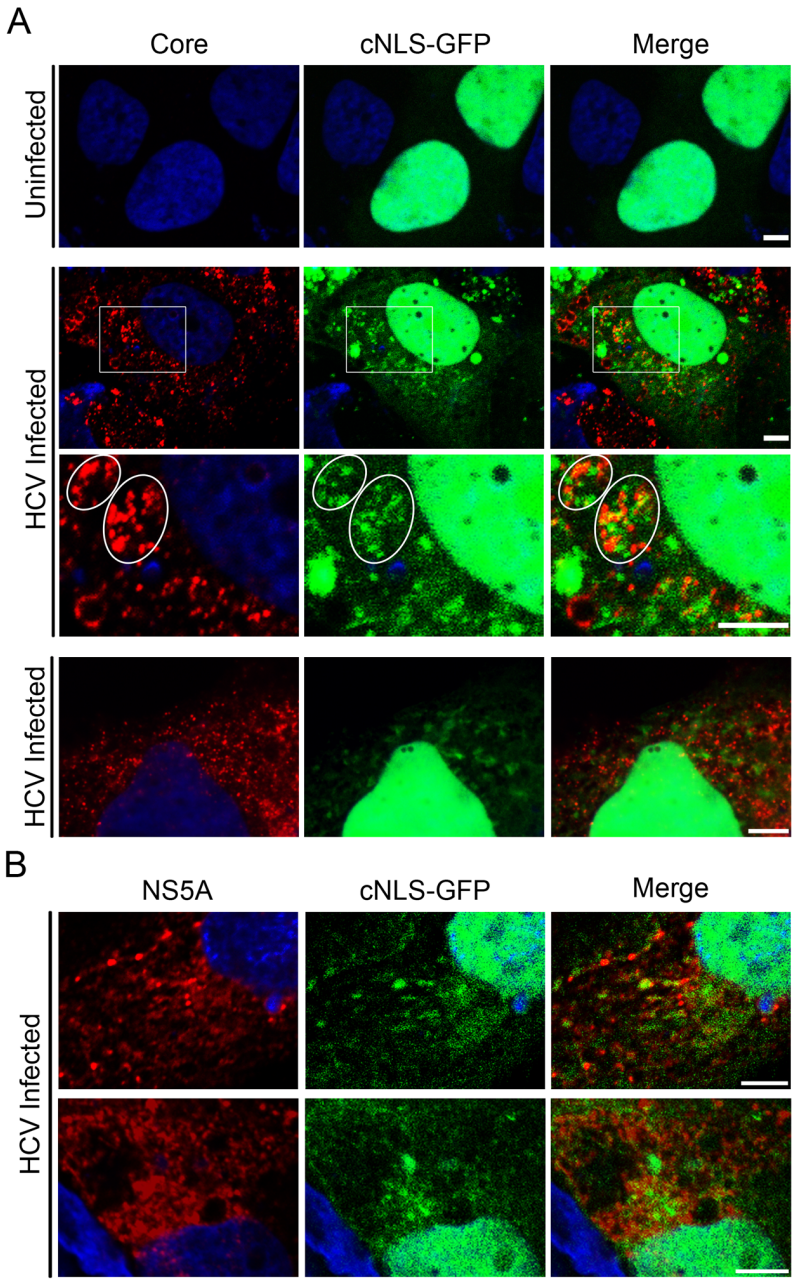

Figure 3-17. Localization of cNLS-GFP reporter protein to the membranous web. Huh7.5 cells were infected with HCV. Two days following infection, cells were transfected with a plasmid-born construct encoding a cNLS-GFP reporter. Four days post infection, the subcellular localization of the cNLS-GFP protein was examined by fluorescence confocal microscopy (green). The localization of the cNLS-GFP fluorescence signal was compared to that of HCV core (red, panel A) or NS5A (red, panel B) by indirect immunofluorescence confocal microscopy using specific antibodies. In panel A, boxed areas in the second rows of images are shown at higher magnification in the third row. Regions enriched for both the cNLS-GFP reporter and HCV core are highlighted in third row with white ovals. In all panels, uninfected Huh7.5 cells producing the cNLS-GFP reporter are also shown. DNA is stained with DAPI (blue). Scale bars, 5 μm.

3.3 Discussion

The organization, composition, and functions of membrane structures induced by positive strand RNA viruses remain largely ill-defined. During HCV infection, it has been postulated that the membranous web functions in viral egress, concentration and synchronization of viral replication and assembly, as well as avoidance from host cytoplasmic PRRs (den Boon et al., 2010; Overby and Weber, 2011). All of these functions are thought to require the existence of a permeability barrier between the cytosol and the interior of the membranous web. Here we report that Nups accumulate in the membranous web at sites of HCV replication or assembly. Consistent with these observations, we detect various HCV proteins in association with specific Nups and Kaps. Importantly, these proteins play a role in HCV infection. Insight into the function of these interactions came from the observation that a reporter protein normally found exclusively in the nucleus is also targeted to regions of the cytoplasm occupied by the membranous web. We hypothesize that Nups and Kaps present in the virus-induced membranous web facilitate virus replication, in part, through their ability to sequester molecules, both host and HCV proteins, required for HCV replication and assembly (Figure 3-18).

The existence of assembled cytoplasmic NPCs crossing ER membranes, or annulate lamellae, has been reported in many cell types (Kessel, 1983; Merisko, 1989). These NPCs are capable of transporting NLS-containing cargo across the ER (Cordes et al., 1997), but the function they play in the cytoplasm is unclear. We have observed that, during HCV infection, multiple Nups are redistributed to cytoplasmic membranes enriched with HCV proteins (Figure 3-2, 3-3, 3-4, 3-5, and 3-8). Indeed, HCV infection resulted in the re-localization of all the Nups examined, representing most of the major subcomplexes of the NPC, to regions of the cytoplasm populated by HCV proteins. These results lead us to conclude that intact cytoplasmic

NPCs, or derivatives of these structures, are present in areas of HCV replication or assembly. This concept is consistent with previous electron microscopy studies of HCV infected cells where various double membrane structures, topologically analogous to ER-like structures housing cytoplasmic NPCs, were detected in the membranous web (Ferraris et al., 2010; Paul et al., 2011; Shimizu et al., 1990).

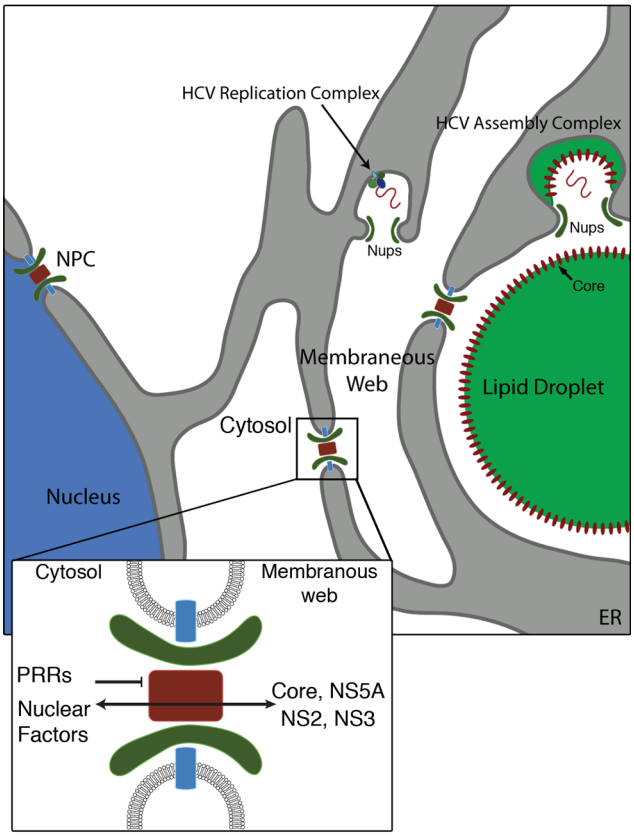

Figure 3-18. Model for the function of cytoplasmic NPCs in HCV infection. In HCV infected cells, cytoplasmically positioned NPCs are predicted to form channels across double membrane structures of the membranous web. These NPCs are proposed to facilitate movement of NLS-containing proteins, such as HCV core, NS2, NS3, NS5A and host nuclear proteins, from the surrounding cytoplasm across double membrane structures of the membranous web while excluding proteins lacking NLS sequences, such as pattern recognition receptors (PRRs), from regions of HCV replication and assembly. We also speculate that Nups (such as Nup155 and Nup153) may be recruited to regions of the membranous web where HCV replication and virion assembly would employ the ability of these Nups to contour membranes.

Changes in the localization of Nups in HCV infected cells led us to investigate corresponding changes in mRNA transcript and protein levels. Our qPCR analysis of Nup and Kap transcript levels revealed that only a subset are elevated in HCV infected cells, indicating that Nups recruited to the membranous web are likely derived from both existing cellular Nup pools and increased synthesis. Several Nups have previously been observed to be up-regulated upon innate immune stimulation of specific cell types (Castelló et al., 2009; Enninga et al., 2002). Similar innate immune activation has also been observed upon HCV infection leading to the possibility that the observed up-regulation of Nups in HCV infected cells may result from HCV-mediated immune activation (Joyce et al., 2009; Walters et al., 2006). However, this does not appear to be the case as treatment of Huh7.5 cells with various immune stimulants did not alter cellular levels of mRNAs encoding many of the Nups examined in this study (Figure 3-11). Thus, the increase in Nup levels observed following HCV infection likely occurs through a mechanism distinct from immune activation.

Immunoprecipitation experiments revealed that several Nups associate with HCV core and NS5A. Additionally, the HCV channel forming protein, p7, has previously been shown to interact with Nup214 in a yeast two-hybrid system (Huang et al., 2005). Importantly, the interactions between Nups and HCV core or NS5A are not mediated by Kaps (Figure 3-12A and 3-13A). Thus, their interactions are unlikely to reflect a transport intermediate where HCV proteins are moving as cargo through the NPC. Rather, these data are consistent with a direct association between HCV proteins and Nups. These interactions are predicted to contribute to the recruitment of specific Nups, as well as associated subcomplexes or assembled NPCs, to the forming membranous web.

It is possible that the interaction of HCV proteins with Nups and kaps could potentially alter host cell nucleocytoplasmic transport in such a way that facilitates HCV replication. For

example some viruses, including polio and influenza, inhibit nuclear transport by inducing Nup degradation, to improve viral replication (Fontoura et al., 2005; Levin et al., 2010a; Satterly et al., 2007). However, it seems less likely that HCV proteins target Nups and Kaps for a similar reason as we do not detect degradation of Nups, and nuclear import of the cNLS-GFP reporter, while exhibiting some cytoplasmic localization, appears robust in HCV-infected cells (Figure 3-2, 3-16, and 3-17). Instead, we hypothesize that interactions of HCV protein and Nups and Kaps reflect two, potentially simultaneously acting, functions conducted by these proteins within the membranous web. One proposed role is based on the observation that a subset of Nups, including Nup107 and Nup155, are structurally related to secretory vesicle coat proteins. These proteins have highly conserved domain structures and their interactions with membranes and membrane proteins is proposed to facilitate the convex membrane curvature of the pore membrane domains that connect the inner and outer nuclear membranes and attach to the scaffold structures of the NPC (Hsia et al., 2007). In addition, while lacking structural similarity to coat proteins, Nup153 interacts with the vesicle coat protein COPI and this association has been linked to the post-mitotic NE membrane assembly (Liu et al., 2003). The association of Nup153 with HCV proteins and COPI is also intriguing in light of studies showing a role for the COPI coatomer complex in HCV replication (Tai et al., 2009). Considering these observations, we speculate that Nups may be recruited to the membranous web, in part, to usurp their functions in contouring of membranes. Importantly, the curvature of membrane domains at sites of viral particle budding into the ER lumen is topologically similar to the pore membrane (Bartenschlager et al., 2010; Shimizu et al., 2011). These ideas are consistent with the physical association of Nup155 and Nup153 with core and NS5A and the visible close association of these Nups with core enriched regions adjacent to lipid droplets (Figure 3-2).

Our data also support a second, more conventional role for Nups within the membranous web as part of assembled or partially assembled NPCs and as regulators of Kap/cargo movement. We envisage that the membranous web-associated NPCs selectively allow NLS-containing molecules to access regions within the membranous web. Such a mechanism would explain several observations. For example, previous studies have identified, or inferred the presence of, NLS-like sequences or NTF binding domains in HCV proteins, including in core (Ide et al., 1996), NS5A (Suzuki et al., 2005), and NS3 (Kim et al., 1999), and our own analysis has also revealed NLS-like sequences in these proteins and NS2 (Levin et al., 2014). Moreover, previous studies have detected interactions between HCV proteins and Kaps (Chung et al., 2000; de Chassey et al., 2008; Isoyama et al., 2002), and we have found that core and NS5A proteins interact with Kap β3/IPO5 and Kap α (Figure 3-12). However, since these proteins are ER-associated and detected in the cytoplasm during infection, we propose that these import signals function in the cytoplasm.

A requirement for a transport regulatory mechanism within the membranous web is inferred by the observed compartmentalization properties of this structure, including several studies showing HCV RNA and proteins within the membranous web are resistant to RNase and protease treatment (Miyanari et al., 2003). This physical separation is also revealed by the exclusion of tubulin from regions of the cytoplasm occupied by HCV proteins (Figure 3-1B and 3-1C). Various HCV and host proteins synthesized in the cytosol must overcome this barrier to enter regions of the web where HCV replication and assembly occurs. We propose that NLS sequences within HCV proteins as well as several host-cell nuclear factors detected in the membranous web (Isken et al., 2007; Lee et al., 2011a) function to facilitate movement of these proteins from the cytosol through NPCs positioned in the membranous web to regions of HCV replication and assembly. Importantly, cytoplasmic proteins lacking NLSs, such as PRRs, would

be inhibited from accessing viral RNA; events potentially contributing to the ability of HCV to maintain a chronic infection. This concept of NPC-mediated transport functioning within the membranous web is directly supported by our observations that a cNLS-GFP reporter protein is visibly enriched in regions of the cytoplasm occupied by HCV proteins (Figure 3-16 and 3-17). Furthermore, the concentration of Kap β3/IPO5 in regions of the cytoplasm occupied by core (Figure 3-12) supports a function for this NTF in the membranous web.

Consistent with these proposed functions for the nuclear transport machinery within the membranous web, we observe that various Nups and Kaps are required for HCV production. For example, we detected an inhibition of HCV replication or assembly following depletion of Nup98, Nup153, or Nup155 (Figure 3-15). Depleted levels of mRNA and protein for each Nup appeared similar (Figure 3-14), however, the consequences of their depletion on HCV replication were not. While depletion of Nup98 or Nup153 reduced both intracellular levels of viral RNA and secreted virus, depletion of Nup155 led to a specific decrease in secreted virus but no significant change in intracellular levels of viral RNA. These results are consistent with Nup98 and Nup153 being required prior to or coincident with in HCV RNA replication. By contrast, Nup155 depleted cells show no defect in intracellular HCV RNA accumulation implying that Nup155 contributes to post-replication processes such as effective viral packaging or egress. These differential effects of Nup depletion remain to be further characterized and we envisage several potential scenarios that would explain these results. They may arise from the different functional roles of these Nups within NPCs, thus depleting individual Nups would lead to distinct changes in the functionality of the NPC, including alterations in the functions of specific transport pathways. In support of this idea, inhibition of Kap α transport by treatment with competitive peptides mirrors the effects of depleting Nup98 or Nup153, namely decreasing both intracellular HCV RNA and secreted virus. Conversely, depletion of Kap β3/IPO5, or

competitive inhibition of its *in vivo* function with peptides, results in a phenotype similar to depletion of Nup155, namely a decrease in secreted virus but no change in the intracellular levels of HCV RNA (Figure 3-15). Thus, distinct transport pathways may have functions at different stages of the HCV lifecycle, likely as defined by their cargos. Alternatively, the structural integrity and general transport functions of the NPC appear to be differentially tolerant to changes in the levels of individual Nups. This is revealed, for example, by depletion of NDC1, where NPCs remain functional despite significant depletion (Stavru et al., 2006) of what is thought to be an essential component of the NPC (Mansfeld et al., 2006a; Mitchell et al., 2010). The presence of depleted, but functional, NPCs would explain our observation that depletion of NDC1 did not significantly alter HCV replication. Another possibility is that these Nups and Kaps also contribute to virus production through additional functions unlinked to transport. For example, as discussed above, Nups such as Nup155 likely influence membrane structure; moreover, various Nups, including Nup98 and Nup155 have been linked to the maintenance of chromatin structure and the regulation of transcription (reviewed in (Arib and Akhtar, 2011; Hsia et al., 2007)).

Our model suggesting that Nups form functional NPCs within the membranous web implies NPCs are capable of functioning outside the confines of the nuclear envelope. Indeed previous studies have shown that annulate lamellae can transport NLS-coupled gold particles across the ER (Cordes et al., 1997). Moreover, a recent report demonstrated that NPCs are present at the transition zone of cilia in mammalian cells and that a transport mechanism similar to that of nucleocytoplasmic transport is utilized to transport proteins between the cilia and the adjacent cytoplasm (Fan et al., 2011; Kee et al., 2012). Interestingly, these cilia associated NPCs appear to lack certain Nups suggesting they represent derivatives of the NE embedded structures. Whether the NPCs we have detected associated with the membranous web also

represent a variant form of NPCs remains to be determined. This seems plausible as our replicon data imply that HCV proteins do not recruit intact NPCs to the membranous web but rather distinct HCV proteins may recruit different subsets of Nups. We can envisage that the concerted activities of the HCV proteins could promote assembly of NPCs or a variant form of this structure in the membranous web.

The ability of HCV to exploit the functions of the Nups and Kaps for the purpose of creating an environment conducive to its replication and assembly may represent a mechanism widely used by positive-strand RNA viruses. For example, we have observed increased amounts of cytoplasmic Nup98-containing foci that likely represent NPCs in cells infected with hepatitis A virus and dengue virus (Figure 3-6). Consistent with this observation, electron microscopy studies have reported increased levels of annulate lamellae in hepatitis A virus infected cells (Marshall et al., 1996), as well as cells infected with Japanese Encephalitis virus and Rubella virus (Courington and Vogt, 1967; Kim and Boatman, 1967; Wang et al., 1997). These results lead us to conclude that Nups represent a conserved target of positive-strand RNA viruses and, with greater mechanistic understanding, a potential target for antiviral intervention.

CHAPTER IV: Exclusion of pattern recognition receptors from the hepatitis C virus-induced membranous web

4.1 Overview

Hepatitis C virus (HCV) is a positive-strand RNA virus of the flavivirus family and a major cause of liver disease worldwide. HCV replicates in the cytoplasm causing extensive rearrangements of host cell membranes to form viral replication and assembly complexes; collectively termed the membranous web. This membranous web has been shown to protect the viral genome from exogenously added nucleases and is predicted to form distinct cytoplasmic compartments. In this study, we used various immunofluorescence techniques to show that cytoplasmic pattern recognition receptors (PRRs), including RIGI and MDA5, are excluded from the membranous web, a phenomenon consistent with its proposed compartmentalization function. We have previously proposed that access to regions within the membranous web is regulated by nuclear pore complex (NPC) like structures recruited into these cytoplasmic structures. Here we show that the addition of a nuclear localization signal (NLS) to PRRs increases colocalization of PRRs with viral proteins, and production of the PRR-NLS fusions inhibits viral replication. Additionally, we used positive- and negative-strand RNA probes as well as subcellular fractionation of HCV infected cells to identified separate compartments within membranous web. One containing the majority of the viral RNA while the other contained significantly more infectious virus. Staining for ribosomes in conjunction with PRRs and viral RNA also revealed that a pool of the viral genome is located outside the membranous web. These results support the existence of district replication and assembly complexes within the membranous web and suggest that there is a spatial separation between viral genome replication and protein production. We propose that the membranous web serves inhibit contact between cytoplasmic PRRs and the viral genome and that this is through the use of resident NPCs, which function to regulate traffic between cytoplasmic compartments in HCV infected cells.

4.2 Results

4.2.1 HCV infection induces the production of cytoplasmic compartments lacking PRRs

Several groups have reported that the membranous web appears to protect viral proteins and RNA from exogenously added nucleases (Hsu et al., 2010; Miyanari et al., 2003; Overby et al., 2010). This compartmentalization is also supported by our observation that HCV proteins present in the membranous web appear in regions of the cytoplasm largely devoid of microtubules (Neufeldt et al., 2013). Importantly, the barrier formed by membrane structures of the web appears to be selectively permeable, and the nuclear transport machinery contributes to controlling access of proteins to viral replication and assembly compartments within the web (Levin et al., 2014; Neufeldt et al., 2013). For example, GFP reporter proteins containing classical NLS (cNLS) sequences are localized to cytoplasmic areas containing HCV proteins, while those containing a functionally distinct NLS sequence (Impβ3 NLS) were excluded from the membranous web (Levin et al., 2014; Neufeldt et al., 2013).

Active exclusion of proteins from the membranous web could represent an innate immune evasion strategy employed by the virus. In order to test this hypothesis, we transfected uninfected or HCV infected cells with constructs encoding FLAG-tagged RIG-I or V5-tagged MDA5 and visualized the cellular distribution of these PRRs by confocal immunofluorescence microscopy (Figure 4-1 and 4-2). In uninfected cells, we observed a diffuse cytoplasmic localization for both RIG-I and MDA5 (Figure 4-1 and 4-2A top panels). By contrast, in HCV infected cells, RIG-I and MDA5 were absent from regions of the cytoplasm that contained the majority of HCV proteins or the viral dsRNA (Figure 4-1 and 4-2A bottom panels). Pearson's colocalization coefficients calculated for the images in Figure 4-1 and 4-2A showed that there was a negative correlation between fluorescent signals observed for the HCV markers and either RIG-I or MDA5, further supporting the conclusion that PRRs are restricted from accessing the

membranous web (Figure 4-1 and 4-2A right panels). On the basis of the localization of dsRNA and RLRs (RIG-I-like receptors) (Figure 4-1 and 4-2), we concluded that RLRs are prevented from entering regions of viral replication. To further evaluate this apparent segregation, we examined the subcellular localization of the MDA5 reporter in Huh7 cells harbouring the JFH-1 subgenomic replicon. In replicon cells transfected with constructs coding for MDA5, we observed that MDA5 and viral proteins were present in distinct, largely non-overlapping regions of the cytoplasm similar to observations in the virus-infected cells (Figure 4-2A and 4-3A). These observations provide support for the hypothesis that viral compartments inhibit entry of PRRs thereby impeding innate immune activation.

A caveat of experiments examining the exogenous expression of RLRs is that overexpression of the active form of RIG-I in HCV infected Huh7.5 cells leads to immune activation, which impedes viral replication (Sumpter et al., 2005). To avoid this complication, we used a point mutant of RIG-I (RIG-I-K270A) that lacks helicase activity and signalling capacity (Takahasi et al., 2008). The observed subcellular localization of Rig-I-K270A was comparable to that of the active RIG-I in uninfected and HCV infected cells (Figure 4-1A and 4-2B). Furthermore, RIG-I-K270A was similarly reduced in regions of the cytoplasm where HCV core and NS4B were concentrated (Figure 4-2B).

Since lipid droplets accumulate within the membranous web and are required for HCV assembly, we also examined the localization of lipid droplets in relation to RIG-I and viral proteins in HCV infected cells harbouring the RIG-I-K270A expression construct. Not surprisingly, in uninfected cells, we observed exclusion of RIG-I-K270A signal from cytoplasmic regions occupied by lipid droplets (Figure 4-3B top panel). In HCV infected cells these regions, as well as extension areas adjacent to the lipid droplets, lacked RIG-I signal (Figure 4-3B bottom

panel). These data further support the hypothesis that RIG-I is excluded from cytoplasmic compartments induced by HCV infection.

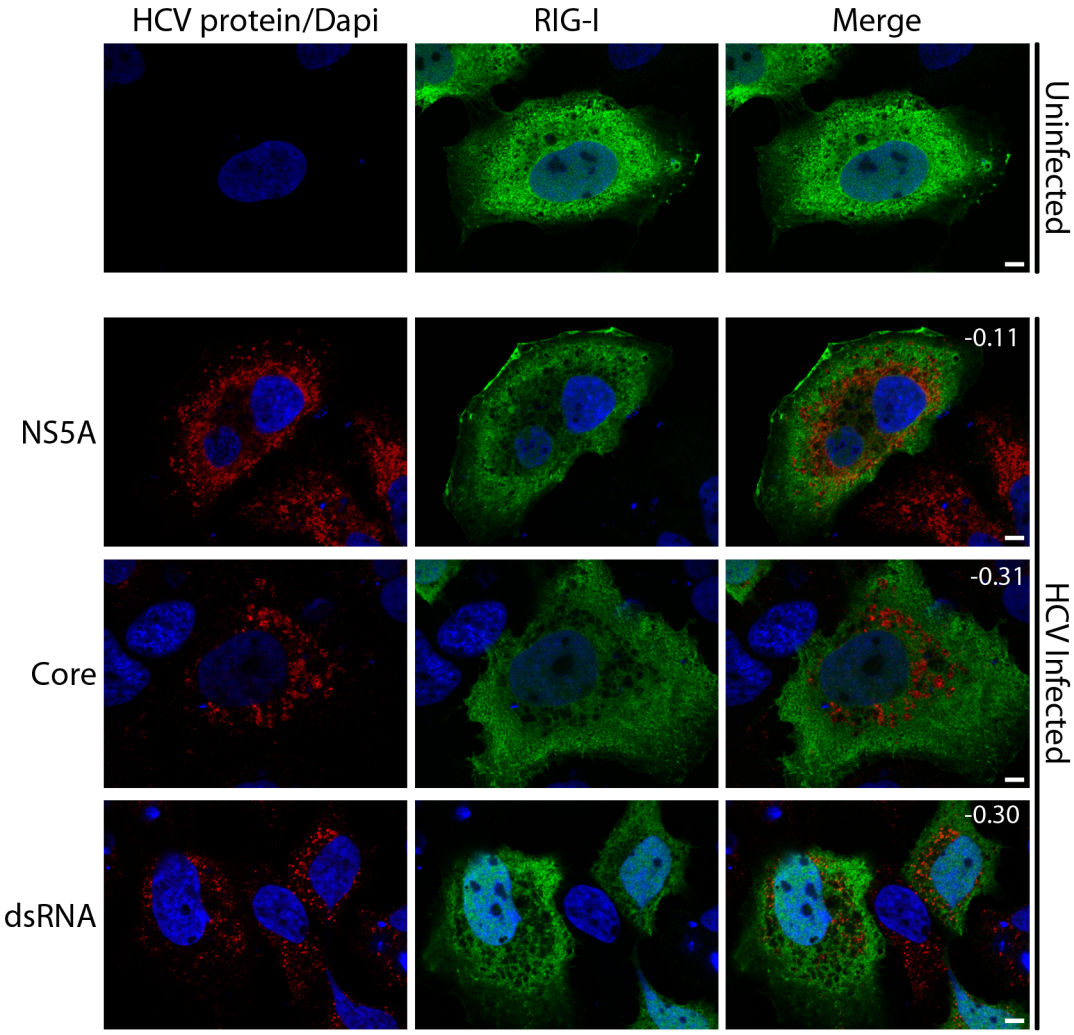

Figure 4-1. Exclusion of PRRs from cytoplasmic regions enriched for HCV proteins. Uninfected or HCV-infected Huh7.5 cells were transfected with constructs encoding for FLAG-tagged RIG-I 2 days after infection. On day 4 after HCV infection, the localization of HCV proteins and PRRs in cells either uninfected or HCV-infected was evaluated by indirect immunofluorescence microscopy using antibodies specific for the indicated HCV protein and either the V5 or FLAG epitope tag. DNA was detected with DAPI (blue) and scale bars represent 5 μm. Pearson's colocalization coefficients were calculated using Coloc2 software in ImageJ.

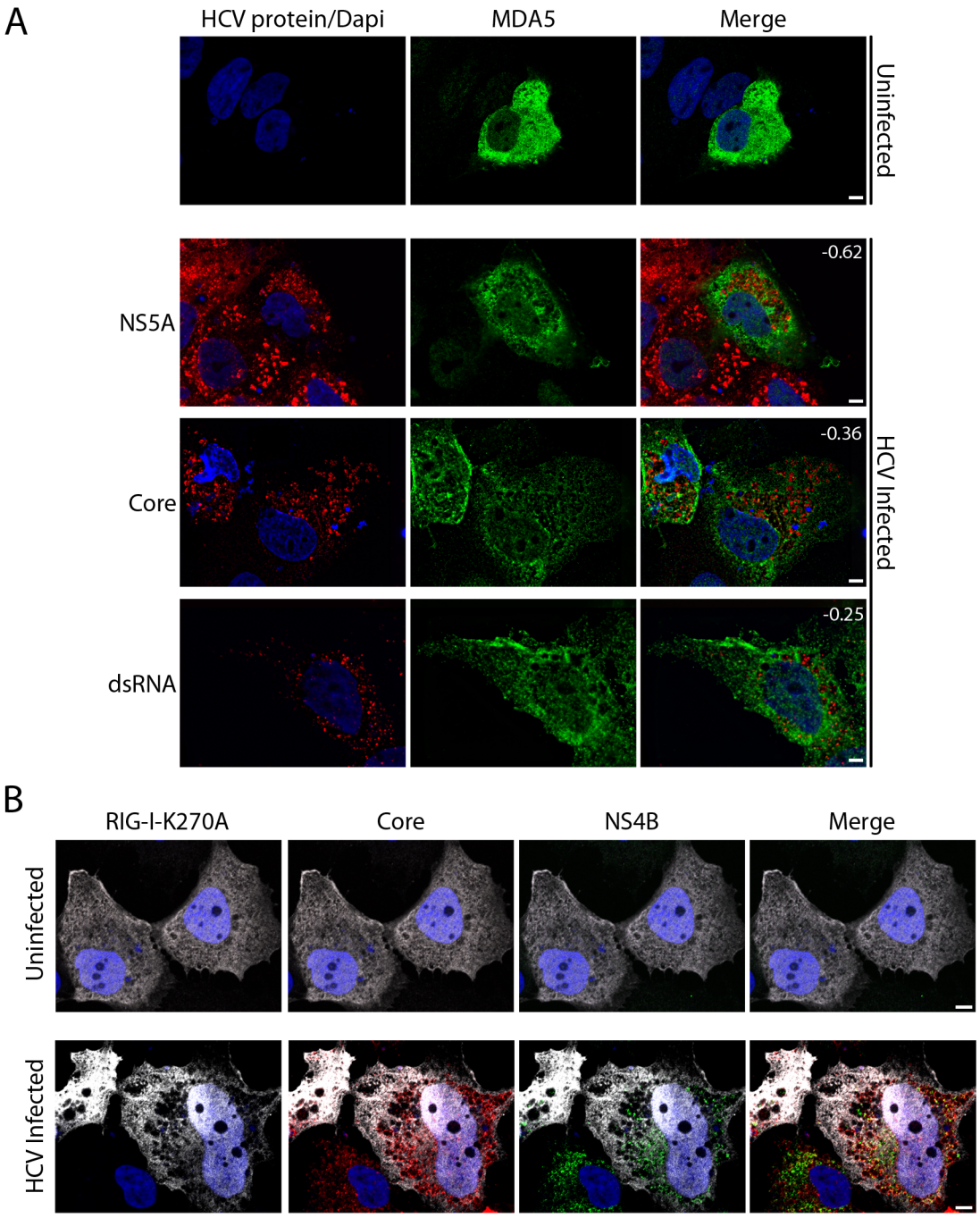

Figure 4-2. Exclusion of PRRs from cytoplasmic regions enriched for HCV proteins. Uninfected or HCV-infected Huh7.5 cells were transfected with constructs encoding for V5-tagged MDA5 (A), or FLAG-tagged RIG-I-K270A (B) 2 days after infection. On day 4 after HCV infection, the localization of HCV proteins and PRRs in cells either uninfected or HCV-infected was evaluated by indirect immunofluorescence microscopy using antibodies specific for the indicated HCV protein and either the V5 or FLAG epitope tag. DNA was detected with DAPI (blue) and scale bars represent 5 μm. Pearson's colocalization coefficients (A) were calculated using Coloc2 software in ImageJ.

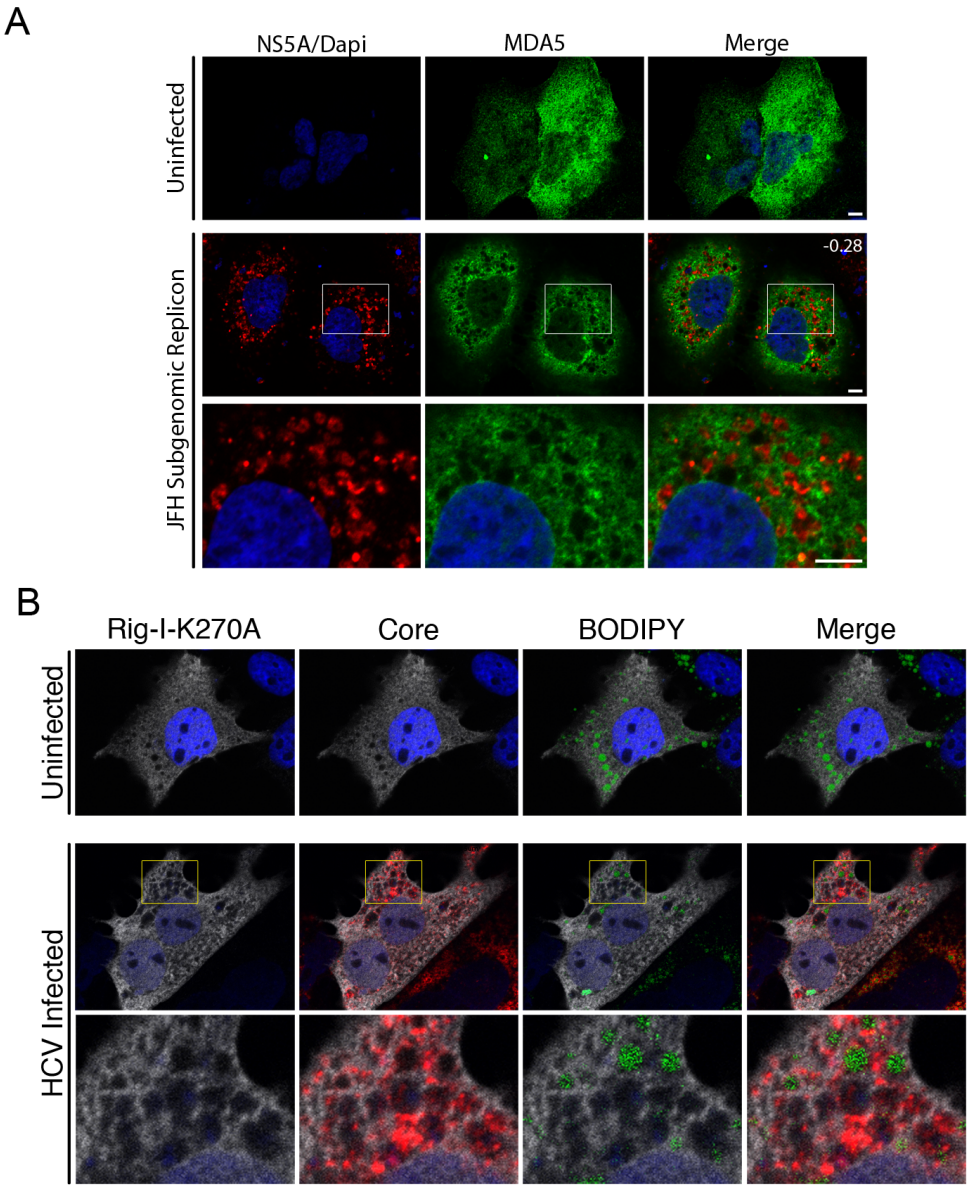

Figure 4-3. Characterization of RLR localization compared to membranous web markers. A. Huh7 cells or Huh7 cells harbouring the JFH-1 subgenomic replicon were transfected with constructs encoding V5-tagged MDA5 and incubated for 48 hours. The localization of HCV proteins and PRRs in cells was evaluated by indirect immunofluorescence microscopy using antibodies specific for the NS5A and the V5 epitope tag. DNA was detected with DAPI and scale bars represent 5 μm. Pearson's colocalization coefficients were calculated using ImageJ software. **B.** Uninfected or HCV-infected Huh7.5 cells were transfected with a construct encoding for FLAG-tagged Rig-I-K207A 2 days after infection. On day 4 after HCV infection, cells were incubated with BODIPY (green) followed by incubation with antibodies directed against the FLAG epitope (grey) and HCV core (red). DNA was detected with DAPI (blue) and scale bars represent 5 μm.

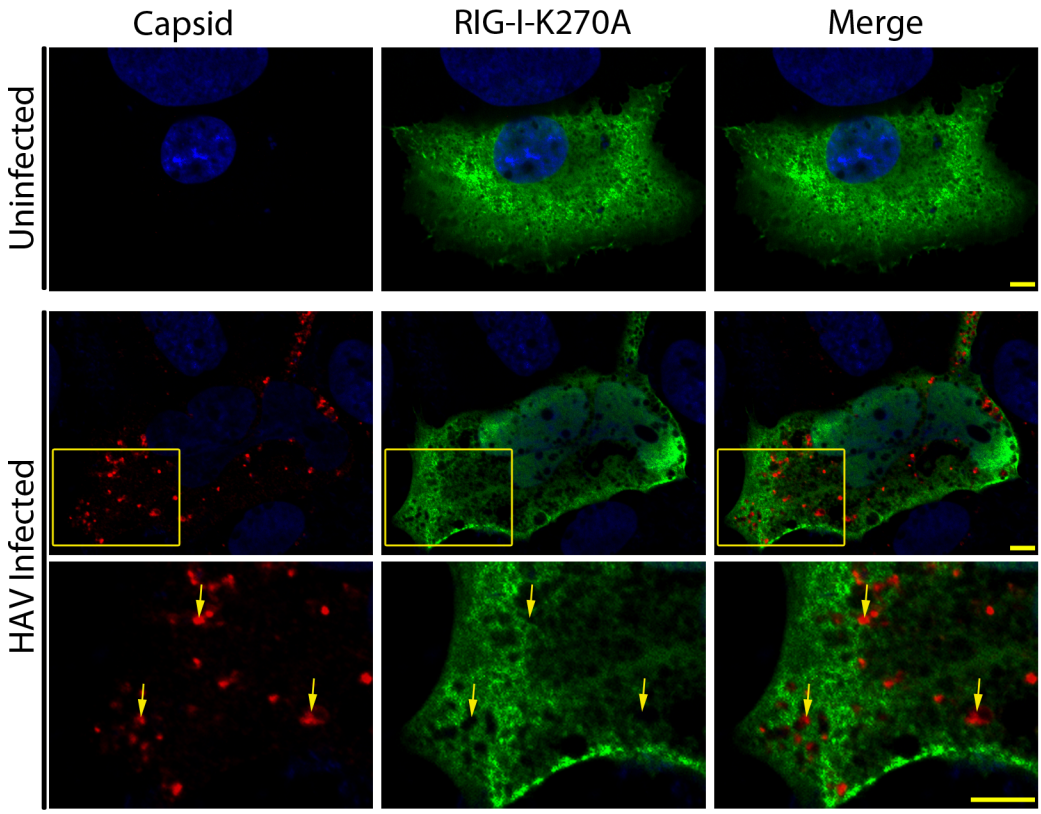

Figure 4-4. Exclusion of PRRs from cytoplasmic regions enriched for HAV proteins. Uninfected or HAV-infected Huh7.5 cells were transfected with constructs encoding for catalytically inactive FLAG-tagged RIG-I-K270A 5 days after viral infection. On day 7 after HAV infection, the localization of RIG-I-K270A (green) and HAV capsid protein (red) we evaluated by indirect immunofluorescence microscopy using specific antibodies. DNA was stained with DAPI and scale bars represent 5 μm.

4.2.2 HAV infection induces cytoplasmic compartments lacking RIG-I

All positive-strand RNA viruses reorganize host cell membranes and, in many cases, have been shown to form distinct replication complexes (den Boon and Ahlquist, 2010; den Boon et al., 2010). To test if the exclusion of PRRs from regions occupied by the HCV-induced membranous web (Figure 4-1 and 4-2) is a phenotype for other positive-strand RNA viruses, we examined the localization of RIG-I-K270A in hepatitis A virus (HAV) infected cells. In HAV infected Huh7.5 cells, we observed exclusion of RIG-I-K270A from cytoplasmic regions containing HAV capsid protein, results similar to that seen in HCV infected cells (Figure 4-4). These results are consistent with the idea that virus-induced cytoplasmic compartments may represent a common immune evasion strategy of positive-strand RNA viruses.

4.2.3 NLS-tagged PRRs colocalize with HCV proteins and inhibit viral replication

The HCV-induced membranous web is composed of numerous vesicles and membrane structures that are concentrated within specific regions of the cytoplasm (Miyanari et al., 2007; Paul et al., 2011; Romero-Brey et al., 2012). We previously reported that GFP-NLS-tagged reporter proteins could enter regions of the cytoplasm occupied by membranous web structures, presumably using associated components of the nuclear transport machinery including NPCs and NLS binding nuclear transport factors (Levin et al., 2014; Neufeldt et al., 2013). As in previous studies, we observed that the GFP-NLS-tagged reporter was found throughout the cytoplasm, including within the regions containing an abundance of HCV core protein but lacking tubulin (Figure 4-5). Building on these data, we hypothesize that placing an NLS on a PRR would overcome the selective barrier between the cytoplasm and the membranous web (Levin et al., 2014; Neufeldt et al., 2013). To test this, uninfected or HCV-infected Huh7.5 cells were transfected with constructs encoding V5-tagged MDA5-I923V, NLS-MDA5-I923V, RIG-

I-K270A or NLS-RIG-I-K270A, and the localization of the reporter proteins was compared to that of HCV NS5A. Similar to the K270A mutation in RIG-I, the I923V mutation inhibits MDA5-mediated activation of immune signalling pathways (Shigemoto et al., 2009). Consistent with results presented in Figure 4-2A, the MDA5-I923V mutant was observed outside cellular regions containing NS5A (Figure 4-6A). In uninfected cells, the NLS-tagged reporter proteins exhibited an increased nuclear signal over those not containing an NLS sequence, demonstrating that the NLS sequence is functional (Figure 4-6A-D, top rows). When the NLS-tagged MDA5 or RIG-I proteins were expressed in HCV-infected cells, the level of overlap between NS5A and the reporter protein significantly increased compared to constructs lacking the NLS (Figure 4-6A-D). We further evaluated this using Pearson's colocalization coefficients, which demonstrate a significant increase in overlap between the fluorescent signals associated with NS5A and NLS-MDA5-I923V as compared to NS5A and MDA5-I923V (Figure 4-6E). These results provide further evidence that the nuclear transport machinery, at least in part, controls access into HCV-induced cytoplasmic compartments.

We further evaluated the consequence of adding an NLS sequence to RLRs by examining the effects of expressing active NLS-tagged RIG-I on HCV infection. Cells were infected with HCV followed by transfection with constructs encoding RIG-I, NLS-RIG-I, NLS-RIG-I-K270A or SLN-RIG-I and total intracellular and extracellular viral RNA levels were determined by real-time PCR. Among these constructs, SLN-RIG-I fusion contains a reverse, non-functional NLS sequence. In uninfected cells, we observed only minimal changes in the levels of immune stimulated genes in cells expressing the NLS-tagged RIG-I compared to those expressing wild type RIG-I, indicating that addition of the NLS tag does not cause to RIG-I-mediated immune activation (Figure 4-7). In HCV infected cells, there was a significant decrease in the levels of HCV RNA following transfection of cells with the NLS-RIG-I constructs

(Figure 4-6F). A small decrease in HCV RNA levels was also observed in cells harbouring the RIG-I construct and no changes were observed in cells transfected with the SLN-RIG-I or NLS-RIG-I-K270A expression constructs. These results provide further evidence for the formation of distinct cytoplasmic compartments in positive-strand RNA virus infected cells, and they implicate the nuclear transport machinery as a regulatory of access to sites of virus replication and assembly.

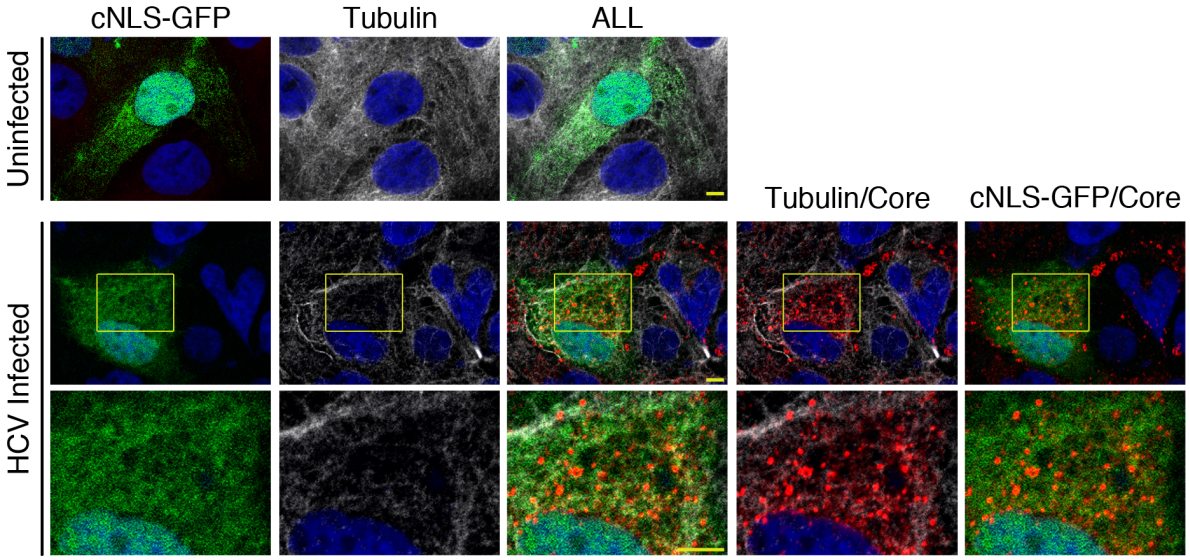

Figure 4-5. Localization of cNLS-GFP reporter to the membranous web. Uninfected or HCV-infected Huh7.5 cells were transfected with a construct encoding a chimeric protein consisting of an N-terminal cNLS sequence followed by two tandemly repeated GFP molecules 2 days after infection. On day 4 after HCV infection, the cNLS-GFP reporter was visualized by fluorescence microscopy (green) and its location compared to Tubulin (grey) and HCV Core (red) detected by immunofluorescence microscopy. DNA was detected with DAPI (blue) and scale bars represent 5 μm. Panels under 'ALL' show a merge image of each of the four colour channels including cNLS-GFP, Tubulin, Core and DAPI.

Figure 4-6. NLS-tagged PRRs colocalize with HCV proteins and inhibit viral replication. **A-B.** Uninfected or HCV-infected Huh7.5 cells were transfected with constructs encoding for either V5-tagged MDA5-I923V (A) or V5-tagged NLS-MDA5-I923V (B) 2 days after infection. On day 4 after HCV infection, the localization of HCV NS5A protein (red) as compared to that of MDA5-I923V or NLS-MDA5-I923V (green) was evaluated by indirect immunofluorescence microscopy using antibodies specific for the HCV NS5A or the V5 epitope tag. DNA was stained with DAPI (blue) and scale bars represent 5 μm. **C-D.** Uninfected or HCV-infected Huh7.5 cells were transfected with constructs encoding for either GFP-tagged RIG-I-K270A (C) or GFP-tagged NLS-RIG-I-K270A (D) 2 days after infection. On day 4 after HCV infection, the localization of HCV NS5A protein (red) as compared to that of RIG-I-K270A or NLS-RIG-I-K270A (green) was evaluated by indirect immunofluorescence microscopy using antibodies specific for the HCV NS5A. DNA was stained with DAPI (blue) and scale bars represent 5 μm. **E.** Pearson's colocalization coefficients for colocalization between HCV core and V5 fluorescence signals from HCV infected cells expressing either V5-tagged MDA5-I923V or V5-tagged NLS-MDA5-I923V. The values presented represent an average over 15 cells and the error bars indicate standard error. **F.** Uninfected or HCV infected Huh7.5 cells were transfected with constructs encoding for RIG-I-GFP, NLS-RIG-I-GFP or SLN-RIG-I-GFP 24 hours after infection. 72 hours after infection, cells were harvested using TRIzol reagent and the total levels of intracellular viral RNA were determined by qPCR using specific primers. Fold change was calculated relative to HCV infected cells transfected with constructs encoding for GFP alone.

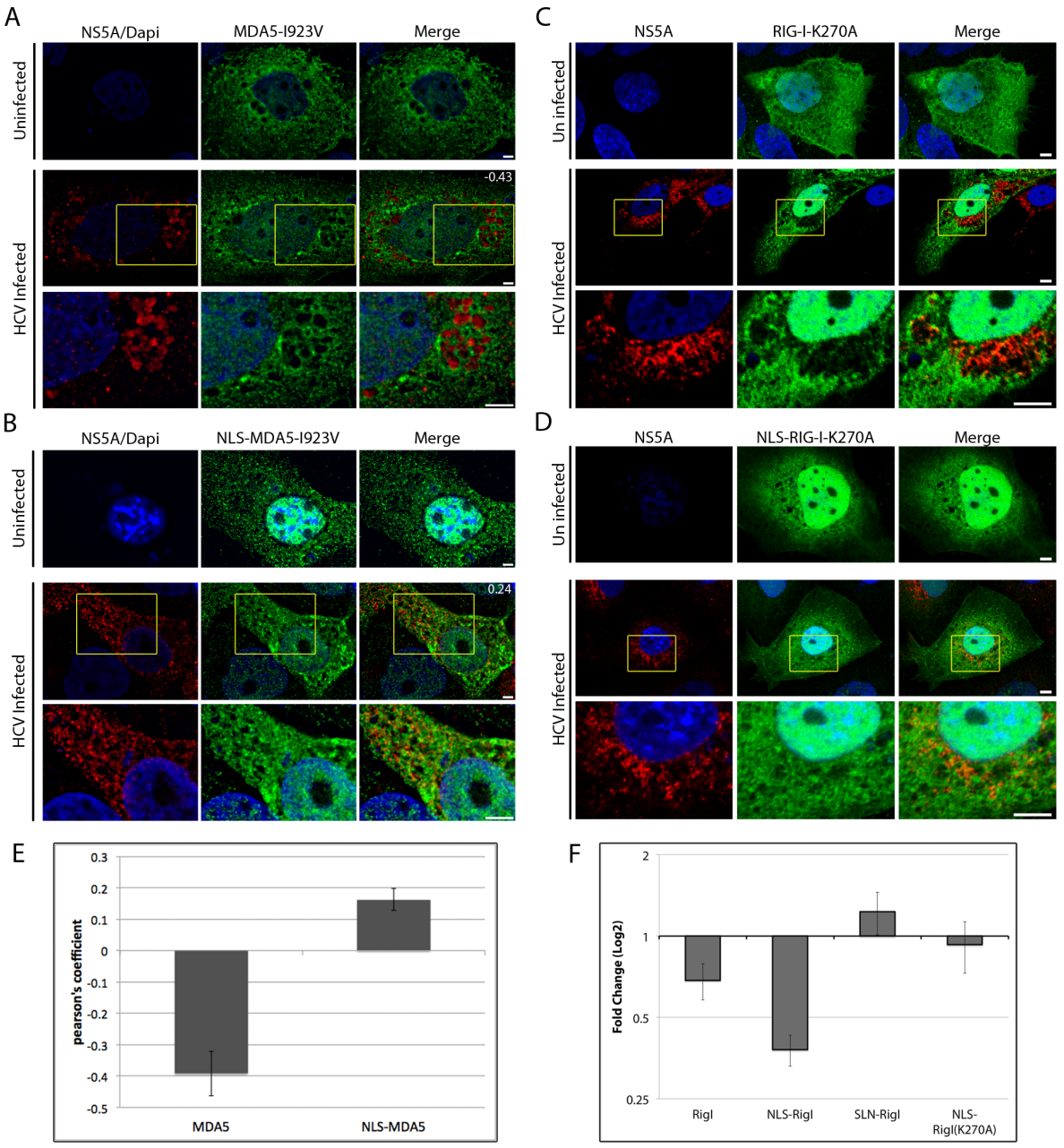

Figure 4-6. NLS-tagged PRRs colocalize with HCV proteins and inhibit viral replication

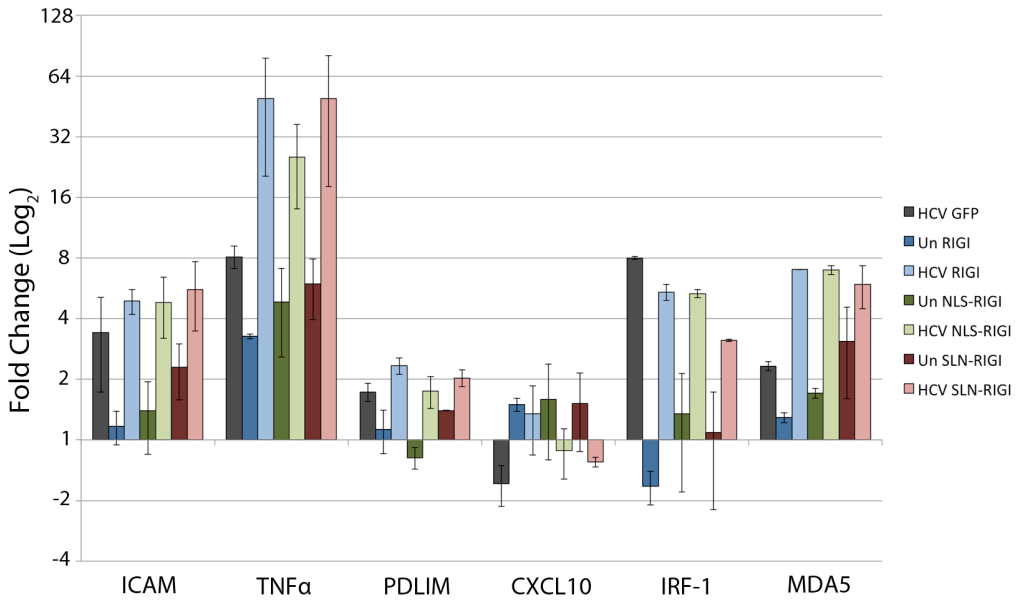

Figure 4-7. Induction of immune transcript by NLS-tagged RIG-I expression. Uninfected or HCV infected Huh7.5 cells were transfected with constructs encoding for RIG-I-GFP, NLS-RIG-I-GFP or SLN-RIG-I-GFP 24 hours after infection. 72 hours after infection, cells were harvested using TRIzol reagent and the levels of immune gene transcripts were determined by qPCR using specific primers. The values presented are relative to uninfected cells not transfected with any of the expression constructs.

4.2.4 RLRs are inhibited for accessing regions of viral replication and assembly

The results presented above suggest that HCV infection induces the formation of cytoplasmic compartments that sequester the viral genome away from RLRs in the surrounding regions of the cytoplasm, presumably to limit the innate immune response. In positive-strand RNA virus infection, viral RNA is involved is several different processes including genome replication, translation, and virion assembly. To better understand the spatial organization of HCV replication and assembly, and to determine the relationship between these processes and RLRs, we used fluorescence microscopy to examine the localization of specific viral RNA markers and we compared these to ectopically expressed RLRs. The localization of different viral RNA species was detected using branched DNA probes directed against either the positive-strand or negative-strand of the HCV genome. This methodology has previously been used for single molecule detection of host cell mRNA transcripts, as well as for detection of viral RNAs (Feeley et al., 2011; Lee et al., 2011b; Yu et al., 2012). For our studies, cells harbouring the FLAG-tagged RIG-I-K270A construct were co-stained with antibodies directed against the FLAG epitope and either HCV core or NS5A and then examined by in situ hybridization using positive-strand or negative-strand RNA probes (Figure 4-8 and 4-9). In cells analyzed for the localization of NS5A, RIG-I-K270A, and negative-strand HCV RNA, we observed that the negative-sense viral RNA was localized to regions that contained NS5A but lacked a RIG-I signal (Figure 4-8A), suggesting access of RIG-I to viral replication compartments is inhibited. Similarly, in HCV infected cells co-stained for core protein, RIG-I-K270A, and positive-strand RNA, both positive-strand RNA and core protein were predominantly localized to cytoplasmic regions lacking RIG-I signal (Figure 4-8B). However, the positive-strand RNA probe was also detected in a less abundant pool of foci distinct form core-containing regions and overlapping with RIG-I signal. These results imply that, although the majority of positive-strand HCV RNA

is present within cytoplasmic compartments that lack RIG-I, another pool exists outside these regions. Moreover, this suggests that viral RNA may traffic between different cytoplasmic compartments.

Figure 4-8. Exclusion of Rig-I from compartments containing both positive-strand and negative-strand viral RNA. A and B. Uninfected or HCV-infected Huh7.5 cells were transfected with constructs encoding for FLAG-tagged RIG-I-K207A 2 days after infection. On day 4 after HCV infection, cells were incubated with antibodies directed against the FLAG epitope (grey) and either HCV core or NS5A. DNA probes (Affymetrix) targeted to either the positive-strand or the negative-strand of the HCV RNA (red) were then hybridized to the viral RNA using the manufacturers protocol. DNA was stained with DAPI (blue) and cells were visualized by confocal immunofluorescence microscopy. Scale bars represent 5 μm.

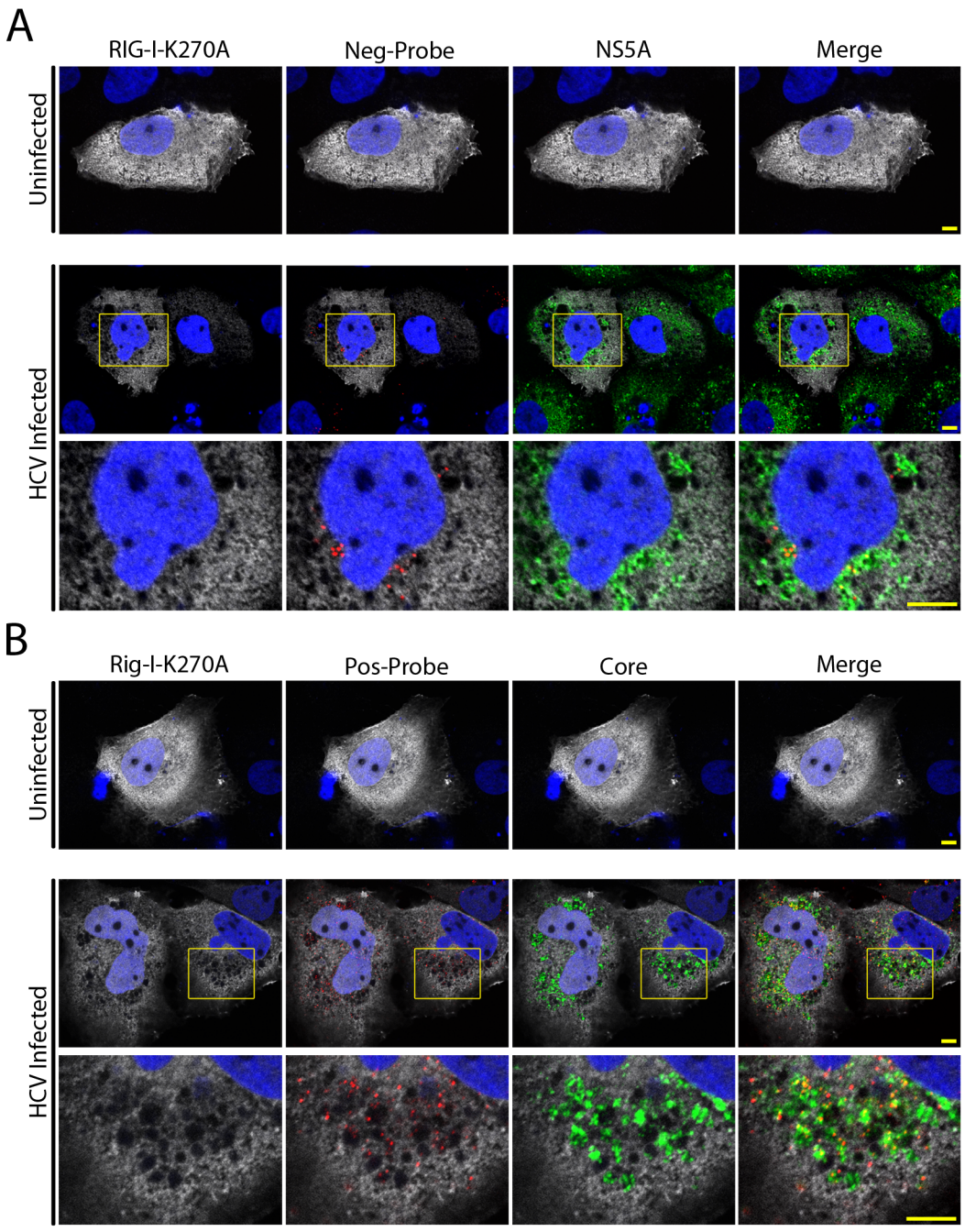

Figure 4-8. Exclusion of Rig-I from compartments containing both positive-strand and negative-strand viral RNA

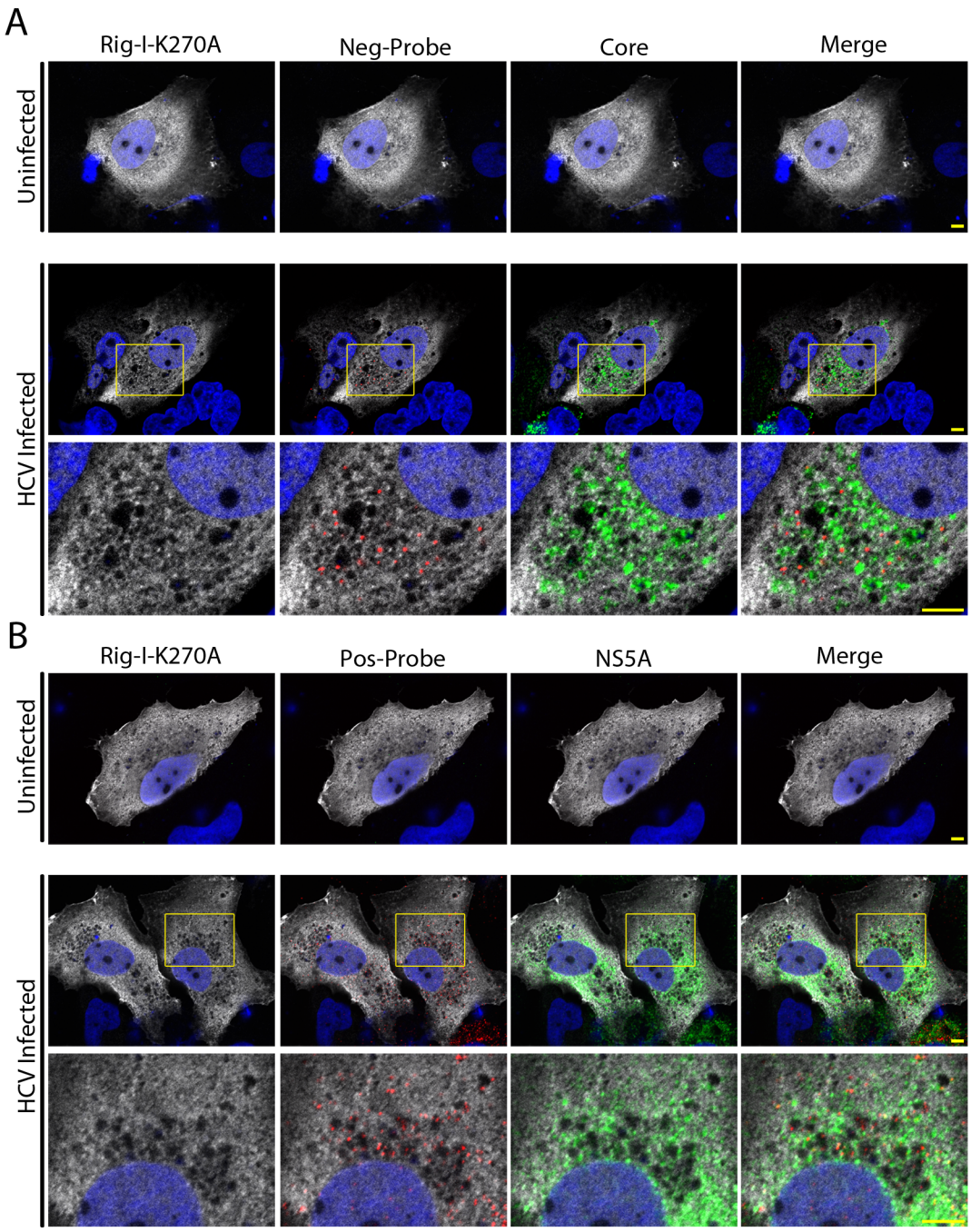

Figure 4-9. Localization of viral proteins and RNA in HCV-infected cells. Uninfected or HCV-infected Huh7.5 cells were transfected with a construct encoding for FLAG-tagged Rig-I-K207A 2 days after infection. On day 4 after HCV infection, cells were incubated with antibodies directed against the FLAG epitope (grey) and either HCV core or NS5A (green). DNA probes (Affymetrix) targeted to either the positive-strand or the negative-strand of the HCV RNA (red) were then hybridized to the samples using the manufacturers protocol. DNA was stained with DAPI (blue) and cells were visualized by confocal immunofluorescence microscopy. Scale bars represent 5 μm.

4.2.5 Isolation of distinct cytoplasmic compartments from HCV infected cells

The extent to which the membranous web is specialized to establish distinct regions, or subcompartments, that function in specific steps of the viral life-cycle, such as genome replication and viral assembly, has been documented or postulated for various positive-strand RNA viruses, including HCV (Counihan et al., 2011; Overby and Weber, 2011; Welsch et al., 2009). Our data in Figure 4-8 reinforce this conclusion as we can detect positive-strand HCV RNA distributed more broadly through out the cytoplasm as compared to negative-strand RNA. While the percent of total viral RNA involved in different processes is unclear, a portion of the positive-strand RNA is present at sites of virus assembly and egress. Previous studies have shown that these processes occur in association with lipid droplets and utilize the host cell VLDL export pathway (Huang et al., 2007; Miyanari et al., 2007; Shavinskaya et al., 2007). Notably, proteins functioning in lipid biogenesis and the VLDL export pathway localized to mitochondrial-associated ER membranes (MAM) linking these membranes to virus assembly (Horner et al., 2011; Huang et al., 2007; Lewin et al., 2002; Miyanari et al., 2007; Rusinol et al., 1994; Shavinskaya et al., 2007; Stone et al., 2009). Consistent with this idea, we have previously detected the enrichment of HCV and nuclear pore complex proteins in membrane fractions with sedimentation characteristics similar to MAM (Neufeldt et al., 2013).

We have used subcellular fractionation and western blot analysis to further examine the distribution and levels of key HCV proteins in various membrane fractions. With this approach, we observed an enrichment of viral polymerase NS5B in the lower density 'microsomal' membrane fractions. By contrast, core and the viral factor NS3 were enriched in the denser 'MAM' fraction (Figure 4-10A). Thus, key components of viral replication or assembly centers were enriched within lower density 'microsomal' membrane fractions or denser 'MAM' fraction, respectively. To further characterize these compartments, we also evaluated the levels of total

viral RNA and the amounts of infections virus present in the microsomal and MAM fractions. We observed that higher levels of total viral RNA were present in the microsomal fraction. By contrast, approximately double the percent of infectious virus was present in the MAM fraction (Figure 4-10B). These fractionation results lead us to conclude that distinct replication and assembly compartments are present in HCV infected cells, with a lower density 'microsomal' membrane fraction enriched for viral replication complexes (NS5B and viral RNA) and a membrane fraction similar in density to 'MAM' enriched for viral assembly complexes (Core, NS3, and infections virus). Moreover, the higher percentage of membrane-bound positive-strand RNA found in association with microsomes (~45% of total RNA) as compared to the denser to 'MAM' fraction (~10% of total RNA) implies that the majority of membrane associated viral RNA is likely engaged in replication or translation, while significantly lower amounts of RNA are present virion assembly sites (Figure 4-10B).

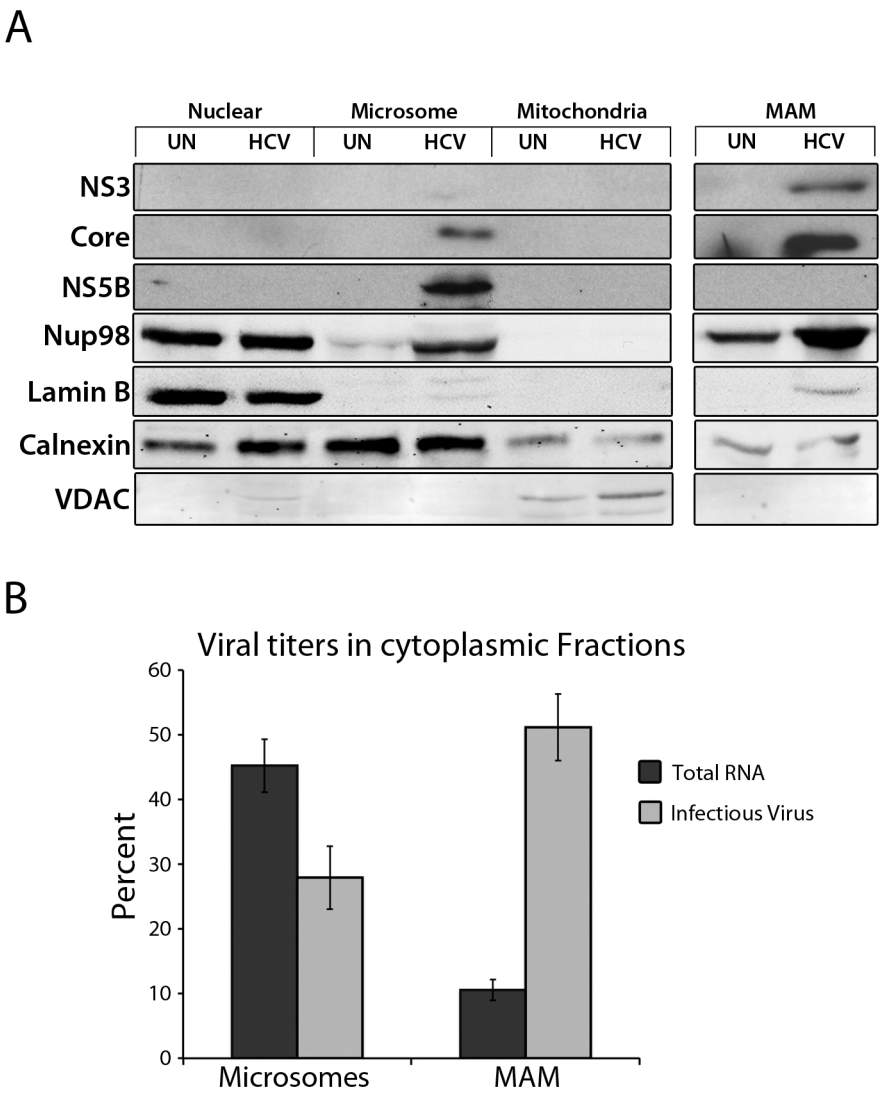

Figure 4-10. HCV infection induces the formation of multiple cytoplasmic compartments. A and B Total cell lysates were isolated from uninfected (UN) or HCV-infected (HCV) Huh7.5 cells and subjected to subcellular fractionation. **A.** Western blotting with antibodies specific for the indicated proteins was used to evaluate the total protein amounts in each of the indicated fractions. Equal amounts of total protein were loaded into each lane. All samples were run on the same gel and images shown are derived from the same membrane. **B.** The total HCV RNA from the microsomal or MAM fractions isolated in A were determined by qPCR. The number of infectious HCV particles microsomal or MAM fractions isolated in A was determined by infecting Huh7.5 cells with a portion of the sample from each fraction followed by counting focus-forming units using indirect immunofluorescence microscopy. Data shown in panel A were produced with the help of R.H. Steenbergen.

4.2.6 Ribosomes colocalize with RIG-I and are inhibited from accessing cytoplasmic regions enriched for HCV core.

Results obtained from the subcellular fraction of HCV infected cells show that the majority of membrane-bound viral RNA is associated with the lower density 'microsomal' fraction. As indicated above, our data lead us to conclude that this pool represents RNA in the process of either viral genome replication or translation. Several previous studies have reported that positive-strand RNA virus replication complexes are formed in association with ribosome-free ER membranes while translation of the HCV polyprotein occurs on membrane-bound ribosomes, suggesting that spatial separation exists between these two processes (Fontana et al., 2010; Gillespie et al., 2010; Knoops et al., 2008; Welsch et al., 2009). Indeed, it has been suggested that this spatial separation of viral replication, translation, and packaging is required to avoid interference between these processes (Paul and Bartenschlager, 2013). We therefore evaluated the localization of ribosomes and their relationship to HCV replication or assembly complexes. We stained uninfected or HCV infected Huh7.5 cells with antibodies directed against the S6 protein component of the 40S ribosomal subunit. In uninfected cells, ribosomes were distributed throughout the cytoplasm (Figure 4-11A, top panel). However, in infected cells the vast majority of the S6 protein was excluded from regions of the cytoplasm containing HCV core protein (Figure 4-11A). The separation of the two fluorescent signals was also supported by negative Pearson's colocalization coefficients (Figure 4-11, right panels). To determine whether the signal observed for ribosomal proteins corresponded with RIG-I, cells were transfected with constructs encoding RIG-I-K270A followed by staining with antibodies directed against the FLAG epitope, S6 ribosomal protein, and HCV core. In both uninfected and HCV infected cells, there was significant overlap was observed between RIG-I-K270A and the S6 protein (Figure 4-11B). This spatial separation between the membranous web and the bulk of the

ribosomal proteins are consistent with a model in which translation of the viral polyprotein occurs on rough ER membranes outside of the membranous web.

Figure 4-11. Exclusion of ribosomes from viral replication compartments. A. Huh7.5 cells were uninfected or infected with HCV for four days. The localization of the S6 protein of the 40S ribosomal subunit (green) and HCV core protein (red) in cells was evaluated by indirect immunofluorescence microscopy using specific antibodies. DNA was stained with DAPI (blue). **B.** Uninfected or HCV-infected Huh7.5 cells were transfected with a construct encoding FLAG-tagged RIG-I-K270A 2 days after infection. On day 4 after HCV infection, cells were incubated with antibodies directed against the FLAG epitope (red/green), HCV core (red) and the S6 protein (green). DNA was stained with DAPI (blue) and cells were visualized by confocal indirect immunofluorescence microscopy. Scale bars represent 5 μm.

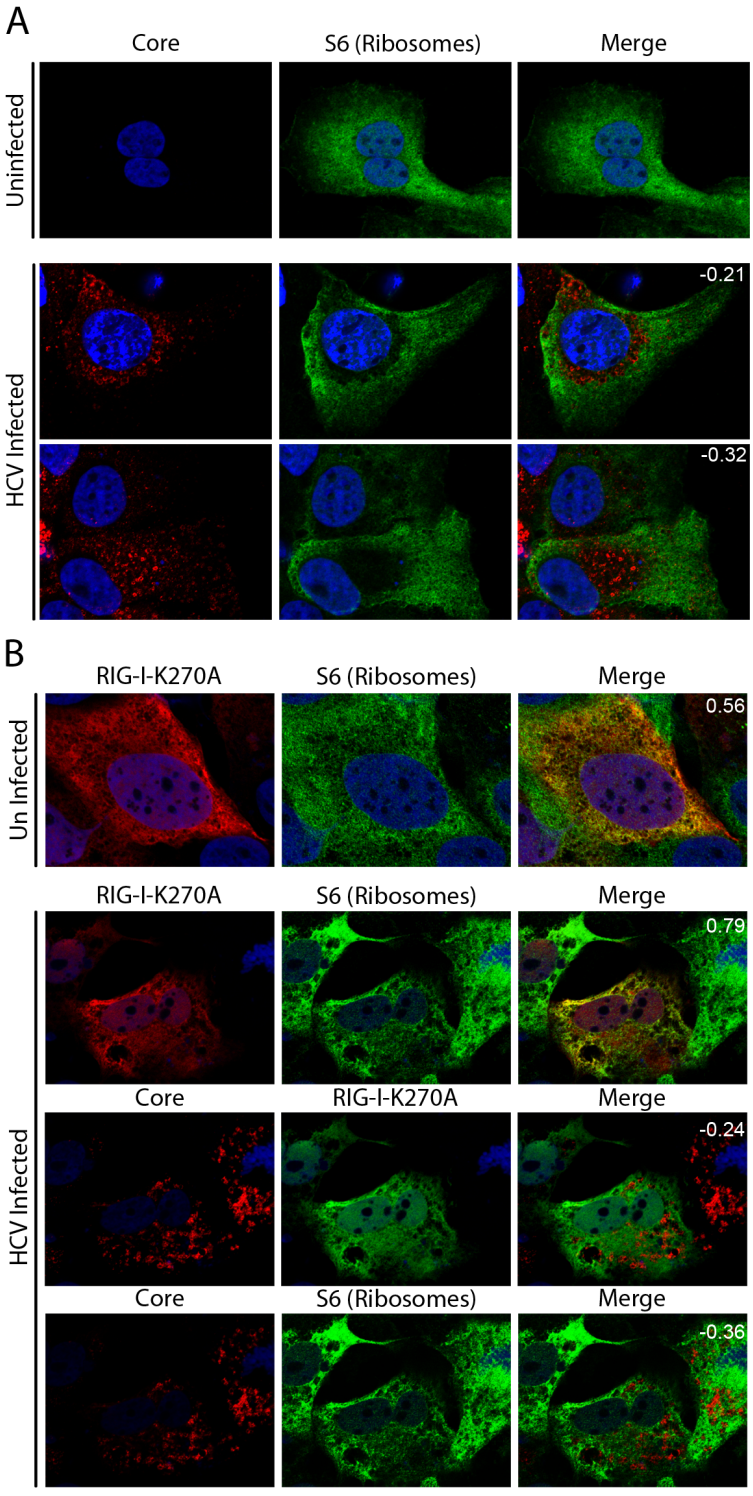

Figure 4-11. Exclusion of ribosomes from viral replication compartments

4.3 Discussion

Although there are significant differences in the organization and architecture of the membrane rearrangements induced by positive-strand RNA viruses, the general function of these compartments is conserved. Much like the formation of membrane bound organelles in eukaryotic cells, the induction of compartmentalized viral replication factories serves to both concentrate proteins within a specific area, thereby increasing efficiency of certain processes, and to spatially separate processes that interfere with one another. An added function of sequestering viral replication complexes away from the surrounding cytosol is the concealment of viral PAMPs from RLRs, thereby inhibiting host cell innate immune activation. On the basis of the data presented here, we propose that a selective permeability barrier exists between the cytosol and replication complexes, and that this barrier promotes viral infection by both allowing passage of metabolites and viral RNA while inhibiting access to RLRs. Our findings support a role for components of the nuclear transport machinery in regulating traffic between these cytoplasmic compartments by demonstrating that addition of NLS sequences to either RIG-I or MDA5 allows these proteins to access the membranous web and impede viral replication. We also demonstrate the existence of multiple viral compartments in HCV infected cells and provide evidence for a spatial separation between viral genome replication and translation. We propose that the nuclear transport machinery is involved in maintaining a selective barrier that allows trafficking of specific molecules between the membranous web and the surrounding cytoplasm.

4.3.1 Compartmentalization of viral replication complexes

Recently, our understanding of the underlying architecture of positive-strand RNA virus-induced replication factories has been greatly increased by EM tomography analysis (reviewed in

(Paul and Bartenschlager, 2013)). These studies have revealed the induction of two distinct types of membrane alterations by positive-strand RNA viruses. The conservation of the membrane alterations induced by viral agents suggests strong evolutionary pressures for maintaining the architecture of these structures. Here, we have evaluated the function of these membrane rearrangements in concealing PAMPs from host RLRs in positive-strand RNA virus infection. Replication factories from both HAV, which induces a perinuclear tubular-vesicular membrane replication complex, and HCV, which forms replication complexes composed predominantly of DMVs, both inhibited entry to RLRs (Figure 4-1, 4-2 and 4-4) (Gosert et al., 2000; Romero-Brey et al., 2012). Additionally, previous studies have shown that viral replication factories produced in Tick-borne encephalitis virus infected cells (InV/spherule-type membrane alterations) also inhibit immune activation by concealing viral dsRNA from cytosolic RLRs (Overby et al., 2010). Collectively, these observations suggest that hiding viral PAMPs from cytosolic immune receptors is a common strategy for immune evasion used by positive-strand RNA viruses.

Compartmentalization of the membranous web creates a functional barrier to both metabolites needed for replication and for the viral RNA. This segregation of viral replication and assembly centers necessitates a transport mechanism capable of regulating traffic between different compartments of the membranous web and the surrounding cytoplasm. In the InV/S type replication factories, narrow channels exist at the neck of the InVs connecting them to the cytosol and these channels have been suggested to transport newly synthesized RNA destined for translation or assembly, as well as allow access to metabolites required for replication (Fontana et al., 2010; Gillespie et al., 2010; Kopek et al., 2007; Welsch et al., 2009). However, the composition of these channels and the mechanisms of RNA export remain unclear. In HCV infected cells, channels between DMVs and the cytosol have only rarely been observed, and they vary significantly in size suggesting a different mechanism is utilized for transport between

compartments of the membranous web and the surrounding cytosol. Previously, we presented data indicating that NPCs are recruited to sites of viral replication and assembly, and that NPC-mediated transport occurs within the membranous web (Levin et al., 2014; Neufeldt et al., 2013). Components of the nuclear transport machinery are involved in numerous cellular processes that could impact viral infection, including forming and maintaining curved membranes, regulating immune responses, mediating mRNA export, and trafficking cargos required for viral infection (Le Sage and Mouland, 2013; Yarbrough et al., 2014). Here we provide evidence supporting a transport function for the NPC and soluble nuclear transport factors in the membranous web by demonstrating that RLRs that are normally inhibited from accessing replication/assembly complexes, colocalize with HCV proteins when they are tagged with an NLS sequence (Figure 4-6). Moreover, we show that the addition of NLS sequences to active RLRs has an inhibitory affect on viral replication (Figure 4-6F). Together, these results provide further evidence for functional NPC-mediated transport between compartments within the membranous web and the surrounding cytoplasm. Thus, virus-induced recruitment of NPCs to the membranous web appears to contribute to the immune evasion strategy of HCV. However, a transport role for NPC-like structures in the membranous web does not exclude the possibility of individual components of the nuclear transport machinery having additional roles in HCV infection.

4.3.2 HCV infection induces the formation of multiple cytoplasmic compartments

In addition to revealing a viral immune evasion tactic, the subcellular localization of RIG-I and its exclusion from regions of the cell occupied by HCV proteins provides an effective marker for the boundaries of the membranous web in infected cells. Previously, visualization of the membranous web by immunofluorescence has been imprecise due to the abundance of HCV proteins in infected cells and the difficulty in interpreting the lack of overlap between viral

proteins involved similar processes. Correlation of adjacent proteins, either viral proteins or host factors, has predominantly been employed to propose associations between proteins within the membranous web. Previous studies have indicated that staining for either NS5A or NS4B proteins represents an approach to defining the location of the membranous web (Paul et al., 2013; Wolk et al., 2008). However, in infected cells, NS5A is observed throughout the cytoplasm where it is proposed to be involved in numerous viral and cellular processes (Figure 4-1 and 4-2)(reviewed in (Joyce and Tyrrell, 2010)). Likewise, NS4B also shows a dispersed cytoplasmic pattern that only periodically overlaps with HCV core (Figure 4-2B)(Paul et al., 2013). Data presented here indicate that HCV proteins and RNA are enriched in regions that inhibit entry to PRRs and that, through an NLS-dependent mechanism, PRRs are actively excluded from virus-induced cytoplasmic compartments (Figure 4-1, 4-2 4-6 and 4-8). From these observations, we propose that staining for overexpressed RIG-I-K270A can provide an effective exclusion marker capable of outlining the membranous web in infected cells using fluorescence microscopy (Figure 4-1, 4-2, 4-8 and 4-11). This technique could be further used to evaluate the role of specific host factors in HCV infected cells, and future experiments using live-cell imaging with inactive RLR constructs may also provide important details about the formation and dynamics of viral replication complexes.

The induction of district cytoplasmic compartments for the purposes of either viral genome replication or virion assembly has been proposed in numerous studies. However, visualization and characterization of these different compartments has been difficult. In this study, we used subcellular fractionation techniques to isolate membrane fractions enriched for either viral replication or assembly components (Figure 4-10). The predominance of the viral polymerase NS5B in the microsomes reflects an enrichment of replication complexes in this membrane fraction, while the concentration of the core protein in a membrane fraction of a

density similar to MAMs suggest that this heavier membrane fraction is enriched for assembly complexes. Consistent with these observations, increased levels of viral RNA co-fractionate with the microsomal fraction while increased levels of infectious virus are associated with the denser MAM membrane fractions (Figure 4-10B). These experiments describe a useful enrichment technique for both replication and assembly complexes and provide a platform for future experiments aimed at understanding the relationship between these distinct viral processes.

Current theories on HCV assembly and egress propose that HCV RNA traffics with core from replication compartments to assembly complexes suggesting a spatial separation between viral replication and assembly complexes (see section 1.3.4 and reviewed in (Joyce and Tyrrell, 2010; Lindenbach and Rice, 2013). Previous studies have shown that the viral core protein goes through a maturation step that involves cleavage of a small C-terminal peptide causing relocalization to LDs followed by NS2/p7-mediated recruitment to assembly compartments (Gentzsch et al., 2013; Jirasko et al., 2010b; Popescu et al., 2011). The viral NS2/p7 protein complex also recruits NS3/4A proteins to the viral assembly compartment where NS3 is thought to function in packaging viral RNA (Beran et al., 2009; Counihan et al., 2011; Phan et al., 2011; Pietschmann et al., 2009). This trafficking of viral components to LDs is thought to act as an initiation step for viral packaging, which is closely linked to lipid export pathways. Our isolation of membranes enriched for each of these complexes by subcellular fractionation supports the idea that there is separation between viral replication and assembly compartments and provides evidence that HCV induces the formation of multiple cytoplasmic compartments (Figure 4-10). Moreover, our immunofluorescence data using probes specific for the positive-strand RNA in parallel with HCV core staining suggest that, in addition to being excluded from viral replication compartments, RIG-I is also inhibited from entering assembly complexes (Figure 4-1, 4-3A and 4-8). This exclusion of PRRs from multiple virus-induced

compartments gives insight into the organization of the membranous web and may indicate that there is a larger and more complex architecture of the membranous web than current EM tomography assays have observed.

4.3.3 Topology and organization of the membranous web

One possible explanation for the exclusion of RLRs from both replication and assembly complexes could be that both viral compartments are located within a single larger membrane structure, which is selectively permeable to the surrounding cytoplasm. Indeed, the staining pattern for overexpressed RLR proteins in HCV infected cells showed the formation of large cytoplasmic compartments containing multiple viral proteins (Figure 4-1, 4-2 and 4-8). Previously, EM studies have defined the membranous web as an accumulation of different vesicle species in areas of viral replication (Romero-Brey et al., 2012). Overexpression of the inactive version of RIG-I or MDA5 defined cytoplasmic compartments that were variable in size, but usually larger than 500 nm in diameter (Figure 4-1 and 4-2). This observation supports the hypothesis that large cytoplasmic regions are compartmentalized to form replication or assembly complexes. The inclusion of NLS-tagged GFP reporter proteins within these regions also demonstrates that there is selective permeability between the membranous web and the surrounding cytosol (Figure 4-5) (Levin et al., 2014; Neufeldt et al., 2013). Together with our data indicating RLRs are excluded from both replication and assembly complexes, these observations may indicate the formation of a compartment that encompasses a larger area of the cytoplasm; however, the nature of the membrane barrier that defines the perimeter of the membranous web remains ill defined.

The complex architecture of the membranous web suggests that mechanisms are in place to organize molecules and process within these compartments. Previously, it has been suggested

that positive-strand RNA viruses coordinate different viral processes, such as replication, translation and assembly, by spatially segregating these processes in different compartments (Paul and Bartenschlager, 2013). Indeed viral capsid proteins and RNA often relocate to different cellular locations at later time points in infection, suggesting coordination between viral replication and assembly that prevents interference between these processes. A similar separation between replication and RNA translation has also been proposed based on evidence that various positive-strand RNA viruses are composed of ribosome-free membranes and the hypothesis that these processes would interfere with one another (Fontana et al., 2010; Gillespie et al., 2010; Knoops et al., 2008; Welsch et al., 2009). Here, we show that bulk ribosomes have a similar subcellular localization to that of RIG-I in HCV infected cells, supporting a spatial separation between genome replication/assembly and translation (Figure 4-10). This is also supported by our observations that a portion of the viral positive-strand RNA is located in regions containing RIG-I (Figure 4-8B). These observations suggest that viral RNA destined for translation may exit the membranous web which would imply that mechanisms exist to target newly replicated viral RNA for either export from the membranous web and translation or retention and targeting to viral assembly centers. Several groups have shown that phosphorylation of NS5A is specifically required for viral assembly and have suggested that this may act as a molecular switch to shift viral RNA from replication to assembly (Kim et al., 2011; Tellinghuisen et al., 2008). It may be that phosphorylation NS5A or a similar mechanism is involved redirecting viral RNA towards assembly compartments rather that translation compartments. Further research into the dynamics of viral RNA and protein trafficking is required to determine how positive-strand RNA viruses spatially organize replication factories.

The previously described activation of RIG-I-mediated immune responses in HCV infected cells indicates that at least a portion of the viral RNA is present in regions of the

cytoplasm containing RIG-I. We envisage several scenarios that might allow RIG-I to interact with viral RNA despite their largely segregated localization patterns in infected cells. First, previous analysis of HCV-induced immune response showed that RIG-I-mediated signalling is activated at early time points after infection (Sumpter et al., 2005). Thus, RIG-I activation in HCV infected cells could occur through an interaction with viral RNA prior to the establishment of a fully compartmentalized membranous web. Alternatively, viral ssRNA, which can associate with and activate RIG-I in the absence of dsRNA, could passively or actively exit the membranous web, potentially for the purpose of translation, to the surrounding cytosol where it could be recognized by RIG-I and initiate immune activation (Saito et al., 2007). Observations that bulk ribosomes colocalize with RIG-I are consistent with the idea that positive-strand viral RNA could bind RIG-I outside the membranous web (Figure 4-11). In both models, a passive strategy for immune evasion through concealment of PAMPs is not sufficient for blocking all immune activation. Importantly, however, in both proposed models, RLRs would only have access to viral positive-strand RNA while double-stranded viral RNA is protected in the membranous web. This may explain why it has been difficult to observe MDA5-mediated immune activation, as MDA5 does not recognize ssRNA.

4.3.4 Conclusions

In addition to previously published data, the observations presented here support a model where NPC-like structures positioned within virus-induced compartments function to conceal replication intermediates from RLRs while still allowing entry to molecules required for replication. Further studies into the structure and function of cytoplasmic NPCs, including their interactions with viral proteins and their ability to facilitate transport of host proteins, viral proteins, and RNA between compartments of the membranous web and the surrounding

cytosol, will have a broad impact on our understanding of their roles in the life cycle of HCV and other positive-strand RNA viruses. Additionally, functional analysis of this pathway may lead to the discovery of general targets for antiviral drugs. Notably, recent results suggest that selectively inhibiting the interactions of HCV proteins with the nuclear transport machinery has inhibitory effects on viral replication with limited cellular toxicity (Levin et al., 2014; Neufeldt et al., 2013).

CHAPTER V: A role for Nup358 in the innate immune response

5.1 Overview

By regulating the transport of proteins and nucleic acids between nuclear and cytoplasmic compartments, the NPC influences a large number of cellular pathways. A growing body of literature has implicated the NPC and specific Nups in controlling processes such as gene expression and sumoylation, through mechanisms unrelated to its transport function. Among the cellular pathways that utilize Nups is the innate immune response. For example, two mammalian Nups, Nup98 and Nup96, are upregulated in response to IFN treatment (Enninga et al., 2002). One function for their increased production is believed to be the release of an mRNA export block implemented by several viruses. To gain further insight into the functions of Nups in immune responses, we have performed quantitative real time PCR on macrophage cells treated with IFNγ to identify expression change in Nup genes. These experiments revealed that, following IFN stimulation, an additional subset of Nups (including Nup358, Nup153, and Nup205) were expressed at elevated levels, whereas other Nups (including Nup155, Nup214 and Nup107) were not affected. Protein analysis confirmed a corresponding change in cellular protein amounts of Nup98, Nup358, Nup155, and Nup153. Moreover, time course experiments showed that upregulation of Nup358 and Nup98 exhibited a biphasic pattern that paralleled trends observed with other IFN-stimulated genes. Immunofluorescence analysis of Nup98 or Nup358 following IFN treatment showed that these proteins are localized to nuclear and cytoplasmic compartments, respectively. Depletion of Nup358 caused increased interferon stimulated gene (ISG) activation indicating an immune regulatory role for Nup358. Further domain and promoter analysis showed that Nup358 is involved in regulating type I IFN responses, and that this might be facilitated by Nup358 SUMO E3 ligase and isopeptidase activity. Moreover, depletion of Nup358 also inhibited HCV replication suggesting that viruses may utilize the immune regulatory function of Nup358 to subvert host cell immune responses.

This function of Nup358 in HCV infection is consistent with our previous data showing that Nup358 is elevated at early time points after infections. From these data, we propose that multiple Nups are involved in innate immune responses and that Nup358 functions in negatively regulating innate immune signalling pathways.

5.2 Results

5.2.1 Immune stimulation increases mRNA expression levels of a subset of nucleoporins

Previous studies have reported that specific NPC components are involved in innate immune responses. Specifically, these studies showed that Nup96 and Nup98 are elevated following stimulation of macrophages with IFNγ, and that each of these Nups functions in promoting expression of immune effector proteins (Enninga et al., 2002; Faria et al., 2006; Satterly et al., 2007; Schmitz et al., 2010). Here, we aimed to evaluate the global effect of immune activation on the NPC by examining the effects of IFNγ treatment on the mRNA transcripts levels of selected Nups present in each of the NPC subcomplexes (Figure 1-5). Nup transcript amounts were analyzed in both an immortalized mouse macrophage cell line (Raw264.7) and in primary mouse peritoneal macrophages over a 24-hour time course of IFNγ treatment (Figure 5-1). Consistent with previously published data, we observed elevated Nup98 transcript levels following IFNγ stimulation in both cell lines. Interestingly, Nup98 upregulation was observed between 12 and 24 hours in Raw264.7 cells and between 2 and 4 hours in primary macrophages highlighting the differences in immune signalling between these cell lines. These differences in immune activation were also seen with a well-defined ISG, IRF-1, when comparing upregulation patterns observed between primary macrophages and Raw264.7 cells (Figure 5-2). In addition to changes in Nup98 mRNA levels, IFN stimulation increased transcript levels for Nup358 in both primary macrophages and Raw264.7 macrophages, whereas Nup88, Nup153 and Nup205 were elevated only in primary macrophages and Nup62 and Nup93 mRNA levels were upregulated only in Raw264.7 cells. The transcript levels of other Nups, including Nup53, Nup93, Nup155 and Nup214, were not significantly altered by IFNγ treatment in either cell line. In contrast to other Nups, Nup358 transcript levels were highly elevated at earlier time points after IFNγ stimulation in both cells lines (at 2 hours in primary

cells and between 4-6 hours in Raw264.7 cells), which was also paralleled by IRF-1 upregulation in both cell lines (Figure 5-1 and 5-2). These results suggest that Nup358 may have a significant role early in the innate immune responses.

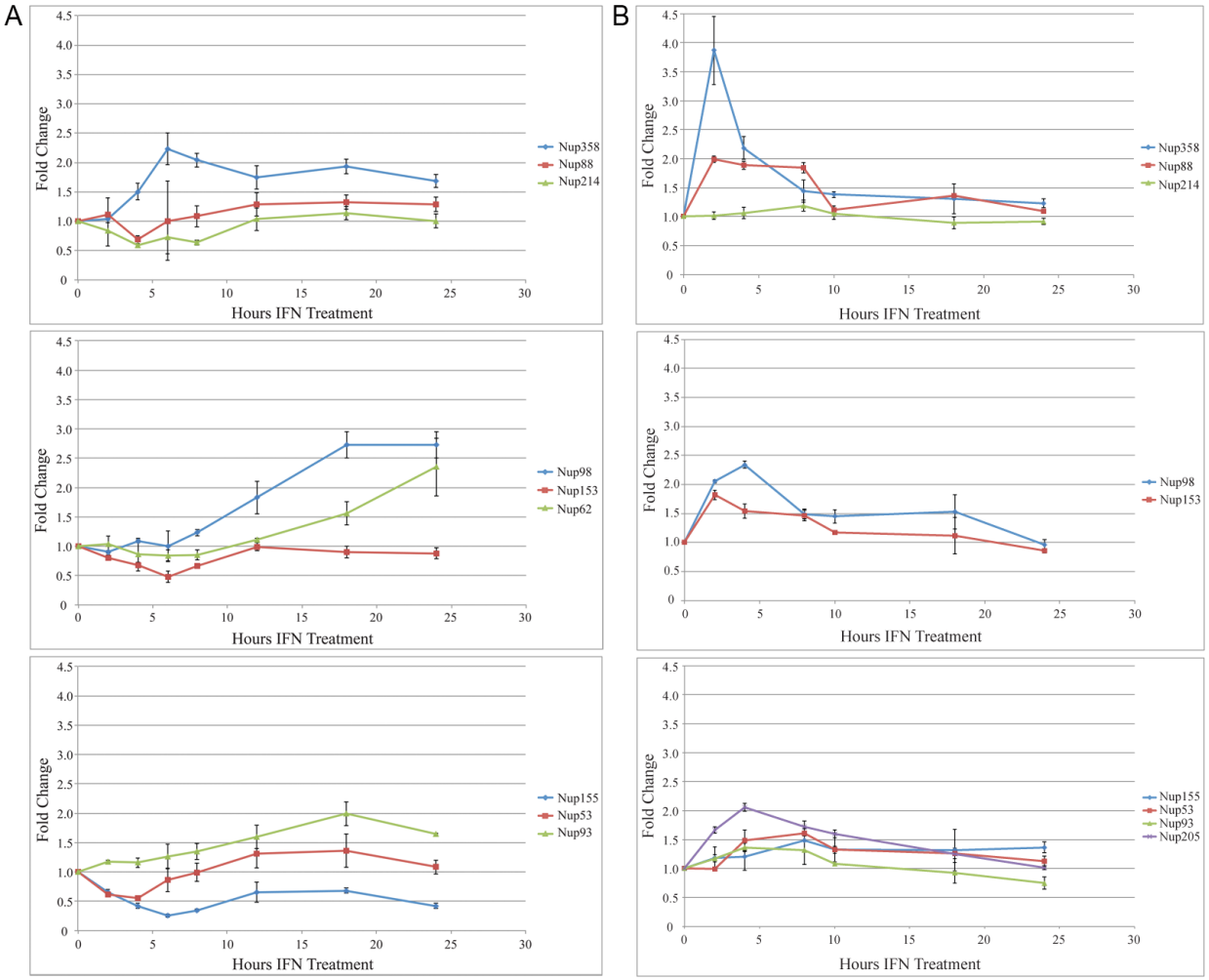

Figure 5-1. IFNγ treatment alters the mRNA transcript levels of a subset of Nups. A and B. Raw264.7 mouse macrophages (column A) and primary mouse macrophages (column B) were treated with 1000 U/mL recombinant mouse IFNγ for 24 hours. The amounts of Nup mRNA transcripts were determined at the indicated time points after addition by qPCR using primer sets specific to each Nup. Values shown for each sample were normalized to HPRT and are expressed as fold-change relative to untreated cells. Error bars were derived from standard error based on at least 3 biological replicates. Primary mouse macrophages were isolated from the mouse peritoneal cavity 4 days after the mice were injected with Concanavalin A. Macrophages were separated from other white blood cells by attachment to tissue culture treated plates.

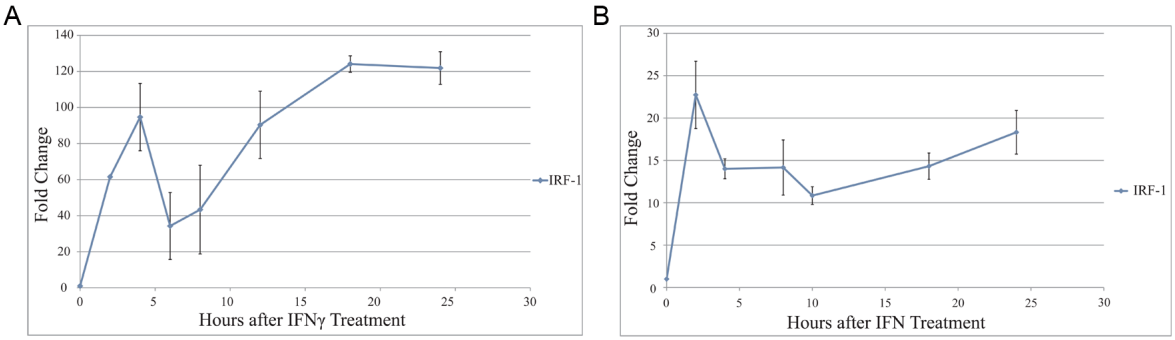

Figure 5-2. IFNγ-induced changes in IRF1 transcript levels. A and B. Raw264.7 mouse macrophages (panel A) and primary mouse macrophages (panel B) were treated with 1000 U/mL recombinant mouse IFNγ for 24 hours. The amounts of IRF1 mRNA transcripts were determined at the indicated time points after addition by qPCR using specific primers. Values shown for each sample were normalized to HPRT and are expressed as fold-change relative to untreated cells. Error bars were derived from standard error based on at least 3 biological replicates. Primary mouse macrophages were isolated from the mouse peritoneal cavity 4 days after the mice were injected with Concanavalin A. Macrophages were separated from other white blood cells by attachment to tissue culture treated plates.

5.2.2 Immune stimulation elevates proteins levels and alters subcellular localization of specific Nups

To determine if an increase in Nup transcripts results in a corresponding increase in protein amounts, we evaluated the changes in total Nup protein following IFNγ treatment by quantitative western blotting. Consistent with our findings in Figure 5-1, we observed a significant increase in Nup98 and Nup358 protein amounts following IFNγ treatment of Raw264.7 cells (Figure 5-3A). Interestingly, the trend of Nup98 and Nup358 upregulation showed a biphasic pattern, which is consistent with trends described for a number of other ISGs (Ivashkiv and Donlin, 2014; Platanias, 2005). The resulting change in Nup proteins could suggest that the NPC associated pools of these proteins have increased, indicating changes in NPC structure or transport capacity. Alternatively, excess Nups produced following IFN stimulation might localize to nucleoplasmic or cytoplasmic compartments where they could facilitate a non-transport related function in innate immune pathways (Enninga et al., 2002). To determine the subcellular localization of specific Nups following IFNγ treatment, we probed cells with antibodies directed against Nup98 or Nup358 and evaluated their location by immunofluorescence microscopy. Consistent with previous studies, we found a significant increase in intra-nuclear levels of Nup98, most notably in distinct nuclear foci, likely representing the previously described 'GLFG bodies' (Figure 5-3B and 5-3C)(Griffis et al., 2002). Additionally, the levels of Nup98 at the NE and in the cytoplasm were not significantly altered, further supporting an intranuclear function for Nup98 in innate immune signalling. Conversely, the cytoplasmic and NE levels of Nup358 were significantly increased following treatment with IFNγ, suggesting that Nup358 may have a cytoplasmic or NPC-related function in the innate immune response (Figure 5-3B and 5-3C). These observations are consistent with Nup358 and Nup98 having different roles in innate immune signalling, and they may suggest their functions in immunity encompass additional functions beyond nuclear transport.

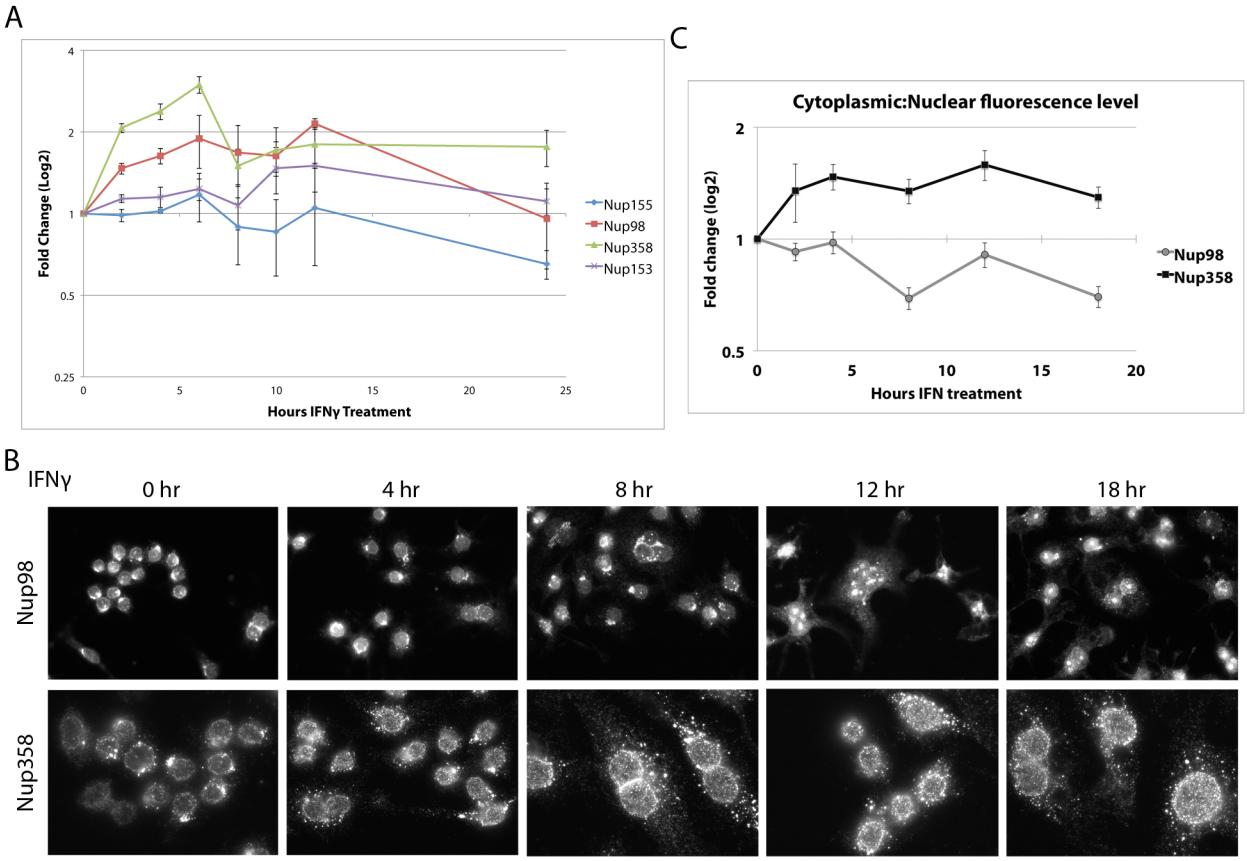

Figure 5-3. IFNγ treatment alters the protein levels and subcellular localization of specific Nups. Raw264.7 cells were treated with 1000 U/mL mouse recombinant IFNγ for the indicated time. **A.** Protein levels were determined by quantitative western blotting using antibodies directed against the indicated Nups. Blots were developed using a Licor infrared system and quantification was done with ImageJ software. The values presented are derived from an average of three biological replicates and error bars represent standard error. **B.** The subcellular localization of Nup98 or Nup358 following INFγ treatment was determined by indirect immunofluorescence microscopy using antibodies directed against Nup98 or Nup358. Exposure time is equal between all Nup98 panels or all Nup358 panels. **C.** The relative cytoplasmic and nuclear fluorescence levels were calculated for each time point shown in B using ImageJ software. The values are expressed as the fold-change of the ratio of cytoplasmic verses nuclear fluorescence levels relative to that of cells prior to IFNγ treatment. Values represent an average of >15 cells and error bars were calculated based on standard error.

5.2.3 Depletion of Nup358 leads to increases in immune activation

Upregulation of Nup358 in response to immune stimulation coupled with previous studies showing that Nup358 negatively regulates transcriptional activation of some immune genes, led us to hypothesize that Nup358 may be involved in negatively regulating immune pathways (Scognamiglio et al., 2008). To better understand the role of Nup358 in transcriptional regulation of immune genes, we examined the effects of depleting Nup358 on mRNA transcript levels of various immune stimulated genes (ISGs) using a qPCR array. Transcript levels of 47 ISGs important in HCV infection were evaluated 72 hours after depletion of Nup358 in Huh7.5 human hepatocytes, which are normally used for HCV infection experiments (Table 5-1). Using this system, we observed a significant increase in the transcript levels of a subset of ISGs following depletion of Nup358 for 72 hours (Figure 5-4). From this array data, we selected several ISGs that were altered by Nup358 depletion to further characterize the function of Nup358 in regulating ISG expression. To examine the effects of Nup358 depletion on the dynamics of ISG activation following IFNγ treatment, we evaluated the changes in transcript amounts for specific ISGs in cells transduced with constructs encoding shRNAs directed against Nup98, Nup155, Nup358, or a scrambled control shRNA construct. For these experiments we used a human macrophages cell line, U937 as these cells respond to IFNγ stimulation. Consistent with our array data, at the first time point before the addition of IFNγ, Nup358 knockdown caused an increase in mRNA transcript levels for a number of immune related genes including IRF-1, MDA5, ICAM1, ULBP2, CXCL9, and OAS3 (Figure 5-5A). When Nup-depleted cells were then treated with IFNγ over a time course of 12 hours, we observed several different effects. In Nup358 depleted cells, the amounts of ISG transcripts were elevated compared to that of the control shRNA treated cells, but the general pattern of upregulation was not significantly altered (Figure 5-5A purple). Depletion of Nup98 had similar transcriptional

effects as Nup358 depletion on some genes but divergent effects on others, further suggesting these two proteins have different roles in immune activation (Figure 5-5 red). By contrast, the upregulation of ISGs did not appear to be altered by Nup155 depletion compared to the shRNA control (Figure 5-5 green). These results suggest that the immune regulatory function of Nup358 may act to generally control the activation of ISGs following immune stimulation.

Table 5-1. List of mRNA transcripts evaluated in the ISG qPCR array.

Initial response genes		Down stream effectors	cytokine/chemokine/HLA	Markers
Activators	Regulators			
RELA (p65)	SOCS1	1FI44	CXCL9	PCNA
IFIH1 (Mda5)	SOCS3	MX1	CXCL10	HSPA5
TICAM1 (TRIFF)	STAT1	OASL	CXCL11	ALB
VISA (IPS1)	STAT2	OAS3	HLA-A	
IRF-7	PDLIM2	ISG20	HLA-C	
IRF-9	OTUD5	IFIT2	HLA-DRA	
IRF-3	NLRX1	IFIT3	HLA-G	
IFNA2		MX1	IL18	
IFNB1		PCNA	IL15	
STAT1		HSPA5	ICAM1	
STAT2		ALB	ULBP2	
IFNG			CCL8	
			MICA	
			CLEC2D	

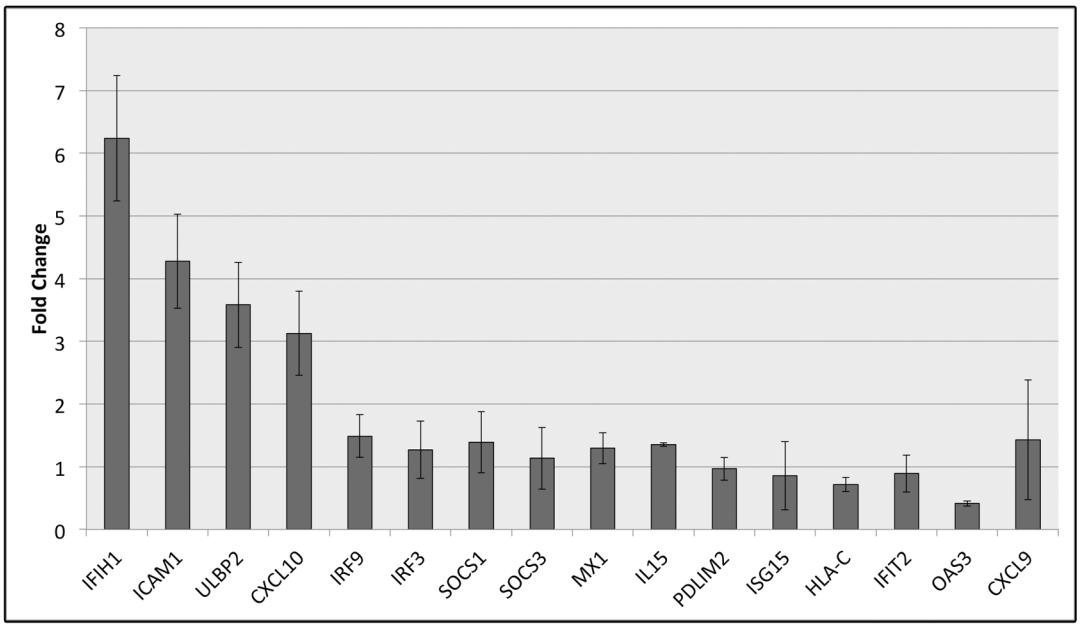

Figure 5-4. Nup358 depletion alters ISG transcript levels. Huh7.5 were infected with lentivirus encoding for shRNAs directed against Nup358 or a scrambled control shRNA sequence. After 3 days, total RNA was isolated from the cells and mRNA transcript levels for immune genes were determined using a TaqMan® OpenArray® RT PCR array (Applied Biosystems). Values are corrected for HPRT transcript levels and fold-change was calculated relative to cells expressing the scrambled shRNA control sequence. The values presented are derived from an average of two biological replicates and error bars represent standard error. The qPCR array includes primes for 48 mRNA transcripts for ISGs that are involved in HCV infection (Table 5-1). Shown here are 17 transcripts from the array that were altered by Nup358 depletion.

Figure 5-5. Depletion of specific Nups alters ISG mRNA transcript levels and promoter activity. U937 cells (A) or HeLa cells (B) were transduced with constructs encoding for shRNAs directed against the indicated Nups, or with a construct encoding a scrambled control shRNA using a lenti viral delivery system. **A.** Three days after transduction, cells were treated with 500 U/mL human recombinant IFNγ for the indicated time. Transcript amounts for the indicated genes were determined by qPCR using specific primers, and fold-change was calculated relative to un-transduced and un-treated cells. **B.** Two days after transduction, cells were transfected with constructs encoding for the luciferase protein regulated by an ISRE, GAS, STAT3, or control promoter region. On day 4 after transduction, cells were lysed using the Promega BrightGlow reagent and the luminescence was measured using a 96-well plate reader. The values shown represent fold-change relative to the luciferase activity of cells transfected with the control construct harbouring the no ISG promoter region.

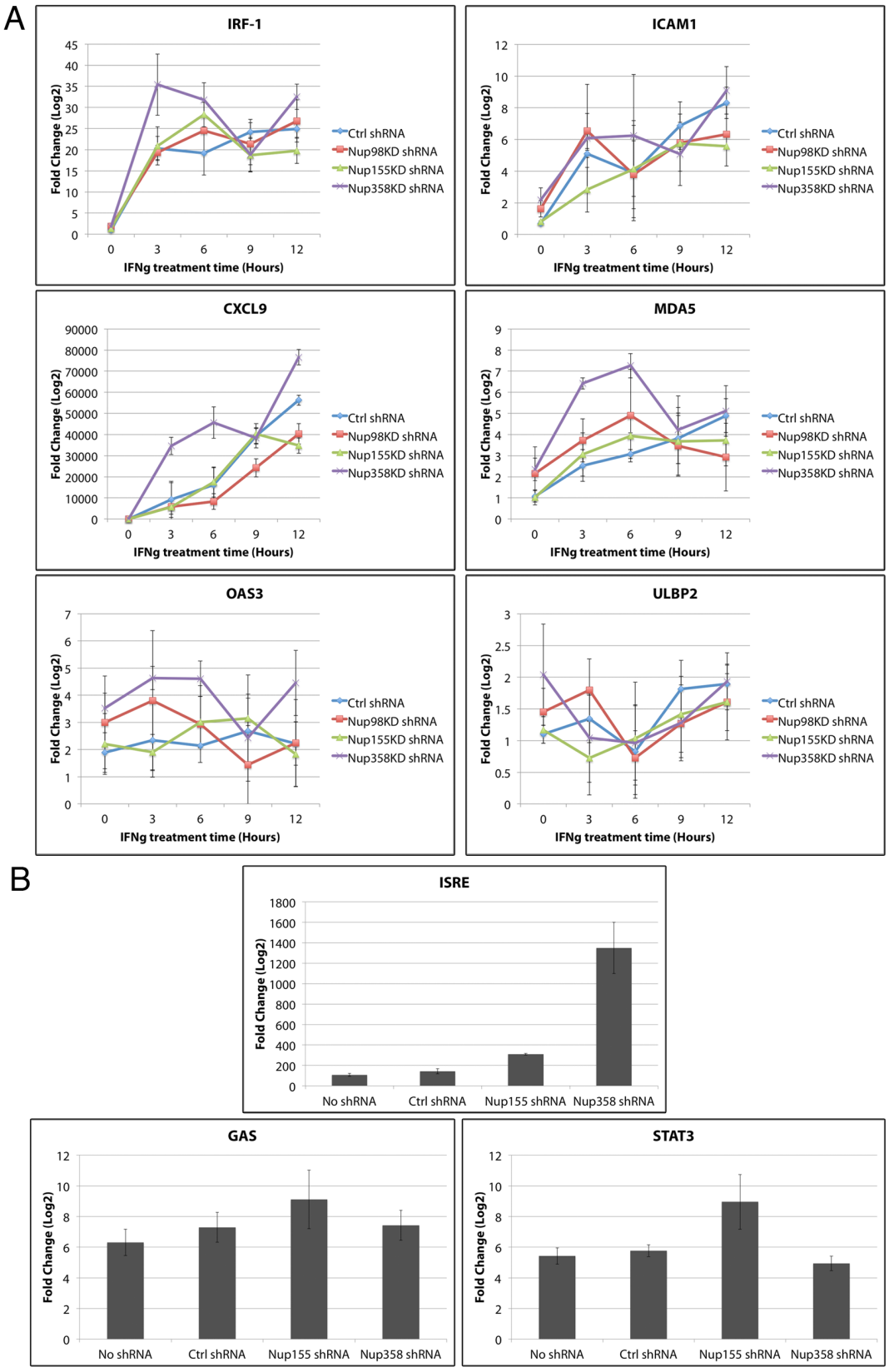

Figure 5-5. Depletion of specific Nups alters ISG mRNA transcript levels and promoter activity.

To better understand the mechanisms by which Nup358 affects transcriptional regulation of ISGs, we examined the activity of known ISG promoter regions following Nup358 depletion. Luciferase reporter systems composed of a luciferase gene regulated by a specific ISG promoter sequence, including the ISRE, GAS, or STAT3 elements, were used to determine which immune pathways are altered by Nup358 depletion. Cells were transduced with shRNA depletion constructs targeted for Nup358, Nup155, or a scrambled control sequence for 72 hours, followed by transfection with a luciferase reporter construct containing an ISRE, GAS, STAT3, or control promoter element. Nup155 was used as a control because it was not increased by IFN treatment (Figure 5-1). Twenty-four hours after transfection, the luciferase activity in cells expressing each of different constructs was measured to determine the relative activity of the specific promoter element. Interestingly, Nup358-depleted cells expressing the luciferase gene with an ISRE promoter element showed a significant increase in luciferase activity compared to control shRNA treated cells (Figure 5-5B top panel). A smaller but still significant increase in luciferase activity was also observed in Nup155-depleted cells. Interestingly, Nup155 depletion but not Nup358 depletion increased STAT3 promoter activity suggesting Nup155 may also have a role in immune regulation (Figure 5-5 bottom right). Cells transfected with the luciferase constructs regulated by the GAS promoter element showed no significant change in luciferase activity between cells harbouring the control shRNA construct and those depleted of Nup358 or Nup155 (Figure 5-5B bottom left). The ISRE promoter element is activated primarily by type I IFN stimulation (Figure 1-4A), suggesting that Nup358 is involved in regulation of the type I IFN signal transduction pathway.

5.2.4 Both the SUMO E3 domain and the cyclophilin domain of Nup358 impact ISG activation

Nup358 contains several functional domains that have the potential to affect innate immune activation. To determine which of these functional domains are involved in regulating immune signalling pathways, we analyzed the effects of individual Nup358 domains on promoter activity using the luciferase reported assay described above (for Nup358 domains see Figure 1-7). Cell lines stably expressing the SUMO E3 ligase domain (IR) or the cyclophilin homology C-terminal domain (CTD) of Nup358 were transfected with the luciferase reporter plasmids containing immune promoter elements described above, which were expressed for 24 hours followed by analysis of luciferase activity. We found that, in cells expressing either the IR or CTD domains, there was a decrease in level of ISRE activation as compared normal cells (Figure 5-6A left). In order to determine the effects of Nup depletion in cells expressing each of the Nup358 domains, HeLa cells stably expressing one of the Nup358 domains were infected with lentivirus containing Nup155, Nup358, or scrambled ctrl shRNA constructs. For these experiments, we chose a Nup358 shRNA sequence that would not deplete the levels of the Nup358 truncations. 72 hours after transduction, cells were transfected with the luciferase reporter plasmids and analyzed for luciferase activity after 24 hours (Figure 5-6). A similar trend in ISRE activation was observed in the IR or CTD cell lines transduced with the control shRNA or when Nup358 was depleted (Figure 5-6). Interestingly, Nup155 depletion also caused an increase in ISRE promoter activation, which was only slightly decreased by expression of the Nup358 domains. Consistent with the data presented in Figure 5-5, specific domains of Nup358 did not significantly alter GAS or STAT3 promoter element activity (Figure 5-6B). These results indicate that both the SUMO ligase and isopeptidase activities of Nup358 may be involved in regulating immune responses.

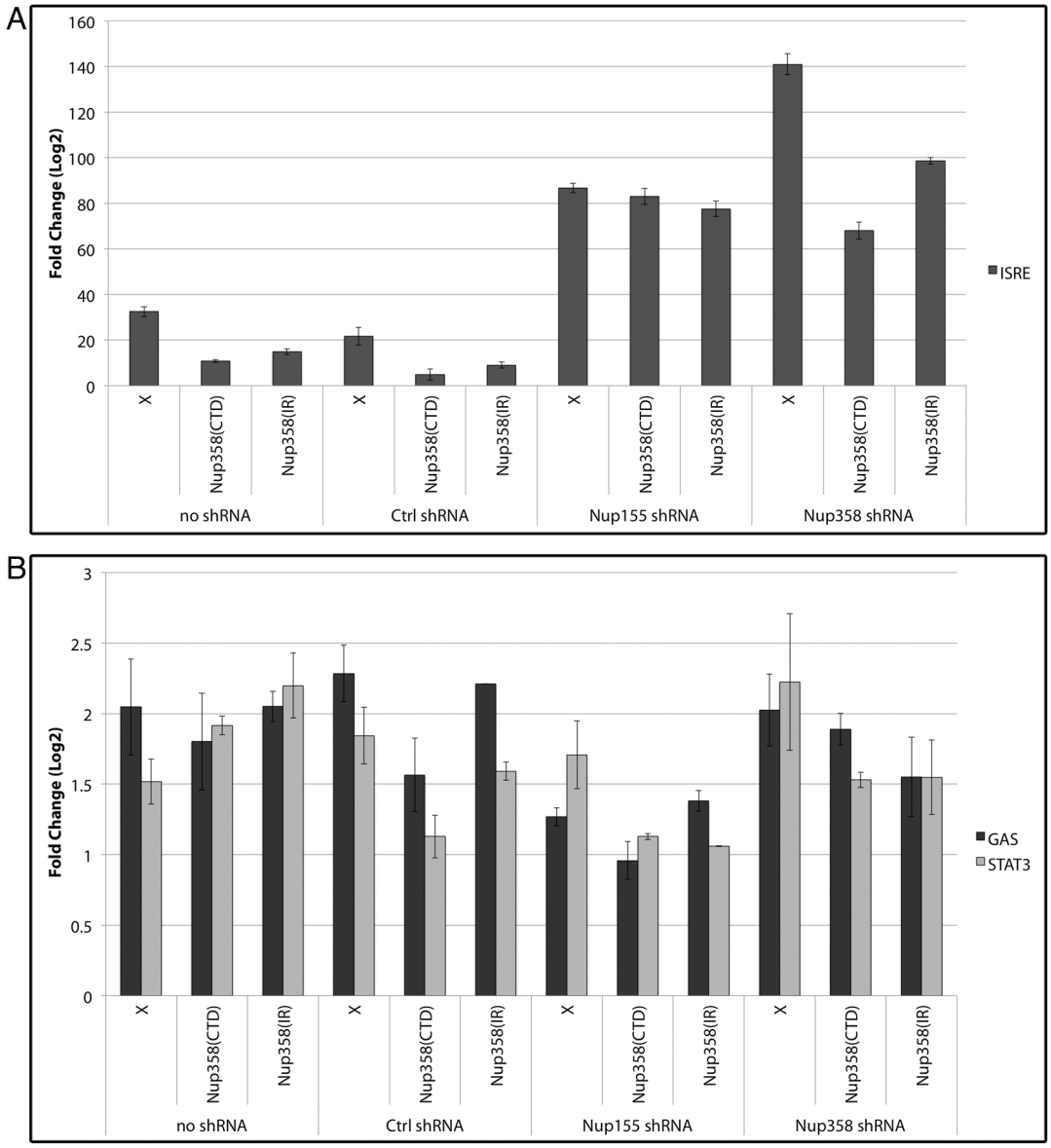

Figure 5-6. Over expression of specific Nup358 domains alters ISRE promoter activity. HeLa cells were transfected with constructs encoding for the Nup358 cyclophilin domain (CTD) or the Nup358 SUMO E3 ligase domain (IR) and incubated with G418 for 2 weeks to produce stable lines. Control HeLa cells and each of the stable lines were transduced with constructs encoding for shRNAs directed against the indicated Nups, or with a construct encoding a scrambled control shRNA using a lenti viral delivery system. Two days after transduction, cells were transfected with constructs encoding for luciferase regulated by an ISRE, GAS, STAT3, or control promoter region. On day 4 after transduction, cells were lysed using the Promega BrightGlow reagent and the luminescence was measured using a 96-well plate reader. The values shown represent fold-change relative to the luciferase activity of normal HeLa cells harbouring the construct with a control promoter region. The data shown are based on one biological replica and the error bars are derived from the standard error or three technical replicas.

5.2.5 Nup358 supports HCV replication

The results presented above suggest that Nup358 has a role in suppressing the transcriptional activation of various ISGs. Taken together with previous observation that Nup358 transcript amounts are elevated at early points after IFNγ stimulation (Figure 5-1), this may indicate that Nup358 is an early negative regulator of immune activation. Moreover, our previous data showing upregulation of Nup358 in HCV infected cells may indicate that this function of Nup358 is utilized by HCV to limit immune activation at early stages in the viral life cycle (Figure 3-10)(Neufeldt et al., 2013). To evaluate the role of Nup358 in HCV infection, we examined the effect of Nup358 depletion on HCV infection. Huh7.5 cells were infected with HCV and, after 24 hours, cells were also infected with lentivirus expressing shRNA sequences directed against Nup98, Nup155, Nup358, or a scrambled control sequence (Figure 5-7). Depletion of Nup98, Nup155, or expression of the shRNA control did not significantly change the levels of intracellular or extracellular HCV RNA within the time frame of these experiments. By contrast, Nup358 depletion caused a significant decrease in both intracellular levels of HCV RNA and the levels of secreted virus (Figure 5-7A). Immunofluorescence analysis of HCV infected cells depleted of Nup358 also showed a significant decrease in the number of infected cells (Figure 5-7B). These results indicate that Nup358 is an important host cell factor in controlling immune responses and in supporting HCV infection.

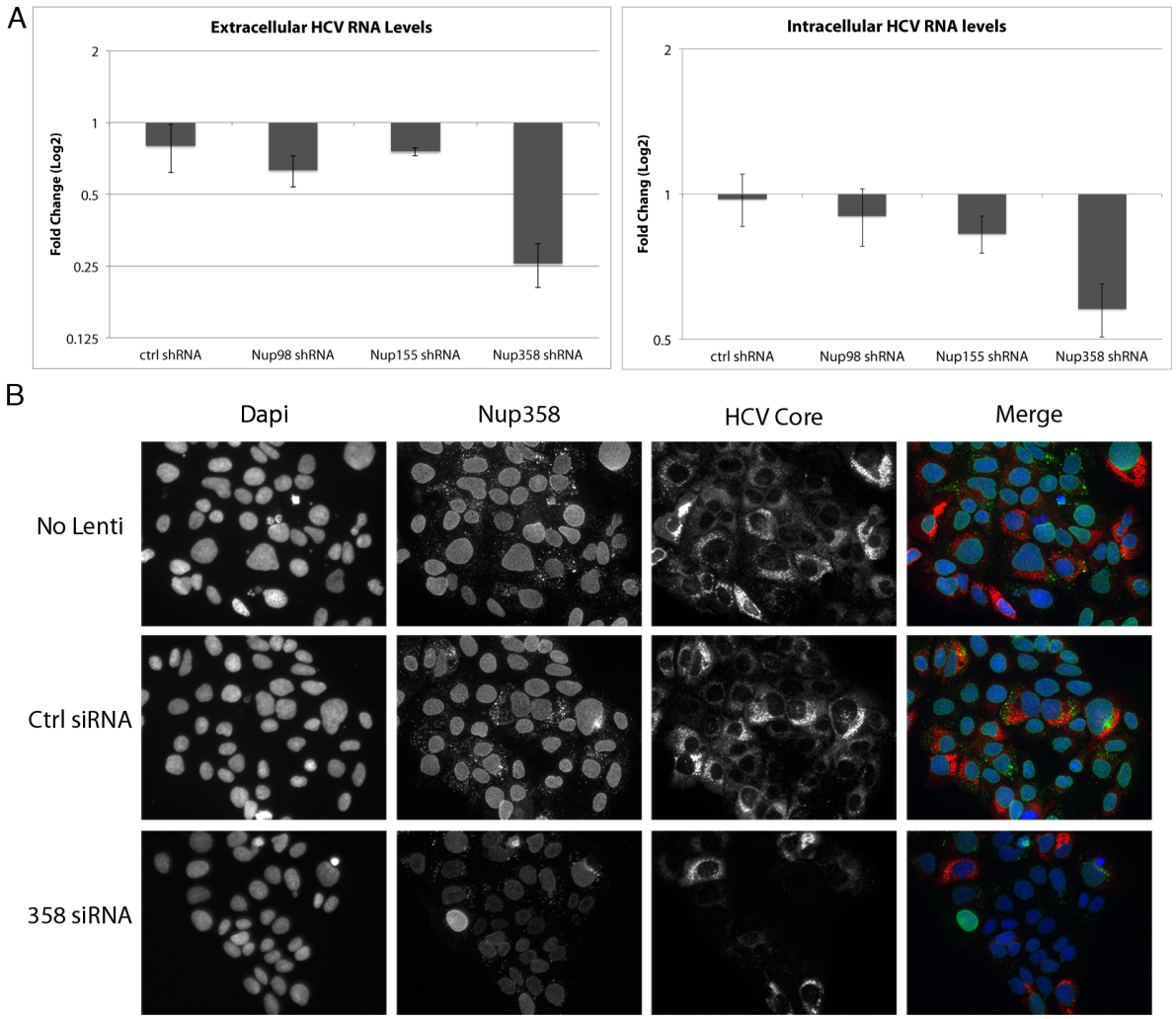

Figure 5-7. Nup358 supports HCV replication. Huh7.5 cells were uninfected or HCV-infected and, 24 hours later, cells were infected with lentivirus harbouring constructs encoding shRNAs directed against Nup98, Nup155, Nup358, or a scrambled control shRNA sequence for three days. **A.** The effects of Nup depletion on HCV titers was evaluated by qPCR analysis of HCV RNA levels in cell extracts (panel A left) or in the culture supernatant (panel A right) from HCV infected Huh7.5 cells co-infected with or without lentivirus. Values for each sample are normalized to HPRT mRNA levels and are expressed as fold-change relative to HCV infected cells not treated with lentivirus. Error bars indicate standard error (based on ≥ 3 experiments). **B.** Localization of Nup358 (green) and HCV core (red) was determined by indirect immunofluorescence using antibodies specific for the indicated proteins. DNA was stained with DAPI (blue).

5.3 Discussion

Host cell immune responses are activated by a complex network of signalling molecules that lead to the stimulation of genes required to combat microbial infections. All of the signalling cascades required for effective immune activation must transit through the NPC to stimulate transcription of immune effector genes, placing the NPC in a key location for interacting with immune signalling molecules. Many immune stimulated gene products function in propagating immune activation and initiating inflammatory responses, while others act directly on invading pathogens. One prominent side effect of immune activation is host cell toxicity, which is a by-product of immune proteins producing inflammatory and cytotoxic responses required to fight infection. The potential for toxic side effects makes regulation of immune signalling critical for the overall effectiveness of immune responses in organisms. Here we provide evidence suggesting that the levels of several components of the NPC are elevated by immune stimulation and we present data supporting a role for the NPC in regulating immune pathways in several different cell lines. Specifically, we show that depletion of Nup358, normally located on the cytoplasmic face of the NPC, leads to elevated levels of several proinflammatory genes suggesting that Nup358 is involved in basal regulation of immune signalling pathways. We also demonstrate that depletion of Nup358 leads to changes in the level of ISG activation following IFNγ stimulation and increases activation of the type I IFN specific ISRE promoter element. Moreover, overexpression of specific regions of Nup358, including its SUMO E3 ligase and cyclophilin homology domains, reduces the level of reporter genes controlled by an ISRE promoter element, suggesting that specific functional domains of Nup358 are involved in the regulation of type I IFN responses. Finally, we show that HCV infection is also negatively affected by Nup358 depletion, demonstrating that Nup358 is an important host factor in HCV infection. Together, our data support a role for Nup358 in negatively regulating type I IFN

responses and suggests that this function of Nup358 may be targeted by viruses the facilitate host cell immune evasion.

5.3.1 The NPC as a key structure in innate immune signalling

A key step in immune signal transduction pathways is the passage of signalling molecules into the nucleus. For instance, in IFN-induced JAK/STAT signalling, trafficking of the STAT transcription factor through the NPC requires the formation of dimers, which is facilitated by JAK phosphorylation of specific serine residues (Figure 1-4A). Similarly, cytoplasmic phosphorylation of IRF transcription factors also initiates the formation of dimers, which can interact with the NPC and transit into the nucleus to activate immune genes. The nuclear import of these active transcription factors necessitates that the NPC interacts with all immune signalling cascades, positioning Nups in an ideal location to regulate immune signalling cascades. Our observations show that the levels of specific Nups are altered following immune stimulation, implying an active role for the NPC or specific Nups in immune signalling (Figure 5-1 and 5-3). We envisage that NPC components could affect immune pathways in several ways. First, changes in the levels or localization of specific Nups could modify the transport properties of the NPC. A similar mechanism has been observed in yeast, where elevated levels of a specific Nup, Nup53p, leads to changes in transport efficiency for specific cargos (Makhnevych et al., 2003; Marelli et al., 2001). Additionally, excess Nups could facilitate or block interactions with transport cargos there by altering nuclear transit of immune-related cargo proteins. Alternatively, changes in Nup levels could stimulate the modification (e.g. by sumoylation) of immune signalling molecules leading to protein inactivation, protein degradation, or a block in transport. Finally, the NPC may also regulate immune signalling by controlling the transport or translation of specific mRNA molecules (Bachi et al., 2000; Faria et al., 2006; Mahadevan et al., 2013). A

combined effect of several of these mechanisms may be critical for the proper activation and regulation of cellular innate immune responses.

5.3.2 Peripheral Nups are upregulated by innate immune activation

Our qPCR screen showed that the majority of Nup transcripts elevated following IFN treatment pertained to asymmetrical Nups, which are located either in the nuclear basket or cytoplasmic filaments of the NPC (Figure 5-1). These asymmetrical Nups often serve as platforms for NPC associated proteins and are connected to numerous cellular pathways, functioning both in NPC-mediated transport and non-transport processes (See sections 1.6.1.3 and 1.7). Therefore, IFN induced changes in the levels of these Nups has the potential to significantly impact cellular systems. This is the case for Nup358, which is a multifaceted Nup linked to numerous cellular pathways that could affect immune activation. Depletion of Nup358 has been shown to decrease the rate of Impα/β- and transportin-mediated import and mutational analysis of Nup358 has demonstrated that different domains of Nup358 are required for the transport of specific cargos, suggesting that Nup358 acts as a platform for the formation of import complexes and the regulation of specific transport pathways (Hutten et al., 2008; Hutten et al., 2009; Walde et al., 2012). Nup358 also contains several binding sites for the GTPase Ran and it interacts with RanGAP, which implicates Nup358 in maintaining efficient nucleocytoplasmic transport (Saitoh et al., 1997; Yokoyama et al., 1995). These functions of Nup358 may also be important for the trafficking of cargos related to immune activation. Alterations in the protein amount of Nup358 following IFN stimulation could lead to changes in the NPCs capacity to transport immune signalling molecules leading to a down regulation of immune activation (Figure 5-1 and 5-3). Additionally, the excess cytoplasmic Nup358 observed in immune-stimulated cells may sequester specific cargos away from the NPC thereby preventing

nuclear import (Figure 5-3). In general, varying levels of Nup358 at the NPC and in the cytoplasm could contribute to modulating the overall transport capacity of the NPC, which represents a potential mechanism by which Nup358 could affect immune responses.

5.3.3 Nup358 negatively regulates innate immune signalling

Nup358 depletion has previously been linked to elevated levels of IRF-1 and TNF-α (Scognamiglio et al., 2008). Building on these data, we show that, in Nup358 depleted cells, there is a significant increase in the levels of numerous ISGs, supporting a regulatory role for Nup358 in innate immune signalling (Figure 5-4 and 5-5). Interestingly, the timing of Nup358 upregulation in macrophage cells closely paralleled that of IRF-1, which is one of the first ISGs activated upon IFN stimulation (Figure 5-1 and 5-2). This suggests that Nup358 is part of an early negative feedback loop for immune signalling, which would be consistent with previous studies showing that IFN stimulation produces an initial burst of ISG activation followed by a quick return to basal levels (Ivashkiv and Donlin, 2014). Interestingly, several SOCS family proteins, which are also involved in negatively regulating IFN signalling, have a similar pattern of upregulation as Nup358 following IFN stimulation (Yoshimura et al., 2007). Our results suggest that Nup358 may have a dual role in innate immune regulation by both blocking basal activation of immune responses and, similar to SOCS proteins, in negatively regulating the initial burst of immune activation following IFN stimulation.

Several functional domains within Nup358 have the potential to influence immune pathways. For example, the Nup358 SUMO E3 ligase domain (IR domain) may impact the immune response through the modification of specific signalling or effector molecules. A significant number of immune transcription factors that transit through the NPC including IRF1, IRF3, IRF5, IRF7, NFκB, and STAT1, are targets of SUMO modification, and, in each

case, sumoylation is linked to transcriptional repression (Kim et al., 2008; Mabb and Miyamoto, 2007; Nakagawa and Yokosawa, 2002; Rogers et al., 2003; Ungureanu et al., 2005). The location of Nup358 coupled with its observed role in regulating immune responses and its SUMO E3 ligase activity may indicate that Nup358 functions to inactivate immune transcription factors, through SUMO modification, as they enter the NPC or in the cytoplasm of cells. Some studies have suggested the Nup358 IR domains can act to generally enhance the transfer of SUMO from UBC9 to target proteins without directly interacting with the target (Pichler et al., 2004). Therefore, Nup358 overexpression following IFN stimulation could function to non-specifically sumoylate proteins trafficking to the nuclear compartment. Normal cellular levels of Nup358 may also suppress the basal activation of the immune responses through a similar mechanism. Furthermore, Nup358 has been shown to promote SUMO modification of HDAC4, which also leads to increased silencing of inflammatory genes (Kirsh et al., 2002). Data presented in Figure 5-6A demonstrate that increased expression of the Nup358 IR domain specifically decreases the levels of type I IFN-mediated immune activity, supporting a role for the Nup358 SUMO ligase activity in regulating immune responses (Figure 5-6A).

The C-terminal domain of Nup358 (Nup358 ^{CTD}), containing homology to cyclophilin A, also has the potential to impact immune responses. Cyclophilins were originally identified as proteins that bind to immunosuppressant molecules such as cyclosporin, FK506/tacrolimus, and rapamycin/sirolimus, and have become important targets for antiviral drugs (Fischer et al., 1989; Takahashi et al., 1989). Building on previous findings, our results indicate that Nup358^{CTD} has a role in immune activation by demonstrating that overexpression of this domain has a negative impact on type I IFN responses (Figure 5-6). In addition to functioning in immune response pathways, cyclophilins have defined roles in several viral infections (See section 1.7)(reviewed in (Zhou et al., 2012)). For example, CypA associates with the HCV replication complex and is

required for viral genome replication in host cells (Hanoulle et al., 2009; Rosnoblet et al., 2012). Indeed, treatment of HCV infected cells with the CypA inhibitor cyclosporine leads to a potent inhibition of HCV replication (Di Nunzio et al., 2012; Hopkins and Gallay, 2012; Kaul et al., 2009; Schaller et al., 2011). The structural homology between CypA and the Nup358^{CTD} may be one explanation for the decrease in HCV replication observed in Nup358-depleted cells (Figure 5-7). This would be consistent with our previous data showing that HCV infection induces both the upregulation of Nup358 at early time points after infection and the relocalization of Nup358 to the membranous web (Figure 3-2)(Neufeldt et al., 2013). These observations may also indicate that, in addition to the previously described transport function for NPC components at the membranous web, Nup358 may also have a direct role in viral replication through the Nup358^{CTD} domain. Alternatively, the regulatory effects of Nup358 on ISRE activity and general immune pathways could indicate that Nup358 affects viral replication by blocking immune activation (Figure 5-5 and 5-6). Further investigation into the role of Nup358 and, more specifically, its IR and CTD domains in immune signalling pathways and viral infection may provide important insights into how viruses manipulate host cells to promote viral genome replication and prevent immune activation.

5.3.4 Regulation of innate immune activation by altering mRNA export

Another avenue by which the NPC could influence innate immune responses is through manipulation of the nuclear export and/or translation of mRNA transcripts. Several Nups that are upregulated in response to IFN, including Nup96, Nup98, Nup153, and Nup358 have prominent roles in the export of mRNA transcripts (Figure 5-1)(Enninga et al., 2002; Faria et al., 2006; Forler et al., 2004a; Ullman et al., 1999). Increases in the protein amounts of specific Nups may be critical to accommodate the increased flow of mRNA transcripts following immune

activation. In particular, elevated levels of Nup98, which is involved in both gene regulation and mRNA processing, may function to increase the efficiency of immune gene expression in cells (reviewed in (Iwamoto et al., 2010)). Additionally, Nup358 may function in a similar capacity as it has been shown to both bind mRNA export factors and promote mRNA release into the cytosol (Forler et al., 2004a). Moreover, the ZF domain of Nup358 has also been linked to efficient translation of ER-targeted mRNA transcripts suggesting that Nup358 forms a link between nuclear export and efficient translation of specific mRNAs (Mahadevan et al., 2013). These functions of Nup358 are likely important for the expression of various cytokines and chemokines that are produced in the ER lumen as well as many other membrane proteins that are required to propagate inflammatory responses. Therefore, the overexpression of Nup358 may function to negatively regulate the activation of new immune genes while still maintaining efficient export and translation of RNA transcripts that are in production or already formed. Interestingly, positive-strand RNA virus transcripts are also targeted to the rough ER for translation, which would make the increased expression of Nup358 by HCV highly beneficial for both its immune regulatory and its translation initiation activities.

5.3.5 Conclusions

Here, we demonstrate that Nup358 is involved in negatively regulating immune responses and we provide evidence suggesting that this function is specific to the type I IFN response. Moreover, domain analysis indicates that both the CTD and IR domains are involved in immune regulation function of Nup358. However, the large number of functional domains located within Nup358 makes determining the precise mechanisms of its immune regulation activity difficult to achieve. It is likely that multiple domains of Nup358 contribute to both the immune and viral functions of Nup358, but further experimentation is required to determine the

mode of action. This multifunctional nature of Nup358 makes it both an intriguing and complex target for studying immune responses and inflammatory diseases. Continued examination of the role of the NPC and specifically Nup358 in immune activation has the potential to greatly increase our understanding of these pathways and may also provide important targets for therapeutics.

CHAPTER VI: Perspectives

6.1 Synopsis

Currently, it is estimated that approximately three percent of the global population is infected with HCV, making it a significant contributor to global human disease. Nearly half of the patients infected with HCV develop a chronic infection that, without treatment, can cause liver cirrhosis leading to end stage liver disease. In order to propagate in infected hepatocytes, HCV induces massive rearrangements of host cell membranes, collectively termed the membranous web, leading to the formation of specialized compartments where viral replication and assembly occurs. In the work presented here, we uncover an intricate interaction network between viral proteins and the NPC, which supports the formation of the membranous web and limits host cell immune activation. Multiple components of the nuclear transport machinery were found to interact with HCV proteins and accumulate in the virus-induced membranous web. Additionally, we show that several Nups and Kaps were found to support HCV infection in Huh7.5 cells. Our observations support a role for the nuclear transport machinery in the formation of distinct viral compartments that maintain a selective barrier with the surrounding cytosol. Moreover, data presented here indicate that this selective barrier limits access to proteins that negatively impact viral replication, such as RLRs, while allowing traffic of proteins containing an NLS sequence. The results described in chapters 4 and 5 present a novel function for the NPC and nuclear transport machinery in positive-strand virus replication and immune evasion. Additionally, we show that Nup358 is specifically upregulated by HCV and also give evidence that Nup358 is involved in negatively regulating immune responses. From these results, we postulate that the specific manipulation of Nup358 levels and relocalization by HCV likely constitutes another viral immune evasion strategy linked to the NPC. In this chapter, I discuss the impact of our observations on the understanding of virus-host interactions and on the role of the nuclear transport machinery in both viral infection and immune activation. Additionally, I

discuss the broader implications of the NPC as a key structure in regulating immune responses and as a recurrent target for human disease.

6.2 The NPC as a common target for viral infections

A growing number of studies are uncovering key functions for the NPC in a diverse range of viral infections. This likely arises, in part, from the critical role for nuclear transport in cellular signalling cascades and gene expression. Subtle alterations in the levels or morphology of specific Nups can lead to changes in the transport capacity of the NPC for specific cargos (Makhnevych et al., 2003; Marelli et al., 2001). Several viruses take advantage of this by manipulating the NPC in such a way as to decrease the efficiency of transport for immune signalling molecules or mRNA transcripts (see section 1.8 and (Yarbrough et al., 2014)). A number of viruses also manipulate or utilize nucleocytoplasmic transport pathways in order to facilitate viral capsid uncoating and traffic the genome into the nucleus (Le Sage and Mouland, 2013). Adenovirus, HSV-1 and influenza virus are all excellent examples of viruses that both utilize and inhibit nuclear transport pathways (Le Sage and Mouland, 2013; Yarbrough et al., 2014). These viruses replicate in the nucleus and require interactions with specific Nups to mediate uncoating and nuclear import of their genome (Le Sage and Mouland, 2013). Additionally, specific proteins encoded by each of these viruses interact with components of the mRNA export machinery, which leads to decreased host mRNA export and increased viral RNA export (Le Sage and Mouland, 2013; Yarbrough et al., 2014). By targeting specific components of the nuclear transport machinery, these viruses can alter the host cell environment to facilitate viral propagation. Expanding on the observations from previous studies, data presented in chapters 3 and 4 indicate a different function for the nuclear transport machinery in viral infection. We demonstrate that HCV infection hijacks the nuclear transport machinery to

cytoplasmic locations in order to promote viral replication. Moreover, we provide evidence suggesting that NPC-mediated transport is active at the membranous web, and that, similar to NPC function at the NE, the nuclear transport machinery is involved in maintaining a selective barrier between cytoplasmic membrane compartments. These experiments present a novel mechanism for the utilization of NPC-mediated transport by viral infections further demonstrating the importance of these pathways for viral infection.

In addition to nuclear transport, Nups regulate a large number of other cellular pathways that make them excellent targets for viruses. Both Nup98 and Nup153 have been identified as common targets in numerous viral infections (Le Sage and Mouland, 2013; Yarbrough et al., 2014). These Nups have roles in regulating gene expression as well as functioning in NPC-mediated transport. Additionally, Nup358, which is involved in regulating numerous NPC-associated processes on cytoplasmic side of the NPC, is a common target of virus including HCV and HIV. Studies examining the function of the nuclear transport system in viral infections have demonstrated the effectiveness of targeting specific Nups in preventing immune responses and promoting virus production. These observations also reveal the dual function of the nuclear transport machinery, demonstrating that Nups can have both pro-viral and anti-viral functions.

The preceding discussion highlights the central functions of the NPC and nuclear transport machinery in numerous viral infections, which also make these pathways an enticing target for the development of antiviral therapies. Studies aimed at uncovering therapeutics that affect the nuclear transport machinery have often focused on the pharmacological modulation of nuclear import either through direct targeting of the NPC or through targeting specific NTFs or import cargos. However, so far these studies have had limited success. One example of a successful NPC targeting drug is the Impα/β import inhibitor Ivermectin, which is a small molecule originally used to treat Onchocerciasis (river blindness) that has also recently been

show to inhibit both DENV and HIV infection (Tay et al., 2013; Wagstaff et al., 2012). Additionally, high throughput screens in influenza A infected cells have uncovered several small molecules that rescue the mRNA export block induced by the viral NS1 protein (Chahine and Pierce, 2009). Though there has so far been limited success in the development of nuclear transport targeting drugs, continued research into therapeutic molecules that target this critical pathway could lead to the discovery of antivirals that have a broad impact on viral diseases. Furthermore, this research has the potential to uncover novel functions for the nuclear transport machinery and increase our understanding of this fundamental pathway.

6.3 Virus-induced replication compartments: the need for a pore

Structural analysis of replication complexes produced in virus-infected cells has revealed several common elements between different viruses. This is exemplified by positive-strand RNA virus replication factories, which have been shown to induce encapsulation of the replication machinery in protected membrane compartments. Several different studies have demonstrated that in positive-strand RNA virus infection, the viral RNA is protected from exogenously added nucleases suggesting that viral replication compartments are sealed from the surrounding cytosol (Paul et al., 2013; Quinkert et al., 2005). However, a sealed viral replication compartment is theoretically problematic, as it would not allow import of metabolites required for replication or export of the viral RNA for translation or virion assembly. Therefore, a transport mechanism must exist to facilitate efficient replication and propagation within the host cell. Indeed, small pores connecting replication compartments to the cytosol have been observed in several positive-strand RNA virus infected cells. In the case of InV/S type membrane alterations; replication compartments appear as vesicular invaginations into existing cellular membranes, often ER membranes, which are connected to the cytoplasm by small uniform pores (reviewed

in (Paul and Bartenschlager, 2013)). DMV type replication complexes also contain openings to the cytoplasm, though, as observed in HCV infection, these openings appear only rarely and are variable in size (Romero-Brey et al., 2012). Results presented in chapters 3 and 4 supports a model where components of the NPC act to form a selective barrier that allows specific transport between cytoplasmic compartments in HCV infected cells. Additionally, we provide evidence indicating that this may be a common function of the NPC in viral infections as both DENV and HAV relocalize Nups to the cytoplasm. Interestingly, the topology of virus-induced replication complexes at the site of the pore shares homology with the membrane curvature of the NE at the NPC (Paul et al., 2013). Both these structures form an interface at the site of membrane fusion between two different cellular compartments. However, the pore structures identified in InV/S or DMV type replication complexes are much smaller than pores that form in the NE (Romero-Brey et al., 2012; Welsch et al., 2009). Significant differences in size between NE channels and those in InV/S replication complexes may suggest that only a subset of Nups are involved in the formation of pores in virus-infected cells. Indeed, we observed that depletion of NDC1 did not significantly alter HCV replication indicating that not all Nups are required for HCV infection (Figure 3-14). The generally accepted hypothesis that a transport mechanism exists between cytosolic and viral replication compartments in combination with our observations strongly suggest that a proteinaceous membrane pore complex comprised of components of the NPC is involved in the selective trafficking of molecules between the cytosol and virus-induced membrane compartments.

6.4 Viral immune evasion through concealment from RLRs

The formation of a selective barrier between viral replication compartments and the cytosol serves multiple functions by both allowing the viral replicase and assembly complexes to

acquire the requisite constituents need to function and protecting these viral complexes from degradation by cellular enzymes or detection by RLRs. The latter function likely represents an important strategy for avoidance of immune activation, as the recognition of viral RNA by RLRs is a critical step in fighting RNA virus infections. In HCV infection, increased activation of RIG-I leads to a significant decrease in HCV replication, which is exemplified by the overproduction of HCV in the RIG-I deficient Huh7.5 cells (Blight et al., 2002; Sumpter et al., 2005). HCV has evolved several mechanisms for the active inhibition of RIG-I signalling and the subsequent IFN response through cleaving or blocking key proteins in these pathways (see section 1.4.6.1). In addition to these active immune avoidance mechanisms, our data support a passive strategy for immune evasion through concealment potential PAMPs from immune recognition. This strategy for immune evasion has been proposed in several studies, but, until recently, no concrete evidence existed for the formation of replication compartments that inhibit entry to RLRs (Overby and Weber, 2011). In chapter 4 we present data suggesting that multiple positive-strand RNA viruses, representing different types of virus-induced membrane alterations, each produce replication compartments that inhibit entry to cytoplasmic RLRs. These observations give tangible evidence for a passive immune evasion strategy utilized by positive-strand RNA viruses. Our data also indicate a role of NPCs in inhibiting entry to RLRs further supporting a function for non-nuclear NPC-mediate transport in positive-strand RNA virus infected cells. These observations give rise to questions about the structure of viral replication complexes and open an interesting avenue for future research into the nature of NPC-mediate transport and viral-host interactions. Moving forward, it will be interesting to see how viruses recruit NPC components away from the NE and to determine the nature of the NPC-like structures that might form in viral replication complexes. Our data suggest that not all Nups are recruited to the membranous web in HCV infected cells, which may indicate that hybrid NPC structures are

recruited to replication compartments. Additional analysis into the roles of Nups and virus-induced membrane alterations in infected cells may generate important information into the function of viral replication compartments in evading immune responses and supporting viral infection.

6.5 Non-transport functions for the nuclear transport machinery in HCV infection

Assembly of the NPC at the NE requires a concerted effort from several integral membrane and membrane associated proteins. A subset of these Nups, including Nup155 and Nup107, function in forming and maintaining the membrane curvature of NE at the NPC. As discussed in section 1.6.1.1, these core scaffold Nups contain several membrane binding motifs that are highly homologous to those found in vesicle coatomer proteins such as COPI (Devos et al., 2004; Hsia et al., 2007). Similarities between these proteins are interesting in light of observations that both COPI and core scaffold Nups are involved in HCV infection (Tai et al., 2009). Additionally, Nup153, which has a defined role in membrane curvature, also associates with both COPI and HCV proteins and is a host factor that supports HCV infection (Liu et al., 2003; Neufeldt et al., 2013). These observations may suggest an alternative role for Nups in HCV infected cells. In addition to a transport function, specific components of the nuclear transport machinery may also have a role in facilitating the membrane alterations induced by viral infections. A role for membrane coat Nups in forming viral replication complexes is also supported by the similarities in the topology between viral replication vesicles and NE membrane curvature (reviewed in (Paul and Bartenschlager, 2013)). Additionally, numerous reports have shown that both Nups and Kaps have important functions outside of nucleocytoplasmic transport and can be found in various cellular organelles. It may be that HCV uses one of these non-transport functions to promote viral propagation within host cell. Though

much of the work presented here has focused on establishing a transport function for the Nups and Kaps in virus-induced replication complexes, our observations do not rule out alternative roles for these proteins in viral infection. Future investigation into the functions of the nuclear transport machinery in positive-strand RNA virus infections may reveal that specific Nups and Kaps have multiple roles in viral infection.

6.6 The NPC as a general regulator of immune signalling and gene activation

In order to generate an immune response, signals that originate in the cytoplasm or on the cell surface must transit to the appropriate gene locus to either activate or suppress transcriptional function. Situated at the interface between the nucleus and cytoplasm, the NPC provides a link between cytoplasmic or cell surface signalling and gene activation. Its localization also provides it with the unique opportunity to generally regulate signalling cascades and protein production. Our data presented in chapter 5 indicate that alterations occur in the levels of specific Nups following immune activation suggesting a role for the NPC in the immune response. Further investigation into one of these Nups, Nup358, demonstrated that it has a key regulatory role in innate immune regulation. The function of Nup358 in negatively regulating immune activation may also be supported by observations that Nup358 protein levels are elevated by HCV infection and that Nup358 supports HCV infection. The convergence of signalling pathways at the NPC situates Nup358 in the ideal position to regulate all signalling activity that transits to the nucleus. From our data, we predict that Nup358 acts to block basal or aberrant activation of immune genes by inhibiting nuclear import of or inactivating key immune signalling molecules. The exponential increase in immune signalling molecule activation following IFN stimulation overcomes the signalling barrier created by basal levels of Nup358 leading to the initial burst of immune activation. This initial surge of immune transcriptional

activation also leads to increased levels of Nup358, which we predict acts in a negative feedback loop involved in limiting immune activation. Similar negative feedback mechanisms have been observed with SOCS proteins, which are rapidly induced by IFN stimulation to extinguish JAK/STAT signalling (reviewed in (Alexander, 2002)). These data indicate that Nup358 is a critical component of the IFN response. Further research into the mechanisms of Nup358 mediated immune regulation will provide important insights into the IFN response pathway and may provide novel targets for therapeutics.

REFERENCES

Abe, T., Y. Kaname, I. Hamamoto, Y. Tsuda, X. Wen, S. Taguwa, K. Moriishi, O. Takeuchi, T. Kawai, T. Kanto, N. Hayashi, S. Akira, and Y. Matsuura. 2007. Hepatitis C virus nonstructural protein 5A modulates the toll-like receptor-MyD88-dependent signaling pathway in macrophage cell lines. *J Virol.* 81:8953-8966.

Adam, E.J., and S.A. Adam. 1994. Identification of cytosolic factors required for nuclear location sequence-mediated binding to the nuclear envelope. *J Cell Biol.* 125:547-555.

Akey, C.W. 1989. Interactions and structure of the nuclear pore complex revealed by cryo-electron microscopy. *J Cell Biol.* 109:955-970.

Akey, C.W., and M. Radermacher. 1993. Architecture of the Xenopus nuclear pore complex revealed by three-dimensional cryo-electron microscopy. *J Cell Biol.* 122:1-19.

Akira, S., and K. Takeda. 2004. Toll-like receptor signalling. *Nat Rev Immunol.* 4:499-511.

Alber, F., S. Dokudovskaya, L.M. Veenhoff, W. Zhang, J. Kipper, D. Devos, A. Suprapto, O. Karni-Schmidt, R. Williams, B.T. Chait, M.P. Rout, and A. Sali. 2007a. Determining the architectures of macromolecular assemblies. *Nature.* 450:683-694.

Alber, F., S. Dokudovskaya, L.M. Veenhoff, W. Zhang, J. Kipper, D. Devos, A. Suprapto, O. Karni-Schmidt, R. Williams, B.T. Chait, A. Sali, and M.P. Rout. 2007b. The molecular architecture of the nuclear pore complex. *Nature.* 450:695-701.

Alexander, W.S. 2002. Suppressors of cytokine signalling (SOCS) in the immune system. *Nat Rev Immunol.* 2:410-416.

Alexopoulou, L., A.C. Holt, R. Medzhitov, and R.A. Flavell. 2001. Recognition of double-stranded RNA and activation of NF-kappaB by Toll-like receptor 3. *Nature.* 413:732-738.

Aligo, J., S. Jia, D. Manna, and K.V. Konan. 2009. Formation and function of hepatitis C virus replication complexes require residues in the carboxy-terminal domain of NS4B protein. *Virology.* 393:68-83.

Alter, M.J., H.S. Margolis, K. Krawczynski, F.N. Judson, A. Mares, W.J. Alexander, P.Y. Hu, J.K. Miller, M.A. Gerber, R.E. Sampliner, and et al. 1992. The natural history of community-acquired hepatitis C in the United States. The Sentinel Counties Chronic non-A, non-B Hepatitis Study Team. *N Engl J Med.* 327:1899-1905.

Andre, P., F. Komurian-Pradel, S. Deforges, M. Perret, J.L. Berland, M. Sodoyer, S. Pol, C. Brechot, G. Paranhos-Baccala, and V. Lotteau. 2002. Characterization of low- and very-low-density hepatitis C virus RNA-containing particles. *J Virol.* 76:6919-6928.

Antonin, W., J. Ellenberg, and E. Dultz. 2008. Nuclear pore complex assembly through the cell cycle: regulation and membrane organization. *FEBS Lett.* 582:2004-2016.

Antonin, W., C. Franz, U. Haselmann, C. Antony, and I.W. Mattaj. 2005. The integral membrane nucleoporin pom121 functionally links nuclear pore complex assembly and nuclear envelope formation. *Mol Cell.* 17:83-92.

Ao, Z., K.D. Jayappa, B. Wang, Y. Zheng, X. Wang, J. Peng, and X. Yao. 2012. Contribution of host nucleoporin 62 in HIV-1 integrase chromatin association and viral DNA integration. *J Biol Chem.* 287:10544-10555.

Appel, N., M. Zayas, S. Miller, J. Krijnse-Locker, T. Schaller, P. Friebe, S. Kallis, U. Engel, and R. Bartenschlager. 2008. Essential role of domain III of nonstructural protein 5A for hepatitis C virus infectious particle assembly. *PLoS pathogens.* 4:e1000035.

Arib, G., and A. Akhtar. 2011. Multiple facets of nuclear periphery in gene expression control. *Curr Opin Cell Biol.* 23:346-353.

Bach, E.A., M. Aguet, and R.D. Schreiber. 1997. The IFN gamma receptor: a paradigm for cytokine receptor signaling. *Annu Rev Immunol.* 15:563-591.

Bachi, A., I.C. Braun, J.P. Rodrigues, N. Pante, K. Ribbeck, C. von Kobbe, U. Kutay, M. Wilm, D. Gorlich, M. Carmo-Fonseca, and E. Izaurralde. 2000. The C-terminal domain of TAP interacts with the nuclear pore complex and promotes export of specific CTE-bearing RNA substrates. *RNA.* 6:136-158.

Backes, P., D. Quinkert, S. Reiss, M. Binder, M. Zayas, U. Rescher, V. Gerke, R. Bartenschlager, and V. Lohmann. 2010. Role of annexin A2 in the production of infectious hepatitis C virus particles. *Journal of virology.* 84:5775-5789.

Barba, G., F. Harper, T. Harada, M. Kohara, S. Goulinet, Y. Matsuura, G. Eder, Z. Schaff, M.J. Chapman, T. Miyamura, and C. Brechot. 1997. Hepatitis C virus core protein shows a cytoplasmic localization and associates to cellular lipid storage droplets. *Proc Natl Acad Sci U S A.* 94:1200-1205.

Bartenschlager, R., F.L. Cosset, and V. Lohmann. 2010. Hepatitis C virus replication cycle. *J Hepatol.* 53:583-585.

Bartosch, B., A. Vitelli, C. Granier, C. Goujon, J. Dubuisson, S. Pascale, E. Scarselli, R. Cortese, A. Nicosia, and F.L. Cosset. 2003. Cell entry of hepatitis C virus requires a set of co-receptors that include the CD81 tetraspanin and the SR-B1 scavenger receptor. *J Biol Chem.* 278:41624-41630.

Belgareh, N., G. Rabut, S.W. Bai, M. van Overbeek, J. Beaudouin, N. Daigle, O.V. Zatsepina, F. Pasteau, V. Labas, M. Fromont-Racine, J. Ellenberg, and V. Doye. 2001. An evolutionarily conserved NPC subcomplex, which redistributes in part to kinetochores in mammalian cells. *J Cell Biol.* 154:1147-1160.

Belov, G.A., P.V. Lidsky, O.V. Mikitas, D. Egger, K.A. Lukyanov, K. Bienz, and V.I. Agol. 2004. Bidirectional increase in permeability of nuclear envelope upon poliovirus infection and accompanying alterations of nuclear pores. *J Virol.* 78:10166-10177.

Belov, G.A., V. Nair, B.T. Hansen, F.H. Hoyt, E.R. Fischer, and E. Ehrenfeld. 2012. Complex dynamic development of poliovirus membranous replication complexes. *J Virol.* 86:302-312.

Belov, G.A., and F.J. van Kuppeveld. 2012. (+)RNA viruses rewire cellular pathways to build replication organelles. *Curr Opin Virol.* 2:740-747.

Benga, W.J., S.E. Krieger, M. Dimitrova, M.B. Zeisel, M. Parnot, J. Lupberger, E. Hildt, G. Luo, J. McLauchlan, T.F. Baumert, and C. Schuster. 2010. Apolipoprotein E interacts with hepatitis C virus nonstructural protein 5A and determines assembly of infectious particles. *Hepatology.* 51:43-53.

Beran, R.K., B.D. Lindenbach, and A.M. Pyle. 2009. The NS4A protein of hepatitis C virus promotes RNA-coupled ATP hydrolysis by the NS3 helicase. *J Virol.* 83:3268-3275.

Berger, K.L., J.D. Cooper, N.S. Heaton, R. Yoon, T.E. Oakland, T.X. Jordan, G. Mateu, A. Grakoui, and G. Randall. 2009. Roles for endocytic trafficking and phosphatidylinositol 4-kinase III alpha in hepatitis C virus replication. *Proc Natl Acad Sci U S A.* 106:7577-7582.

Berke, I.C., T. Boehmer, G. Blobel, and T.U. Schwartz. 2004. Structural and functional analysis of Nup133 domains reveals modular building blocks of the nuclear pore complex. *J Cell Biol.* 167:591-597.

Berke, I.C., and Y. Modis. 2012. MDA5 cooperatively forms dimers and ATP-sensitive filaments upon binding double-stranded RNA. *Embo J.* 31:1714-1726.

Bernad, R., D. Engelsma, H. Sanderson, H. Pickersgill, and M. Fornerod. 2006. Nup214-Nup88 nucleoporin subcomplex is required for CRM1-mediated 60 S preribosomal nuclear export. *J Biol Chem.* 281:19378-19386.

Bernad, R., H. van der Velde, M. Fornerod, and H. Pickersgill. 2004. Nup358/RanBP2 attaches to the nuclear pore complex via association with Nup88 and Nup214/CAN and plays a supporting role in CRM1-mediated nuclear protein export. *Mol Cell Biol.* 24:2373-2384.

Bhattacharya, S., R. Eckner, S. Grossman, E. Oldread, Z. Arany, A. D'Andrea, and D.M. Livingston. 1996. Cooperation of Stat2 and p300/CBP in signalling induced by interferon-alpha. *Nature.* 383:344-347.

Bhattacharya, S., W.C. HuangFu, G. Dong, J. Qian, D.P. Baker, J. Karar, C. Koumenis, J.A. Diehl, and S.Y. Fuchs. 2013. Anti-tumorigenic effects of Type 1 interferon are subdued by integrated stress responses. *Oncogene.* 32:4214-4221.

Bianco, A., V. Reghellin, L. Donnici, S. Fenu, R. Alvarez, C. Baruffa, F. Peri, M. Pagani, S. Abrignani, P. Neddermann, and R. De Francesco. 2012. Metabolism of phosphatidylinositol 4-kinase IIIalpha-dependent PI4P Is subverted by HCV and is targeted by a 4-anilino quinazoline with antiviral activity. *PLoS Pathog.* 8:e1002576.

Bigger, C.B., K.M. Brasky, and R.E. Lanford. 2001. DNA microarray analysis of chimpanzee liver during acute resolving hepatitis C virus infection. *J Virol.* 75:7059-7066.

Bigger, C.B., B. Guerra, K.M. Brasky, G. Hubbard, M.R. Beard, B.A. Luxon, S.M. Lemon, and R.E. Lanford. 2004. Intrahepatic gene expression during chronic hepatitis C virus infection in chimpanzees. *J Virol.* 78:13779-13792.

Bischoff, F.R., and D. Gorlich. 1997. RanBP1 is crucial for the release of RanGTP from importin beta-related nuclear transport factors. *FEBS Lett.* 419:249-254.

Bischoff, F.R., and H. Ponstingl. 1991. Catalysis of guanine nucleotide exchange on Ran by the mitotic regulator RCC1. *Nature.* 354:80-82.

Blanchard, E., S. Belouzard, L. Goueslain, T. Wakita, J. Dubuisson, C. Wychowski, and Y. Rouille. 2006. Hepatitis C virus entry depends on clathrin-mediated endocytosis. *J Virol.* 80:6964-6972.

Blight, K.J., J.A. McKeating, and C.M. Rice. 2002. Highly permissive cell lines for subgenomic and genomic hepatitis C virus RNA replication. *J Virol.* 76:13001-13014.

Blindenbacher, A., F.H. Duong, L. Hunziker, S.T. Stutvoet, X. Wang, L. Terracciano, D. Moradpour, H.E. Blum, T. Alonzi, M. Tripodi, N. La Monica, and M.H. Heim. 2003. Expression of hepatitis c virus proteins inhibits interferon alpha signaling in the liver of transgenic mice. *Gastroenterology.* 124:1465-1475.

Bode, J.G., S. Ludwig, C. Ehrhardt, U. Albrecht, A. Erhardt, F. Schaper, P.C. Heinrich, and D. Haussinger. 2003. IFN-alpha antagonistic activity of HCV core protein involves induction of suppressor of cytokine signaling-3. *Faseb J.* 17:488-490.

Bodoor, K., S. Shaikh, D. Salina, W.H. Raharjo, R. Bastos, M. Lohka, and B. Burke. 1999. Sequential recruitment of NPC proteins to the nuclear periphery at the end of mitosis. *J. Cell Sci.* 112 (Pt 13):2253-2264.

Bogerd, H.P., A. Echarri, T.M. Ross, and B.R. Cullen. 1998. Inhibition of human immunodeficiency virus Rev and human T-cell leukemia virus Rex function, but not Mason-Pfizer monkey virus constitutive transport element activity, by a mutant human nucleoporin targeted to Crm1. *J Virol.* 72:8627-8635.

Boson, B., O. Granio, R. Bartenschlager, and F.L. Cosset. 2011. A concerted action of hepatitis C virus p7 and nonstructural protein 2 regulates core localization at the endoplasmic reticulum and virus assembly. *PLoS pathogens.* 7:e1002144.

Boulant, S., P. Targett-Adams, and J. McLauchlan. 2007. Disrupting the association of hepatitis C virus core protein with lipid droplets correlates with a loss in production of infectious virus. *J Gen Virol.* 88:2204-2213.

Boulant, S., C. Vanbelle, C. Ebel, F. Penin, and J.P. Lavergne. 2005. Hepatitis C virus core protein is a dimeric alpha-helical protein exhibiting membrane protein features. *J Virol.* 79:11353-11365.

Bracarda, S., A.M. Eggermont, and J. Samuelsson. 2010. Redefining the role of interferon in the treatment of malignant diseases. *European journal of cancer*. 46:284-297.

Brass, A.L., D.M. Dykxhoorn, Y. Benita, N. Yan, A. Engelman, R.J. Xavier, J. Lieberman, and S.J. Elledge. 2008. Identification of host proteins required for HIV infection through a functional genomic screen. *Science*. 319:921-926.

Brazzoli, M., A. Bianchi, S. Filippini, A. Weiner, Q. Zhu, M. Pizza, and S. Crotta. 2008. CD81 is a central regulator of cellular events required for hepatitis C virus infection of human hepatocytes. *J Virol*. 82:8316-8329.

Brickner, D.G., I. Cajigas, Y. Fondufe-Mittendorf, S. Ahmed, P.C. Lee, J. Widom, and J.H. Brickner. 2007. H2A.Z-mediated localization of genes at the nuclear periphery confers epigenetic memory of previous transcriptional state. *PLoS Biol*. 5:e81.

Brohawn, S.G., N.C. Leksa, E.D. Spear, K.R. Rajashankar, and T.U. Schwartz. 2008. Structural evidence for common ancestry of the nuclear pore complex and vesicle coats. *Science*. 322:1369-1373.

Burke, B., and C.L. Stewart. 2013. The nuclear lamins: flexibility in function. *Nature reviews. Molecular cell biology*. 14:13-24.

Campbell, M.S., G.K. Chan, and T.J. Yen. 2001. Mitotic checkpoint proteins HsMAD1 and HsMAD2 are associated with nuclear pore complexes in interphase. *J Cell Sci*. 114:953-963.

Capelson, M., Y. Liang, R. Schulte, W. Mair, U. Wagner, and M.W. Hetzer. 2010. Chromatin-bound nuclear pore components regulate gene expression in higher eukaryotes. *Cell*. 140:372-383.

Cardarelli, F., M. Serresi, R. Bizzarri, M. Giacca, and F. Beltram. 2007. In vivo study of HIV-1 Tat arginine-rich motif unveils its transport properties. *Mol Ther*. 15:1313-1322.

Castelló, A., J. Izquierdo, E. Welnowska, and L. Carrasco. 2009. RNA nuclear export is blocked by poliovirus 2A protease and is concomitant with nucleoporin cleavage. *J Cell Sci*. 122:3799-3809.

Catanese, M.T., H. Ansuini, R. Graziani, T. Huby, M. Moreau, J.K. Ball, G. Paonessa, C.M. Rice, R. Cortese, A. Vitelli, and A. Nicosia. 2010. Role of scavenger receptor class B type I in hepatitis C virus entry: kinetics and molecular determinants. *J Virol*. 84:34-43.

Cerutti, A., P. Maillard, R. Minisini, P.O. Vidalain, F. Roohvand, E.I. Pecheur, M. Pirisi, and A. Budkowska. 2011. Identification of a functional, CRM-1-dependent nuclear export signal in hepatitis C virus core protein. *PLoS One*. 6:e25854.

Chadrin, A., B. Hess, M. San Roman, X. Gatti, B. Lombard, D. Loew, Y. Barral, B. Palancade, and V. Doye. 2010. Pom33, a novel transmembrane nucleoporin required for proper nuclear pore complex distribution. *J Cell Biol*. 189:795-811.

Chahine, M.N., and G.N. Pierce. 2009. Therapeutic targeting of nuclear protein import in pathological cell conditions. *Pharmacological reviews*. 61:358-372.

Chang, H.M., M. Paulson, M. Holko, C.M. Rice, B.R. Williams, I. Marie, and D.E. Levy. 2004. Induction of interferon-stimulated gene expression and antiviral responses require protein deacetylase activity. *Proc Natl Acad Sci U S A*. 101:9578-9583.

Chao, T.C., W.C. Su, J.Y. Huang, Y.C. Chen, K.S. Jeng, H.D. Wang, and M.M. Lai. 2012. Proline-serine-threonine phosphatase-interacting protein 2 (PSTPIP2), a host membrane-deforming protein, is critical for membranous web formation in hepatitis C virus replication. *J Virol*. 86:1739-1749.

Chaudhary, N., and J.C. Courvalin. 1993. Stepwise reassembly of the nuclear envelope at the end of mitosis. *J. Cell Biol*. 122:295-306.

Chen, L., I. Borozan, J. Feld, J. Sun, L.L. Tannis, C. Coltescu, J. Heathcote, A.M. Edwards, and I.D. McGilvray. 2005. Hepatic gene expression discriminates responders and nonresponders in treatment of chronic hepatitis C viral infection. *Gastroenterology*. 128:1437-1444.

Chi, N.C., E.J. Adam, and S.A. Adam. 1995. Sequence and characterization of cytoplasmic nuclear protein import factor p97. *J Cell Biol*. 130:265-274.

Choo, Q.L., G. Kuo, A.J. Weiner, L.R. Overby, D.W. Bradley, and M. Houghton. 1989. Isolation of a cDNA clone derived from a blood-borne non-A, non-B viral hepatitis genome. *Science*. 244:359-362.

Chow, K.H., S. Elgort, M. Dasso, and K.S. Ullman. 2012. Two distinct sites in Nup153 mediate interaction with the SUMO proteases SENP1 and SENP2. *Nucleus*. 3:349-358.

Chung, K., J. Lee, J. Kim, O. Song, S. Cho, J. Lim, M. Seedorf, B. Hahm, and S. Jang. 2000. Nonstructural protein 5A of hepatitis C virus inhibits the function of karyopherin beta3. *J Virol*. 74:5233-5241.

Coller, K.E., N.S. Heaton, K.L. Berger, J.D. Cooper, J.L. Saunders, and G. Randall. 2012. Molecular determinants and dynamics of hepatitis C virus secretion. *PLoS Pathog*. 8:e1002466.

Copeland, A.M., W.W. Newcomb, and J.C. Brown. 2009. Herpes simplex virus replication: roles of viral proteins and nucleoporins in capsid-nucleus attachment. *J Virol*. 83:1660-1668.

Cordes, V.C., H.R. Rackwitz, and S. Reidenbach. 1997. Mediators of nuclear protein import target karyophilic proteins to pore complexes of cytoplasmic annulate lamellae. *Exp Cell Res*. 237:419-433.

Cormier, E.G., F. Tsamis, F. Kajumo, R.J. Durso, J.P. Gardner, and T. Dragic. 2004. CD81 is an entry coreceptor for hepatitis C virus. *Proc Natl Acad Sci U S A*. 101:7270-7274.

Counihan, N.A., S.M. Rawlinson, and B.D. Lindenbach. 2011. Trafficking of hepatitis C virus core protein during virus particle assembly. *PLoS Pathog.* 7:e1002302.

Courington, D., and P.K. Vogt. 1967. Electron microscopy of chick fibroblasts infected by defective rous sarcoma virus and its helper. *J. Virol.* 1:400-414.

Croft, J.A., J.M. Bridger, S. Boyle, P. Perry, P. Teague, and W.A. Bickmore. 1999. Differences in the localization and morphology of chromosomes in the human nucleus. *J Cell Biol.* 145:1119-1131.

Cronshaw, J.M., A.N. Krutchinsky, W. Zhang, B.T. Chait, and M.J. Matunis. 2002. Proteomic analysis of the mammalian nuclear pore complex. *J Cell Biol.* 158:915-927.

Da Costa, D., M. Turek, D.J. Felmlee, E. Girardi, S. Pfeffer, G. Long, R. Bartenschlager, M.B. Zeisel, and T.F. Baumert. 2012. Reconstitution of the entire hepatitis C virus life cycle in nonhepatic cells. *J Virol.* 86:11919-11925.

Dacks, J.B., and M.C. Field. 2007. Evolution of the eukaryotic membrane-trafficking system: origin, tempo and mode. *J Cell Sci.* 120:2977-2985.

DaFonseca, C.J., F. Shu, and J.J. Zhang. 2001. Identification of two residues in MCM5 critical for the assembly of MCM complexes and Stat1-mediated transcription activation in response to IFN-gamma. *Proc Natl Acad Sci U S A.* 98:3034-3039.

Darnell, J.E., Jr. 1997. STATs and gene regulation. *Science.* 277:1630-1635.

Darnell, J.E., Jr., I.M. Kerr, and G.R. Stark. 1994. Jak-STAT pathways and transcriptional activation in response to IFNs and other extracellular signaling proteins. *Science.* 264:1415-1421.

Davis, T.L., J.R. Walker, V. Campagna-Slater, P.J. Finerty, R. Paramanathan, G. Bernstein, F. MacKenzie, W. Tempel, H. Ouyang, W.H. Lee, E.Z. Eisenmesser, and S. Dhe-Paganon. 2010. Structural and biochemical characterization of the human cyclophilin family of peptidyl-prolyl isomerases. *PLoS Biol.* 8:e1000439.

Dawlaty, M.M., L. Malureanu, K.B. Jeganathan, E. Kao, C. Sustmann, S. Tahk, K. Shuai, R. Grosschedl, and J.M. van Deursen. 2008. Resolution of sister centromeres requires RanBP2-mediated SUMOylation of topoisomerase IIalpha. *Cell.* 133:103-115.

de Chassey, B., V. Navratil, L. Tafforeau, M. Hiet, A. Aublin-Gex, S. Agaugué, G. Meiffren, F. Pradezynski, B. Faria, T. Chantier, M. Le Breton, J. Pellet, N. Davoust, P. Mangeot, A. Chaboud, F. Penin, Y. Jacob, P. Vidalain, M. Vidal, P. André, C. Rabourdin-Combe, and V. Lotteau. 2008. Hepatitis C virus infection protein network. *Mol Syst Biol.* 4:230.

de Lucas, S., J. Bartolome, and V. Carreno. 2005. Hepatitis C virus core protein down-regulates transcription of interferon-induced antiviral genes. *J Infect Dis.* 191:93-99.

de Weerd, N.A., and T. Nguyen. 2012. The interferons and their receptors--distribution and regulation. *Immunol Cell Biol.* 90:483-491.

Debler, E.W., Y. Ma, H.S. Seo, K.C. Hsia, T.R. Noriega, G. Blobel, and A. Hoelz. 2008. A fence-like coat for the nuclear pore membrane. *Mol Cell*. 32:815-826.

DeGrasse, J.A., K.N. DuBois, D. Devos, T.N. Siegel, A. Sali, M.C. Field, M.P. Rout, and B.T. Chait. 2009. Evidence for a shared nuclear pore complex architecture that is conserved from the last common eukaryotic ancestor. *Molecular & cellular proteomics : MCP*. 8:2119-2130.

Deleersnyder, V., A. Pillez, C. Wychowski, K. Blight, J. Xu, Y.S. Hahn, C.M. Rice, and J. Dubuisson. 1997. Formation of native hepatitis C virus glycoprotein complexes. *J Virol*. 71:697-704.

den Boon, J.A., and P. Ahlquist. 2010. Organelle-like membrane compartmentalization of positive-strand RNA virus replication factories. *Annu Rev Microbiol*. 64:241-256.

den Boon, J.A., A. Diaz, and P. Ahlquist. 2010. Cytoplasmic viral replication complexes. *Cell Host Microbe*. 8:77-85.

Denning, D.P., S.S. Patel, V. Uversky, A.L. Fink, and M. Rexach. 2003. Disorder in the nuclear pore complex: the FG repeat regions of nucleoporins are natively unfolded. *Proc Natl Acad Sci U S A*. 100:2450-2455.

Der, S.D., A. Zhou, B.R. Williams, and R.H. Silverman. 1998. Identification of genes differentially regulated by interferon alpha, beta, or gamma using oligonucleotide arrays. *Proc Natl Acad Sci U S A*. 95:15623-15628.

Devos, D., S. Dokudovskaya, F. Alber, R. Williams, B.T. Chait, A. Sali, and M.P. Rout. 2004. Components of coated vesicles and nuclear pore complexes share a common molecular architecture. *PLoS Biol*. 2:e380.

Devos, D., S. Dokudovskaya, R. Williams, F. Alber, N. Eswar, B.T. Chait, M.P. Rout, and A. Sali. 2006. Simple fold composition and modular architecture of the nuclear pore complex. *Proc Natl Acad Sci U S A*. 103:2172-2177.

Di Nunzio, F., A. Danckaert, T. Fricke, P. Perez, J. Fernandez, E. Perret, P. Roux, S. Shorte, P. Charneau, F. Diaz-Griffero, and N.J. Arhel. 2012. Human nucleoporins promote HIV-1 docking at the nuclear pore, nuclear import and integration. *PLoS One*. 7:e46037.

Di Nunzio, F., T. Fricke, A. Miccio, J.C. Valle-Casuso, P. Perez, P. Souque, E. Rizzi, M. Severgnini, F. Mavilio, P. Charneau, and F. Diaz-Griffero. 2013. Nup153 and Nup98 bind the HIV-1 core and contribute to the early steps of HIV-1 replication. *Virology*. 440:8-18.

Diebold, S.S., T. Kaisho, H. Hemmi, S. Akira, and C. Reis e Sousa. 2004. Innate antiviral responses by means of TLR7-mediated recognition of single-stranded RNA. *Science*. 303:1529-1531.

Dingwall, C., J. Robbins, S.M. Dilworth, B. Roberts, and W.D. Richardson. 1988. The nucleoplasmin nuclear location sequence is larger and more complex than that of SV-40 large T antigen. *J Cell Biol.* 107:841-849.

Doucet, C.M., J.A. Talamas, and M.W. Hetzer. 2010. Cell cycle-dependent differences in nuclear pore complex assembly in metazoa. *Cell.* 141:1030-1041.

Dreux, M., P. Gastaminza, S.F. Wieland, and F.V. Chisari. 2009. The autophagy machinery is required to initiate hepatitis C virus replication. *Proc Natl Acad Sci U S A.* 106:14046-14051.

Du, Z., Y. Shen, W. Yang, I. Mecklenbrauker, B.G. Neel, and L.B. Ivashkiv. 2005. Inhibition of IFN-alpha signaling by a PKC- and protein tyrosine phosphatase SHP-2-dependent pathway. *Proc Natl Acad Sci U S A.* 102:10267-10272.

Dultz, E., and J. Ellenberg. 2010. Live imaging of single nuclear pores reveals unique assembly kinetics and mechanism in interphase. *J Cell Biol.* 191:15-22.

Dultz, E., E. Zanin, C. Wurzenberger, M. Braun, G. Rabut, L. Sironi, and J. Ellenberg. 2008. Systematic kinetic analysis of mitotic dis- and reassembly of the nuclear pore in living cells. *J Cell Biol.* 180:857-865.

Duong, F.H., M. Filipowicz, M. Tripodi, N. La Monica, and M.H. Heim. 2004. Hepatitis C virus inhibits interferon signaling through up-regulation of protein phosphatase 2A. *Gastroenterology.* 126:263-277.

Egger, D., B. Wölk, R. Gosert, L. Bianchi, H. Blum, D. Moradpour, and K. Bienz. 2002. Expression of hepatitis C virus proteins induces distinct membrane alterations including a candidate viral replication complex. *J Virol.* 76:5974-5984.

Elton, D., M. Simpson-Holley, K. Archer, L. Medcalf, R. Hallam, J. McCauley, and P. Digard. 2001. Interaction of the influenza virus nucleoprotein with the cellular CRM1-mediated nuclear export pathway. *J Virol.* 75:408-419.

Enninga, J., D. Levy, G. Blobel, and B. Fontoura. 2002. Role of nucleoporin induction in releasing an mRNA nuclear export block. *Science.* 295:1523-1525.

Evans, M.J., C.M. Rice, and S.P. Goff. 2004. Phosphorylation of hepatitis C virus nonstructural protein 5A modulates its protein interactions and viral RNA replication. *Proc Natl Acad Sci U S A.* 101:13038-13043.

Evans, M.J., T. von Hahn, D.M. Tscherne, A.J. Syder, M. Panis, B. Wolk, T. Hatziioannou, J.A. McKeating, P.D. Bieniasz, and C.M. Rice. 2007. Claudin-1 is a hepatitis C virus co-receptor required for a late step in entry. *Nature.* 446:801-805.

Fan, S., E.L. Whiteman, T.W. Hurd, J.C. McIntyre, J.F. Dishinger, C.J. Liu, J.R. Martens, K.J. Verhey, U. Sajjan, and B. Margolis. 2011. Induction of Ran GTP drives ciliogenesis. *Mol. Biol. Cell.* 22:4539-4548.

Faria, A.M., A. Levay, Y. Wang, A.O. Kamphorst, M.L. Rosa, D.R. Nussenzveig, W. Balkan, Y.M. Chook, D.E. Levy, and B.M. Fontoura. 2006. The nucleoporin Nup96 is required for proper expression of interferon-regulated proteins and functions. *Immunity*. 24:295-304.

Faria, P., P. Chakraborty, A. Levay, G. Barber, H. Ezelle, J. Enninga, C. Arana, J. van Deursen, and B. Fontoura. 2005. VSV disrupts the Rae1/mrnp41 mRNA nuclear export pathway. *Mol Cell*. 17:93-102.

Feeley, E.M., J.S. Sims, S.P. John, C.R. Chin, T. Pertel, L.M. Chen, G.D. Gaiha, B.J. Ryan, R.O. Donis, S.J. Elledge, and A.L. Brass. 2011. IFITM3 inhibits influenza A virus infection by preventing cytosolic entry. *PLoS Pathog*. 7:e1002337.

Feeney, E.R., and R.T. Chung. 2014. Antiviral treatment of hepatitis C. *Bmj*. 348:g3308.

Feldherr, C.M., and D. Akin. 1997. The location of the transport gate in the nuclear pore complex. *J Cell Sci*. 110 (Pt 24):3065-3070.

Feldherr, C.M., E. Kallenbach, and N. Schultz. 1984. Movement of a karyophilic protein through the nuclear pores of oocytes. *J Cell Biol*. 99:2216-2222.

Felix, R.S., G.W. Colleoni, O.L. Caballero, M. Yamamoto, M.S. Almeida, V.C. Andrade, L. Chauffaille Mde, W.A. Silva, Jr., M.D. Begnami, F.A. Soares, A.J. Simpson, M.A. Zago, and A.L. Vettore. 2009. SAGE analysis highlights the importance of p53csv, ddx5, mapkapk2 and ranbp2 to multiple myeloma tumorigenesis. *Cancer Lett*. 278:41-48.

Feng, Z., L. Hensley, K.L. McKnight, F. Hu, V. Madden, L. Ping, S.H. Jeong, C. Walker, R.E. Lanford, and S.M. Lemon. 2013. A pathogenic picornavirus acquires an envelope by hijacking cellular membranes. *Nature*. 496:367-371.

Ferraris, P., E. Blanchard, and P. Roingeard. 2010. Ultrastructural and biochemical analyses of hepatitis C virus-associated host cell membranes. *J Gen Virol*. 91:2230-2237.

Ferreira, P.A., J.T. Hom, and W.L. Pak. 1995. Retina-specifically expressed novel subtypes of bovine cyclophilin. *J Biol Chem*. 270:23179-23188.

Ferreon, J.C., A.C. Ferreon, K. Li, and S.M. Lemon. 2005. Molecular determinants of TRIF proteolysis mediated by the hepatitis C virus NS3/4A protease. *J Biol Chem*.

Field, M.C., and J.B. Dacks. 2009. First and last ancestors: reconstructing evolution of the endomembrane system with ESCRTs, vesicle coat proteins, and nuclear pore complexes. *Curr Opin Cell Biol*. 21:4-13.

Field, M.C., A. Sali, and M.P. Rout. 2011. Evolution: On a bender--BARs, ESCRTs, COPs, and finally getting your coat. *J Cell Biol*. 193:963-972.

Finlay, D.R., E. Meier, P. Bradley, J. Horecka, and D.J. Forbes. 1991. A complex of nuclear pore proteins required for pore function. *J Cell Biol*. 114:169-183.

Fischer, G., B. Wittmann-Liebold, K. Lang, T. Kiefhaber, and F.X. Schmid. 1989. Cyclophilin and peptidyl-prolyl cis-trans isomerase are probably identical proteins. *Nature*. 337:476-478.

Fitzgerald, K.A., S.M. McWhirter, K.L. Faia, D.C. Rowe, E. Latz, D.T. Golenbock, A.J. Coyle, S.M. Liao, and T. Maniatis. 2003. IKKepsilon and TBK1 are essential components of the IRF3 signaling pathway. *Nature immunology*. 4:491-496.

Flotho, A., and F. Melchior. 2013. Sumoylation: a regulatory protein modification in health and disease. *Annual review of biochemistry*. 82:357-385.

Fontana, J., C. Lopez-Iglesias, W.P. Tzeng, T.K. Frey, J.J. Fernandez, and C. Risco. 2010. Three-dimensional structure of Rubella virus factories. *Virology*. 405:579-591.

Fontoura, B.M., P.A. Faria, and D.R. Nussenzveig. 2005. Viral interactions with the nuclear transport machinery: discovering and disrupting pathways. *IUBMB Life*. 57:65-72.

Forler, D., G. Rabut, F. Ciccarelli, A. Herold, T. Köcher, R. Niggeweg, P. Bork, J. Ellenberg, and E. Izaurralde. 2004a. RanBP2/Nup358 provides a major binding site for NXF1-p15 dimers at the nuclear pore complex and functions in nuclear mRNA export. *Mol Cell Biol*. 24:1155-1167.

Forler, D., G. Rabut, F.D. Ciccarelli, A. Herold, T. Kocher, R. Niggeweg, P. Bork, J. Ellenberg, and E. Izaurralde. 2004b. RanBP2/Nup358 provides a major binding site for NXF1-p15 dimers at the nuclear pore complex and functions in nuclear mRNA export. *Mol Cell Biol*. 24:1155-1167.

Fornerod, M., M. Ohno, M. Yoshida, and I.W. Mattaj. 1997a. CRM1 is an export receptor for leucine-rich nuclear export signals. *Cell*. 90:1051-1060.

Fornerod, M., J. van Deursen, S. van Baal, A. Reynolds, D. Davis, K.G. Murti, J. Fransen, and G. Grosveld. 1997b. The human homologue of yeast CRM1 is in a dynamic subcomplex with CAN/Nup214 and a novel nuclear pore component Nup88. *Embo J*. 16:807-816.

Foster, T.L., P. Gallay, N.J. Stonehouse, and M. Harris. 2011. Cyclophilin A interacts with domain II of hepatitis C virus NS5A and stimulates RNA binding in an isomerase-dependent manner. *J Virol*. 85:7460-7464.

Fraser, C.S., and J.A. Doudna. 2007. Structural and mechanistic insights into hepatitis C viral translation initiation. *Nature reviews. Microbiology*. 5:29-38.

Frey, S., and D. Gorlich. 2007. A saturated FG-repeat hydrogel can reproduce the permeability properties of nuclear pore complexes. *Cell*. 130:512-523.

Frey, S., R.P. Richter, and D. Gorlich. 2006. FG-rich repeats of nuclear pore proteins form a three-dimensional meshwork with hydrogel-like properties. *Science*. 314:815-817.

Friebe, P., J. Boudet, J.P. Simorre, and R. Bartenschlager. 2005. Kissing-loop interaction in the 3' end of the hepatitis C virus genome essential for RNA replication. *J Virol*. 79:380-392.

Fried, H., and U. Kutay. 2003. Nucleocytoplasmic transport: taking an inventory. *Cellular and molecular life sciences : CMLS*. 60:1659-1688.

Fried, M.W., M.L. Shiffman, K.R. Reddy, C. Smith, G. Marinos, F.L. Goncales, Jr., D. Haussinger, M. Diago, G. Carosi, D. Dhumeaux, A. Craxi, A. Lin, J. Hoffman, and J. Yu. 2002. Peginterferon alfa-2a plus ribavirin for chronic hepatitis C virus infection. *N Engl J Med*. 347:975-982.

Frieman, M., B. Yount, M. Heise, S.A. Kopecky-Bromberg, P. Palese, and R.S. Baric. 2007. Severe acute respiratory syndrome coronavirus ORF6 antagonizes STAT1 function by sequestering nuclear import factors on the rough endoplasmic reticulum/Golgi membrane. *J Virol*. 81:9812-9824.

Frolova, E.I., R. Gorchakov, L. Pereboeva, S. Atasheva, and I. Frolov. 2010. Functional Sindbis virus replicative complexes are formed at the plasma membrane. *J Virol*. 84:11679-11695.

Fuchs, S.Y. 2013. Hope and fear for interferon: the receptor-centric outlook on the future of interferon therapy. *J Interferon Cytokine Res*. 33:211-225.

Fukuda, M., S. Asano, T. Nakamura, M. Adachi, M. Yoshida, M. Yanagida, and E. Nishida. 1997. CRM1 is responsible for intracellular transport mediated by the nuclear export signal. *Nature*. 390:308-311.

Funakoshi, T., M. Clever, A. Watanabe, and N. Imamoto. 2011. Localization of Pom121 to the inner nuclear membrane is required for an early step of interphase nuclear pore complex assembly. *Mol Biol Cell*. 22:1058-1069.

Gale, M., Jr., C.M. Blakely, B. Kwieciszewski, S.L. Tan, M. Dossett, N.M. Tang, M.J. Korth, S.J. Polyak, D.R. Gretch, and M.G. Katze. 1998. Control of PKR protein kinase by hepatitis C virus nonstructural 5A protein: molecular mechanisms of kinase regulation. *Mol Cell Biol*. 18:5208-5218.

Gastaminza, P., G. Cheng, S. Wieland, J. Zhong, W. Liao, and F.V. Chisari. 2008. Cellular determinants of hepatitis C virus assembly, maturation, degradation, and secretion. *J Virol*. 82:2120-2129.

Gentzsch, J., C. Brohm, E. Steinmann, M. Friesland, N. Menzel, G. Vieyres, P.M. Perin, A. Frentzen, L. Kaderali, and T. Pietschmann. 2013. hepatitis c Virus p7 is critical for capsid assembly and envelopment. *PLoS Pathog*. 9:e1003355.

Gerace, L., Y. Ottaviano, and C. Kondor-Koch. 1982. Identification of a major polypeptide of the nuclear pore complex. *J Cell Biol*. 95:826-837.

Germain, M.A., L. Chatel-Chaix, B. Gagne, E. Bonneil, P. Thibault, F. Pradezynski, B. de Chassey, L. Meyniel-Schicklin, V. Lotteau, M. Baril, and D. Lamarre. 2014. Elucidating novel hepatitis C virus-host interactions using combined mass spectrometry and functional genomics approaches. *Molecular & cellular proteomics : MCP*. 13:184-203.

Germi, R., J.M. Crance, D. Garin, J. Guimet, H. Lortat-Jacob, R.W. Ruigrok, J.P. Zarski, and E. Drouet. 2002. Cellular glycosaminoglycans and low density lipoprotein receptor are involved in hepatitis C virus adsorption. *J Med Virol.* 68:206-215.

Ghildyal, R., B. Jordan, D. Li, H. Dagher, P.G. Bardin, J.E. Gern, and D.A. Jans. 2009. Rhinovirus 3C protease can localize in the nucleus and alter active and passive nucleocytoplasmic transport. *J Virol.* 83:7349-7352.

Gilchrist, D.A., G. Fromm, G. dos Santos, L.N. Pham, I.E. McDaniel, A. Burkholder, D.C. Fargo, and K. Adelman. 2012. Regulating the regulators: the pervasive effects of Pol II pausing on stimulus-responsive gene networks. *Genes Dev.* 26:933-944.

Gillespie, L.K., A. Hoenen, G. Morgan, and J.M. Mackenzie. 2010. The endoplasmic reticulum provides the membrane platform for biogenesis of the flavivirus replication complex. *J Virol.* 84:10438-10447.

Goldfarb, D.S., A.H. Corbett, D.A. Mason, M.T. Harreman, and S.A. Adam. 2004. Importin alpha: a multipurpose nuclear-transport receptor. *Trends Cell Biol.* 14:505-514.

Goldfarb, D.S., J. Gariepy, G. Schoolnik, and R.D. Kornberg. 1986. Synthetic peptides as nuclear localization signals. *Nature.* 322:641-644.

Goldman, R.D., D.K. Shumaker, M.R. Erdos, M. Eriksson, A.E. Goldman, L.B. Gordon, Y. Gruenbaum, S. Khuon, M. Mendez, R. Varga, and F.S. Collins. 2004. Accumulation of mutant lamin A causes progressive changes in nuclear architecture in Hutchinson-Gilford progeria syndrome. *Proc Natl Acad Sci U S A.* 101:8963-8968.

Gorlich, D., N. Pante, U. Kutay, U. Aebi, and F.R. Bischoff. 1996. Identification of different roles for RanGDP and RanGTP in nuclear protein import. *Embo J.* 15:5584-5594.

Gorlich, D., S. Prehn, R.A. Laskey, and E. Hartmann. 1994. Isolation of a protein that is essential for the first step of nuclear protein import. *Cell.* 79:767-778.

Gosert, R., D. Egger, and K. Bienz. 2000. A cytopathic and a cell culture adapted hepatitis A virus strain differ in cell killing but not in intracellular membrane rearrangements. *Virology.* 266:157-169.

Gosert, R., D. Egger, V. Lohmann, R. Bartenschlager, H. Blum, K. Bienz, and D. Moradpour. 2003. Identification of the hepatitis C virus RNA replication complex in Huh-7 cells harboring subgenomic replicons. *J Virol.* 77:5487-5492.

Gough, S.M., C.I. Slape, and P.D. Aplan. 2011. NUP98 gene fusions and hematopoietic malignancies: common themes and new biologic insights. *Blood.* 118:6247-6257.

Gouttenoire, J., P. Roingeard, F. Penin, and D. Moradpour. 2010. Amphipathic alpha-helix AH2 is a major determinant for the oligomerization of hepatitis C virus nonstructural protein 4B. *J Virol.* 84:12529-12537.

Gower, E., C. Estes, S. Blach, K. Razavi-Shearer, and H. Razavi. 2014. Global epidemiology and genotype distribution of the hepatitis C virus infection. *J Hepatol.*

Gracias, D.T., E. Stelekati, J.L. Hope, A.C. Boesteanu, T.A. Doering, J. Norton, Y.M. Mueller, J.A. Fraietta, E.J. Wherry, M. Turner, and P.D. Katsikis. 2013. The microRNA miR-155 controls CD8(+) T cell responses by regulating interferon signaling. *Nature immunology.* 14:593-602.

Grandi, P., T. Dang, N. Pane, A. Shevchenko, M. Mann, D. Forbes, and E. Hurt. 1997. Nup93, a vertebrate homologue of yeast Nic96p, forms a complex with a novel 205-kDa protein and is required for correct nuclear pore assembly. *Mol Biol Cell.* 8:2017-2038.

Green, A.M., P.R. Beatty, A. Hadjilaou, and E. Harris. 2014. Innate immunity to dengue virus infection and subversion of antiviral responses. *J Mol Biol.* 426:1148-1160.

Greenberg, H.B., R.B. Pollard, L.I. Lutwick, P.B. Gregory, W.S. Robinson, and T.C. Merigan. 1976. Effect of human leukocyte interferon on hepatitis B virus infection in patients with chronic active hepatitis. *N Engl J Med.* 295:517-522.

Griffis, E.R., N. Altan, J. Lippincott-Schwartz, and M.A. Powers. 2002. Nup98 is a mobile nucleoporin with transcription-dependent dynamics. *Molecular biology of the cell.* 13:1282-1297.

Griffis, E.R., B. Craige, C. Dimaano, K.S. Ullman, and M.A. Powers. 2004. Distinct functional domains within nucleoporins Nup153 and Nup98 mediate transcription-dependent mobility. *Molecular biology of the cell.* 15:1991-2002.

Guan, T., S. Muller, G. Klier, N. Pante, J.M. Blevitt, M. Haner, B. Paschal, U. Aebi, and L. Gerace. 1995. Structural analysis of the p62 complex, an assembly of O-linked glycoproteins that localizes near the central gated channel of the nuclear pore complex. *Mol Biol Cell.* 6:1591-1603.

Guillen, J., A. Gonzalez-Alvarez, and J. Villalain. 2010. A membranotropic region in the C-terminal domain of hepatitis C virus protein NS4B interaction with membranes. *Biochim Biophys Acta.* 1798:327-337.

Gustin, K.E., and P. Sarnow. 2001. Effects of poliovirus infection on nucleo-cytoplasmic trafficking and nuclear pore complex composition. *Embo J.* 20:240-249.

Gustin, K.E., and P. Sarnow. 2002. Inhibition of nuclear import and alteration of nuclear pore complex composition by rhinovirus. *J Virol.* 76:8787-8796.

Guttler, T., and D. Gorlich. 2011. Ran-dependent nuclear export mediators: a structural perspective. *Embo J.* 30:3457-3474.

Hadziyannis, S.J., H. Sette, Jr., T.R. Morgan, V. Balan, M. Diago, P. Marcellin, G. Ramadori, H. Bodenheimer, Jr., D. Bernstein, M. Rizzetto, S. Zeuzem, P.J. Pockros, A. Lin, A.M. Ackrill, and P.I.S. Group. 2004. Peginterferon-alpha2a and ribavirin combination therapy

in chronic hepatitis C: a randomized study of treatment duration and ribavirin dose. *Annals of internal medicine*. 140:346-355.

Hallberg, E., R.W. Wozniak, and G. Blobel. 1993. An integral membrane protein of the pore membrane domain of the nuclear envelope contains a nucleoporin-like region. *J Cell Biol.* 122:513-521.

Hang, J., and M. Dasso. 2002. Association of the human SUMO-1 protease SENP2 with the nuclear pore. *J Biol Chem*. 277:19961-19966.

Hanoulle, X., A. Badillo, J.M. Wieruszeski, D. Verdegem, I. Landrieu, R. Bartenschlager, F. Penin, and G. Lippens. 2009. Hepatitis C virus NS5A protein is a substrate for the peptidyl-prolyl cis/trans isomerase activity of cyclophilins A and B. *The Journal of biological chemistry*. 284:13589-13601.

Harel, A., and D.J. Forbes. 2004. Importin beta: conducting a much larger cellular symphony. *Mol. cell.* 16:319-330.

Harel, A., A.V. Orjalo, T. Vincent, A. Lachish-Zalait, S. Vasu, S. Shah, E. Zimmerman, M. Elbaum, and D.J. Forbes. 2003. Removal of a single pore subcomplex results in vertebrate nuclei devoid of nuclear pores. *Mol Cell.* 11:853-864.

Hawryluk-Gara, L., M. Platani, R. Santarella, R. Wozniak, and I. Mattaj. 2008. Nup53 is required for nuclear envelope and nuclear pore complex assembly. *Mol Biol Cell.* 19:1753-1762.

Hawryluk-Gara, L., E. Shibuya, and R. Wozniak. 2005. Vertebrate Nup53 interacts with the nuclear lamina and is required for the assembly of a Nup93-containing complex. *Mol Biol Cell.* 16:2382-2394.

Hayes, C.N., and K. Chayama. 2014. Emerging treatments for chronic hepatitis C. *Journal of the Formosan Medical Association = Taiwan yi zhi.*

Hebbes, T.R., A.W. Thorne, and C. Crane-Robinson. 1988. A direct link between core histone acetylation and transcriptionally active chromatin. *Embo J.* 7:1395-1402.

Heil, F., H. Hemmi, H. Hochrein, F. Ampenberger, C. Kirschning, S. Akira, G. Lipford, H. Wagner, and S. Bauer. 2004. Species-specific recognition of single-stranded RNA via toll-like receptor 7 and 8. *Science.* 303:1526-1529.

Heim, M.H. 2013. 25 years of interferon-based treatment of chronic hepatitis C: an epoch coming to an end. *Nat Rev Immunol.* 13:535-542.

Heim, M.H., D. Moradpour, and H.E. Blum. 1999. Expression of hepatitis C virus proteins inhibits signal transduction through the Jak-STAT pathway. *J Virol.* 73:8469-8475.

Helbig, K.J., D.T. Lau, L. Semendric, H.A. Harley, and M.R. Beard. 2005. Analysis of ISG expression in chronic hepatitis C identifies viperin as a potential antiviral effector. *Hepatology*. 42:702-710.

Hemmi, H., O. Takeuchi, T. Kawai, T. Kaisho, S. Sato, H. Sanjo, M. Matsumoto, K. Hoshino, H. Wagner, K. Takeda, and S. Akira. 2000. A Toll-like receptor recognizes bacterial DNA. *Nature*. 408:740-745.

Henke, J.I., D. Goergen, J. Zheng, Y. Song, C.G. Schuttler, C. Fehr, C. Junemann, and M. Niepmann. 2008. microRNA-122 stimulates translation of hepatitis C virus RNA. *Embo J*. 27:3300-3310.

Herker, E., C. Harris, C. Hernandez, A. Carpentier, K. Kaehlcke, A.R. Rosenberg, R.V. Farese, Jr., and M. Ott. 2010. Efficient hepatitis C virus particle formation requires diacylglycerol acyltransferase-1. *Nat Med*. 16:1295-1298.

Hetzer, M.W. 2010. The nuclear envelope. *Cold Spring Harb Perspect Biol*. 2:a000539.

Hetzer, M.W., T.C. Walther, and I.W. Mattaj. 2005. Pushing the envelope: structure, function, and dynamics of the nuclear periphery. *Annual review of cell and developmental biology*. 21:347-380.

Hetzer, M.W., and S.R. Wente. 2009. Border control at the nucleus: biogenesis and organization of the nuclear membrane and pore complexes. *Dev Cell*. 17:606-616.

Hijikata, M., N. Kato, Y. Ootsuyama, M. Nakagawa, and K. Shimotohno. 1991. Gene mapping of the putative structural region of the hepatitis C virus genome by in vitro processing analysis. *Proc Natl Acad Sci U S A*. 88:5547-5551.

Hinson, E.R., and P. Cresswell. 2009. The N-terminal amphipathic alpha-helix of viperin mediates localization to the cytosolic face of the endoplasmic reticulum and inhibits protein secretion. *J Biol Chem*. 284:4705-4712.

Ho, H.H., and L.B. Ivashkiv. 2006. Role of STAT3 in type I interferon responses. Negative regulation of STAT1-dependent inflammatory gene activation. *J Biol Chem*. 281:14111-14118.

Hoebe, K., X. Du, P. Georgel, E. Janssen, K. Tabeta, S.O. Kim, J. Goode, P. Lin, N. Mann, S. Mudd, K. Crozat, S. Sovath, J. Han, and B. Beutler. 2003. Identification of Lps2 as a key transducer of MyD88-independent TIR signalling. *Nature*. 424:743-748.

Hoelz, A., E.W. Debler, and G. Blobel. 2011. The structure of the nuclear pore complex. *Annual review of biochemistry*. 80:613-643.

Holwell, T.A., S.C. Schweitzer, M.E. Reyland, and R.M. Evans. 1999. Vimentin-dependent utilization of LDL-cholesterol in human adrenal tumor cells is not associated with the level of expression of apoE, sterol carrier protein-2, or caveolin. *J Lipid Res*. 40:1440-1452.

Hoofnagle, J.H., K.D. Mullen, D.B. Jones, V. Rustgi, A. Di Bisceglie, M. Peters, J.G. Waggoner, Y. Park, and E.A. Jones. 1986. Treatment of chronic non-A,non-B hepatitis with recombinant human alpha interferon. A preliminary report. *N Engl J Med*. 315:1575-1578.

Hopkins, S., and P. Gallay. 2012. Cyclophilin inhibitors: an emerging class of therapeutics for the treatment of chronic hepatitis C infection. *Viruses*. 4:2558-2577.

Horner, S.M., and M. Gale, Jr. 2009. Intracellular innate immune cascades and interferon defenses that control hepatitis C virus. *J Interferon Cytokine Res*. 29:489-498.

Horner, S.M., H.M. Liu, H.S. Park, J. Briley, and M. Gale, Jr. 2011. Mitochondrial-associated endoplasmic reticulum membranes (MAM) form innate immune synapses and are targeted by hepatitis C virus. *Proc Natl Acad Sci*. 108:14590-14595.

Horner, S.M., H.S. Park, and M. Gale, Jr. 2012. Control of innate immune signaling and membrane targeting by the hepatitis C virus NS3/4A protease are governed by the NS3 helix alpha0. *Journal of virology*.

Hornung, V., J. Ellegast, S. Kim, K. Brzozka, A. Jung, H. Kato, H. Poeck, S. Akira, K.K. Conzelmann, M. Schlee, S. Endres, and G. Hartmann. 2006. 5'-Triphosphate RNA is the ligand for RIG-I. *Science*. 314:994-997.

Hou, F., L. Sun, H. Zheng, B. Skaug, Q.X. Jiang, and Z.J. Chen. 2011. MAVS forms functional prion-like aggregates to activate and propagate antiviral innate immune response. *Cell*. 146:448-461.

Hsia, K.C., P. Stavropoulos, G. Blobel, and A. Hoelz. 2007. Architecture of a coat for the nuclear pore membrane. *Cell*. 131:1313-1326.

Hsu, N.Y., O. Ilnytska, G. Belov, M. Santiana, Y.H. Chen, P.M. Takvorian, C. Pau, H. van der Schaar, N. Kaushik-Basu, T. Balla, C.E. Cameron, E. Ehrenfeld, F.J. van Kuppeveld, and N. Altan-Bonnet. 2010. Viral reorganization of the secretory pathway generates distinct organelles for RNA replication. *Cell*. 141:799-811.

Huang, H., F. Sun, D.M. Owen, W. Li, Y. Chen, M. Gale, Jr., and J. Ye. 2007. Hepatitis C virus production by human hepatocytes dependent on assembly and secretion of very low-density lipoproteins. *Proc Natl Acad Sci U S A*. 104:5848-5853.

Huang, Y.P., S.L. Zhang, J. Cheng, L. Wang, J. Guo, Y. Liu, Y. Yang, L.Y. Zhang, G.Q. Bai, X.S. Gao, D. Ji, S.M. Lin, Y.W. Zhong, and Q. Shao. 2005. Screening of genes of proteins interacting with p7 protein of hepatitis C virus from human liver cDNA library by yeast two-hybrid system. *World J. Gastroenterol*. 11:4709-4714.

Huangfu, W.C., J. Qian, C. Liu, J. Liu, A.E. Lokshin, D.P. Baker, H. Rui, and S.Y. Fuchs. 2012. Inflammatory signaling compromises cell responses to interferon alpha. *Oncogene*. 31:161-172.

Hutten, S., A. Flotho, F. Melchior, and R. Kehlenbach. 2008. The Nup358-RanGAP complex is required for efficient importin alpha/beta-dependent nuclear import. *Mol Biol Cell*. 19:2300-2310.

Hutten, S., S. Wälde, C. Spillner, J. Hauber, and R. Kehlenbach. 2009. The nuclear pore component Nup358 promotes transportin-dependent nuclear import. *J Cell Sci.* 122:1100-1110.

Ide, Y., L. Zhang, M. Chen, G. Inchauspe, C. Bahl, Y. Sasaguri, and R. Padmanabhan. 1996. Characterization of the nuclear localization signal and subcellular distribution of hepatitis C virus nonstructural protein NS5A. *Gene.* 182:203-211.

Imamoto, N., T. Shimamoto, S. Kose, T. Takao, T. Tachibana, M. Matsubae, T. Sekimoto, Y. Shimonishi, and Y. Yoneda. 1995. The nuclear pore-targeting complex binds to nuclear pores after association with a karyophile. *FEBS Lett.* 368:415-419.

Iouk, T., O. Kerscher, R.J. Scott, M.A. Basrai, and R.W. Wozniak. 2002. The yeast nuclear pore complex functionally interacts with components of the spindle assembly checkpoint. *J Cell Biol.* 159:807-819.

Isaacs, A., and J. Lindenmann. 1957. Virus interference. I. The interferon. *Proceedings of the Royal Society of London. Series B, Containing papers of a Biological character. Royal Society.* 147:258-267.

Isken, O., M. Baroth, C.W. Grassmann, S. Weinlich, D.H. Ostareck, A. Ostareck-Lederer, and S.E. Behrens. 2007. Nuclear factors are involved in hepatitis C virus RNA replication. *Rna.* 13:1675-1692.

Isoyama, T., S. Kuge, and A. Nomoto. 2002. The core protein of hepatitis C virus is imported into the nucleus by transport receptor Kap123p but inhibits Kap121p-dependent nuclear import of yeast AP1-like transcription factor in yeast cells. *J Biol Chem.* 277:39634-39641.

Ivashkiv, L.B., and L.T. Donlin. 2014. Regulation of type I interferon responses. *Nat Rev Immunol.* 14:36-49.

Iwamoto, M., H. Asakawa, Y. Hiraoka, and T. Haraguchi. 2010. Nucleoporin Nup98: a gatekeeper in the eukaryotic kingdoms. *Genes to cells : devoted to molecular & cellular mechanisms.* 15:661-669.

Janeway, C.A., Jr. 1989. Approaching the asymptote? Evolution and revolution in immunology. *Cold Spring Harb Symp Quant Biol.* 54 Pt 1:1-13.

Janeway, C.A., Jr., and R. Medzhitov. 2002. Innate immune recognition. *Annu Rev Immunol.* 20:197-216.

Jayappa, K.D., Z. Ao, and X. Yao. 2012. The HIV-1 passage from cytoplasm to nucleus: the process involving a complex exchange between the components of HIV-1 and cellular machinery to access nucleus and successful integration. *International journal of biochemistry and molecular biology.* 3:70-85.

Jiang, F., A. Ramanathan, M.T. Miller, G.Q. Tang, M. Gale, Jr., S.S. Patel, and J. Marcotrigiano. 2011. Structural basis of RNA recognition and activation by innate immune receptor RIG-I. *Nature.* 479:423-427.

Jiang, J., and G. Luo. 2009. Apolipoprotein E but not B is required for the formation of infectious hepatitis C virus particles. *J Virol.* 83:12680-12691.

Jirasko, V., R. Montserret, J.Y. Lee, J. Gouttenoire, D. Moradpour, F. Penin, and R. Bartenschlager. 2010a. Structural and functional studies of nonstructural protein 2 of the hepatitis C virus reveal its key role as organizer of virion assembly. *PLoS pathogens.* 6:e1001233.

Jirasko, V., R. Montserret, J.Y. Lee, J. Gouttenoire, D. Moradpour, F. Penin, and R. Bartenschlager. 2010b. Structural and functional studies of nonstructural protein 2 of the hepatitis C virus reveal its key role as organizer of virion assembly. *PLoS Pathog.* 6:e1001233.

Jopling, C.L., M. Yi, A.M. Lancaster, S.M. Lemon, and P. Sarnow. 2005. Modulation of hepatitis C virus RNA abundance by a liver-specific MicroRNA. *Science.* 309:1577-1581.

Joseph, J., S.T. Liu, S.A. Jablonski, T.J. Yen, and M. Dasso. 2004. The RanGAP1-RanBP2 complex is essential for microtubule-kinetochore interactions in vivo. *Curr. Biol.* 14:611-617.

Joseph, J., S.H. Tan, T.S. Karpova, J.G. McNally, and M. Dasso. 2002. SUMO-1 targets RanGAP1 to kinetochores and mitotic spindles. *J Cell Biol.* 156:595-602.

Joyce, M., and D. Tyrrell. 2010. The cell biology of hepatitis C virus. *Microbes Infect.* 12:263-271.

Joyce, M., K. Walters, S. Lamb, M. Yeh, L. Zhu, N. Kneteman, J. Doyle, M. Katze, and D. Tyrrell. 2009. HCV induces oxidative and ER stress, and sensitizes infected cells to apoptosis in SCID/Alb-uPA mice. *PLoS Pathog.* 5:e1000291.

Kalderon, D., B.L. Roberts, W.D. Richardson, and A.E. Smith. 1984. A short amino acid sequence able to specify nuclear location. *Cell.* 39:499-509.

Karin, M., and Y. Ben-Neriah. 2000. Phosphorylation meets ubiquitination: the control of NF-[kappa]B activity. *Annu Rev Immunol.* 18:621-663.

Kassube, S.A., T. Stuwe, D.H. Lin, C.D. Antonuk, J. Napetschnig, G. Blobel, and A. Hoelz. 2012. Crystal structure of the N-terminal domain of Nup358/RanBP2. *J Mol Biol.* 423:752-765.

Katahira, J., K. Strasser, A. Podtelejnikov, M. Mann, J.U. Jung, and E. Hurt. 1999. The Mex67p-mediated nuclear mRNA export pathway is conserved from yeast to human. *Embo J.* 18:2593-2609.

Kato, H., O. Takeuchi, S. Sato, M. Yoneyama, M. Yamamoto, K. Matsui, S. Uematsu, A. Jung, T. Kawai, K.J. Ishii, O. Yamaguchi, K. Otsu, T. Tsujimura, C.S. Koh, C. Reis e Sousa, Y. Matsuura, T. Fujita, and S. Akira. 2006. Differential roles of MDA5 and RIG-I helicases in the recognition of RNA viruses. *Nature.* 441:101-105.

Kaul, A., S. Stauffer, C. Berger, T. Pertel, J. Schmitt, S. Kallis, M. Zayas, V. Lohmann, J. Luban, and R. Bartenschlager. 2009. Essential role of cyclophilin A for hepatitis C virus replication and virus production and possible link to polyprotein cleavage kinetics. *PLoS pathogens*. 5:e1000546.

Ke, P.Y., and S.S. Chen. 2011. Activation of the unfolded protein response and autophagy after hepatitis C virus infection suppresses innate antiviral immunity in vitro. *J Clin Invest*. 121:37-56.

Kee, H.L., J.F. Dishinger, T. Lynne Blasius, C.J. Liu, B. Margolis, and K.J. Verhey. 2012. A size-exclusion permeability barrier and nucleoporins characterize a ciliary pore complex that regulates transport into cilia. *Nat. Cell Biol.* 14:431-437.

Keminer, O., and R. Peters. 1999. Permeability of single nuclear pores. *Biophys J*. 77:217-228.

Kessel, R.G. 1983. The structure and function of annulate lamellae: porous cytoplasmic and intranuclear membranes. *Int Rev Cytol.* 82:181-303.

Kim, E., J. Park, and S. Um. 2008. Ubc9-mediated sumoylation leads to transcriptional repression of IRF-1. *Biochem Biophys Res Commun*. 377:952-956.

Kim, J.E., W.K. Song, K.M. Chung, S.H. Back, and S.K. Jang. 1999. Subcellular localization of hepatitis C viral proteins in mammalian cells. *Arch Virol.* 144:329-343.

Kim, K.S., and E.S. Boatman. 1967. Electron microscopy of monkey kidney cell cultures infected with rubella virus. *J. Virol.* 1:205-214.

Kim, S., C. Welsch, M. Yi, and S.M. Lemon. 2011. Regulation of the production of infectious genotype 1a hepatitis C virus by NS5A domain III. *J Virol.* 85:6645-6656.

Kirsh, O., J.S. Seeler, A. Pichler, A. Gast, S. Muller, E. Miska, M. Mathieu, A. Harel-Bellan, T. Kouzarides, F. Melchior, and A. Dejean. 2002. The SUMO E3 ligase RanBP2 promotes modification of the HDAC4 deacetylase. *Embo J*. 21:2682-2691.

Knoops, K., M. Barcena, R.W. Limpens, A.J. Koster, A.M. Mommaas, and E.J. Snijder. 2012. Ultrastructural characterization of arterivirus replication structures: reshaping the endoplasmic reticulum to accommodate viral RNA synthesis. *J Virol.* 86:2474-2487.

Knoops, K., M. Kikkert, S.H. Worm, J.C. Zevenhoven-Dobbe, Y. van der Meer, A.J. Koster, A.M. Mommaas, and E.J. Snijder. 2008. SARS-coronavirus replication is supported by a reticulovesicular network of modified endoplasmic reticulum. *PLoS Biol.* 6:e226.

Kohli, A., A. Shaffer, A. Sherman, and S. Kottilil. 2014. Treatment of hepatitis C: a systematic review. *JAMA*. 312:631-640.

Konig, R., Y. Zhou, D. Elleder, T.L. Diamond, G.M. Bonamy, J.T. Irelan, C.Y. Chiang, B.P. Tu, P.D. De Jesus, C.E. Lilley, S. Seidel, A.M. Opaluch, J.S. Caldwell, M.D. Weitzman, K.L. Kuhen, S. Bandyopadhyay, T. Ideker, A.P. Orth, L.J. Miraglia, F.D. Bushman, J.A.

Young, and S.K. Chanda. 2008. Global analysis of host-pathogen interactions that regulate early-stage HIV-1 replication. *Cell*. 135:49-60.

Kopecky-Bromberg, S.A., L. Martinez-Sobrido, M. Frieman, R.A. Baric, and P. Palese. 2007. Severe acute respiratory syndrome coronavirus open reading frame (ORF) 3b, ORF 6, and nucleocapsid proteins function as interferon antagonists. *J Virol*. 81:548-557.

Kopek, B.G., G. Perkins, D.J. Miller, M.H. Ellisman, and P. Ahlquist. 2007. Three-dimensional analysis of a viral RNA replication complex reveals a virus-induced mini-organelle. *PLoS Biol*. 5:e220.

Kotenko, S.V., G. Gallagher, V.V. Baurin, A. Lewis-Antes, M. Shen, N.K. Shah, J.A. Langer, F. Sheikh, H. Dickensheets, and R.P. Donnelly. 2003. IFN-lambdas mediate antiviral protection through a distinct class II cytokine receptor complex. *Nature immunology*. 4:69-77.

Kowalinski, E., T. Lunardi, A.A. McCarthy, J. Louber, J. Brunel, B. Grigorov, D. Gerlier, and S. Cusack. 2011. Structural basis for the activation of innate immune pattern-recognition receptor RIG-I by viral RNA. *Cell*. 147:423-435.

Krull, S., J. Dorries, B. Boysen, S. Reidenbach, L. Magnius, H. Norder, J. Thyberg, and V.C. Cordes. 2010. Protein Tpr is required for establishing nuclear pore-associated zones of heterochromatin exclusion. *Embo J*. 29:1659-1673.

Kubota, T., M. Matsuoka, T. Chang, P. Tailor, T. Sasaki, M. Tashiro, A. Kato, and K. Ozato. 2008. Virus infection triggers SUMOylation of IRF3 and IRF7, leading to the negative regulation of type I interferon gene expression. *J Biol Chem*. 283:25660-25670.

Kujala, P., A. Ikaheimonen, N. Ehsani, H. Vihinen, P. Auvinen, and L. Kaariainen. 2001. Biogenesis of the Semliki Forest virus RNA replication complex. *J Virol*. 75:3873-3884.

Kushima, Y., T. Wakita, and M. Hijikata. 2010. A disulfide-bonded dimer of the core protein of hepatitis C virus is important for virus-like particle production. *J Virol*. 84:9118-9127.

Lanford, R.E., B. Guerra, H. Lee, D. Chavez, K.M. Brasky, and C.B. Bigger. 2006. Genomic response to interferon-alpha in chimpanzees: implications of rapid downregulation for hepatitis C kinetics. *Hepatology*. 43:961-972.

Lavillette, D., E.I. Pecheur, P. Donot, J. Fresquet, J. Molle, R. Corbau, M. Dreux, F. Penin, and F.L. Cosset. 2007. Characterization of fusion determinants points to the involvement of three discrete regions of both E1 and E2 glycoproteins in the membrane fusion process of hepatitis C virus. *J Virol*. 81:8752-8765.

Le Sage, V., and A.J. Mouland. 2013. Viral subversion of the nuclear pore complex. *Viruses*. 5:2019-2042.

Lee, J.W., P.C. Liao, K.C. Young, C.L. Chang, S.S. Chen, T.T. Chang, M.D. Lai, and S.W. Wang. 2011a. Identification of hnRNPH1, NF45, and C14orf166 as novel host interacting partners of the mature hepatitis C virus core protein. *J Proteome Res*. 10:4522-4534.

Lee, K., Z. Ambrose, T.D. Martin, I. Oztop, A. Mulky, J.G. Julias, N. Vandegraaff, J.G. Baumann, R. Wang, W. Yuen, T. Takemura, K. Shelton, I. Taniuchi, Y. Li, J. Sodroski, D.R. Littman, J.M. Coffin, S.H. Hughes, D. Unutmaz, A. Engelman, and V.N. KewalRamani. 2010. Flexible use of nuclear import pathways by HIV-1. *Cell Host Microbe*. 7:221-233.

Lee, K., N. Kunkeaw, S.H. Jeon, I. Lee, B.H. Johnson, G.Y. Kang, J.Y. Bang, H.S. Park, C. Leelayuwat, and Y.S. Lee. 2011b. Precursor miR-886, a novel noncoding RNA repressed in cancer, associates with PKR and modulates its activity. *RNA*. 17:1076-1089.

Levin, A., Z. Hayouka, A. Friedler, and A. Loyter. 2010a. Transportin 3 and importin alpha are required for effective nuclear import of HIV-1 integrase in virus-infected cells. *Nucleus*. 1:422-431.

Levin, A., Z. Hayouka, M. Helfer, R. Brack-Werner, A. Friedler, and A. Loyter. 2009. Peptides derived from HIV-1 integrase that bind Rev stimulate viral genome integration. *PLoS One*. 4:e4155.

Levin, A., C.J. Neufeldt, D. Pang, K. Wilson, D. Loewen-Dobler, M.A. Joyce, R.W. Wozniak, and D.L. Tyrrell. 2014. Functional characterization of nuclear localization and export signals in hepatitis C virus proteins and their role in the membranous web. *PLoS One*. 9:e114629.

Levin, A., J. Rosenbluh, Z. Hayouka, A. Friedler, and A. Loyter. 2010b. Integration of HIV-1 DNA is regulated by interplay between viral rev and cellular LEDGF/p75 proteins. *Mol Med*. 16:34-44.

Lewin, T.M., C.G. Van Horn, S.K. Krisans, and R.A. Coleman. 2002. Rat liver acyl-CoA synthetase 4 is a peripheral-membrane protein located in two distinct subcellular organelles, peroxisomes, and mitochondrial-associated membrane. *Arch Biochem Biophys*. 404:263-270.

Li, H., X. Yang, G. Yang, Z. Hong, L. Zhou, P. Yin, Y. Xiao, L. Chen, R.T. Chung, and L. Zhang. 2014. Hepatitis C virus NS5A hijacks ARFGAP1 to maintain a phosphatidylinositol 4-phosphate-enriched microenvironment. *J Virol*. 88:5956-5966.

Li, Q., A.L. Brass, A. Ng, Z. Hu, R.J. Xavier, T.J. Liang, and S.J. Elledge. 2009. A genome-wide genetic screen for host factors required for hepatitis C virus propagation. *Proc Natl Acad Sci U S A*. 106:16410-16415.

Li, Q., and I.M. Verma. 2002. NF-kappaB regulation in the immune system. *Nat Rev Immunol*. 2:725-734.

Lim, R.Y., B. Fahrenkrog, J. Koser, K. Schwarz-Herion, J. Deng, and U. Aebi. 2007. Nanomechanical basis of selective gating by the nuclear pore complex. *Science*. 318:640-643.

Lim, R.Y., N.P. Huang, J. Koser, J. Deng, K.H. Lau, K. Schwarz-Herion, B. Fahrenkrog, and U. Aebi. 2006. Flexible phenylalanine-glycine nucleoporins as entropic barriers to nucleocytoplasmic transport. *Proc Natl Acad Sci U S A*. 103:9512-9517.

Limpens, R.W., H.M. van der Schaar, D. Kumar, A.J. Koster, E.J. Snijder, F.J. van Kuppeveld, and M. Barcena. 2011. The transformation of enterovirus replication structures: a three-dimensional study of single- and double-membrane compartments. *mBio*. 2.

Lin, D.H., S. Zimmermann, T. Stuwe, E. Stuwe, and A. Hoelz. 2013. Structural and functional analysis of the C-terminal domain of Nup358/RanBP2. *Journal of molecular biology*. 425:1318-1329.

Lin, R., C. Heylbroeck, P.M. Pitha, and J. Hiscott. 1998. Virus-dependent phosphorylation of the IRF-3 transcription factor regulates nuclear translocation, transactivation potential, and proteasome-mediated degradation. *Mol Cell Biol*. 18:2986-2996.

Lin, W., S.S. Kim, E. Yeung, Y. Kamegaya, J.T. Blackard, K.A. Kim, M.J. Holtzman, and R.T. Chung. 2006. Hepatitis C virus core protein blocks interferon signaling by interaction with the STAT1 SH2 domain. *J Virol*. 80:9226-9235.

Lindenbach, B.D., M.J. Evans, A.J. Syder, B. Wolk, T.L. Tellinghuisen, C.C. Liu, T. Maruyama, R.O. Hynes, D.R. Burton, J.A. McKeating, and C.M. Rice. 2005. Complete replication of hepatitis C virus in cell culture. *Science*. 309:623-626.

Lindenbach, B.D., and C.M. Rice. 2013. The ins and outs of hepatitis C virus entry and assembly. *Nature reviews. Microbiology*. 11:688-700.

Liu, B., S. Mink, K.A. Wong, N. Stein, C. Getman, P.W. Dempsey, H. Wu, and K. Shuai. 2004. PIAS1 selectively inhibits interferon-inducible genes and is important in innate immunity. *Nature immunology*. 5:891-898.

Liu, H.M., and M. Gale. 2010. Hepatitis C Virus Evasion from RIG-I-Dependent Hepatic Innate Immunity. *Gastroenterology research and practice*. 2010:548390.

Liu, J., W.C. HuangFu, K.G. Kumar, J. Qian, J.P. Casey, R.B. Hamanaka, C. Grigoriadou, R. Aldabe, J.A. Diehl, and S.Y. Fuchs. 2009. Virus-induced unfolded protein response attenuates antiviral defenses via phosphorylation-dependent degradation of the type I interferon receptor. *Cell Host Microbe*. 5:72-83.

Liu, J., A.J. Prunuske, A.M. Fager, and K.S. Ullman. 2003. The COPI complex functions in nuclear envelope breakdown and is recruited by the nucleoporin Nup153. *Dev. cell*. 5:487-498.

Lohmann, V., F. Korner, J. Koch, U. Herian, L. Theilmann, and R. Bartenschlager. 1999. Replication of subgenomic hepatitis C virus RNAs in a hepatoma cell line. *Science*. 285:110-113.

Loiodice, I., A. Alves, G. Rabut, M. Van Overbeek, J. Ellenberg, J.B. Sibarita, and V. Doye. 2004. The entire Nup107-160 complex, including three new members, is targeted as one entity to kinetochores in mitosis. *Mol Biol Cell*. 15:3333-3344.

Long, G., M.S. Hiet, M.P. Windisch, J.Y. Lee, V. Lohmann, and R. Bartenschlager. 2011. Mouse hepatic cells support assembly of infectious hepatitis C virus particles. *Gastroenterology*. 141:1057-1066.

Lu, L.F., M.P. Boldin, A. Chaudhry, L.L. Lin, K.D. Taganov, T. Hanada, A. Yoshimura, D. Baltimore, and A.Y. Rudensky. 2010. Function of miR-146a in controlling Treg cell-mediated regulation of Th1 responses. *Cell*. 142:914-929.

Lund, J., L. Alexopoulou, A. Sato, M. Karow, N. Adams, N. Gale, A. Iwasaki, and R. Flavell. 2004. Recognition of single-stranded RNA viruses by Toll-like receptor 7. *Proc Natl Acad Sci U S A*. 101:5598-5603.

Lupberger, J., M.B. Zeisel, F. Xiao, C. Thumann, I. Fofana, L. Zona, C. Davis, C.J. Mee, M. Turek, S. Gorke, C. Royer, B. Fischer, M.N. Zahid, D. Lavillette, J. Fresquet, F.L. Cosset, S.M. Rothenberg, T. Pietschmann, A.H. Patel, P. Pessaux, M. Doffoel, W. Raffelsberger, O. Poch, J.A. McKeating, L. Brino, and T.F. Baumert. 2011. EGFR and EphA2 are host factors for hepatitis C virus entry and possible targets for antiviral therapy. *Nat Med*. 17:589-595.

Lutzmann, M., R. Kunze, A. Buerer, U. Aebi, and E. Hurt. 2002. Modular self-assembly of a Y-shaped multiprotein complex from seven nucleoporins. *Embo J*. 21:387-397.

Ma, Z., D.A. Hill, M.H. Collins, S.W. Morris, J. Sumegi, M. Zhou, C. Zuppan, and J.A. Bridge. 2003. Fusion of ALK to the Ran-binding protein 2 (RANBP2) gene in inflammatory myofibroblastic tumor. *Genes Chromosomes Cancer*. 37:98-105.

Mabb, A.M., and S. Miyamoto. 2007. SUMO and NF-kappaB ties. *Cellular and molecular life sciences : CMLS*. 64:1979-1996.

Madrid, A.S., J. Mancuso, W.Z. Cande, and K. Weis. 2006. The role of the integral membrane nucleoporins Ndc1p and Pom152p in nuclear pore complex assembly and function. *J Cell Biol*. 173:361-371.

Mahadevan, K., H. Zhang, A. Akef, X.A. Cui, S. Gueroussov, C. Cenik, F.P. Roth, and A.F. Palazzo. 2013. RanBP2/Nup358 potentiates the translation of a subset of mRNAs encoding secretory proteins. *PLoS biology*. 11:e1001545.

Mahajan, R., C. Delphin, T. Guan, L. Gerace, and F. Melchior. 1997. A small ubiquitin-related polypeptide involved in targeting RanGAP1 to nuclear pore complex protein RanBP2. *Cell*. 88:97-107.

Makhnevych, T., C. Lusk, A. Anderson, J. Aitchison, and R. Wozniak. 2003. Cell cycle regulated transport controlled by alterations in the nuclear pore complex. *Cell*. 115:813-823.

Mamiya, N., and H.J. Worman. 1999. Hepatitis C virus core protein binds to a DEAD box RNA helicase. *J Biol Chem*. 274:15751-15756.

Manders, E.M., J. Stap, G.J. Brakenhoff, R. van Driel, and J.A. Aten. 1992. Dynamics of three-dimensional replication patterns during the S-phase, analysed by double labelling of DNA and confocal microscopy. *Journal of cell science*. 103 (Pt 3):857-862.

Manders, E.M.M., F.J. Verbeek, and J.A. Aten. 1993. Measurement of Colocalization of Objects in Dual-Color Confocal Images. *J Microsc-Oxford*. 169:375-382.

Manns, M.P., J.G. McHutchison, S.C. Gordon, V.K. Rustgi, M. Shiffman, R. Reindollar, Z.D. Goodman, K. Koury, M. Ling, and J.K. Albrecht. 2001. Peginterferon alfa-2b plus ribavirin compared with interferon alfa-2b plus ribavirin for initial treatment of chronic hepatitis C: a randomised trial. *Lancet*. 358:958-965.

Mans, B.J., V. Anantharaman, L. Aravind, and E.V. Koonin. 2004. Comparative genomics, evolution and origins of the nuclear envelope and nuclear pore complex. *Cell cycle*. 3:1612-1637.

Mansfeld, J., S. Güttinger, L. Hawryluk-Gara, N. Panté, M. Mall, V. Galy, U. Haselmann, P. Mühlhäusser, R. Wozniak, I. Mattaj, U. Kutay, and W. Antonin. 2006a. The conserved transmembrane nucleoporin NDC1 is required for nuclear pore complex assembly in vertebrate cells. *Mol Cell*. 22:93-103.

Mansfeld, J., S. Guttinger, L.A. Hawryluk-Gara, N. Pante, M. Mall, V. Galy, U. Haselmann, P. Muhlhausser, R.W. Wozniak, I.W. Mattaj, U. Kutay, and W. Antonin. 2006b. The conserved transmembrane nucleoporin NDC1 is required for nuclear pore complex assembly in vertebrate cells. *Molecular cell*. 22:93-103.

Mansfeld, J., S. Guttinger, L.A. Hawryluk-Gara, N. Pante, M. Mall, V. Galy, U. Haselmann, P. Muhlhausser, R.W. Wozniak, I.W. Mattaj, U. Kutay, and W. Antonin. 2006c. The conserved transmembrane nucleoporin NDC1 is required for nuclear pore complex assembly in vertebrate cells. *Mol Cell*. 22:93-103.

Maraldi, N.M., G. Lattanzi, C. Capanni, M. Columbaro, E. Mattioli, P. Sabatelli, S. Squarzoni, and F.A. Manzoli. 2006. Laminopathies: a chromatin affair. *Advances in enzyme regulation*. 46:33-49.

Marelli, M., C.P. Lusk, H. Chan, J.D. Aitchison, and R.W. Wozniak. 2001. A link between the synthesis of nucleoporins and the biogenesis of the nuclear envelope. *J Cell Biol*. 153:709-724.

Marshall, J.A., J. Borg, A.G. Coulepis, and D.A. Anderson. 1996. Annulate lamellae and lytic HAV infection in vitro. *Tissue Cell*. 28:205-214.

Martin, D.N., and S.L. Uprichard. 2013. Identification of transferrin receptor 1 as a hepatitis C virus entry factor. *Proc Natl Acad Sci U S A*. 110:10777-10782.

Masaki, T., R. Suzuki, K. Murakami, H. Aizaki, K. Ishii, A. Murayama, T. Date, Y. Matsuura, T. Miyamura, T. Wakita, and T. Suzuki. 2008. Interaction of hepatitis C virus nonstructural protein 5A with core protein is critical for the production of infectious virus particles. *J Virol.* 82:7964-7976.

Mateo, M., S.P. Reid, L.W. Leung, C.F. Basler, and V.E. Volchkov. 2010. Ebolavirus VP24 binding to karyopherins is required for inhibition of interferon signaling. *J Virol.* 84:1169-1175.

Matreyek, K.A., and A. Engelman. 2011. The requirement for nucleoporin NUP153 during human immunodeficiency virus type 1 infection is determined by the viral capsid. *J Virol.* 85:7818-7827.

Matsumoto, M., S.B. Hwang, K.S. Jeng, N. Zhu, and M.M. Lai. 1996. Homotypic interaction and multimerization of hepatitis C virus core protein. *Virology.* 218:43-51.

Matunis, M.J., E. Coutavas, and G. Blobel. 1996. A novel ubiquitin-like modification modulates the partitioning of the Ran-GTPase-activating protein RanGAP1 between the cytosol and the nuclear pore complex. *J Cell Biol.* 135:1457-1470.

Matunis, M.J., J. Wu, and G. Blobel. 1998. SUMO-1 modification and its role in targeting the Ran GTPase-activating protein, RanGAP1, to the nuclear pore complex. *J Cell Biol.* 140:499-509.

McHutchison, J.G., S.C. Gordon, E.R. Schiff, M.L. Shiffman, W.M. Lee, V.K. Rustgi, Z.D. Goodman, M.H. Ling, S. Cort, and J.K. Albrecht. 1998. Interferon alfa-2b alone or in combination with ribavirin as initial treatment for chronic hepatitis C. Hepatitis Interventional Therapy Group. *N Engl J Med.* 339:1485-1492.

Meehan, A.M., D.T. Saenz, R. Guevera, J.H. Morrison, M. Peretz, H.J. Fadel, M. Hamada, J. van Deursen, and E.M. Poeschla. 2014. A cyclophilin homology domain-independent role for Nup358 in HIV-1 infection. *PLoS Pathog.* 10:e1003969.

Melcak, I., A. Hoelz, and G. Blobel. 2007. Structure of Nup58/45 suggests flexible nuclear pore diameter by intermolecular sliding. *Science.* 315:1729-1732.

Melen, K., R. Fagerlund, M. Nyqvist, P. Keskinen, and I. Julkunen. 2004. Expression of hepatitis C virus core protein inhibits interferon-induced nuclear import of STATs. *J Med Virol.* 73:536-547.

Menzel, N., W. Fischl, K. Hueging, D. Bankwitz, A. Frentzen, S. Haid, J. Gentzsch, L. Kaderali, R. Bartenschlager, and T. Pietschmann. 2012. MAP-kinase regulated cytosolic phospholipase A2 activity is essential for production of infectious hepatitis C virus particles. *PLoS Pathog.* 8:e1002829.

Merisko, E.M. 1989. Annulate lamellae: an organelle in search of a function. *Tissue Cell.* 21:343-354.

Merz, A., G. Long, M.S. Hiet, B. Brugger, P. Chlanda, P. Andre, F. Wieland, J. Krijnse-Locker, and R. Bartenschlager. 2011. Biochemical and morphological properties of hepatitis C virus particles and determination of their lipidome. *The Journal of biological chemistry*. 286:3018-3032.

Metz, P., E. Dazert, A. Ruggieri, J. Mazur, L. Kaderali, A. Kaul, U. Zeuge, M.P. Windisch, M. Trippler, V. Lohmann, M. Binder, M. Frese, and R. Bartenschlager. 2012. Identification of type I and type II interferon-induced effectors controlling hepatitis C virus replication. *Hepatology*. 56:2082-2093.

Meuleman, P., J. Hesselgesser, M. Paulson, T. Vanwolleghem, I. Desombere, H. Reiser, and G. Leroux-Roels. 2008. Anti-CD81 antibodies can prevent a hepatitis C virus infection in vivo. *Hepatology*. 48:1761-1768.

Meylan, E., J. Curran, K. Hofmann, D. Moradpour, M. Binder, R. Bartenschlager, and J. Tschopp. 2005. Cardif is an adaptor protein in the RIG-I antiviral pathway and is targeted by hepatitis C virus. *Nature*. 437:1167-1172.

Mitchell, J.M., J. Mansfeld, J. Capitanio, U. Kutay, and R.W. Wozniak. 2010. Pom121 links two essential subcomplexes of the nuclear pore complex core to the membrane. *J. Cell Biol.* 191:505-521.

Miyamoto, H., H. Okamoto, K. Sato, T. Tanaka, and S. Mishiro. 1992. Extraordinarily low density of hepatitis C virus estimated by sucrose density gradient centrifugation and the polymerase chain reaction. *J Gen Virol.* 73 (Pt 3):715-718.

Miyanari, Y., K. Atsuzawa, N. Usuda, K. Watashi, T. Hishiki, M. Zayas, R. Bartenschlager, T. Wakita, M. Hijikata, and K. Shimotohno. 2007. The lipid droplet is an important organelle for hepatitis C virus production. *Nat Cell Biol.* 9:1089-1097.

Miyanari, Y., M. Hijikata, M. Yamaji, M. Hosaka, H. Takahashi, and K. Shimotohno. 2003. Hepatitis C virus non-structural proteins in the probable membranous compartment function in viral genome replication. *J. Biol. Chem.* 278:50301-50308.

Molina, S., V. Castet, C. Fournier-Wirth, L. Pichard-Garcia, R. Avner, D. Harats, J. Roitelman, R. Barbaras, P. Graber, P. Ghersa, M. Smolarsky, A. Funaro, F. Malavasi, D. Larrey, J. Coste, J.M. Fabre, A. Sa-Cunha, and P. Maurel. 2007. The low-density lipoprotein receptor plays a role in the infection of primary human hepatocytes by hepatitis C virus. *J Hepatol.* 46:411-419.

Monette, A., N. Pante, and A.J. Mouland. 2011. HIV-1 remodels the nuclear pore complex. *J Cell Biol.* 193:619-631.

Montpetit, B., N.D. Thomsen, K.J. Helmke, M.A. Seeliger, J.M. Berger, and K. Weis. 2011. A conserved mechanism of DEAD-box ATPase activation by nucleoporins and InsP6 in mRNA export. *Nature*. 472:238-242.

Moore, M.S., and G. Blobel. 1992. The two steps of nuclear import, targeting to the nuclear envelope and translocation through the nuclear pore, require different cytosolic factors. *Cell.* 69:939-950.

Moore, M.S., and G. Blobel. 1993. The GTP-binding protein Ran/TC4 is required for protein import into the nucleus. *Nature.* 365:661-663.

Moradpour, D., C. Englert, T. Wakita, and J.R. Wands. 1996. Characterization of cell lines allowing tightly regulated expression of hepatitis C virus core protein. *Virology.* 222:51-63.

Moriya, K., H. Yotsuyanagi, Y. Shintani, H. Fujie, K. Ishibashi, Y. Matsuura, T. Miyamura, and K. Koike. 1997. Hepatitis C virus core protein induces hepatic steatosis in transgenic mice. *J Gen Virol.* 78 (Pt 7):1527-1531.

Mosmann, T. 1983. Rapid colorimetric assay for cellular growth and survival: application to proliferation and cytotoxicity assays. *J Immunol Methods.* 65:55-63.

Muir, A.J., M.L. Shiffman, A. Zaman, B. Yoffe, A. de la Torre, S. Flamm, S.C. Gordon, P. Marotta, J.M. Vierling, J.C. Lopez-Talavera, K. Byrnes-Blake, D. Fontana, J. Freeman, T. Gray, D. Hausman, N.N. Hunder, and E. Lawitz. 2010. Phase 1b study of pegylated interferon lambda 1 with or without ribavirin in patients with chronic genotype 1 hepatitis C virus infection. *Hepatology.* 52:822-832.

Muller, M., J. Briscoe, C. Laxton, D. Guschin, A. Ziemiecki, O. Silvennoinen, A.G. Harpur, G. Barbieri, B.A. Witthuhn, C. Schindler, and et al. 1993. The protein tyrosine kinase JAK1 complements defects in interferon-alpha/beta and -gamma signal transduction. *Nature.* 366:129-135.

Muller, U., U. Steinhoff, L.F. Reis, S. Hemmi, J. Pavlovic, R.M. Zinkernagel, and M. Aguet. 1994. Functional role of type I and type II interferons in antiviral defense. *Science.* 264:1918-1921.

Murray, P.J. 2007. The JAK-STAT signaling pathway: input and output integration. *J Immunol.* 178:2623-2629.

Nahmias, Y., J. Goldwasser, M. Casali, D. van Poll, T. Wakita, R.T. Chung, and M.L. Yarmush. 2008. Apolipoprotein B-dependent hepatitis C virus secretion is inhibited by the grapefruit flavonoid naringenin. *Hepatology.* 47:1437-1445.

Nakagawa, K., and H. Yokosawa. 2002. PIAS3 induces SUMO-1 modification and transcriptional repression of IRF-1. *FEBS Lett.* 530:204-208.

Nakai, K., T. Okamoto, T. Kimura-Someya, K. Ishii, C.K. Lim, H. Tani, E. Matsuo, T. Abe, Y. Mori, T. Suzuki, T. Miyamura, J.H. Nunberg, K. Moriishi, and Y. Matsuura. 2006. Oligomerization of hepatitis C virus core protein is crucial for interaction with the cytoplasmic domain of E1 envelope protein. *J Virol.* 80:11265-11273.

Napetschnig, J., S.A. Kassube, E.W. Debler, R.W. Wong, G. Blobel, and A. Hoelz. 2009. Structural and functional analysis of the interaction between the nucleoporin Nup214 and the DEAD-box helicase Ddx19. *Proc Natl Acad Sci U S A*. 106:3089-3094.

Neilson, D.E., M.D. Adams, C.M. Orr, D.K. Schelling, R.M. Eiben, D.S. Kerr, J. Anderson, A.G. Bassuk, A.M. Bye, A.M. Childs, A. Clarke, Y.J. Crow, M. Di Rocco, C. Dohna-Schwake, G. Dueckers, A.E. Fasano, A.D. Gika, D. Gionnis, M.P. Gorman, P.J. Grattan-Smith, A. Hackenberg, A. Kuster, M.G. Lentschig, E. Lopez-Laso, E.J. Marco, S. Mastroyianni, J. Perrier, T. Schmitt-Mechelke, S. Servidei, A. Skardoutsou, P. Uldall, M.S. van der Knaap, K.C. Goglin, D.L. Tefft, C. Aubin, P. de Jager, D. Hafler, and M.L. Warman. 2009. Infection-triggered familial or recurrent cases of acute necrotizing encephalopathy caused by mutations in a component of the nuclear pore, RANBP2. *American journal of human genetics*. 84:44-51.

Nemergut, M.E., C.A. Mizzen, T. Stukenberg, C.D. Allis, and I.G. Macara. 2001. Chromatin docking and exchange activity enhancement of RCC1 by histones H2A and H2B. *Science*. 292:1540-1543.

Neufeldt, C.J., M.A. Joyce, A. Levin, R.H. Steenbergen, D. Pang, J. Shields, D.L. Tyrrell, and R.W. Wozniak. 2013. Hepatitis C virus-induced cytoplasmic organelles use the nuclear transport machinery to establish an environment conducive to virus replication. *PLoS Pathog*. 9:e1003744.

Niepmann, M. 2009. Internal translation initiation of picornaviruses and hepatitis C virus. *Biochim Biophys Acta*. 1789:529-541.

Nieva, J.L., V. Madan, and L. Carrasco. 2012. Viroporins: structure and biological functions. *Nature reviews. Microbiology*. 10:563-574.

Nusinzon, I., and C.M. Horvath. 2003. Interferon-stimulated transcription and innate antiviral immunity require deacetylase activity and histone deacetylase 1. *Proc Natl Acad Sci U S A*. 100:14742-14747.

O'Neill, L.A., K.A. Fitzgerald, and A.G. Bowie. 2003. The Toll-IL-1 receptor adaptor family grows to five members. *Trends Immunol*. 24:286-290.

Ohtsubo, M., H. Okazaki, and T. Nishimoto. 1989. The RCC1 protein, a regulator for the onset of chromosome condensation locates in the nucleus and binds to DNA. *J Cell Biol*. 109:1389-1397.

Ojala, P.M., B. Sodeik, M.W. Ebersold, U. Kutay, and A. Helenius. 2000. Herpes simplex virus type 1 entry into host cells: reconstitution of capsid binding and uncoating at the nuclear pore complex in vitro. *Mol Cell Biol*. 20:4922-4931.

Olmstead, A.D., W. Knecht, I. Lazarov, S.B. Dixit, and F. Jean. 2012. Human subtilase SKI-1/S1P is a master regulator of the HCV Lifecycle and a potential host cell target for developing indirect-acting antiviral agents. *PLoS Pathog*. 8:e1002468.

Onischenko, E., L.H. Stanton, A.S. Madrid, T. Kieselbach, and K. Weis. 2009. Role of the Ndc1 interaction network in yeast nuclear pore complex assembly and maintenance. *J Cell Biol.* 185:475-491.

Op De Beeck, A., C. Voisset, B. Bartosch, Y. Ciczora, L. Cocquerel, Z. Keck, S. Foung, F.L. Cosset, and J. Dubuisson. 2004. Characterization of functional hepatitis C virus envelope glycoproteins. *J Virol.* 78:2994-3002.

Oshiumi, H., M. Matsumoto, K. Funami, T. Akazawa, and T. Seya. 2003. TICAM-1, an adaptor molecule that participates in Toll-like receptor 3-mediated interferon-beta induction. *Nature immunology*. 4:161-167.

OuYang, B., S. Xie, M.J. Berardi, X. Zhao, J. Dev, W. Yu, B. Sun, and J.J. Chou. 2013. Unusual architecture of the p7 channel from hepatitis C virus. *Nature*. 498:521-525.

Overby, A.K., V.L. Popov, M. Niedrig, and F. Weber. 2010. Tick-borne encephalitis virus delays interferon induction and hides its double-stranded RNA in intracellular membrane vesicles. *J Virol.* 84:8470-8483.

Overby, A.K., and F. Weber. 2011. Hiding from intracellular pattern recognition receptors, a passive strategy of flavivirus immune evasion. *Virulence*. 2:238-240.

Owen, D.M., H. Huang, J. Ye, and M. Gale, Jr. 2009. Apolipoprotein E on hepatitis C virion facilitates infection through interaction with low-density lipoprotein receptor. *Virology*.

Owsianka, A.M., and A.H. Patel. 1999. Hepatitis C virus core protein interacts with a human DEAD box protein DDX3. *Virology*. 257:330-340.

Palomares-Jerez, M.F., H. Nemesio, and J. Villalain. 2012. Interaction with membranes of the full C-terminal domain of protein NS4B from hepatitis C virus. *Biochim Biophys Acta.* 1818:2536-2549.

Pante, N., and M. Kann. 2002. Nuclear pore complex is able to transport macromolecules with diameters of about 39 nm. *Mol Biol Cell.* 13:425-434.

Papadopoulou, A.S., J. Dooley, M.A. Linterman, W. Pierson, O. Ucar, B. Kyewski, S. Zuklys, G.A. Hollander, P. Matthys, D.H. Gray, B. De Strooper, and A. Liston. 2012. The thymic epithelial microRNA network elevates the threshold for infection-associated thymic involution via miR-29a mediated suppression of the IFN-alpha receptor. *Nature immunology*. 13:181-187.

Park, J.H., S. Park, J.S. Yang, O.S. Kwon, S. Kim, and S.K. Jang. 2013. Discovery of cellular proteins required for the early steps of HCV infection using integrative genomics. *PLoS One*. 8:e60333.

Park, N., P. Katikaneni, T. Skern, and K.E. Gustin. 2008. Differential targeting of nuclear pore complex proteins in poliovirus-infected cells. *J Virol.* 82:1647-1655.

Park, N., T. Skern, and K.E. Gustin. 2010. Specific cleavage of the nuclear pore complex protein Nup62 by a viral protease. *J Biol Chem*. 285:28796-28805.

Pasdeloup, D., D. Blondel, A.L. Isidro, and F.J. Rixon. 2009. Herpesvirus capsid association with the nuclear pore complex and viral DNA release involve the nucleoporin CAN/Nup214 and the capsid protein pUL25. *J Virol*. 83:6610-6623.

Patel, S.S., B.J. Belmont, J.M. Sante, and M.F. Rexach. 2007. Natively unfolded nucleoporins gate protein diffusion across the nuclear pore complex. *Cell*. 129:83-96.

Paul, D., and R. Bartenschlager. 2013. Architecture and biogenesis of plus-strand RNA virus replication factories. *World journal of virology*. 2:32-48.

Paul, D., S. Hoppe, G. Saher, J. Krijnse-Locker, and R. Bartenschlager. 2013. Morphological and biochemical characterization of the membranous hepatitis C virus replication compartment. *J Virol*. 87:10612-10627.

Paul, D., I. Romero-Brey, J. Gouttenoire, S. Stoitsova, J. Krijnse-Locker, D. Moradpour, and R. Bartenschlager. 2011. NS4B self-interaction through conserved C-terminal elements is required for the establishment of functional hepatitis C virus replication complexes. *J. Virol*. 85:6963-6976.

Peisley, A., B. Wu, H. Xu, Z.J. Chen, and S. Hur. 2014. Structural basis for ubiquitin-mediated antiviral signal activation by RIG-I. *Nature*. 509:110-114.

Pemberton, L.F., and B.M. Paschal. 2005. Mechanisms of receptor-mediated nuclear import and nuclear export. *Traffic*. 6:187-198.

Pestka, S., S.V. Kotenko, G. Muthukumaran, L.S. Izotova, J.R. Cook, and G. Garotta. 1997. The interferon gamma (IFN-gamma) receptor: a paradigm for the multichain cytokine receptor. *Cytokine Growth Factor Rev*. 8:189-206.

Pflugheber, J., B. Fredericksen, R. Sumpter, Jr., C. Wang, F. Ware, D.L. Sodora, and M. Gale, Jr. 2002. Regulation of PKR and IRF-1 during hepatitis C virus RNA replication. *Proc Natl Acad Sci U S A*. 99:4650-4655.

Phan, T., A. Kohlway, P. Dimberu, A.M. Pyle, and B.D. Lindenbach. 2011. The acidic domain of hepatitis C virus NS4A contributes to RNA replication and virus particle assembly. *J Virol*. 85:1193-1204.

Pichler, A., A. Gast, J. Seeler, A. Dejean, and F. Melchior. 2002. The nucleoporin RanBP2 has SUMO1 E3 ligase activity. *Cell*. 108:109-120.

Pichler, A., P. Knipscheer, H. Saitoh, T.K. Sixma, and F. Melchior. 2004. The RanBP2 SUMO E3 ligase is neither HECT- nor RING-type. *Nature structural & molecular biology*. 11:984-991.

Pichlmair, A., O. Schulz, C.P. Tan, T.I. Naslund, P. Liljestrom, F. Weber, and C. Reis e Sousa. 2006. RIG-I-mediated antiviral responses to single-stranded RNA bearing 5'-phosphates. *Science*. 314:997-1001.

Pickersgill, H., B. Kalverda, E. de Wit, W. Talhout, M. Fornerod, and B. van Steensel. 2006. Characterization of the Drosophila melanogaster genome at the nuclear lamina. *Nature genetics*. 38:1005-1014.

Pietersz, G.A., W. Li, and V. Apostolopoulos. 2001. A 16-mer peptide (RQIKIWFQNRRMKWKK) from antennapedia preferentially targets the Class I pathway. *Vaccine*. 19:1397-1405.

Pietschmann, T., M. Zayas, P. Meuleman, G. Long, N. Appel, G. Koutsoudakis, S. Kallis, G. Leroux-Roels, V. Lohmann, and R. Bartenschlager. 2009. Production of infectious genotype 1b virus particles in cell culture and impairment by replication enhancing mutations. *PLoS pathogens*. 5:e1000475.

Pileri, P., Y. Uematsu, S. Campagnoli, G. Galli, F. Falugi, R. Petracca, A.J. Weiner, M. Houghton, D. Rosa, G. Grandi, and S. Abrignani. 1998. Binding of hepatitis C virus to CD81. *Science*. 282:938-941.

Pineiro, D., and E. Martinez-Salas. 2012. RNA structural elements of hepatitis C virus controlling viral RNA translation and the implications for viral pathogenesis. *Viruses*. 4:2233-2250.

Platanias, L.C. 2005. Mechanisms of type-I- and type-II-interferon-mediated signalling. *Nat Rev Immunol*. 5:375-386.

Ploss, A., M.J. Evans, V.A. Gaysinskaya, M. Panis, H. You, Y.P. de Jong, and C.M. Rice. 2009. Human occludin is a hepatitis C virus entry factor required for infection of mouse cells. *Nature*. 457:882-886.

Polyak, S.J., K.S. Khabar, D.M. Paschal, H.J. Ezelle, G. Duverlie, G.N. Barber, D.E. Levy, N. Mukaida, and D.R. Gretch. 2001a. Hepatitis C virus nonstructural 5A protein induces interleukin-8, leading to partial inhibition of the interferon-induced antiviral response. *J Virol*. 75:6095-6106.

Polyak, S.J., K.S. Khabar, M. Rezeiq, and D.R. Gretch. 2001b. Elevated levels of interleukin-8 in serum are associated with hepatitis C virus infection and resistance to interferon therapy. *J Virol*. 75:6209-6211.

Popescu, C.I., N. Callens, D. Trinel, P. Roingeard, D. Moradpour, V. Descamps, G. Duverlie, F. Penin, L. Heliot, Y. Rouille, and J. Dubuisson. 2011. NS2 protein of hepatitis C virus interacts with structural and non-structural proteins towards virus assembly. *PLoS Pathog*. 7:e1001278.

Porter, F.W., Y.A. Bochkov, A.J. Albee, C. Wiese, and A.C. Palmenberg. 2006. A picornavirus protein interacts with Ran-GTPase and disrupts nucleocytoplasmic transport. *Proc Natl Acad Sci U S A*. 103:12417-12422.

Porter, F.W., and A.C. Palmenberg. 2009. Leader-induced phosphorylation of nucleoporins correlates with nuclear trafficking inhibition by cardioviruses. *J Virol.* 83:1941-1951.

Poynard, T., P. Bedossa, M. Chevallier, P. Mathurin, C. Lemonnier, C. Trepo, P. Couzigou, J.L. Payen, M. Sajus, and J.M. Costa. 1995. A comparison of three interferon alfa-2b regimens for the long-term treatment of chronic non-A, non-B hepatitis. Multicenter Study Group. *N Engl J Med.* 332:1457-1462.

Prunuske, A., J. Liu, S. Elgort, J. Joseph, M. Dasso, and K. Ullman. 2006. Nuclear envelope breakdown is coordinated by both Nup358/RanBP2 and Nup153, two nucleoporins with zinc finger modules. *Mol Biol Cell.* 17:760-769.

Qiao, Y., E.G. Giannopoulou, C.H. Chan, S.H. Park, S. Gong, J. Chen, X. Hu, O. Elemento, and L.B. Ivashkiv. 2013. Synergistic activation of inflammatory cytokine genes by interferon-gamma-induced chromatin remodeling and toll-like receptor signaling. *Immunity.* 39:454-469.

Quan, B., H.S. Seo, G. Blobel, and Y. Ren. 2014. Vesiculoviral matrix (M) protein occupies nucleic acid binding site at nucleoporin pair (Rae1 * Nup98). *Proc Natl Acad Sci U S A.* 111:9127-9132.

Quinkert, D., R. Bartenschlager, and V. Lohmann. 2005. Quantitative analysis of the hepatitis C virus replication complex. *Journal of virology.* 79:13594-13605.

Rabl, C. 1885. Über Zelltheilung. *Morphol. Jahrb.* 10:214-300.

Radu, A., G. Blobel, and M.S. Moore. 1995a. Identification of a protein complex that is required for nuclear protein import and mediates docking of import substrate to distinct nucleoporins. *Proc Natl Acad Sci U S A.* 92:1769-1773.

Radu, A., M.S. Moore, and G. Blobel. 1995b. The peptide repeat domain of nucleoporin Nup98 functions as a docking site in transport across the nuclear pore complex. *Cell.* 81:215-222.

Ramos, E.L. 2010. Preclinical and clinical development of pegylated interferon-lambda 1 in chronic hepatitis C. *J Interferon Cytokine Res.* 30:591-595.

Reid, S.P., L.W. Leung, A.L. Hartman, O. Martinez, M.L. Shaw, C. Carbonnelle, V.E. Volchkov, S.T. Nichol, and C.F. Basler. 2006. Ebola virus VP24 binds karyopherin alpha1 and blocks STAT1 nuclear accumulation. *J Virol.* 80:5156-5167.

Reiss, S., I. Rebhan, P. Backes, I. Romero-Brey, H. Erfle, P. Matula, L. Kaderali, M. Poenisch, H. Blankenburg, M.S. Hiet, T. Longerich, S. Diehl, F. Ramirez, T. Balla, K. Rohr, A. Kaul, S. Buhler, R. Pepperkok, T. Lengauer, M. Albrecht, R. Eils, P. Schirmacher, V. Lohmann, and R. Bartenschlager. 2011. Recruitment and activation of a lipid kinase by hepatitis C virus NS5A is essential for integrity of the membranous replication compartment. *Cell Host Microbe.* 9:32-45.

Reverter, D., and C. Lima. 2005. Insights into E3 ligase activity revealed by a SUMO-RanGAP1-Ubc9-Nup358 complex. *Nature*. 435:687-692.

Rexach, M., and G. Blobel. 1995. Protein import into nuclei: association and dissociation reactions involving transport substrate, transport factors, and nucleoporins. *Cell*. 83:683-692.

Ribbeck, K., and D. Gorlich. 2001. Kinetic analysis of translocation through nuclear pore complexes. *Embo J*. 20:1320-1330.

Ribbeck, K., and D. Gorlich. 2002. The permeability barrier of nuclear pore complexes appears to operate via hydrophobic exclusion. *Embo J*. 21:2664-2671.

Ribbeck, K., G. Lipowsky, H.M. Kent, M. Stewart, and D. Gorlich. 1998. NTF2 mediates nuclear import of Ran. *Embo J*. 17:6587-6598.

Roberts, M.S., D.C. Angus, C.L. Bryce, Z. Valenta, and L. Weissfeld. 2004. Survival after liver transplantation in the United States: a disease-specific analysis of the UNOS database. *Liver Transpl*. 10:886-897.

Rogers, R., C. Horvath, and M. Matunis. 2003. SUMO modification of STAT1 and its role in PIAS-mediated inhibition of gene activation. *J Biol Chem*. 278:30091-30097.

Romero-Brey, I., A. Merz, A. Chiramel, J.Y. Lee, P. Chlanda, U. Haselman, R. Santarella-Mellwig, A. Habermann, S. Hoppe, S. Kallis, P. Walther, C. Antony, J. Krijnse-Locker, and R. Bartenschlager. 2012. Three-dimensional architecture and biogenesis of membrane structures associated with hepatitis C virus replication. *PLoS pathogens*. 8:e1003056.

Romero-Lopez, C., and A. Berzal-Herranz. 2009. A long-range RNA-RNA interaction between the 5' and 3' ends of the HCV genome. *Rna*. 15:1740-1752.

Romero-Lopez, C., and A. Berzal-Herranz. 2012. The functional RNA domain 5BSL3.2 within the NS5B coding sequence influences hepatitis C virus IRES-mediated translation. *Cellular and molecular life sciences : CMLS*. 69:103-113.

Rosnoblet, C., B. Fritzinger, D. Legrand, H. Launay, J.M. Wieruszeski, G. Lippens, and X. Hanoulle. 2012. Hepatitis C virus NS5B and host cyclophilin A share a common binding site on NS5A. *J Biol Chem*. 287:44249-44260.

Rout, M.P., J.D. Aitchison, M.O. Magnasco, and B.T. Chait. 2003. Virtual gating and nuclear transport: the hole picture. *Trends Cell Biol*. 13:622-628.

Rout, M.P., J.D. Aitchison, A. Suprapto, K. Hjertaas, Y. Zhao, and B.T. Chait. 2000. The yeast nuclear pore complex: composition, architecture, and transport mechanism. *J Cell Biol*. 148:635-651.

Rusinol, A.E., Z. Cui, M.H. Chen, and J.E. Vance. 1994. A unique mitochondria-associated membrane fraction from rat liver has a high capacity for lipid synthesis and contains pre-Golgi secretory proteins including nascent lipoproteins. *J Biol Chem.* 269:27494-27502.

Sainz, B., Jr., N. Barretto, D.N. Martin, N. Hiraga, M. Imamura, S. Hussain, K.A. Marsh, X. Yu, K. Chayama, W.A. Alrefai, and S.L. Uprichard. 2012. Identification of the Niemann-Pick C1-like 1 cholesterol absorption receptor as a new hepatitis C virus entry factor. *Nat Med.* 18:281-285.

Saito, T., R. Hirai, Y.M. Loo, D. Owen, C.L. Johnson, S.C. Sinha, S. Akira, T. Fujita, and M. Gale, Jr. 2007. Regulation of innate antiviral defenses through a shared repressor domain in RIG-I and LGP2. *Proc Natl Acad Sci U S A.* 104:582-587.

Saitoh, H., R. Pu, M. Cavenagh, and M. Dasso. 1997. RanBP2 associates with Ubc9p and a modified form of RanGAP1. *Proc Natl Acad Sci U S A.* 94:3736-3741.

Saitoh, N., Y. Uchimura, T. Tachibana, S. Sugahara, H. Saitoh, and M. Nakao. 2006. In situ SUMOylation analysis reveals a modulatory role of RanBP2 in the nuclear rim and PML bodies. *Exp Cell Res.* 312:1418-1430.

Sakamoto, S., R. Potla, and A.C. Larner. 2004. Histone deacetylase activity is required to recruit RNA polymerase II to the promoters of selected interferon-stimulated early response genes. *J Biol Chem.* 279:40362-40367.

Santolini, E., G. Migliaccio, and N. La Monica. 1994. Biosynthesis and biochemical properties of the hepatitis C virus core protein. *J Virol.* 68:3631-3641.

Sarasin-Filipowicz, M., E.J. Oakeley, F.H. Duong, V. Christen, L. Terracciano, W. Filipowicz, and M.H. Heim. 2008. Interferon signaling and treatment outcome in chronic hepatitis C. *Proc Natl Acad Sci U S A.* 105:7034-7039.

Sarasin-Filipowicz, M., X. Wang, M. Yan, F.H. Duong, V. Poli, D.J. Hilton, D.E. Zhang, and M.H. Heim. 2009. Alpha interferon induces long-lasting refractoriness of JAK-STAT signaling in the mouse liver through induction of USP18/UBP43. *Mol Cell Biol.* 29:4841-4851.

Sato, M., N. Tanaka, N. Hata, E. Oda, and T. Taniguchi. 1998. Involvement of the IRF family transcription factor IRF-3 in virus-induced activation of the IFN-beta gene. *FEBS Lett.* 425:112-116.

Satterly, N., P. Tsai, J. van Deursen, D. Nussenzveig, Y. Wang, P. Faria, A. Levay, D. Levy, and B. Fontoura. 2007. Influenza virus targets the mRNA export machinery and the nuclear pore complex. *Proc Natl Acad Sci.* 104:1853-1858.

Scarselli, E., H. Ansuini, R. Cerino, R.M. Roccasecca, S. Acali, G. Filocamo, C. Traboni, A. Nicosia, R. Cortese, and A. Vitelli. 2002. The human scavenger receptor class B type I is a novel candidate receptor for the hepatitis C virus. *Embo J.* 21:5017-5025.

Schaller, T., K.E. Ocwieja, J. Rasaiyaah, A.J. Price, T.L. Brady, S.L. Roth, S. Hue, A.J. Fletcher, K. Lee, V.N. KewalRamani, M. Noursadeghi, R.G. Jenner, L.C. James, F.D. Bushman, and G.J. Towers. 2011. HIV-1 capsid-cyclophilin interactions determine nuclear import pathway, integration targeting and replication efficiency. *PLoS pathogens*. 7:e1002439.

Schindler, C., K. Shuai, V.R. Prezioso, and J.E. Darnell, Jr. 1992. Interferon-dependent tyrosine phosphorylation of a latent cytoplasmic transcription factor. *Science*. 257:809-813.

Schmid, M., G. Arib, C. Laemmli, J. Nishikawa, T. Durussel, and U.K. Laemmli. 2006. Nup-PI: the nucleopore-promoter interaction of genes in yeast. *Mol Cell*. 21:379-391.

Schmitz, A., A. Schwarz, M. Foss, L. Zhou, B. Rabe, J. Hoellenriegel, M. Stoeber, N. Panté, and M. Kann. 2010. Nucleoporin 153 arrests the nuclear import of hepatitis B virus capsids in the nuclear basket. *PLoS Pathog*. 6:e1000741.

Schoggins, J.W., S.J. Wilson, M. Panis, M.Y. Murphy, C.T. Jones, P. Bieniasz, and C.M. Rice. 2011. A diverse range of gene products are effectors of the type I interferon antiviral response. *Nature*. 472:481-485.

Schooley, A., B. Vollmer, and W. Antonin. 2012. Building a nuclear envelope at the end of mitosis: coordinating membrane reorganization, nuclear pore complex assembly, and chromatin de-condensation. *Chromosoma*. 121:539-554.

Schregel, V., S. Jacobi, F. Penin, and N. Tautz. 2009. Hepatitis C virus NS2 is a protease stimulated by cofactor domains in NS3. *Proc Natl Acad Sci U S A*. 106:5342-5347.

Schroder, M., M. Baran, and A.G. Bowie. 2008. Viral targeting of DEAD box protein 3 reveals its role in TBK1/IKKepsilon-mediated IRF activation. *Embo J*. 27:2147-2157.

Schwartz, T.U. 2005. Modularity within the architecture of the nuclear pore complex. *Curr Opin Struct Biol*. 15:221-226.

Schwer, B., S. Ren, T. Pietschmann, J. Kartenbeck, K. Kaehlcke, R. Bartenschlager, T.S. Yen, and M. Ott. 2004. Targeting of hepatitis C virus core protein to mitochondria through a novel C-terminal localization motif. *J Virol*. 78:7958-7968.

Scognamiglio, A., A. Nebbioso, F. Manzo, S. Valente, A. Mai, and L. Altucci. 2008. HDAC-class II specific inhibition involves HDAC proteasome-dependent degradation mediated by RANBP2. *Biochim Biophys Acta*. 1783:2030-2038.

Scott, R., L. Cairo, D. Van de Vosse, and R. Wozniak. 2009. The nuclear export factor Xpo1p targets Mad1p to kinetochores in yeast. *J Cell Biol*. 184:21-29.

Scott, R.J., C.P. Lusk, D.J. Dilworth, J.D. Aitchison, and R.W. Wozniak. 2005. Interactions between Mad1p and the nuclear transport machinery in the yeast Saccharomyces cerevisiae. *Mol Biol Cell*. 16:4362-4374.

Seki, T., N. Hayashi, and T. Nishimoto. 1996. RCC1 in the Ran pathway. *Journal of biochemistry*. 120:207-214.

Sewry, C.A., S.C. Brown, E. Mercuri, G. Bonne, L. Feng, G. Camici, G.E. Morris, and F. Muntoni. 2001. Skeletal muscle pathology in autosomal dominant Emery-Dreifuss muscular dystrophy with lamin A/C mutations. *Neuropathology and applied neurobiology*. 27:281-290.

Shavinskaya, A., S. Boulant, F. Penin, J. McLauchlan, and R. Bartenschlager. 2007. The lipid droplet binding domain of hepatitis C virus core protein is a major determinant for efficient virus assembly. *The Journal of biological chemistry*. 282:37158-37169.

Shigemoto, T., M. Kageyama, R. Hirai, J. Zheng, M. Yoneyama, and T. Fujita. 2009. Identification of loss of function mutations in human genes encoding RIG-I and MDA5: implications for resistance to type I diabetes. *J Biol Chem*. 284:13348-13354.

Shimizu, Y., T. Hishiki, S. Ujino, K. Sugiyama, K. Funami, and K. Shimotohno. 2011. Lipoprotein component associated with hepatitis C virus is essential for virus infectivity. *Curr Opin Virol*. 1:19-26.

Shimizu, Y.K., A.J. Weiner, J. Rosenblatt, D.C. Wong, M. Shapiro, T. Popkin, M. Houghton, H.J. Alter, and R.H. Purcell. 1990. Early events in hepatitis C virus infection of chimpanzees. *Proc. Natl. Acad. Sci.* 87:6441-6444.

Shuai, K., and B. Liu. 2005. Regulation of gene-activation pathways by PIAS proteins in the immune system. *Nat Rev Immunol*. 5:593-605.

Silvennoinen, O., J.N. Ihle, J. Schlessinger, and D.E. Levy. 1993. Interferon-induced nuclear signalling by Jak protein tyrosine kinases. *Nature*. 366:583-585.

Simmonds, P., J. Bukh, C. Combet, G. Deleage, N. Enomoto, S. Feinstone, P. Halfon, G. Inchauspe, C. Kuiken, G. Maertens, M. Mizokami, D.G. Murphy, H. Okamoto, J.M. Pawlotsky, F. Penin, E. Sablon, I.T. Shin, L.J. Stuyver, H.J. Thiel, S. Viazov, A.J. Weiner, and A. Widell. 2005. Consensus proposals for a unified system of nomenclature of hepatitis C virus genotypes. *Hepatology*. 42:962-973.

Sir, D., C.F. Kuo, Y. Tian, H.M. Liu, E.J. Huang, J.U. Jung, K. Machida, and J.H. Ou. 2012. Replication of hepatitis C virus RNA on autophagosomal membranes. *J Biol Chem*. 287:18036-18043.

Sklan, E.H., R.L. Serrano, S. Einav, S.R. Pfeffer, D.G. Lambright, and J.S. Glenn. 2007. TBC1D20 is a Rab1 GTPase-activating protein that mediates hepatitis C virus replication. *J Biol Chem*. 282:36354-36361.

Smith, M.W., Z.N. Yue, M.J. Korth, H.A. Do, L. Boix, N. Fausto, J. Bruix, R.L. Carithers, Jr., and M.G. Katze. 2003. Hepatitis C virus and liver disease: global transcriptional profiling and identification of potential markers. *Hepatology*. 38:1458-1467.

Solmaz, S.R., G. Blobel, and I. Melcak. 2013. Ring cycle for dilating and constricting the nuclear pore. *Proc Natl Acad Sci U S A*. 110:5858-5863.

Solmaz, S.R., R. Chauhan, G. Blobel, and I. Melcak. 2011. Molecular architecture of the transport channel of the nuclear pore complex. *Cell.* 147:590-602.

Song, Y., P. Friebe, E. Tzima, C. Junemann, R. Bartenschlager, and M. Niepmann. 2006. The hepatitis C virus RNA 3'-untranslated region strongly enhances translation directed by the internal ribosome entry site. *J Virol.* 80:11579-11588.

Sosa, B.A., A. Rothballer, U. Kutay, and T.U. Schwartz. 2012. LINC complexes form by binding of three KASH peptides to domain interfaces of trimeric SUN proteins. *Cell.* 149:1035-1047.

Stade, K., C.S. Ford, C. Guthrie, and K. Weis. 1997. Exportin 1 (Crm1p) is an essential nuclear export factor. *Cell.* 90:1041-1050.

Stapleford, K.A., and B.D. Lindenbach. 2011. Hepatitis C virus NS2 coordinates virus particle assembly through physical interactions with the E1-E2 glycoprotein and NS3-NS4A enzyme complexes. *J Virol.* 85:1706-1717.

Stavru, F., B.B. Hulsmann, A. Spang, E. Hartmann, V.C. Cordes, and D. Gorlich. 2006. NDC1: a crucial membrane-integral nucleoporin of metazoan nuclear pore complexes. *J. cell Biol.* 173:509-519.

Steenbergen, R.H., M.A. Joyce, B.S. Thomas, D. Jones, J. Law, R. Russell, M. Houghton, and D.L. Tyrrell. 2013. Human serum leads to differentiation of human hepatoma cells, restoration of very-low-density lipoprotein secretion, and a 1000-fold increase in HCV Japanese fulminant hepatitis type 1 titers. *Hepatology.* 58:1907-1917.

Steinkuhler, C., A. Urbani, L. Tomei, G. Biasiol, M. Sardana, E. Bianchi, A. Pessi, and R. De Francesco. 1996. Activity of purified hepatitis C virus protease NS3 on peptide substrates. *J Virol.* 70:6694-6700.

Stewart, M. 2007. Molecular mechanism of the nuclear protein import cycle. *Nature reviews. Molecular cell biology.* 8:195-208.

Stewart, M. 2010. Nuclear export of mRNA. *Trends in biochemical sciences.* 35:609-617.

Stoffler, D., K.N. Goldie, B. Feja, and U. Aebi. 1999. Calcium-mediated structural changes of native nuclear pore complexes monitored by time-lapse atomic force microscopy. *J Mol Biol.* 287:741-752.

Stone, M., S. Jia, W.D. Heo, T. Meyer, and K.V. Konan. 2007. Participation of rab5, an early endosome protein, in hepatitis C virus RNA replication machinery. *J Virol.* 81:4551-4563.

Stone, S.J., M.C. Levin, P. Zhou, J. Han, T.C. Walther, and R.V. Farese, Jr. 2009. The endoplasmic reticulum enzyme DGAT2 is found in mitochondria-associated membranes and has a mitochondrial targeting signal that promotes its association with mitochondria. *J Biol Chem.* 284:5352-5361.

Strambio-De-Castillia, C., M. Niepel, and M.P. Rout. 2010. The nuclear pore complex: bridging nuclear transport and gene regulation. *Nature reviews. Molecular cell biology*. 11:490-501.

Strawn, L.A., T. Shen, N. Shulga, D.S. Goldfarb, and S.R. Wente. 2004. Minimal nuclear pore complexes define FG repeat domains essential for transport. *Nat Cell Biol*. 6:197-206.

Strunze, S., M.F. Engelke, I.H. Wang, D. Puntener, K. Boucke, S. Schleich, M. Way, P. Schoenenberger, C.J. Burckhardt, and U.F. Greber. 2011. Kinesin-1-mediated capsid disassembly and disruption of the nuclear pore complex promote virus infection. *Cell Host Microbe*. 10:210-223.

Strunze, S., L.C. Trotman, K. Boucke, and U.F. Greber. 2005. Nuclear targeting of adenovirus type 2 requires CRM1-mediated nuclear export. *Mol Biol Cell*. 16:2999-3009.

Su, A.I., J.P. Pezacki, L. Wodicka, A.D. Brideau, L. Supekova, R. Thimme, S. Wieland, J. Bukh, R.H. Purcell, P.G. Schultz, and F.V. Chisari. 2002. Genomic analysis of the host response to hepatitis C virus infection. *Proc Natl Acad Sci U S A*. 99:15669-15674.

Sumpter, R., Jr., Y.M. Loo, E. Foy, K. Li, M. Yoneyama, T. Fujita, S.M. Lemon, and M. Gale, Jr. 2005. Regulating intracellular antiviral defense and permissiveness to hepatitis C virus RNA replication through a cellular RNA helicase, RIG-I. *J Virol*. 79:2689-2699.

Suzuki, R., S. Sakamoto, T. Tsutsumi, A. Rikimaru, K. Tanaka, T. Shimoike, K. Moriishi, T. Iwasaki, K. Mizumoto, Y. Matsuura, T. Miyamura, and T. Suzuki. 2005. Molecular determinants for subcellular localization of hepatitis C virus core protein. *J. Virol*. 79:1271-1281.

Taddei, A., G. Van Houwe, F. Hediger, V. Kalck, F. Cubizolles, H. Schober, and S.M. Gasser. 2006. Nuclear pore association confers optimal expression levels for an inducible yeast gene. *Nature*. 441:774-778.

Tahk, S., B. Liu, V. Chernishof, K.A. Wong, H. Wu, and K. Shuai. 2007. Control of specificity and magnitude of NF-kappa B and STAT1-mediated gene activation through PIASy and PIAS1 cooperation. *Proc Natl Acad Sci U S A*. 104:11643-11648.

Tai, A.W., Y. Benita, L.F. Peng, S.S. Kim, N. Sakamoto, R.J. Xavier, and R.T. Chung. 2009. A functional genomic screen identifies cellular cofactors of hepatitis C virus replication. *Cell Host Microbe*. 5:298-307.

Takahashi, N., T. Hayano, and M. Suzuki. 1989. Peptidyl-prolyl cis-trans isomerase is the cyclosporin A-binding protein cyclophilin. *Nature*. 337:473-475.

Takahasi, K., M. Yoneyama, T. Nishihori, R. Hirai, H. Kumeta, R. Narita, M. Gale, Jr., F. Inagaki, and T. Fujita. 2008. Nonself RNA-sensing mechanism of RIG-I helicase and activation of antiviral immune responses. *Mol Cell*. 29:428-440.

Takeda, A., and N.R. Yaseen. 2014. Nucleoporins and nucleocytoplasmic transport in hematologic malignancies. *Seminars in cancer biology*. 27:3-10.

Talamas, J.A., and M.W. Hetzer. 2011. POM121 and Sun1 play a role in early steps of interphase NPC assembly. *J Cell Biol.* 194:27-37.

Tamura, T., H. Yanai, D. Savitsky, and T. Taniguchi. 2008. The IRF family transcription factors in immunity and oncogenesis. *Annu Rev Immunol.* 26:535-584.

Tanida, I., M. Fukasawa, T. Ueno, E. Kominami, T. Wakita, and K. Hanada. 2009. Knockdown of autophagy-related gene decreases the production of infectious hepatitis C virus particles. *Autophagy.* 5:937-945.

Tatham, M.H., S. Kim, E. Jaffray, J. Song, Y. Chen, and R.T. Hay. 2005. Unique binding interactions among Ubc9, SUMO and RanBP2 reveal a mechanism for SUMO paralog selection. *Nature structural & molecular biology.* 12:67-74.

Tay, M.Y., J.E. Fraser, W.K. Chan, N.J. Moreland, A.P. Rathore, C. Wang, S.G. Vasudevan, and D.A. Jans. 2013. Nuclear localization of dengue virus (DENV) 1-4 non-structural protein 5; protection against all 4 DENV serotypes by the inhibitor Ivermectin. *Antiviral Res.* 99:301-306.

Taylor, D.R., M. Puig, M.E. Darnell, K. Mihalik, and S.M. Feinstone. 2005. New antiviral pathway that mediates hepatitis C virus replicon interferon sensitivity through ADAR1. *J Virol.* 79:6291-6298.

Taylor, D.R., S.T. Shi, P.R. Romano, G.N. Barber, and M.M. Lai. 1999. Inhibition of the interferon-inducible protein kinase PKR by HCV E2 protein. *Science.* 285:107-110.

Tellinghuisen, T.L., K.L. Foss, and J. Treadaway. 2008. Regulation of hepatitis C virion production via phosphorylation of the NS5A protein. *PLoS Pathog.* 4:e1000032.

Therizols, P., C. Fairhead, G.G. Cabal, A. Genovesio, J.C. Olivo-Marin, B. Dujon, and E. Fabre. 2006. Telomere tethering at the nuclear periphery is essential for efficient DNA double strand break repair in subtelomeric region. *J Cell Biol.* 172:189-199.

Trotman, L.C., N. Mosberger, M. Fornerod, R.P. Stidwill, and U.F. Greber. 2001. Import of adenovirus DNA involves the nuclear pore complex receptor CAN/Nup214 and histone H1. *Nat Cell Biol.* 3:1092-1100.

Ullman, K.S., S. Shah, M.A. Powers, and D.J. Forbes. 1999. The nucleoporin nup153 plays a critical role in multiple types of nuclear export. *Molecular biology of the cell.* 10:649-664.

Ungureanu, D., S. Vanhatupa, J. Grönholm, J. Palvimo, and O. Silvennoinen. 2005. SUMO-1 conjugation selectively modulates STAT1-mediated gene responses. *Blood.* 106:224-226.

Ungureanu, D., S. Vanhatupa, N. Kotaja, J. Yang, S. Aittomaki, O. Jänne, J. Palvimo, and O. Silvennoinen. 2003. PIAS proteins promote SUMO-1 conjugation to STAT1. *Blood.* 102:3311-3313.

Unwin, P.N., and R.A. Milligan. 1982. A large particle associated with the perimeter of the nuclear pore complex. *J Cell Biol.* 93:63-75.

Van de Vosse, D.W., Y. Wan, D.L. Lapetina, W.M. Chen, J.H. Chiang, J.D. Aitchison, and R.W. Wozniak. 2013. A role for the nucleoporin Nup170p in chromatin structure and gene silencing. *Cell*. 152:969-983.

Van de Vosse, D.W., Y. Wan, R.W. Wozniak, and J.D. Aitchison. 2011. Role of the nuclear envelope in genome organization and gene expression. *Wiley interdisciplinary reviews. Systems biology and medicine*. 3:147-166.

Varinou, L., K. Ramsauer, M. Karaghiosoff, T. Kolbe, K. Pfeffer, M. Muller, and T. Decker. 2003. Phosphorylation of the Stat1 transactivation domain is required for full-fledged IFN-gamma-dependent innate immunity. *Immunity*. 19:793-802.

Velazquez, L., M. Fellous, G.R. Stark, and S. Pellegrini. 1992. A protein tyrosine kinase in the interferon alpha/beta signaling pathway. *Cell*. 70:313-322.

Verdegem, D., A. Badillo, J.M. Wieruszeski, I. Landrieu, A. Leroy, R. Bartenschlager, F. Penin, G. Lippens, and X. Hanoulle. 2011. Domain 3 of NS5A protein from the hepatitis C virus has intrinsic alpha-helical propensity and is a substrate of cyclophilin A. *The Journal of biological chemistry*. 286:20441-20454.

Verga, L., M. Concardi, A. Pilotto, O. Bellini, M. Pasotti, A. Repetto, L. Tavazzi, and E. Arbustini. 2003. Loss of lamin A/C expression revealed by immuno-electron microscopy in dilated cardiomyopathy with atrioventricular block caused by LMNA gene defects. *Virchows Archiv : an international journal of pathology*. 443:664-671.

Wagstaff, K.M., H. Sivakumaran, S.M. Heaton, D. Harrich, and D.A. Jans. 2012. Ivermectin is a specific inhibitor of importin alpha/beta-mediated nuclear import able to inhibit replication of HIV-1 and dengue virus. *Biochem J*. 443:851-856.

Wakita, T., T. Pietschmann, T. Kato, T. Date, M. Miyamoto, Z. Zhao, K. Murthy, A. Habermann, H.G. Krausslich, M. Mizokami, R. Bartenschlager, and T.J. Liang. 2005. Production of infectious hepatitis C virus in tissue culture from a cloned viral genome. *Nat Med*. 11:791-796.

Walde, S., K. Thakar, S. Hutten, C. Spillner, A. Nath, U. Rothbauer, S. Wiemann, and R.H. Kehlenbach. 2012. The nucleoporin Nup358/RanBP2 promotes nuclear import in a cargo- and transport receptor-specific manner. *Traffic*. 13:218-233.

Walters, K.A., M.A. Joyce, J.C. Thompson, M.W. Smith, M.M. Yeh, S. Proll, L.F. Zhu, T.J. Gao, N.M. Kneteman, D.L. Tyrrell, and M.G. Katze. 2006. Host-specific response to HCV infection in the chimeric SCID-beige/Alb-uPA mouse model: role of the innate antiviral immune response. *PLoS Pathog*. 2:e59.

Walther, T.C., A. Alves, H. Pickersgill, I. Loiodice, M. Hetzer, V. Galy, B.B. Hulsmann, T. Kocher, M. Wilm, T. Allen, I.W. Mattaj, and V. Doye. 2003. The conserved Nup107-160 complex is critical for nuclear pore complex assembly. *Cell*. 113:195-206.

Wang, C., J. Pflugheber, R. Sumpter, Jr., D.L. Sodora, D. Hui, G.C. Sen, and M. Gale, Jr. 2003. Alpha interferon induces distinct translational control programs to suppress hepatitis C virus RNA replication. *J Virol.* 77:3898-3912.

Wang, G.G., L. Cai, M.P. Pasillas, and M.P. Kamps. 2007. NUP98-NSD1 links H3K36 methylation to Hox-A gene activation and leukaemogenesis. *Nat Cell Biol.* 9:804-812.

Wang, J.J., C.L. Liao, Y.W. Chiou, C.T. Chiou, Y.L. Huang, and L.K. Chen. 1997. Ultrastructure and localization of E proteins in cultured neuron cells infected with Japanese encephalitis virus. *Virology.* 238:30-39.

Wang, L., R.A. Gordon, L. Huynh, X. Su, K.H. Park Min, J. Han, J.S. Arthur, G.D. Kalliolias, and L.B. Ivashkiv. 2010. Indirect inhibition of Toll-like receptor and type I interferon responses by ITAM-coupled receptors and integrins. *Immunity.* 32:518-530.

Wang, Y.E., O. Pernet, and B. Lee. 2012. Regulation of the nucleocytoplasmic trafficking of viral and cellular proteins by ubiquitin and small ubiquitin-related modifiers. *Biol Cell.* 104:121-138.

Waris, G., D.J. Felmlee, F. Negro, and A. Siddiqui. 2007. Hepatitis C virus induces proteolytic cleavage of sterol regulatory element binding proteins and stimulates their phosphorylation via oxidative stress. *J Virol.* 81:8122-8130.

Watanabe, K., N. Takizawa, M. Katoh, K. Hoshida, N. Kobayashi, and K. Nagata. 2001. Inhibition of nuclear export of ribonucleoprotein complexes of influenza virus by leptomycin B. *Virus Res.* 77:31-42.

Watling, D., D. Guschin, M. Muller, O. Silvennoinen, B.A. Witthuhn, F.W. Quelle, N.C. Rogers, C. Schindler, G.R. Stark, J.N. Ihle, and et al. 1993. Complementation by the protein tyrosine kinase JAK2 of a mutant cell line defective in the interferon-gamma signal transduction pathway. *Nature.* 366:166-170.

Watson, M.L. 1954. Pores in the mammalian nuclear membrane. *Biochim Biophys Acta.* 15:475-479.

Watters, K., and A.C. Palmenberg. 2011. Differential processing of nuclear pore complex proteins by rhinovirus 2A proteases from different species and serotypes. *J Virol.* 85:10874-10883.

Weaver, B.K., K.P. Kumar, and N.C. Reich. 1998. Interferon regulatory factor 3 and CREB-binding protein/p300 are subunits of double-stranded RNA-activated transcription factor DRAF1. *Mol Cell Biol.* 18:1359-1368.

Welsch, S., S. Miller, I. Romero-Brey, A. Merz, C.K. Bleck, P. Walther, S.D. Fuller, C. Antony, J. Krijnse-Locker, and R. Bartenschlager. 2009. Composition and three-dimensional architecture of the dengue virus replication and assembly sites. *Cell Host Microbe.* 5:365-375.

Wen, W., J.L. Meinkoth, R.Y. Tsien, and S.S. Taylor. 1995. Identification of a signal for rapid export of proteins from the nucleus. *Cell.* 82:463-473.

Wente, S.R., and M.P. Rout. 2010. The nuclear pore complex and nuclear transport. *Cold Spring Harb Perspect Biol.* 2:a000562.

Werner, A., A. Flotho, and F. Melchior. 2012. The RanBP2/RanGAP1*SUMO1/Ubc9 complex is a multisubunit SUMO E3 ligase. *Mol Cell.* 46:287-298.

Werner, A., M. Moutty, U. Möller, and F. Melchior. 2009. Performing in vitro sumoylation reactions using recombinant enzymes. *Methods Mol Biol.* 497:187-199.

Wieckowski, M.R., C. Giorgi, M. Lebiedzinska, J. Duszynski, and P. Pinton. 2009. Isolation of mitochondria-associated membranes and mitochondria from animal tissues and cells. *Nat Protoc.* 4:1582-1590.

Wilson, J.A., S. Jayasena, A. Khvorova, S. Sabatinos, I.G. Rodrigue-Gervais, S. Arya, F. Sarangi, M. Harris-Brandts, S. Beaulieu, and C.D. Richardson. 2003. RNA interference blocks gene expression and RNA synthesis from hepatitis C replicons propagated in human liver cells. *Proc. Natl. Acad. Sci.* 100:2783-2788.

Witte, K., G. Gruetz, H.D. Volk, A.C. Looman, K. Asadullah, W. Sterry, R. Sabat, and K. Wolk. 2009. Despite IFN-lambda receptor expression, blood immune cells, but not keratinocytes or melanocytes, have an impaired response to type III interferons: implications for therapeutic applications of these cytokines. *Genes Immun.* 10:702-714.

Wolk, B., B. Buchele, D. Moradpour, and C.M. Rice. 2008. A dynamic view of hepatitis C virus replication complexes. *J Virol.* 82:10519-10531.

Wolk, B., D. Sansonno, H.G. Krausslich, F. Dammacco, C.M. Rice, H.E. Blum, and D. Moradpour. 2000. Subcellular localization, stability, and trans-cleavage competence of the hepatitis C virus NS3-NS4A complex expressed in tetracycline-regulated cell lines. *J Virol.* 74:2293-2304.

Wozniak, A.L., S. Griffin, D. Rowlands, M. Harris, M. Yi, S.M. Lemon, and S.A. Weinman. 2010. Intracellular proton conductance of the hepatitis C virus p7 protein and its contribution to infectious virus production. *PLoS Pathog.* 6:e1001087.

Wu, J., M.J. Matunis, D. Kraemer, G. Blobel, and E. Coutavas. 1995. Nup358, a cytoplasmically exposed nucleoporin with peptide repeats, Ran-GTP binding sites, zinc fingers, a cyclophilin A homologous domain, and a leucine-rich region. *J Biol Chem.* 270:14209-14213.

Xu, H., X. He, H. Zheng, L.J. Huang, F. Hou, Z. Yu, M.J. de la Cruz, B. Borkowski, X. Zhang, Z.J. Chen, and Q.X. Jiang. 2014. Structural basis for the prion-like MAVS filaments in antiviral innate immunity. *eLife.* 3:e01489.

Xylourgidis, N., P. Roth, N. Sabri, V. Tsarouhas, and C. Samakovlis. 2006. The nucleoporin Nup214 sequesters CRM1 at the nuclear rim and modulates NFkappaB activation in Drosophila. *J Cell Sci*. 119:4409-4419.

Yamamoto, M., S. Sato, H. Hemmi, K. Hoshino, T. Kaisho, H. Sanjo, O. Takeuchi, M. Sugiyama, M. Okabe, K. Takeda, and S. Akira. 2003. Role of adaptor TRIF in the MyD88-independent toll-like receptor signaling pathway. *Science*. 301:640-643.

Yamamoto, M., S. Sato, K. Mori, K. Hoshino, O. Takeuchi, K. Takeda, and S. Akira. 2002. Cutting edge: a novel Toll/IL-1 receptor domain-containing adapter that preferentially activates the IFN-beta promoter in the Toll-like receptor signaling. *J Immunol*. 169:6668-6672.

Yanagi, M., M. St Claire, S.U. Emerson, R.H. Purcell, and J. Bukh. 1999. In vivo analysis of the 3' untranslated region of the hepatitis C virus after in vitro mutagenesis of an infectious cDNA clone. *Proc Natl Acad Sci U S A*. 96:2291-2295.

Yang, F., J.M. Robotham, H. Grise, S. Frausto, V. Madan, M. Zayas, R. Bartenschlager, M. Robinson, A.E. Greenstein, A. Nag, T.M. Logan, E. Bienkiewicz, and H. Tang. 2010. A major determinant of cyclophilin dependence and cyclosporine susceptibility of hepatitis C virus identified by a genetic approach. *PLoS pathogens*. 6:e1001118.

Yarbrough, M.L., M.A. Mata, R. Sakthivel, and B.M. Fontoura. 2014. Viral subversion of nucleocytoplasmic trafficking. *Traffic*. 15:127-140.

Yatherajam, G., W. Huang, and S.J. Flint. 2011. Export of adenoviral late mRNA from the nucleus requires the Nxf1/Tap export receptor. *J Virol*. 85:1429-1438.

Yi, H., J.L. Friedman, and P.A. Ferreira. 2007. The cyclophilin-like domain of Ran-binding protein-2 modulates selectively the activity of the ubiquitin-proteasome system and protein biogenesis. *The Journal of biological chemistry*. 282:34770-34778.

Yi, M., Y. Ma, J. Yates, and S.M. Lemon. 2009. Trans-complementation of an NS2 defect in a late step in hepatitis C virus (HCV) particle assembly and maturation. *PLoS Pathog*. 5:e1000403.

Yi, S., Y. Chen, L. Wen, L. Yang, and G. Cui. 2012. Downregulation of nucleoporin 88 and 214 induced by oridonin may protect OCIM2 acute erythroleukemia cells from apoptosis through regulation of nucleocytoplasmic transport of NF-kappaB. *Int J Mol Med*. 30:877-883.

Yokoyama, N., N. Hayashi, T. Seki, N. Pante, T. Ohba, K. Nishii, K. Kuma, T. Hayashida, T. Miyata, U. Aebi, and et al. 1995. A giant nucleopore protein that binds Ran/TC4. *Nature*. 376:184-188.

Yoneyama, M., M. Kikuchi, K. Matsumoto, T. Imaizumi, M. Miyagishi, K. Taira, E. Foy, Y.M. Loo, M. Gale, Jr., S. Akira, S. Yonehara, A. Kato, and T. Fujita. 2005. Shared and unique functions of the DExD/H-box helicases RIG-I, MDA5, and LGP2 in antiviral innate immunity. *J Immunol*. 175:2851-2858.

Yoneyama, M., M. Kikuchi, T. Natsukawa, N. Shinobu, T. Imaizumi, M. Miyagishi, K. Taira, S. Akira, and T. Fujita. 2004. The RNA helicase RIG-I has an essential function in double-stranded RNA-induced innate antiviral responses. *Nature immunology*. 5:730-737.

Yoneyama, M., W. Suhara, Y. Fukuhara, M. Fukuda, E. Nishida, and T. Fujita. 1998. Direct triggering of the type I interferon system by virus infection: activation of a transcription factor complex containing IRF-3 and CBP/p300. *Embo J*. 17:1087-1095.

Yoshimura, A., T. Naka, and M. Kubo. 2007. SOCS proteins, cytokine signalling and immune regulation. *Nat Rev Immunol*. 7:454-465.

You, L.R., C.M. Chen, T.S. Yeh, T.Y. Tsai, R.T. Mai, C.H. Lin, and Y.H. Lee. 1999. Hepatitis C virus core protein interacts with cellular putative RNA helicase. *J Virol*. 73:2841-2853.

You, S., and C.M. Rice. 2008. 3' RNA elements in hepatitis C virus replication: kissing partners and long poly(U). *J Virol*. 82:184-195.

Yu, K.L., S.I. Jang, and J.C. You. 2009. Identification of in vivo interaction between Hepatitis C Virus core protein and 5' and 3' UTR RNA. *Virus Res*. 145:285-292.

Yu, M., D.T. Ting, S.L. Stott, B.S. Wittner, F. Ozsolak, S. Paul, J.C. Ciciliano, M.E. Smas, D. Winokur, A.J. Gilman, M.J. Ulman, K. Xega, G. Contino, B. Alagesan, B.W. Brannigan, P.M. Milos, D.P. Ryan, L.V. Sequist, N. Bardeesy, S. Ramaswamy, M. Toner, S. Maheswaran, and D.A. Haber. 2012. RNA sequencing of pancreatic circulating tumour cells implicates WNT signalling in metastasis. *Nature*. 487:510-513.

Zeisel, M.B., G. Koutsoudakis, E.K. Schnober, A. Haberstroh, H.E. Blum, F.L. Cosset, T. Wakita, D. Jaeck, M. Doffoel, C. Royer, E. Soulier, E. Schvoerer, C. Schuster, F. Stoll-Keller, R. Bartenschlager, T. Pietschmann, H. Barth, and T.F. Baumert. 2007. Scavenger receptor class B type I is a key host factor for hepatitis C virus infection required for an entry step closely linked to CD81. *Hepatology*. 46:1722-1731.

Zeitler, B., and K. Weis. 2004. The FG-repeat asymmetry of the nuclear pore complex is dispensable for bulk nucleocytoplasmic transport in vivo. *J Cell Biol*. 167:583-590.

Zhang, H., H. Saitoh, and M.J. Matunis. 2002. Enzymes of the SUMO modification pathway localize to filaments of the nuclear pore complex. *Mol Cell Biol*. 22:6498-6508.

Zhang, J.J., U. Vinkemeier, W. Gu, D. Chakravarti, C.M. Horvath, and J.E. Darnell, Jr. 1996. Two contact regions between Stat1 and CBP/p300 in interferon gamma signaling. *Proc Natl Acad Sci U S A*. 93:15092-15096.

Zhang, J.J., Y. Zhao, B.T. Chait, W.W. Lathem, M. Ritzi, R. Knippers, and J.E. Darnell, Jr. 1998. Ser727-dependent recruitment of MCM5 by Stat1alpha in IFN-gamma-induced transcriptional activation. *Embo J*. 17:6963-6971.

Zhou, D., Q. Mei, J. Li, and H. He. 2012. Cyclophilin A and viral infections. *Biochemical and biophysical research communications*. 424:647-650.

Zhou, H., M. Xu, Q. Huang, A.T. Gates, X.D. Zhang, J.C. Castle, E. Stec, M. Ferrer, B. Strulovici, D.J. Hazuda, and A.S. Espeseth. 2008. Genome-scale RNAi screen for host factors required for HIV replication. *Cell Host Microbe*. 4:495-504.

Zhu, S., H. Zhang, and M.J. Matunis. 2006. SUMO modification through rapamycin-mediated heterodimerization reveals a dual role for Ubc9 in targeting RanGAP1 to nuclear pore complexes. *Exp Cell Res*. 312:1042-1049.

Zuleger, N., M.I. Robson, and E.C. Schirmer. 2011. The nuclear envelope as a chromatin organizer. *Nucleus*. 2:339-349.